# ANALYSIS OF DEFORMATIONS OF SOILS BASED ON THE THEORY OF PLASTICITY AND ITS APPLICATION TO SETTLEMENT OF EMBANKMENTS

Hideki OHTA

Kyoto University

October , 1971.

# ANALYSIS OF DEFORMATIONS OF SOILS BASED ON THE THEORY OF PLASTICITY AND ITS APPLICATION TO SETTLEMENT OF EMBANKMENTS

Hideki OHTA

Kyoto University

October , 1971.

## SUMMARY

This thesis presents the analysis of the deformation of soils based on the theory of plasticity and its application to the settlement of embankments. As the basis of the settlement analyses of embankments, the constitutive relations for both the isotropically and anisotropically pre-consolidated soils are derived from the flow rule of elastic-plastic materials which is given its thermodynamical base. Based on the constitutive relations for soils, three dimensional consolidation analysis and stability analysis of the embankments at the end of construction are established. Using the constitutive relations for soils, the immediate and consolidation settlement of the embankments are analysed.

CONTENTS

PREFACE

CHAPTER 1 INTRODUCTION . . . . . 1

CHAPTER 2 PRELIMINARY CONSIDERATIONS ON THE MECHANICAL BEHAVIOR OF SOILS . . . . . 5

2.1 Introduction . . . . . 5

2.2 Principle of Effective Stress . . . . . 5

2.3 Consolidation and Dilatancy . . . . . 8

2.4 Stress-Strain Relations . . . . . 12

2.5 Conclusions . . . . . 13

CHAPTER 3 THERMODYNAMICAL BASE OF THE FLOW RULE . . . . . 15

3.1 Introduction . . . . . 15

3.2 Reversible and Irreversible Deformation . . . . . 17

3.3 Constitutive Relations for Irreversible Process. . 19

3.4 Normality Rule in the Strain Space . . . . . 24

3.5 Normality Rule in the Stress Space . . . . . 28

3.6 Conclusions . . . . . 29

CHAPTER 4 CONSTITUTIVE RELATIONS FOR ISOTROPICALLY CONSOLIDATED SOILS . . . . . 31

4.1 Introduction . . . . . 31

4.2 State Surface and Swelling Wall. . . . . 34

1. Definition of Mechanical State of Clays . . . . . 34

2. Time and Path Dependent Behaviors of Clays . . . 35

3. Volume Change of Clays. . . . . 37

4. State Surface and Swelling Wall . . . . . 42

4.3 State Paths under Various Conditions . . . . . 46

1. Undrained Shear . . . . . 46

2. Triaxial Drained Shear. . . . . 47

3. $\sigma_m'$-constant Shear . . . . . 50

4. $\tau_{oct}/\sigma_m'$-constant Shear. . . . . 51

4.4 Stress-Strain Relations. . . . . 53

1. Yield Surface . . . . . 53

2. Incremental Stress-Plastic Strain Relations . . . 55
3. Stress-Elastic Strain Relations . . . . . 57
4. Critical State. . . . . 60
5. Normality Rule in the Octahedral Stress Space . . 63
Appendix . . . . . 65
6. Stress-Strain Relations under Various Conditions. 68
*Undrained Shear — Drained Shear — $\sigma'_m$-constant Shear — $\tau_{oct}/\sigma'_m$-constant Shear — $K_0$-Consolidation*
4.5 Extension of the Theory to Sands and Silts . . . . 80
4.6 Stress-Strain-Temperature Relations . . . . . 83
4.7 Conclusions . . . . . 86

CHAPTER 5 CONSTITUTIVE RELATIONS FOR ANISOTROPICALLY CONSOLIDATED SOILS . . . . . 88
5.1 Introduction . . . . . 88
5.2 State Surface and Swelling Wall. . . . . 88
1. State Surface and Swelling Wall . . . . . 88
2. State Paths under Various Conditions . . . . . 92
*Undrained Shear — Triaxial Drained Shear — $\sigma'_m$-constant Shear*
5.3 Stress-Strain Relations . . . . . .101
1. Critical State . . . . . .101
2. Stress-Strain Relations under Various Conditions.103
*Incremental Stress-Strain Relations — Undrained Shear — Triaxial Drained Shear — $\sigma'_m$-constant Shear*
5.4 Stress Condition for Plane Strain Deformation. . .111
5.5 Comparison with the Cambridge Energy Theory . . .114
5.6 Conclusions . . . . . .116

CHAPTER 6 EXPERIMENTAL EXAMINATIONS . . . . . .117
6.1 Introduction . . . . . .117
6.2 Sample Preparation and Test Procedures . . . . . .118
1. The Clay Used in the Investigations . . . . . .118
2. Test Procedure . . . . . .118

*Triaxial Test — Shear Box Test*
6.3 Consolidation Test . . . . . 119
6.4 Undrained Stress Paths . . . . . 120
1. Normally Consolidated Clay . . . . . 120
2. Overconsolidated Clay . . . . . 121
3. Shear Box Test . . . . . 121
6.5 Analysis on Drained Test . . . . . 123
1. Normally Consolidated Clay . . . . . 123
2. Overconsolidated Clay . . . . . 125
6.6 Stress-Shear Strain Relations . . . . . 126
6.7 Experimental Results by Other Researchers . . . 126
6.8 Conclusions . . . . . 129

CHAPTER 7 THREE DIMENSIONAL CONSOLIDATION ANALYSIS . . . . 131
7.1 Introduction . . . . . 131
7.2 Three Dimensional Consolidation Process . . . . 132
1. Stress-Strain Relations . . . . . 132
2. Dissipation Process of Pore Water Pressure . . 133
*Continuity of the Water — Darcy's Law — Fundamental Equations for Clay in Elastic-Plastic State — Discussion*
3. Deformation of Clay due to the Dissipation of Pore Water Pressure . . . . . 139
7.3 Anisotropic Consolidation . . . . . 139
7.4 Conclusions . . . . . 142

CHAPTER 8 IMMEDIATE SETTLEMENT OF EMBANKMENTS ANALYSED BY FINITE ELEMENT METHOD . . . . . 143
8.1 Introduction . . . . . 143
8.2 Procedures of Analysis . . . . . 144
8.3 Remarks on the Calculation Results . . . . . 145
8.4 Conclusions . . . . . 156

CHAPTER 9 CONSOLIDATION SETTLEMENT OF EMBANKMENTS . . . . . 157
9.1 Introduction . . . . . 157
9.2 Procedures of Analysis . . . . . 157
1. Stress Distributions . . . . . 157
*Initial Stress Distribution — Additional Stress Distribution due to Loading — Total Stress Distribution — Effective Stress Distribution (just after loading)*
2. Immediate Settlement . . . . . 159
*Stress-Strain Relations — Immediate Settlement*
3. Consolidation Settlement . . . . . 160
*Dissipation of Set up Pore Water Pressure — Consolidation Settlement*
9.3 Immediate Settlement . . . . . 162
9.4 Consolidation Settlement . . . . . 169
9.5 Final Settlement due to Consolidation . . . . . 172
9.6 Conclusions . . . . . 173
CHAPTER 10 CRITICAL STATE OF EMBANKMENTS . . . . . 175
10.1 Introduction . . . . . 175
10.2 Failure Conditions . . . . . 175
1. Failure Conditions in Terms of Effective Stress . 175
2. Failure Conditions in Terms of Total Stress . . . 178
10.3 Characteristics Field . . . . . 182
10.4 Critical State of Embankments . . . . . 186
1. Short-Term Stability . . . . . 186
2. Long-Term Stability . . . . . 187
10.5 Conclusions . . . . . 189
CHAPTER 11 CONCLUSIONS . . . . . 191
REFERENCES . . . . . 193

## LIST OF FIGURES


Figure

2-1 Schematic Picture of the Deformation Process in Clay (After Pusch)

2-2 Characteristics of Dilatancy

3-1 Reversible and Irreversible Deformation

3-2 Internal Dissipation Rate

3-3 Loading Cycle ABCD

3-4 Plastic Component of Free Energy

3-5 Elastic Compoment of Free Energy

3-6 Stress-Elastic Strain Relation

3-7 Stress-Plastic Strain Relation

4-1 Effects of Stress History (After Henkel)

4-2 $w$-log p Relations (After Henkel)

4-3 Consolidation Characteristics

4-4 $(w)_f$-$(\log\sigma_m')$ Relations (After Bjerrum)

4-5 Normal Consolidation and Swelling

4-6 Dilatancy of Normally Consolidated Clay (After Shibata)

4-7 Dilatancy Characteristics

4-8 State Surface and Swelling Wall of Isotropically Consolidated Clay

4-9 State Surface and State Paths

4-10 Undrained Stress Paths of Normally Consolidated Clays

4-11 Undrained State Paths

4-12 Undrained Stress Paths of the Clays Pre-Consolidated with the Same Pressure of $\sigma_m'$

4-13 Undrained Stress Paths of the Clays whose $e_i$ are identical

4-14 State Paths in Drained Triaxial Compression Test

4-15 $e$-$\sigma_m'$ Relations in Drained Triaxial Compression Test

4-16 State Paths in $\sigma_m'$-Constant Shear

4-17 Construction of State Surface

4-18 State Paths in $\tau_{oct}/\sigma_m'$-Constant Shear

Figure


4-19 $e$-ln$\sigma'_m$ Relations in $\tau_{oct}/\sigma'_m$-Constant Shear

4-20 Yield Conditions and Yield Loci

4-21 Loading Cyclcle

4-22 $(\sigma'_1 - \sigma'_3)_{max}$ Envelope

4-23 Associated Flow Rule

4-24 Stress Paths and Plastic Strain Increments (Undrained shear)

4-25 Stress Paths and Plastic Strain Increments (Drained Compression Test)

4-26 Stress Paths and Plastic Strain Increments ($\sigma'_m$-Constant shear)

4-27 Stress Paths and Plastic Strain Increments ($\tau_{oct}/\sigma'_m$-Constant Shear

4-28 Consolidation of Sands (After Vesic and Clough)

4-29 Undrained Stress Paths of Loose Sand

4-30 Influence of Temperature (After Matsuo and Kamon)

4-31 Influence of Temperature (After Matsuo and Kamon)

5-1(a) (b) Isometric View of State Surface of Anisotropically Consolidated Clay

5-2 Swelling Wall of Anisotropically Consolidated Clay (Wetter Side)

5-3 State Paths in Undrained Shear

5-4 Stress Paths in Undrained Shear

5-5 $e$-$\sigma'_m$ Relations in Undrained Shear

5-6 State Paths in Drained Shear ($\sigma_a$; increase, $\sigma_r$; constant)

5-7(a) Stress Paths of Conventional Drained Tests (wetter than critical)

(b) Stress Paths of Conventional Drained Tests (drier than critical)

5-8 $e$-$\sigma'_m$ Relations in Drained Shear ($\sigma_a$: increase $\sigma_r$: constant)

5-9 State Paths in $\sigma'_m$-Constant Shear

5-10 Stress Paths in $\sigma'_m$-Constant Shear

5-11 $e$-$\sigma'_m$ Relations in $\sigma'_m$-Constant Shear

Figure


5-12(a) Critical State Line and Yield Loci (wetter than critical)
(b) Critical State Line and Yield Loci (drier than critical)

5-13 Yield Locus in the Rendulic Plane

5-14 Associated Flow Rule

5-15 Stress Paths and Plastic Strain Increments
(a) Undrained Shear, Wetter than Critical
(b) Undrained Shear, Drier than Critical

5-16 Stress-Strain Relations (undrained shear)

5-17 Stress Paths and Plastic Strain Increments
($\sigma_a$: increase, $\sigma_r$: constant)
(a) Wetter than Critical
(b) Drier than Critical

5-18 Stress-Strain Relations ($\sigma_a$: increase, $\sigma_r$: constant)

5-19(a) Stress Paths in Undrained and Drained Shear
(b) Stress-Strain Relations in Undrained and Drained Shear

5-20 Stress Paths and Plastic Strain Increments
($\sigma_m'$-Constant Shear)

5-21 Stress-Strain Relations in $\sigma_m'$-Constant Shear

6-1 Time Dependent Behavior of a Clay under Undrained Shear

6-2 $w$-log p Plot

6-3 Stress Path of the Normally Consolidated Clay under Undrained Shear

6-4 Stress-Strain Relation of the Overconsolidated Clay

6-5 Stress Paths of the Clays under Undrained Shear

6-6 Stress Paths of Normally Consolidated Clays under Shear in Shear Box

6-7 Stress State on the $\phi'$ Maximum Mobilized Plane

6-8 Theoretical Stress Paths of Clays in Shear Box

6-9 Expelled Water Time Relation of Consolidated Clay

6-10 $e$-$\sigma_m'$ Relation of the Normally Consolidated Clay under Drained Shear

6-11 Stress Paths of the Normally Consolidated Clays

6-12 $\tau_{oct}/\sigma_m'$ : Constant Lines for the Normally Consolidated Clays

6-13 $\sigma_m'$ - Constant Test on the Overconsolidated Clay

6-14 Stress-Shear Strain Relations in the Cases of Undrained and Drained Shear

Figure


6-15 Energy Balance (After Roscoe et al.)
(a) Theory
(b) Experiments

6-16 Stress Ratio-Constant Lines (After Roscoe et al.)
(a) In the Stress Space
(b) On the *e-p* Diagram

6-17 Stress Path in Undrained Shear (After Schofield and Wroth)

6-18 Undrained Shear Test (After Schofield and Wroth)
(a) Stress Path
(b) Stress-Shear Strain Relation

7-1 Continuity of the Water

7-2 Yielding of Clay

8-1 Division of Quadrilateral Element

8-2 Stress Increments (Case 1)
(a) Increments of $\sigma_x$
(b) Increments of $\sigma_y$
(c) Increments of $\tau_{xy}$

8-3 Stress Increments (Case 2)
(a) Increments of $\sigma_x$
(b) Increments of $\sigma_y$
(c) Increments of $\tau_{xy}$

8-4 Stress Increments (Case 3)
(a) Increments of $\sigma_x$
(b) Increments of $\sigma_y$
(c) Increments of $\tau_{xy}$

8-5 Stress Ratios
(a) Case 1
(b) Case 2
(c) Case 3

8-6 Induced Pore Water Pressure
(a) Case 1
(b) Case 2
(c) Case 3

8-7 Strain Increments (Case 1)
(a) Increments of $\varepsilon_x$
(b) Increments of $\varepsilon_y$
(c) Increments of $\gamma_{xy}$

8-8 Strain Increments (Case 2)
(a) Increments of $\varepsilon_x$
(b) Increments of $\varepsilon_y$

Figure


8-8 (c) Increments of $\gamma_{xy}$

8-9 Strain Increments (Case 3)
(a) Increments of $\varepsilon_x$
(b) Increments of $\varepsilon_y$
(c) Increments of $\gamma_{xy}$

8-10 Immediate Settlement
(a) Case 1
(b) Case 2
(c) Case 3

9-1 Stress Field Induced by Strip Loading (after Akai)

9-2 Distribution of Pore Water Pressure

9-3 Key Sketches of the Problem
(a) Case 1,2,3
(b) Case 4

9-4 Stress Field (Case 1)
(a) $\sigma_x$
(b) $\sigma_y$
(c) $\tau_{xy}$

9-5 Stress Field (Case 2)
(a) $\sigma_x$
(b) $\sigma_y$
(c) $\tau_{xy}$

9-6 Induced Pore Water Pressure
(a) Case 1
(b) Case 2
(c) Case 3
(d) Case 4

9-7 Strain Field (undrained, Case 1)
(a) $\varepsilon_x$
(b) $\varepsilon_y$
(c) $\gamma_{xy}$

9-8 Strain Field (undrained, Case 2)
(a) $\varepsilon_x$
(b) $\varepsilon_y$

9-9 Strain Field (undrained, Case 3)
(a) $\varepsilon_x$
(b) $\varepsilon_y$

9-10 Strain Field (undrained, Case 4)
(a) $\varepsilon_x$
(b) $\varepsilon_y$

Figure

9-11 Immediate Settlement
(a) Case 1
(b) Case 2
(c) Case 3
(d) Case 4

9-12 Development of Critical State Zone (undrained condition)

9-13 Dissipation of Pore Water Pressure (Case 4)

9-14 Pore Pressure Dissipation and Surface Settlement (Case 1)

9-15 (a) Just under the Center of Strip Load
(b) 2 m from the Center of Strip Load
(c) 4 m from the Center of Strip Load
(d) 6 m from the Center of Strip Load

9-15 Pore Pressure Dissipation and Surface Settlement (Case 4)
(a) Just under the Center of Strip Load
(b) 4 m from the Center of Strip Load

9-16 Deformation after 100 Days (Case 1)

9-17 Deformation after 10000 Days (Case 4)

9-18 Key Sketch of the Problem

9-19 Final Settlement

10-1 Consolidation and Swelling Process without Lateral Deformation (after Henkel and Sowa)

10-2 Direction of Maximum Principal Stress

10-3 Effective Mean Principal Stress at the Critical State

## LIST OF TABLES

Table

6-1 Physical Properties of Clay Specimen

6-2 Strain Rate of the Shear Box Test

# PREFACE

This thesis is concerned with the analysis of the deformation of soils and with its application to the settlement of the embankments. In most of the textbooks of soil mechanics, we cannot find any chapter describing the deformation characteristics of soils as a whole. This fact may seem strange to the readers who are familiar to continuum mechanics including the theories of elasticity, plasticity, fluid mechanics, etc. in which the stress-strain relations of the materials are the most fundamental subjects. Throughout this thesis the author tries to make the deformation characteristics of soils easier to understand, and chooses, as the example, the settlement of embankments which are very familiar to the engineers in the field of soil mechanics and foundation engineering.

The present paper is prepared from the author's research works carried on for five years. The author is fortunate to have the opportunity to study soil mechanics and construction engineering as a graduate student under the supervision of Professor Shojiro Hata during these five years. To Professor Shojiro Hata, the author should express his special thanks for his encouragement and criticism on these investigations. And the author is indepbted to Professors Toru Shibata, Minoru Matsuo and Toshihisa Adachi for their helpful criticisms and suggestions. The author is also grateful to Messrs. Susumu Yoshitani and Makoto Kaneuji for their calculations.

# CHAPTER 1

# INTRODUCTION

Embankments have been one of the most important and popular structures in the field of civil engineering. With the development of railways and highways, and with the increasing necessity of the flood control, the importance of the embankments is swelling.

In advance of the construction of embankments, the civil engineers must be engaged in design works in which used are many theories based on the assumptions about the mechanical behaviors of soils. But at the present stage, the assumptions about the mechanical behavior of soils, on which the current methods of analyses of soil structures are based, are not able to represent the mechanical behavior of real soils with the satisfactory accuracy. Even in the routine works by means of the current analyses of soil structures, engineers are expected to have the proper understanding of the mechanical behavior of soils. And in future, new analyses of soil structures based on the more reliable representaion of the mechanical behavior of soils, especially of the constitutive rotations of soils are to be established.

Most analyses concerning the deformation of soil structures are based on the constitutive equations of linear elastic material, but the mechanical behavior of soils suggests that the soils have to be considered the elastic-plastic materials. In this thesis, the author tries to construct a theory which can explain the mechanical behavior of soils to the satisfactory extent from the viewpoint of practical engineering and tries to make the mechanical behavior of soils easier to understand.

The proposed new methods to analyse the behavior of embankments under and after construction are in such a primitive stage that the practical use of them in the routine works is not so easy. But the informations given by new methods of analyses show the accuracies and limitations of the current analytical methods. And in addition to

that we have the more systematic understanding of the change of the mechanical state of soils due to the change of effective stress state during and after the construction of embankments. These informations on the change of mechanical state of soil are useful for the safe and complete construction of embankments.

Analysis of deformation of soils and its application to the settlement of embankments is presented in this thesis which consists of eleven chapters. This is a brief introduction of the main subjects of each chapter.

In Chapter 2, presented are some preliminary considerations on the mechanical behavior of soils, especially on the principle of effective stress which plays the important role through this thesis and on the consolidation and dilatancy of clays on which the theory presented in this thesis is based. The constitutive relations for soils are derived from the concept of flow rule in plasticity in the theory mentioned in this thesis. Then in Chapter 3, the thermodynamical base of the flow rule for the rate dependent elastic-plastic materials is discussed from the viewpoint of irreversible thermodynamics.

In Chapter 4, constitutive relations for isotropically consolidated soils are presented. And in Chapter 5, the theory mentioned in Chapter 4 is expanded in order to make the theory applicable for anisotropically consolidated soils. The subjects discussed in Chapters 4 and 5 are fundamental analyses of deformation of soils that should be applied to the practical analyses in soil mechanics and foundation engineering. Experimental examinations of the theoretical results are presented in Chapter 6 in order to give some confirmations to the theory.

In Chapter 7, three dimensional consolidation analysis is presented based on the constitutive relations for soils given in Chapters 4 and 5. The contents of Chapters 2 - 7 are rather of academic interest. Then we apply these fundamental considerations to the practical engineering problems in foundation and constructing

engineering in the following chapters.

In Chapter 8 presented is the immediate settlement of embankment analysed by using the finite element method based on the stress-strain relations for clay given in Chapter 5 and some discussions are given on the current method of estimation of immediate settlement with the informations of the calculated results.

In Chapter 9, immediate and consolidation settlement of embankments are calculated by using the three dimensional consolidation theory given in Chapter 7, assuming that the stress distribution set up by the construction of embankments is determined by elasticity. Based on the informations from calculated results, the current estimation method determining the development of settlement are discussed. And the accuracy of the current estimation method of final settlement due to consolidation is discussed.

In Chapter 10 the critical state of embankment is discussed. This problem is what is called stability problem of soil structure. In this chapter, the theory of characteristics field of stress is developed based on the stress condition for the critical state derived from the constitutive relations for soils presented in Chapter 5. And with the informations obtained from the theory, the proper use of the current analyses to the stability problem of soil structures is discussed.

It has been considered that the practical design method should be simple. Then, the researchers in the field of soil mechanics have tried to construct simple analyses. But recently the situation is changing.

In the routine design works of analysing the deformation and stability of embankments under and after construction, we are going to have the excellent ability of numerical analysis with the rapid progress of electronic computer. Then, we need not try to represent the mechanical behavior of soils in extremely simple forms. In place of the simplification, the necessity of more reliable and logically self-consistent descriptions of the mechanical behavior of soils

is increasing. Based on such a reliable representaion of mechanical behavior of soils, new methods to analyse the soil structures are to be established. The investigations presented in this thesis are motivated by the thought mentioned above.

# CHAPTER 2

# PRELIMINARY CONSIDERATIONS ON THE MECHANICAL BEHAVIOR OF SOILS

## 2.1 Introduction

In this chapter we have some preliminary considerations on the mechanical behavior of soils in advance of the construction of the theory presented in the following chapters. The principle of effective stress has played the important role in the analysis of mechanical behavior of soils and therefore at first we consider on this subject. The term effective stress peculiar to soil mechanics is used in this thesis throughout and the physical meaning of effective stress should be clarified here.

The theoretical consideration presented in this thesis are based on the characteristics of consolidation and dilatancy of soils and therefore these two characteristics of soil should be reviewed and their definitions should be clasified. In the last part of this chapter presented is the short survey on the stress-strain relations for soils.

## 2.2 Principle of Effective Stress

In these two decades, some researchers in the field of applied mathematics and applied mechanics have developed the mechanics for generalized continua by constructing systematically elasticity, plasticity, fluid mechanics and thermodynamics into the classical field theory. At this present stage, one of the topics interested by researchers is to construct the theories for materials whose mechanical behaviors have not been represented by the ready made theory to the extent of satisfactory practical use in engineering design. Soil is also such a material with the complex mechanical properties.

One of the causes of the apparent complex mechanical behavior of soil arises from the fact that the soil is a multiphase composite material composed of gas, fluid and solid. Difficulty arising from

such a cause has been eliminated by the *Principle of effective stress* initially proposed by Rendulic (1936) and confirmed to some extent by Henkel (1960). Principle of effective stress is a postulate that the mechanical behaviors of the three phases constituting the soil are independently determined by their allotted stresses respectively. *Effective stress* is defined as the allotted stress of the soil skelton composed of the soil grains and particles. The principle of effective stress is easily accepted intuitively and it leads to the fairly simple representation of apparently complex mechanical behavior of soil.

In the field of soil mechanics, effective stress, defined by Terzaghi as

$$\sigma'_{ij} = \sigma_{ij} - \delta_{ij}u \tag{2.2.1}$$

has been commonly used for the completely saturated soils, where $\delta_{ij}$ is Kronecker's delta. Terzaghi's effective stress is an approximate representation of the stress allotted to soil skelton and its limitation was studied in detail. On the other hand, Biot (1954) gave the definition of effective stress as

$$\sigma'_{ij} = \sigma_{ij} - \delta_{ij}u\,\frac{e}{1+e} \tag{2.2.2}$$

where $e$ is the void ratio of soil.

Judging from the mathematical derivations for obtaining these two definitions of the effective stress, the author considers Biot's effective stress more reasonable. However, Biot's effective stress has a difficulty as follows. The pore water pressure increment $\Delta u$ induced by the application of additional hydrostatic pressure $\Delta\sigma$ under undrained condition in a completely saturated soil specimen compressed isotropically is given by (2.2.1) and (2.2.2) as

$$\Delta\sigma = \Delta\sigma' + \Delta u \tag{2.2.3}$$

$$\Delta\sigma = \Delta\sigma' + \frac{e}{1+e}\,\Delta u \tag{2.2.4}$$

The assumption that the unchanged void ratio $e$ proves unchanging

effective stress $\sigma'$ leads to the conclusion of $\Delta\sigma' = 0$. Therefore, from eq. (2.2.3) and eq. (2.2.4), it follows :

$$\Delta u = \Delta\sigma \tag{2.2.5}$$

$$\Delta u = \frac{1 + e}{e} \Delta\sigma > \Delta\sigma \tag{2.2.6}$$

The physical meaning suggested by eq. (2.2.6) is contrary to the idea commonly accepted in the field of soil mechanics.

But it is note worthy that this experience that is contrary to the derivation given by eq. (2.2.6) is carried on by the application of total stress to soil specimen by means of the increasing cell water pressure which is separated by a thin rubber membrane from the soil specimen. Under such a condition, the induced additional stress in the soil skelton and in the water are of both same value on the boundary of the specimen which is covered by a rubber membrane. And it is apparent that, under such a boundary condition, Biot's definition of effective stress cannot be derived. Comparing eqs. (2.2.1) and (2.2.2), we can easily understand that these two definitions of effective stress coincide with each other when the void ratio is sufficiently large compared with unit.

This conclusion is supported by Skempton (1960) from the different viewpoint who stated that the principle of effective stress is adaptable to soils when the area of contact between the particles per unit gross area of the soil is sufficiently small. Skempton (1960) proposed three definitions of effective stress but he insisted that such a consideration on the exact definition of effective stress was of no more than academic interest. And in the practical sense the definition of effective stress proposed by Terzaghi in 1923 had sufficient accuracy. His conclusions were essentially the same as those given by Bishop (1955). As mentioned above the definition of effective stress has many unclarified questions, but in this thesis the effective stress defined by Terzaghi is used throughout.

Bishop (1955) insisted that Tergaghi's effective stress gave the reasonable understanding not only of the deformation and volume change

in soils but also of the strength characteristics of soils. The usefulness of the effective stress is also emphasized by Whitman (1960) and Bjerrum (1955) who proposed the several methods to obtain the Hvorslev strength parameters.

## 2.3 Consolidation and Dilatancy

As shown by Rendulic (1936) and Henkel (1960) the unique relationship between the effective stress and the void ratio for normally consolidated clay is to some extent confirmed. Now in order to make some further consderations about the stress and void ratio relation, it is convenient to consider the volume change of stressed clay consists of two components: consolidation and dilatancy.

Consolidation is defined as the deformation process of the clay stressed by the proportional loading, i.e., $\sigma'_{ij} / \sigma'_{kl}$ - constant loading system. This stress ratio constant loading is called anisotropic consolidation in which the isotropic consolidation caused by the application of only the hydrostatic effective stress $\sigma'_m$ is included. It is well known characteristics of consolidation process that the void ratio and the logarithm of applied effective hydrostatic stress $\sigma'_m$ are related linearly. But this well confirmed $e$-$\ln\sigma'_m$ linearity of the consolidation process has been only the emperical relation. The study on the microscopic mechanism of this consolidatio process has been out of the attentions of researchers, although it is known that the clay particles tend to rearrange parallel each other normal to the maximum principal stress during the anisotropic consolidation.

Here we try to make the mechanical model explaining the rearrangement of clay particles during anisotropic consolidation based on the behavior of the microstructure of clay. An example of isometric view of clay skelton given by Pusch (1970) is shown in Fig. 2.1.(a). During anisotropic consolidation the links of particles connecting the network of small aggregates break down successively at increasing shear deformation as shown in Fig. 2.1.(b).
Now let us consider the anisotropic consolidation process in which

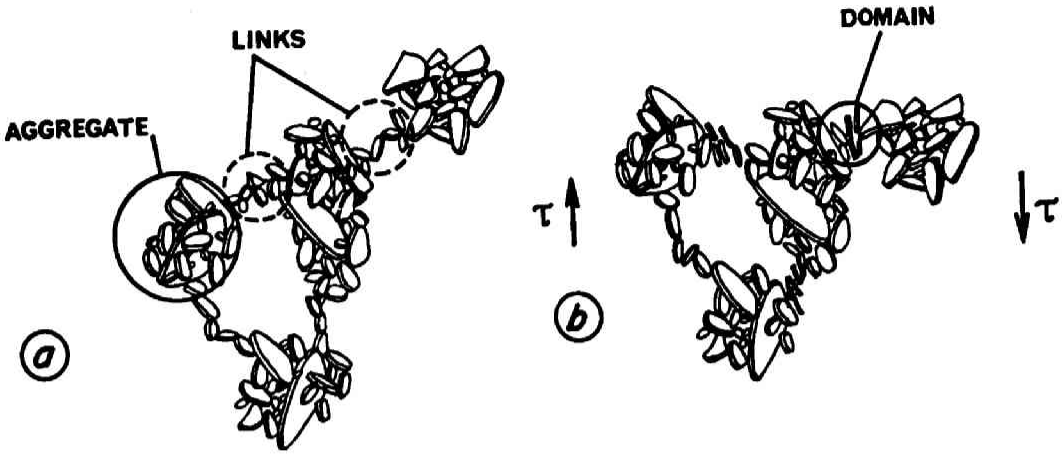


Fig. 2.1. Schematic picture of the deformation process in clay. (After Pusch)

the direction of the maximum principal stress is not altered. Since the anisotropic consolidation process is characterized by the proportional loading, the interparticle forces induced in the clay skelton by the application of additional stresses are also approximately and proportionally increasing during the anisotropic consolidation process. Assuming that the clay particles are not crushed by the increasing proportional forces, relative movements between clay particles cannot be induced if the compressibility of clay particles is negligiblly small.

Therefore it is natural to assume that the volume change due to consolidation process can be caused by only the buckling of the clay skelton. But this buckling is possible to the parts of clay skelton approximately parallel to the direction of maximum principal stress. The clay particles constructing the pole like parts of the clay skelton parallel to the direction of the maximum principal stress tend to rearrange themselves normal to the direction of the maximum principal stress, because during the progressive buckling process the clay particles initially directed to the maximum principal stress

rearrange themselves to the direction normal to the maximum principal stress when the links break down by buckling. These considerations suggest that the rotation of the maximum principal stress during anisoropical consolidation induces excess change compared with the case of irrotational maximum principal stress.

Here we must comment on the isotropic consolidation process in which the direction of maximum principal stress is not fixed. It can be easily supposed that, in the isotropically consolidated clay specimen, the local anisotropic consolidation processes are progressing. This hypothesis gives a reasonable understanding that the clay particles are to be aligned to the particular direction locally as shown by Roscoe, Schofield and Thurairajah (1963).

Now let us consider the dilatancy process of clay. Here we define the dilatancy process as the deformation process of clay stressed with constant effect mean principal stress $\sigma_m'$.
The characteristics of dilatancy have been clarified by serial works by Shibata (1963), Shibata and Karube (1965) and Karube and Kurihara (1966). They concluded that the void ratio change due to dilatancy is related linearly with applied stress ratio $\tau_{oct}/\sigma_m'$. It has been considered in the field of soil mechanics that dilatancy effect is accompanied with the distortional deformation of soil. But it is note worthy that the volume changes due to dilatancy, as defined here, do not occur in the anisotropic consolidation process in which the rails deform distortionally to some extent.

Here let us consider the microscopic mechanism of dilatancy. It is easily understood that all the frame works constructed with clay particles reduce their total volumes when they deform distortionally as shown in Fig. 2.2 briefly. With the assumption that the length of the perimeter are not shortened by buckling or by another sort of reasons this sort of volume change are essentially different from the consolidation mechanism explained before. But the mechanism of dilatancy of soils is not so simple because, as shown in Fig. 2.1, the lengths of perimeters of the frameworks constructed

with clay particles are shortened by the application of shear stress. Then in addition to the volume reduction explained in Fig.2.2, another sort of volume reduction due to the shortening of the perimeters of the frameworks of soil skelton does exist

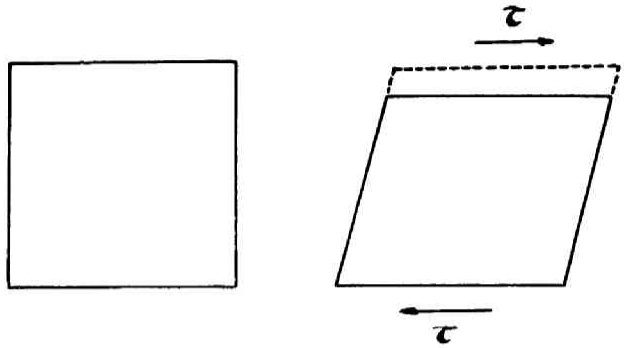


Fig. 2.2. Characteristics of dilatancy.

The extent of the shortening of the perimeters depends on the microstructure of soil. But it is likely that the floculent structure shows the eminent tendency of dilatancy compared with well aligned structure of soil skelton.

The distortional deformation explained in Fig. 2.2 cannot become so large that all the voids vanish, because the aggregates constructed with clay particles which is forming the perimeters of the framework of clay skelton touch each other at the large distortional deformation and prevent the clay skelton from deforming further. At this critical state the frameworks of the clay skelton behave as if they were the grains of sand and further distortional deformation of soil is promoted by the rotation of the clusters (the assemblages of the aggregated clay particles). In such a state clays behave as if they were sands. This state may correspond to so called critical state defined by Roscoe et al.

It is said that the sand grains do not rotate during the shear process until it reaches the critical state and after arriving at the critical state they begin to rotate each other. During the shear

process of sand, before the critical state, the distortional deformation of sand is mainly due to the relative sliding between the sand grains, not mainly due to the rotation of sand grains.

## 2.4 Stress-Strain Relations

Stress-strain relations for soils are the most important to solve the many practical problems in soil mechanics and foundation engineering. Most of the present methods to analyse engineering problems of soil structures are based on the simplified stress-strain relations for soils which cannot represent the complicated stress-strain relations of soils with sufficient accuracy.

Since 1960´s some research groups have been constructing the logically self-consistent theories of stress-strain relations for soils. The research group with Roscoe as the central figure has been developing its theory named "*Critical state energy theory*" based on the estimation of dissipated energy and using the concept of normality in plasticity. The researches of this group have been carried on at Cambridge and published in the serial papers by Roscoe, Schofield and Wroth (1958). Roscoe, and Poorooshasb (1963), Roscoe, Schofield and Thurairajah (1963), Burland (1965), Roscoe and Burland (1968), Schofield and Wroth (1968) and Burland and Lewin (1970).

Almost since the same time of the publication of Cambridge theory, the research group initiated by Rowe (1962) has been also publishing its works "*Stress-Dilatancy Theory*" based on the energy balance from the view point of the particulate mechanics which is arising from the recognition that the soils are the assemblages of granular materials.

Quite independently established theories are there at Kyoto University. One of them has been constructed by Murayama in the serial works (1964, 1965) and succeeded by Murayama and Matsuoka (1971) from the view point of particulate mechanics. In their theories the distribution of the contact angles between grains plays important role. The other work at Kyoto University is the direct

research of the dilatancy of clay initiated by Shibata (1963) and successively continued by Shibata and Karube (1965), Karube and Kurihara (1966), Hata, and Ohta (1968), Hata and Ohta (1969), Hata, Ohta and Yoshitani (1969 a,b), Ohta and Hata (1971), Ohta and Hata (1971 a,b). Ohta and Hata (to appear, a,b), Adachi and Ohta (to appear). This thesis is the consequence of the works of the last research group initiated by Shibata.

## 2.5 Conclusions

In this chapter some preliminary considerations on the mechanical behavior of soils are made in advance of developing the theory in the following chapters. In this chapter, the concept of effective stress is clarified and the limitation of its use is discussed. The principle of effective stress which plays the important role in this thesis is rationalized in the discussions although the concept of effective stress itself includes many physical vagueness.

The main part of this chapter is occupied by the considerations of the microscopic mechanisms of the consolidation and dilatancy processes of clay on which the theory presented later is based. In the discussions the qualitative tendency of clay during consolidation and dilatancy is clarified and reasoned out to some extent.

In addition to these discussions, a brief survey of the previous research works on the stress-strain relations of soils is presented to make the standpoint of the author's study lightened.

# CHAPTER 3

# THERMODYNAMICAL BASE OF THE FLOW RULE

## 3.1 Introduction

In this thesis, the constitutive relations for soils are derived based on the concept of associated flow rule which demands the incremental plastic strain vector to be normal to the current yield surface given in the stress space. Generally speaking, the concept of flow rule of plastic material deforming irreversiblly with work-hardening or work-softening effect is characterized by the assumtion of the existence of plastic potentials as functions of stress tensor. Drucker (1951, 1958, 1962) gave the rationalized explanations of the associated flow rule for the stable plastic materials with convex yield surfaces. Palmer (1965), Palmer, Marier and Drucker (1967) expanded the Drucker's explanation to the unstable materials. Applications of the flow rule to soil mechanics have been tried by Drucker and Prager (1952), Drucker (1954), Drucker, Gibson and Henkel (1957) assuming the Mohr-Coulomb failure condition to be the plastic potential. But in the author's opinion, the Mohr-Coulomb condition is not suitable to be considered as the plastic potential. Palmer (1966) and Weidler and Paslay (1969) tried to give the plastic potential for soils from the standpoint of using the non-associated flow rule.

In this chapter considered are the constitutive equations for a rate dependent elastic-plastic material by using thermodynamic equations.

In microscopic view, the plastic strain (in general, irreversible deformation) associated with internal dissipation differs the material behavior from elastic one. It is always noticed that the mechanical response of real materials shows definite rate effect. Thus, elastic (reversible) and plastic (irreversible) strains and those time rates are assumed to be state variables in addition to temperature and temperature gradient. The 2nd time derivatives of the strains are

postulated to be response functions of the state variables.

Although, the existence of yielding function in stress space is usually assumed in classical plastic theory, we give attention to the above constitutive assumptions and their interrelation to free energy in this chapter.

After Truesdell and Toupin's general thermodynamic frame work (1960), the outstanding papers by Coleman and Noll (1963) and Coleman and Mizel (1964) gave a definite idea how 2nd law of thermodynamics to place restrictions on the constitutive equations of ideal materials. Since then, their technique have been broadly used to construct constitutive equations of ideal materials.

Green and Naghdi (1965) studied on invisid elastic-plastic material and extended to a viscoelastic-plastic material (1967) They used elastic and plastic strains as state variables and assumed the existence of yield function in stress space as classical plastic theory.

Colemen and Gurtin (1967) developed a phenomenological theory of dissipation for viscous-stress type material by introducing internal state variables (hidden state variables).

The applications of this theory to plastic material were done by Leigh (1969) and Kratochvil and Dillon, Jr. (1969). Leigh chose plastic deformation gradient as an internal state variable and assumed a plastic-straining function of state variables which was different from classical yield function and served as a constitutive assumption for plastic strain rate. Kratochvil and Dillon, Jr.'s paper was almost similar to Leigh's except they introduced dislocation arrangement tensor as an additional internal state variable to attempt to clarify the effect of microscopic dislocation phenomenon on macroscopic plastic behaviors.

For isothermal plastic material, Valanis (1970) proposed a different way of consideration. He postulated that the internal dissipation energy was a function of the current state of stress and stress increments. His view was different from others in selecting

state variables. There were, however, some questions in the use of Drucker's stability postulate (1951) to derive his plastic constitutive equations in addition to the 2nd law of thermodynamics.

After above review, the author's work lies on extension and some modification of the works by Green and Naghdi and Coleman and Gurtin.

In Sec.2, presented is an analysis of the interrelation of elastic and plastic strains and their time rate.

Thermodynamics equations and the constitutive assumptions are given in Sec.3. Also, the discussion is extended to the restrictions on the constitutive assumptions by the 2nd law of thermodynamics. Certain simplified cases are also studied.

In order to give physical interplitation of the obtained constitutive equations, we discuss the result in strain space than stress space, in Sec.4.

Finally, in Sec.5, we attempt to map the discussion in Sec.4 to in stress space which are usually done in classical theory of plasticity.

## 3.2 Reversible and Irreversible Deformation

For simplicity, our discussion is fixed in rectangular Cartesian coordinate system through this chapter. The position of any particle of a body is represented by $X(X_K)$ for the state at rest, chosen to be a reference state, $x'(x_K)$ for the deformed state, and $X'(X'_K)$ for the state after the removal of applied stresses. Thus, the total displacement of an arbitrary particle of the body is given by $x-X$, irreversible displacement is given by $X'-X$, reversible displacement of the particle is given by $X'-x$ as shown in Fig. 3.1. Therefore, the position vector of any particle of the substance is given by eqs. (3.2.1) or (3.2.2):

$$x_k = x_k(X_K, t) \tag{3.2.1}$$

$$X'_K = X'_K(X_K, t) \tag{3.2.2}$$

at time t. Here we concider that the functions $x_k$, $X'_K$ are single valued functions of $X_K$ and t. The line elements of the substance at

rest, under deformation and after the removal of applied stress are respectively defined by eqs. (3.2.3), (3.2.4) and (3.2.5):

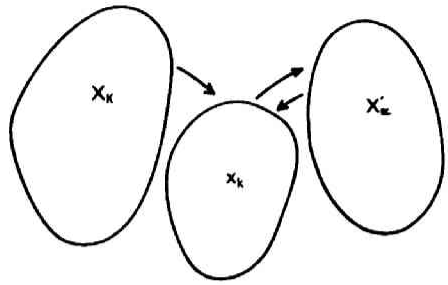


Fig.3.1. Reversible and irreversible deformation

$$dS^2 = dX_K \cdot dX_K \tag{3.2.3}$$

$$ds^2 = dx_k \cdot dx_k = x_{k,K}x_{k,L}dX_K dX_L$$
$$= x_{k,\kappa}x_{k,\lambda}dX'_\kappa dX'_\lambda \tag{3.2.4}$$

$$dS'^2 = dX'_\kappa dX'_\kappa = X'_{\kappa,K}X'_{\kappa,L}dX_K dX_L \tag{3.2.5}$$

and we define the total strain tensor, elastic strain tensor and plastic strain tensor as follows:

$$ds^2 - dS^2 = (x_{k,K}x_{k,L} - \delta_{KL})dX_K dX_L$$
$$\equiv 2E_{KL}dX_K dX_L \tag{3.2.6}$$

$$ds^2 - dS'^2 = (x_{k,\kappa}x_{k,\lambda} - \delta_{\kappa\lambda})dX'_\kappa dX'_\lambda$$
$$\equiv 2E^e_{\kappa\lambda}dX'_\kappa dX'_\lambda \tag{3.2.7}$$

$$dS'^2 - dS'^2 = (X'_{\kappa,K}X'_{\lambda,L} - \delta_{KL})dX_K dX_L$$
$$\equiv 2E^p_{KL}dX_K dX_L \tag{3.2.8}$$

where $E_{KL}$, $E^e_{\kappa\lambda}$ and $E^p_{KL}$ are the total strain tensor, elastic strain tensor and plastic strain tensor respectively Eliminating the terms of left hand side of eqs. (3.2.6), (3.2.7), ves the

following relation:

$$E^{e}_{\kappa\lambda} dX'_{\kappa} dX'_{\lambda} = (E_{KL} - E^{p}_{KL}) dX_K dX_L \tag{3.2.9}$$

and then by using:

$$dX'_{\kappa} = X'_{\kappa},_K dX_K \quad , \quad dX'_{\lambda} = X'_{\lambda},_L dX_L$$

we obtain the relationship between total strain tensor, elastic strain tensor and plastic strain tensor as follows:

$$E^{e}_{\kappa\lambda} X'_{\kappa},_K X'_{\lambda},_L = E_{KL} - E^{p}_{KL} \tag{3.2.10}$$

If we confine our attention to the case of infinitesimal deformation, we get:

$$E^{e}_{KL} = E_{KL} - E^{p}_{KL} \tag{3.2.11}$$

where the relations $X'_{\kappa},_K = \delta_{\kappa K}$ , $X'_{\lambda},_L = \delta_{\lambda L}$ are used, Eq. (3.2.11) shows that the total strain tensor is given by simple sum of elastic strain tensor and plastic strain tensor only for the infinitesimal deformation.

## 3.3 Constitutive Relations for Irreversible Process

Let define the equation of energy balance:

$$\rho\dot{\varepsilon} = t_{(kl)} d_{kl} - m_{klm} w_{kl,m} - q_{k,k} + \rho r \tag{3.3.1}$$

where $\varepsilon$ denotes the specific internal energy, $\rho$ is the specific density, $t_{kl}$ and $m_{klm}$ are the stress tensor and the couple stress tensor, $d_{kl}$ and $w_{kl}$ are the deformation rate tensor and spin tensor and $q_k$, r are the heat flux and heat supply by radiation respectively. Now on we consider only non-polar case, then eq. (3.3.1) is reduced to:

$$\rho\dot{\varepsilon} = t_{kl} d_{kl} - q_{k},_k + \rho r \tag{3.3.2}$$

Introducing:

$$r - \frac{1}{\rho} q_{k},_k \equiv \dot{Q} \tag{3.3.3}$$

eq. (3.3.2) yields as follows:

$$\dot{\varepsilon} - \frac{1}{\rho_o} t_{kl} d_{kl} = \dot{Q} \tag{3.3.4}$$

Substituting the relationship between deformation rate tensor $d_{kl}$ and and Lagrangean strain tensor $E_{kl}$:

$$d_{kl} = \dot{E}_{KL} X_{K,k} X_{L,l} \tag{3.3.5}$$

and the relationship between the stress tensor $t_{kl}$ and Piola-Kirchhoff stress tensor $T_{KL}$:

$$t_{kl} = \frac{\rho}{\rho_o} x_{k,K} x_{l,L} T_{KL} \tag{3.3.6}$$

into eq. (3.3.4), we get the equation of energy balance as:

$$\dot{\varepsilon} - \frac{1}{\rho_o} T_{KL} \dot{E}_{KL} = \dot{Q} \tag{3.3.7}$$

If $\psi$ is the free energy defined by:

$$\psi = \varepsilon - \theta\eta \tag{3.3.8}$$

where $\theta$ is the absolute temperature and $\eta$ is the specific entropy, we get:

$$\dot{\psi} = \dot{\varepsilon} - \dot{\theta}\eta - \theta\dot{\eta} \tag{3.3.9}$$

Combining eqs. (3.3.7) and (3.3.9) it follows:

$$\dot{\psi} + \dot{\theta}\eta + \theta\dot{\eta} - \frac{1}{\rho_o} T_{KL} \dot{E}_{KL} = \dot{Q} \tag{3.3.10}$$

We define the irreversible deformation process of the substance as follows:

$$\theta\sigma = \theta\dot{\eta} - \dot{Q} \geqq 0 \tag{3.3.11}$$

where $\sigma$ is internal dissipation introduced by Coleman and Gurtin (1967). The substitution of eq. (3.3.10) into eq. (3.3.11) gives:

$$\frac{1}{\rho_o} T_{KL} \dot{E}_{KL} - \dot{\psi} - \dot{\theta}\eta \geqq 0 \tag{3.3.12}$$

The material derivative of eq. (3.2.10) leads:

$$\begin{aligned} \dot{E}_{KL} = {} & \dot{E}^{p}_{KL} + \dot{E}^{e}_{\kappa\lambda} X'_{\kappa,K} X'_{\lambda,L} \\ & + E^{e}_{\kappa\lambda} \left( V'_{\kappa;\alpha} X'_{\alpha,K} X'_{\lambda,L} + V'_{\lambda;\beta} X'_{\beta,L} X'_{\kappa,K} \right) \end{aligned} \tag{3.3.13}$$

where $V'_{\kappa}$ is velocity at $X'$. Substituting eq. (3.3.13) into

eq. (3.3.12). we get:

$$T_{KL}\dot{E}^{p}_{KL} + T_{KL}\dot{E}^{e}_{\kappa\lambda}X'_{\kappa},_{K}X'_{\lambda},_{L} + T_{KL}E^{e}_{\kappa\lambda}\ (V'_{\kappa;\alpha}X'_{\alpha},_{K}X'_{\lambda L}$$
$$+ V'_{\lambda;\beta}\ X'_{\beta},_{L}X'_{\kappa},_{K}) - \rho_0\dot{\psi} - \rho_o\ \dot{\theta}\eta \geqq 0 \qquad (3.3.14)$$

For the case of infinitesimal deformation, eq. (3.3.14) is reduced to:

$$T_{KL}\dot{E}^{p}_{KL} + T_{KL}\dot{E}^{e}_{KL} - \rho_0\dot{\psi} - \rho_o\ \dot{\theta}\eta \geqq 0 \qquad (3.3.15)$$

We postulate the constitutive assumption for the substance whose mechanical behavior is rate dependent as

$$\psi = \psi\ (E^{e}_{\kappa\lambda},\ E^{p}_{KL},\ \dot{E}^{e}_{\kappa\lambda},\ \dot{E}^{p}_{KL},\ \theta,\ \theta,_{k}) \qquad (3.3.16\text{-a})$$

$$\eta = \eta\ (E^{e}_{\kappa\lambda},\ E^{p}_{KL},\ \dot{E}^{e}_{\kappa\lambda},\ \dot{E}^{p}_{KL},\ \theta,\ \theta,_{k}) \qquad (3.3.16\text{-b})$$

$$T_{KL} = T_{KL}\ (E^{e}_{\kappa\lambda},E^{p}_{KL},\ \dot{E}^{e}_{\kappa\lambda},\ \dot{E}^{p}_{KL},\ \theta,\ \theta,_{k}) \qquad (3.3.16\text{-c})$$

$$q_p = q_p\ (E^{e}_{\kappa\lambda},\ E^{p}_{KL},\ \dot{E}^{e}_{\kappa\lambda},\ \dot{E}^{p}_{KL},\ \theta,\ \theta,_{k}) \qquad (3.3.16\text{-d})$$

Material time derivative of eq. (3.3.16-a) leads:

$$\dot{\psi} = \frac{\partial\psi}{\partial E^{e}_{\kappa\lambda}}\ \dot{E}_{\kappa\lambda} + \frac{\partial\psi}{\partial E^{p}_{KL}}\ \dot{E}^{p}_{KL} + \frac{\partial\psi}{\partial\dot{E}^{e}_{\kappa\lambda}}\ \dot{E}^{\cdot e}_{\kappa\lambda} + \frac{\partial\psi}{\partial\dot{E}^{p}_{KL}}\ \dot{E}^{\cdot p}_{KL}$$
$$+ \frac{\partial\psi}{\partial\theta}\dot{\theta} + \frac{\partial\psi}{\partial\theta,_{k}}\ \dot{\theta},_{k} \qquad (3.3.17)$$

From eqs. (3.3.14) and (3.3.17), we get the thermodynamic restriction for the rate dependent elastic-plastic material as follows:

$$(T_{KL} - \rho_o\ \frac{\partial\psi}{\partial E^{p}_{KL}})\ \dot{E}^{p}_{KL} - \rho_o\ \frac{\partial\psi}{\partial\dot{E}^{p}_{KL}}\ \dot{E}^{\cdot p}_{KL} + (T_{KL}X'_{\kappa},_{K}X'_{\lambda},_{L}$$
$$- \rho_o\ \frac{\partial\psi}{\partial E^{e}_{\kappa\lambda}})\ \dot{E}^{e}_{\kappa\lambda} - \rho_o\ \frac{\partial\psi}{\partial\dot{E}^{e}_{\kappa\lambda}}\ \dot{E}^{\cdot e}_{\kappa\lambda} + T_{KL}E^{e}_{\kappa\lambda}(V'_{\kappa;\alpha}X'_{\alpha},_{K}X'_{\lambda},_{L}$$
$$+ V'_{\lambda;\beta}X'_{\beta},_{L}X'_{\kappa},_{K}) - \rho_o\ (\eta + \frac{\partial\psi}{\partial\theta}\ )\dot{\theta} - \rho_o\ \frac{\partial\psi}{\partial\theta,_{k}}\ \dot{\theta},_{k} \geqq 0 \qquad (3.3.18)$$

When we confine our attention to the case of infinitesimal deformation eq. (3.3.18) is reduced to:

$$(T_{KL} - \rho_o \frac{\partial\psi}{\partial E^p_{KL}}) \dot{E}^p_{KL} - \rho_o \frac{\partial\psi}{\partial \dot{E}^p_{KL}} \ddot{E}^p_{KL} + (T_{KL} - \rho_o \frac{\partial\psi}{\partial E^e_{KL}}) \dot{E}^e_{KL}$$

$$- \rho_o \frac{\partial\psi}{\partial \dot{E}^e_{KL}} \ddot{E}^e_{KL} - \rho_o (\eta + \frac{\partial\psi}{\partial\theta})\dot{\theta} - \rho_o \frac{\partial\psi}{\partial\theta_{,k}}\dot{\theta}_{,k} \geqq 0 \tag{3.3.19}$$

Eq. (3.3.19) gives the general thermodynamic restriction for the rate dependent elastic-plastic material in the case of infinitesimal deformation with which we deal in the later discussion.

(a) The case that the free energy $\psi$ is independent of the strain rate. As a special case of the constitutive assumptions given by eqs. (3.3.16), we first discuss the rate independent behavior of material:

$$\frac{\partial\psi}{\partial \dot{E}^e_{KL}} = \frac{\partial\psi}{\partial \dot{E}^p_{KL}} = 0 \tag{3.3.20}$$

In this case eq. (3.3.19) is reduced to:

$$(T_{KL} - \rho_o \frac{\partial\psi}{\partial E^p_{KL}}) \dot{E}^p_{KL} + (T_{KL} - \rho_o \frac{\partial\psi}{\partial E^e_{KL}})\dot{E}^e_{KL} - \rho_o (\eta + \frac{\partial\psi}{\partial\theta}) \dot{\theta}$$

$$- \rho_o \frac{\partial\psi}{\partial\theta_{,k}} \dot{\theta}_{,k} \geqq 0 \tag{3.3.21}$$

With the assumption that:

$$\dot{E}^p_{KL} = \dot{E}^p_{KL}(E^e_{KL}, E^p_{KL}, \theta, \theta_{,k}) \tag{3.3.22}$$

and considering the dissipative energy loss to be induced by plastic deformation, we can derive the following relations according to Coleman and Noll technique:

$$T_{KL} = \rho_o \frac{\partial\psi}{E^e_{KL}} \tag{3.3.23}$$

$$\eta = - \frac{\partial\psi}{\partial\theta} \tag{3.3.24}$$

$$\frac{\partial\psi}{\partial\theta_{,k}} = 0 \tag{3.3.25}$$

$$(T_{KL} - \rho_o \frac{\partial\psi}{\partial E^P_{KL}})\dot{E}^P_{KL} \geqq 0 \tag{3.3.26}$$

Eqs. (3.3.23) - (3.3.26) are the sufficient condition, but not the necessary condition for eq. (3.3.21). Therefore it is possible to image the ideal material which does not behave according to eqs. (3.3.23) - (3.3.26) in spite of its rate independent mechanical characteristics. Eqs. (3.3.23) - (3.3.26) have already given by Green and Naghdi (1965).

(b) The case that the free energy $\psi$ is depend on the strain rate. In this case, we have:

$$\frac{\partial\psi}{\partial\dot{E}^{e}_{KL}} \neq 0 \quad , \quad \frac{\partial\psi}{\partial\dot{E}^{p}_{KL}} \neq 0 \tag{3.3.27}$$

In order to develop our discussion let us limit our interests into the case for which the following relations are approximately valid:

$$\dot{\dot{E}}^{e}_{KL} = \alpha(E^{e}_{KL},\ E^{p}_{KL},\ \theta,\ \theta_{,k})\dot{E}^{e}_{KL} \tag{3.3.28}$$

$$\dot{\dot{E}}^{p}_{KL} = \beta(E^{e}_{KL},\ E^{p}_{KL},\ \theta,\ \theta_{,k})\dot{E}^{p}_{KL} \tag{3.3.29}$$

where $\alpha$ and $\beta$ are continuous rate independent functions. Substitution of eqs. (3.3.28) and (3.3.29) into eq. (3.3.19) leads the following inequality:

$$(T_{KL} - \rho_o\frac{\partial\psi}{\partial E^{p}_{KL}} - \rho_o\beta\frac{\partial\psi}{\partial\dot{E}^{p}_{KL}})\dot{E}^{p}_{KL} + (T_{KL} - \rho_o\frac{\partial\psi}{\partial E^{e}_{KL}} - \rho_o\alpha\frac{\partial\psi}{\partial\dot{E}^{e}_{KL}})\dot{E}^{e}_{KL}$$

$$- \rho_o(\eta + \frac{\partial\psi}{\partial\theta})\dot{\theta} - \rho_o\frac{\partial\psi}{\partial\theta_{,k}}\dot{\theta}_{,k} \geqq 0 \tag{3.3.30}$$

With the assumption given by eq. (3.3.22), we get the sufficient condition for the inequality (3.3.30) because of the same reason mentioned in case (a):

$$T_{KL} = \rho_o\frac{\partial\psi}{\partial E^{e}_{KL}} + \rho_o\alpha\frac{\partial\psi}{\partial\dot{E}^{e}_{KL}} \tag{3.3.31}$$

$$\eta = -\frac{\partial\psi}{\partial\theta} \tag{3.3.32}$$

$$\frac{\partial\psi}{\partial\theta_{,k}} = 0 \tag{3.3.33}$$

$$\theta\sigma = (T_{KL} - \rho_o\frac{\partial\psi}{\partial E^{p}_{KL}} - \rho_o\beta\frac{\partial\psi}{\partial\dot{E}^{p}_{KL}})\dot{E}^{p}_{KL} \geqq 0 \tag{3.3.34}$$

Eq. (3.3.34) gives the non-negative internal dissipation for the elastic-plastic material whose mechanical behavior is dependent on the deformation rate. Eqs. (3.3.23) - (3.3.26) are included in eqs. (3.3.31) - (3.3.34) as a special case. Eqs. (3.3.31) - (3.3.33) make the $\theta_{,k}$ be dropped out from the constitutive assumptions given by eqs. (3.3.16-a,b,c) as follows:

$$\psi = \psi(E^e_{KL}, E^p_{KL}, \dot{E}^e_{KL}, \dot{E}^p_{KL}, \theta) \tag{3.3.35-a}$$

$$\eta = \eta(E^e_{KL}, E^p_{KL}, \dot{E}^e_{KL}, \dot{E}^p_{KL}, \theta) \tag{3.3.35-b}$$

$$T_{KL} = T_{KL}(E^e_{KL}, E^p_{KL}, \dot{E}^e_{KL}, \dot{E}^p_{KL}, \theta) \tag{3.3.35-c}$$

$$q_p = q_p(E^e_{KL}, E^p_{KL}, \dot{E}^e_{KL}, \dot{E}^p_{KL}, \theta, \theta_{,k}) \tag{3.3.35-d}$$

## 3.4 Normality Rule in the Strain Space

Eq. (3.3.34) shows that dissipative mechanical work of the material should be non-negative. Here we give the physical interpretation of eq. (3.3.34) and then, based on the some considerations, derive the flow rule of plasticity.

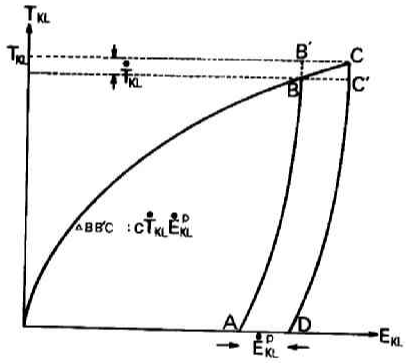


Fig.3.2. Internal dissipation rate

Let us consider the loading cycle ABCD in Fig. 3.2 for the rate dependent elastic-plastic material under isothermal condition. In the loading cycle ABCD, dealt is the special case when the functions $\psi$ and $\alpha$ are chosen so that the elastic loading curve AB completely coincides with the elastic unloading curve CD. Therefore, $\frac{\partial\psi}{\partial E^e_{KL}}$ and $\alpha$ must be independent of the plastic strain tensor $E^p_{KL}$ and the elastic strain rates $\dot{E}^e_{KL}$

on the loading and unloading process must be selected to the same value at the same stress level. Under these conditions, the elastic stress-strain curve ABB'; and DC'C are completely similar. The area given by ABCD is purely internal dissipation energy rate $\theta\sigma$ which is mathematically given by eq. (3.4.1):

$$\begin{aligned}\theta\sigma &= T_{KL}\dot{E}^{p}_{KL} - c\dot{T}_{KL}\dot{E}^{p}_{KL} \\ &= (T_{KL} - c\dot{T}_{KL})\dot{E}^{p}_{KL}\end{aligned} \tag{3.4.1}$$

where the coefficient c is a scalar function of $E^{e}_{KL}$, $E^{p}_{KL}$, $\dot{E}^{e}_{KL}$, $\dot{E}^{p}_{KL}$, $\theta$ and should be in the range of:

$0 \leqq c \leqq 1$ for the work-hardening process,

$-1 \leqq c \leqq 0$ for the work-softening process.

Comparing eqs. (3.3.34) and (3.4.1), we can easily derive:

$$c\dot{T}_{KL} = \rho_o \frac{\partial\psi}{\partial E^{p}_{KL}} + \rho_o \beta \frac{\partial\psi}{\partial \dot{E}^{p}_{KL}} \tag{3.4.2}$$

Therefore we get the constitutive equations for rate dependent elastic-plastic material as follows:

$$T_{KL} = \rho_o \frac{\partial\psi}{\partial E^{e}_{KL}} + \rho_o \alpha \frac{\partial\psi}{\partial \dot{E}^{e}_{KL}} \tag{3.4.3}$$

$$\dot{T} = \frac{\rho_o}{c}\left\{\frac{\partial\psi}{\partial E^{p}_{KL}} + \beta\frac{\partial\psi}{\partial \dot{E}^{p}_{KL}}\right\} \tag{3.4.4}$$

For convenience sake, $T_{KL}$ and $\dot{T}_{KL}$ are devided into two parts:

$$T_{KL} = T_{(1)KL} + T_{(2)KL} \tag{3.4.5-a}$$

where

$$T_{(1)KL} = \rho_o \frac{\partial\psi}{\partial E^{e}_{KL}} \tag{3.4.5-b}$$

$$T_{(2)KL} = \rho_o \alpha \frac{\partial\psi}{\partial \dot{E}^{e}_{KL}} \tag{3.4.5-c}$$

$$\dot{T}_{KL} = \dot{T}_{(1)KL} + \dot{T}_{(2)KL} \tag{3.4.6-a}$$

where

$$\dot{T}_{(1)KL} = \frac{\rho_o}{c}\frac{\partial\psi}{\partial E^p_{KL}} \tag{3.4.6-b}$$

$$\dot{T}_{(2)KL} = \frac{\rho_o\beta}{c}\frac{\partial\psi}{\partial \dot{E}^p_{KL}} \tag{3.4.6-c}$$

It is note worthy that even in the constant strain rates process in which the coefficient $\alpha$ and $\beta$ equal to zero, $T_{KL}$ and $\dot{T}_{KL}$ are rate dependent, because the free energy $\psi$ is the function of the strain rate and therefore $T_{(1)KL}$ and $\dot{T}_{(1)KL}$ are also rate dependent. Eqs. (3.4.5-b,c) and (3.4.6-b,c) show that $T_{(1)KL}$, $T_{(2)KL}$ and $\dot{T}_{(1)KL}$, $\dot{T}_{(2)KL}$ are nothing else but the gradients of the free energy $\psi$ in the strain space and in the strain rate space respectively. Therefore we can conclude that $T_{(1)KL}$ and $\dot{T}_{(1)KL}$ are directed normal to the $\psi$-constant contours respectively in $E^e_{KL}$ and $E^p_{KL}$ space and that $T_{(2)KL}$ and $\dot{T}_{(2)KL}$ are also directed normal to the $\psi$-constant contours in the $\dot{E}^e_{KL}$ space and the $\dot{E}^p_{KL}$ space respectively. These relations can be called the normality in the strain space and in the strain rate space.

Now let us add another restrictions to our consideration, i.e. constant strain rate deformation in which the coefficients $\alpha$ and $\beta$ are selected to be zero. In such a constant elastic and plastic strain rate deformation, the stress $T_{KL}$ and $\dot{T}_{KL}$ are identical to $T_{(1)KL}$ and $\dot{T}_{(1)KL}$. Assuming this constant elastic and plastic strain rate deformation process ABCD as shown in Fig. 3.3, we can find that $T_{(1)KL}$ is completely identical at the stage A and D:

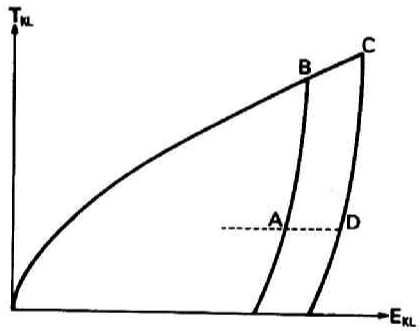


Fig.3.3 Loading cycle ABCD

$$(T_{(1)KL})_A = (\rho_o \frac{\partial\psi}{\partial E^e_{KL}})_A = (\rho_o \frac{\partial\psi}{\partial E^e_{KL}})_D = (T_{(1)KL})_D$$

At point A and D, the elastic strain is same:

$$(E^e_{KL})_A = (E^e_{KL})_D$$

then, we can conclude that $\frac{\partial\psi}{\partial E^e_{KL}}$ is independent of $E^p_{KL}$ and $\dot{E}^p_{KL}$, i.e.:

$$\psi(E^e_{KL}, E^p_{KL}, \dot{E}^e_{KL}, \dot{E}^p_{KL}, \theta)$$
$$= \psi^e(E^e_{KL}, \dot{E}^e_{KL}, \theta) + \psi^p(E^p_{KL}, \dot{E}^p_{KL}, \theta) \qquad (3.4.7)$$

On the process from B to C in Fig. 3.3, plastic strain rate $\dot{E}$ caused by the stress increment $\dot{T}_{KL}$ which is given by

$$\dot{T}_{KL} = (\frac{\rho_o}{c} \frac{\partial\psi^p}{\partial E^p_{KL}})_C$$

as shown in Fig. 3.4. The elastic strain rate $\dot{E}^e_{KL}$ increases as shown in Fig. 3.5 and the applied stress $T_{KL}$ at the stage C is given by

$$T_{KL} = (\rho_o \frac{\partial\psi^e}{\partial E^e_{KL}})_C$$

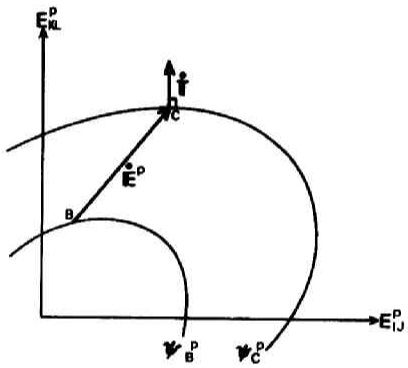


Fig.3.4. Plastic component of free energy

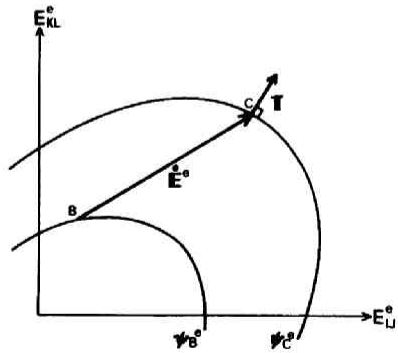


Fig.3.5. Elastic component of free energy

## 3.5 Normality Rule in the Stress Space

Here we confine our discussion in the case of constant temperature and constant elastic and plastic strain rate in which only $T_{(1)KL}$, $\dot{T}_{(1)KL}$ are dealt. Under such a condition $\dot{\psi}^e$ is given as follows:

$$\dot{\psi}^e = \frac{\partial \psi^e}{\partial E^e_{KL}} \dot{E}^e_{KL} \tag{3.5.1}$$

because

$$\dot{\theta} = \dot{E}^e_{KL} = 0.$$

Combining eqs. (3.4.5), (3.4.7) and (3.5.1), we get:

$$\rho_o \dot{\psi}^e = T_{KL} \dot{E}^e_{KL} \tag{3.5.2}$$

By means of the same manner, we get $\dot{\psi}^p$ as follows:

$$\dot{\psi}^p = \frac{\partial \psi^p}{\partial E^p_{KL}} \dot{E}^p_{KL} \tag{3.5.3}$$

From eqs. (3.4.6-b), (3.4.7) and (3.5.3), the following relation is derived:

$$\rho_o \dot{\psi}^p = c\dot{T}_{KL} \dot{E}^p_{KL} \tag{3.5.4}$$

Now let us consider the complementary elastic free energy $\psi^e$ for the elastic free energy $\psi^{e*}$ as shown in Fig. 3.6. We can easily get the following equation:

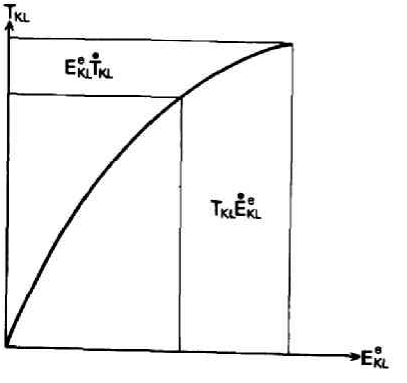


Fig.3.6. Stress-elastic strain relation

$$\rho_o \dot{\psi}^{e*} = E^e_{KL} \dot{T}_{KL} \tag{3.5.5}$$

It follows:

$$E^e_{KL} = \rho_o \frac{\partial \psi^{e*}}{\partial T_{KL}} \tag{3.5.6}$$

In the same manner, we consider to complementary plastic free free energy $\psi^{p*}$ for $\psi^p$ as shown in Fig. 3.7 and we get:

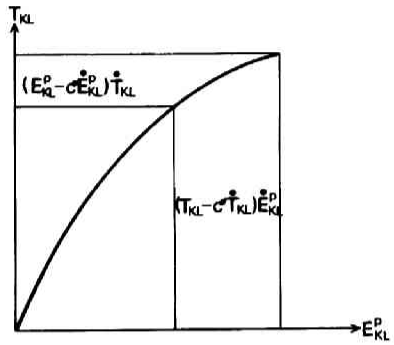


Fig.3.7. Stress-plastic strain relation

$$\rho_o \dot{\psi}^{p*} = c^* \dot{E}^p_{KL} \dot{T}_{KL} \tag{3.5.7}$$

where $c^* = 1 - c$ and then, we get:

$$\dot{E}^p_{KL} = \frac{\rho_o}{c^*} \frac{\partial \psi^{p*}}{\partial T_{KL}} \tag{3.5.8}$$

Eqs. (3.5.6) and (3.5.8) are very familiar to us in the field of elasticity and plasticity. Eq. (3.5.8) is nothing else but the normality rule in plasticity and shows that, under the constant temperature and constant elastic and plastic strain rate, the normality rule are applicable for the apparent yield surface which is the function of temperature and strain rate.

## 3.6 Conclusions

In order to give the physical interpretations to flow rule in plasticity from the viewpoint of thermodynamics, some considerations are made in this chapter. Based on newly proposed definitions of reversible and irreversible deformation, thermodynamical constitutive

relations for rate dependent irreversible process are constructed. By means of physical interpretation of the derived thermodynamical restrictions, normality rule in the strain space is reasoned out. And then the so called normality rule for rate dependent plastic materials in the stress space is obtained under some restrictions. It can be concluded that the plastic potential represented in terms of strain and strain rate has much broader physical meaning than those in terms of stress and stress rate. But by the investigations presented in this chapter, the use of normality flow rule in the following chapters is rationalized to some extent.

The investigations given in this chapter were not achieved to the present stage unless the cooperation of Prof. T. Adachi. It should be noted that the definitions of reversible and irrrversible deformation are of his original idea.

# CHAPTER 4

# CONSTITUTIVE RELATIONS FOR ISOTROPICALLY CONSOLIDATED SOILS

## 4.1 Introduction

Many engineering problems in respect to the stability of soil structures have been practically treated with the assumption that soils were rigid-plastic materials. This simple assumption and the subsequent simple analysis were very convenient to design soil structures upon or under complicated subgrade. This analysis is based on the following conditions;

(a) the equilibrium condition of mass

(b) the failure condition of a soil element (ordinarily Mohr-Coulomb failure condition is used)

and places no restrictions on the deformation of mass. Therefore it is the inherent defect that this analysis is useless for the practical problems with respect to the deformation of soil structures. For such problems the analyses based upon stress-strain relation of soils are necessary. One of them is elasticity. Elasticity is used very often to solve the stress or strain in the soil mass under loading, but it is not so reliable because of its assumptions that are not appropriate to mechanical properties of soils under shear. A new analysis based upon the stress-strain relation adequate to soils is necessary.

It might be more easy to establish a theoretical system of mechanical behaviors of soils including stress-strain relation to detect entire shearing process than to concentrate our attention on the failure point whose definition is physically quite vague. Strength properties are the limited part of mechanical properties of clays under shear.

One of the most reasonable approaches to stress-strain relation of clays is to consider the clays as the work-hardening materials. Incremental stress-strain relation for work-hardening (stable) materials with convex yield surfaces are explained by Drucker (1951).

But the concept of yield surface and normality are not necessarily applied to clays. Because it is still unknown whether the assumptions on which the theory is based are satisfied by clays. Many difficulties arising from the path dependent behaviors should be overcome before practically useful stress-strain relations of clays are found out. Some people tried to propose the reasonable yield surface of clays. Drucker, Gibson and Henkel (1957) proposed cone shaped yield surface with spherical cap for normally and over consolidated clays. The proposed yield surface itself could not thoroughly explain the plastic deformation of clays, but had eminent influence upon the following researches for stress-strain relation of soils.

Roscoe, Schofield and Wroth (1958) studied the state boundary surface (yield surface). In their theory, the concept of critical state line (critical void ratio line) played the important role. Roscoe, Schofield and Thurairajah (1963) developed the energy theory combining the concepts of normality. critical state, state boundary surface and yield locus suggested by Calladine (1963) in the discussion to Roscoe and Poorooshasb (1963) who gave the relation between strains for the undrained shear test and for the anisotropic consolidation. Roscoe, Schofield and Thurairajah (1963) have also derived the incremental stress-strain relations for normally consolidated clays by means of Drucker's postulate (1959) of the incremental stress-plastic strain relations for stable materials with convex yield loci. Palmer (1967) proposed a new energy theory for clays. Schofield and Wroth (1968) derived the stress-strain relations, based on the energy theory. for the idealized soils, Granta gravel and Cam clay. An empirical strain equation was proposed for sands by Wroth and Bassett (1965) and for normally consolidated clays under undrained shear by Wroth (1965). Wroth's stress-strain relation coincides with that given by Schofield and Wroth (1968). Roscoe and Burland (1968) presented the generalized stress-strain relations for "wet" clay based on the modified energy theory proposed

by Burland (1965). Chaplin (1969) proposed another type of stress-strain relations.

The subject of this chapter is to show the state surface and swelling wall (the assemblage of state paths of the soils which had been consolidated with the same hydrostatic pressure) and to derive the stress-strain relations for the idealized isotropically consolidated soils stressed under various conditions with a rather slow strain rate.

After deriving them, the author found that some of the results of this chapter had already been given by Schofield and Wroth (1968) in spite of the quite different, at least apparently, basic assumptions. Of course, there are some differences, in detail, arising from the different basic assumptions, but they are not essential. It is likely that the rate of dissipated energy during shear depends not only on the distortional strain increment but also on the volumetric strain increment. From this viewpoint, it seems that the modified energy theory proposed by Burland (1965), Roscoe and Burland (1968) is more appropriate than the original energy theory given by Roscoe, Schofield and Thurairajah (1963). Schofield and Wroth (1968). But the results of our study support, on the contrary, the derivatives from the original energy theory. Whether or not the coincidence of the results of our study and the original energy theory is merely fortuitous will be clarified later.

These theories mentioned above do not deal with the "elastic" component of distortional strain. Murayama (1968), (1969) constructed a general theory on stress-strain relations by developing his preceding theory (1964) for sands in the elastic state. General stress-strain relations derived from Murayama's theory belong to the so-called hyperbolic type initially proposed by Kondner (1963) and Kondner and Zelasko (1963), to whom Hansen (1963) proposed three types of stress-strain relations.

## 4.2 State Surface and Swelling Wall

### 1. Definition of Mechanical State of Clays

In this chapter the word "stress" means the "effective stress". Effective stress is the macroscopic conventional concept, and is not equal to the interparticle stress. Therefore effective stress is not suitable to discuss the microscopic mechanics of clay skelton under shear. Then our following discussion on the mechanical behaviors of clays has limited accuracy.

Many physical components come forward as the candidates for the essential variables (*state parameters*) expressing the mechanical state of clays. Most popular candidates are the three of shear stress $\tau$ and normal stress $\sigma'$ applied on the potential failure plane and void ratio $e$. These three state parameters were used by Hvorslev (1960). In spite of many experimental studies on the mechanical characteristics of soils concerning the effects of these components, no theory or hypothesis can explain these effects systematically with adjustment, because these effects are too complex to analyse. Therefore, it is necessary to reduce the number of parameters defining the mechanical state of a soil element. One of the most radical questions in soil mechanics might be the selection of these parameters. Generally speaking, at least stress, strain, time and temperature should be included in these parameters. In other words, the mechanical state of a soil element might be represented as a point on a surface given by the constitutive equation in the space defined by stress, strain, time and temperature. The effects of other physical components are represented by some soil constants.

An important problem following the selection of these parameters is how to mathematically represent the mechanical behavior (i.e. the transient process of the mechanical state) of a soil element. The mechanical behavior of soils has been studied from various viewpoints for instance, shear strength, deformation, rheological properties,

consolidation, microscopic structure of the soil skeleton and so on. At the present stage, the available information from these studies seems to be miscellaneous. To represent these various aspects of the mechanical behavior of soils with mathematical idealization, it is necessary to find the most convenient point of view in order to keep the logical consistency through the representation. This problem is, in the figurative sense, similar to the selection of the most proper reference frame to represent a geometrically complex body. Here the mechanical state of clays are expressed by the points in ($\tau_{oct}$, $\sigma_m$, $e$) space. These points are called "*state points*" and this space is called "*state space*". It might not be sufficient to define the mechanical state of clays by these three components, but this set of physical components is one of the most convenient set to define the mechanical state of clays. A transition of the mechanical state of a clay element is shown by a locus of the state point. This locus is called "*state path*" It will be shown later that a rule governing the movement of state points does exist. All state points should move in the state space under the rule described later with the change of conditions.

2. Time and Path Dependent Behaviors of Clays

The deformation of clays (both isotropic and distortional deformation) causes the rearrangement of the structure of clay skelton. The deformation of clays means that the structure of skelton constructed of clay particles changes to keep equilibrium. The necessary duration for this rearrangement of clay skelton induced by the external agency is considerable. The experimental studies on consolidation and creep or relaxation show the existence of this time lag. We must not ignore the fact that this time lag is considerably long. The interval of loading in conventional stress controlled tests and strain rate in conventional strain controlled tests are decided unreasonably. In this chapter only experimental data with sufficient duration for rearrangement of clay skelton are interesting, because in such a case clay can be considered as a

elastic-plastic material with hardening effect.

The mechanical behavior of clay (for instance, state path) is governed by the rearrangement of clay skelton caused by the external agency, and then depends not only on the present state but also on the stress history. The clays whose pre-consolidation pressures are same behave variously with various overconsolidation ratio. Fig.4.1 shows

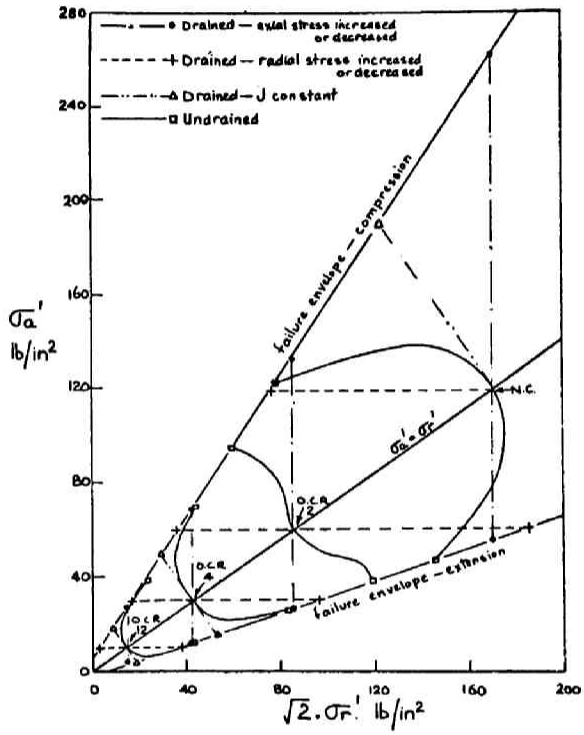


Fig.4.1. Effects of stress history (after Henkel)

an example of such a history dependent behavior of clay given by Henkel (1959). A theory on mechanical behavior of clay should be adaptable not only to normally consolidated clays but also to over-consolidated clays.

Path dependent behavior mentioned above is the mechanical behavior of clay depending on stress history. It is noteworthy that there exist another sort of path dependent behavior of clay. This is the mechanical behavior of clay depending on strain history. The mechanical behavior of a normally consolidated clay under shear with smoothly and monotonously increasing shear strain differ from that of

the same normally consolidated clay under shear with cyclic increasing and decreasing shear strain. This path dependent behavior relating to strain is shown experimentally by Murayama and Kurihara (1968) and Sangrey, Henkel and Esrig (1969). The physical meaning of stress history is quite equivalent to that of strain history in a stable clays, but not in an unstable clays, for instance, heavily overconsolidated clays, because in the latter case the shear strain increases while the shear stress decreases.

Here only the mechanical behaviors of clays under shear with smoothly and monotonously increasing shear strain are interesting.

3. Volume Change of Clays

It is convenient to consider the volume change of clays to be consisting of two components; consolidation and dilatancy component of volume change. On the consolidation volume change of clays, there is well ascertained experimental law; $e$-log$\sigma'_m$ linear relation for normally consolidated clays. Fig.4.2 is the typical $w$-log$\sigma'_m$ relation for normally and overconsolidated clays given by Henkel (1956). The linearity between $e$ and log$\sigma'_m$ for swelling curve and reloading curve is not recognized in strict sense, but is acceptable approximation.

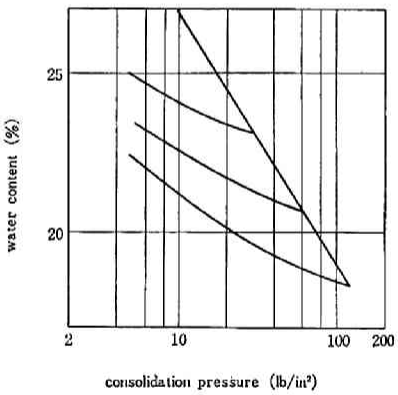


Fig.4.2. $w$-log$\sigma'_m$ relations (after Henkel)

The $e$-log$\sigma'_m$ linear relation is represented by the following equation:

$$e=e_0-C\ln\frac{\sigma'_m}{\sigma'_{m0}} \qquad (4.2.1)$$

where the coefficient $C$ equals to $\lambda$ and $\kappa$ for normal consolidation curve and swelling curve respectively. The point ($\sigma'_{m0}$, $e_0$)

is an arbitrary point on the normal consolidation curve as shown in Fig.4.3. The coefficient $\kappa$ is not necessarily a constant for a clay, but a variable depending on the consolidation pressure applied to the clay before swelling. The coefficient $C$ in the anisotropic consolidation is also equal to $\lambda$ for normally consolidated clays.

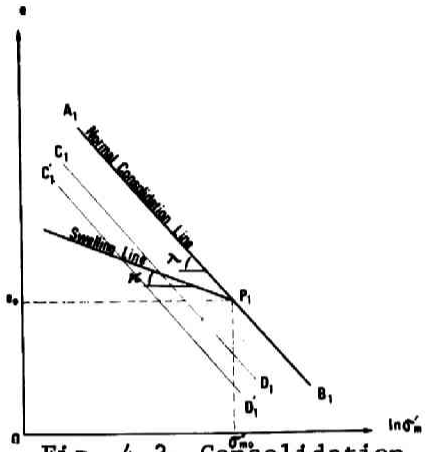


Fig. 4.3. Consolidation characteristics

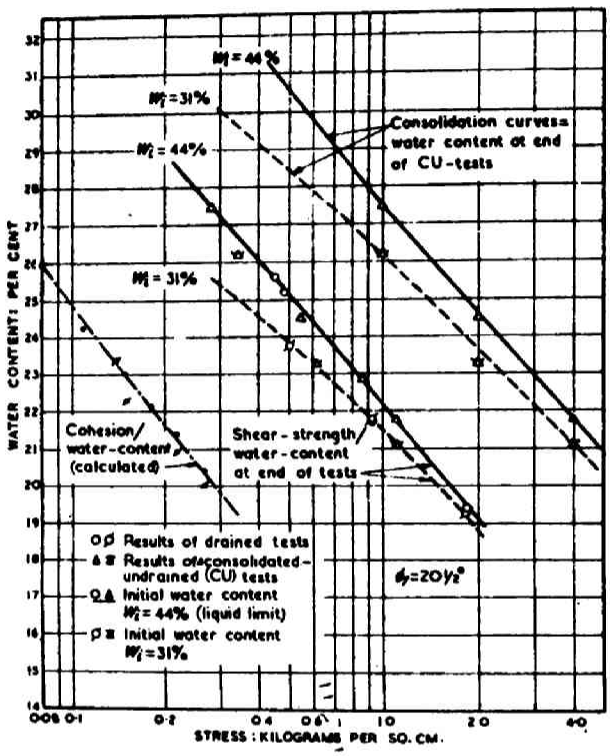


Fig.4.4. $(w)_f$-$(\log\sigma'_m)$ relations (after Bjerrum)

Bjerrum (1951) showed that the failure points ploted on $(e)_f$-$(\ln\sigma'_m)_f$ diagram are also represented by eq.(4.2.1), and the coefficient $C$ equals to $\lambda$ for normally consolidated clays as shown in Fig.4.4. The stress ratio $\tau_{oct}/\sigma'_m$ in anisotropic consolidation or at failure is constant judging from the experimental data up to date. These facts suggest that $e$-$\ln\sigma'_m$ linearity under the condition of $\tau_{oct}/\sigma'_m$: constant is one of the fundamental properties of clays.

The void ratio change on the consolidation process ($\tau_{oct}/\sigma'_m$ - constant) represented in the $e$-$\sigma'_m$ diagram is given in Fig.4.5. Normal consolidation line is a sort of stress-deformation curve on

the loading process and swelling curve is that on the unloading and reloading process. Therefore whereas the swelling process induces only the reversible void ratio change, the normal consolidation process induces not only the reversible void ratio change but also the irreversible void ratio change. This means that the swelling line shows the elastic process and the normal consolidation process shows the elastic-plastic process.

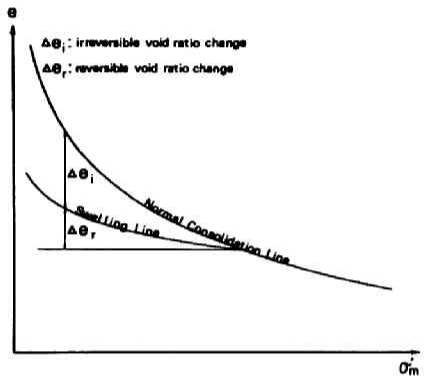


Fig.4.5. Normal consolidation and swelling

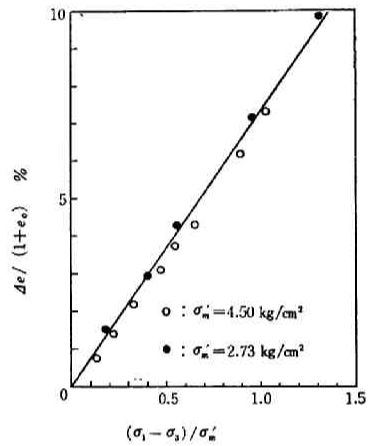


Fig.4.6. Dilatancy of normally consolidated clay (after Shibata)

Differentiating eq.(4.2.1):

$$de=-\lambda\frac{d\sigma'_m}{\sigma'_m} \quad : \quad \text{elastic-plastic state} \tag{4.2.2}$$

$$de=-\kappa\frac{d\sigma'_m}{\sigma'_m} \quad : \quad \text{elastic state} \tag{4.2.3}$$

are obtained while the stress ratio $\tau_{oct}/\sigma'_m$ is kept constant.

Shibata (1963) gave the relationship between applied stresses and volume change accompanied with distortional deformation by means of drained tests of normally consolidated clays keeping $\sigma'_m$ constant

as shown in Fig.4.6. Karube and Kurihara (1966) made further discussion on dilatancy. From the works carried by Shibata, Karube and Kurihara, volume change accompanied with distortional deformation is given by the following equation:

$$\frac{\Delta e}{1+e_0} = -\mu\Delta\left(\frac{\tau_{oct}}{\sigma_m'} - k_1\right) \tag{4.2.4}$$

where the coefficient $\mu$ is a constant for normally consolidated clay, and the symbol $\Delta$ means the total change. Until the magnitude of the ratio of applied octahedral shear stress $\tau_{oct}$ to effective mean stress $\sigma_m'$ exceeds the constant $k_1$, dilatancy does not take place. As shown later, the interpretation of the data given by Richardson and Whitman (1963) tells that the non-dilatant stress ratio $k_1$ is a increasing function of strain rate. Using their words, *the behavior at the fast strain-rate may be characterized by saying that the specimens "hung together" to larger strains, and thus developed more shear resistance*. And $k_1$ might be essentially zero when the shearing speed is thoroughly slow so that the rearrangement of soil skelton can occur completely.

Eq.(4.2.4) is based on the experimental facts in drained tests keeping $\sigma_m'$ constant or in undrained tests of normally consolidated clays with the suitable interpretation. Then it is not guaranteed directly by experiments that eq.(4.2.4) is able to represent dilatancy when $\sigma_m'$ increases in the process of shearing. This problem will be discussed later with drained test data.

From eq.(4.2.4) it is apparent that $\tau_{oct}/\sigma_m'$ -constant means that the volume change of dilatancy does not take place. In the case of $k_1$=0, the loading and unloading processes of dilatancy ($\sigma_m'$-constant) can be represented as Fig.4.7. Here the reversible void ratio change is assumed to be negligiblly small. Then, differentiating eq.(4.2.4), we get:

$$de=\mu(1+e_0)\left(-\frac{d\tau_{oct}}{\sigma_m'} + \frac{\tau_{oct}}{\sigma_m'}\frac{d\sigma_m'}{\sigma_m'}\right) \quad \text{: elastic-plastic state} \tag{4.2.5}$$

$de \fallingdotseq 0$ : elastic state (4.2.6)

Eqs. (4.2.5) and (4.2.6) mean that the dilatancy process is purely plastic.

General stress state of clay under shear consists of two components; one is the hydrostatic component and the other is deviatoric component. Therefore the volume change of clays under general stress state includes consolidation and dilatancy. But consolidation and dilatancy are not necessarily independent of each other on the shearing process, and then the volume change of a clay might not equal to the simple summation of consolidation and dilatancy independent from each other.

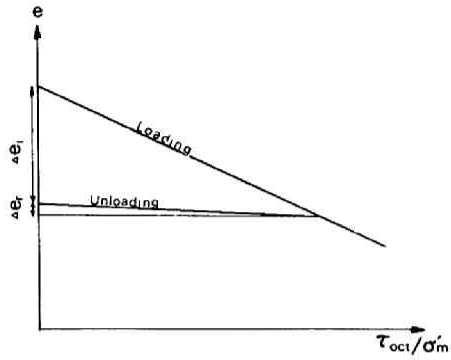


Fig.4.7. Dilatancy characteristics

However the infinitesimal volume change induced by the infinitesimal stress change may be equal to the summation of infinitesimal consolidation and infinitesimal dilatancy, neglecting the second order coupling effect of consolidation and dilatancy. Based on these consideration, the infinitesimal void ratio change of clay is to be derived by summing up eqs.(4.2.2) and (4.2.5) for the clay in elastic-plastic state and eqs.(4.2.3) and (4.2.6) for the clay in elastic state as follows:

$$de=-\lambda\frac{d\sigma'_m}{\sigma'_m}+(1+e_0)\mu\left(\frac{\tau_{oct}}{\sigma'_m}\frac{d\sigma'_m}{\sigma'_m}-\frac{d\tau_{oct}}{\sigma'_m}\right)$$

: elastic-plastic state (4.2.7)

$$de=-\kappa\frac{d\sigma'_m}{\sigma'_m}$$ : elastic state (4.2.8)

Eqs.(4.2.7) and (4.2.8) are the approximate equations which the state parameters $\tau_{oct}$, $\sigma'_m$, $e$ of a stressed clay should satisfy. Eqs. (4.2.7) and (4.2.8) may be altered judging from the more reliable

experimental data and more general theoretical consideration in future.

4. State Surface and Swelling Wall

The surface in the state space given by the solution of eq. (4.2.7) is named the "*state surface*" which is a similar concept of "*state boundary surface*" defined by Roscoe, *et al.* (1958,1963).

As mentioned above, the state point of clay in elastic-plastic state under any stress state must be on the state surface. Let us consider a normally irotropically consolidated clay specimen with the pressure of $\sigma'_{m0}$. The void ratio of this specimen is $e_0$. Then, the state point of this specimen is on the normal consolidation curve lying on the $\tau_{oct}=0$ plane in state space. Some sorts of additional stress system, for instance, the undrained shear or triaxial drained compression, necessarily bring the irreversible deformation to the specimen. This well-known experimental fact shows that the initial state point ($\tau_{oct}=0$, $\sigma'_m=\sigma'_{m0}$, $e=e_0$) of isotropically normally consolidated clay belongs to the state surface before the application of additional external agency.

The solution of eq.(4.2.7) is derived as follows with the boundary condition that the state point ($\tau_{oct}=0$, $\sigma'_m=\sigma'_{m0}$, $e=e_0$) is on the state surface given by the solution:

$$e-e_0+\lambda \ln\frac{\sigma'_m}{\sigma'_{m0}}+(1+e_0)\mu\frac{\tau_{oct}}{\sigma'_m}=0 \qquad (4.2.9)$$

Fig.4.8 is the isometric view of state surface for clays. CZD is the critical state line defined later. APB is the normal consolidation curve and the state point P is represented as ($\tau_{oct}=0$, $\sigma'_m=\sigma'_{m0}$, $e=e_0$). On the other hand, the state point of clay in elastic state must be on a surface given by eq.(4.2.8). This surface is named *swelling wall*. Swelling wall is a similar concept of *elastic wall* or *elastic surface* defined by Roscoe, *et al.*(1963). Now let us consider the normally isotropically consolidated clay specimen again. If the applied effective hydrostatic pressure is

reduced from the initial value of $\sigma'_{m0}$, the specimen swells elastically. Then we can easily conclude that the initial state point ($\tau_{oct}=0$, $\sigma'_m=\sigma'_{m0}$, $e=e_0$) is also on the swelling wall. Solving eq.(4.2.8) with such a boundary condition, we get:

$$e-e_0+\kappa\ln\frac{\sigma'_m}{\sigma'_{m0}}=0 \qquad (4.2.10)$$

Swelling wall given by eq.(4.2.10) is independent of the value of $\tau_{oct}$, and therefore is a wall like surface standing normally on the $\tau_{oct}=0$ plane as shown in Fig.4.8.

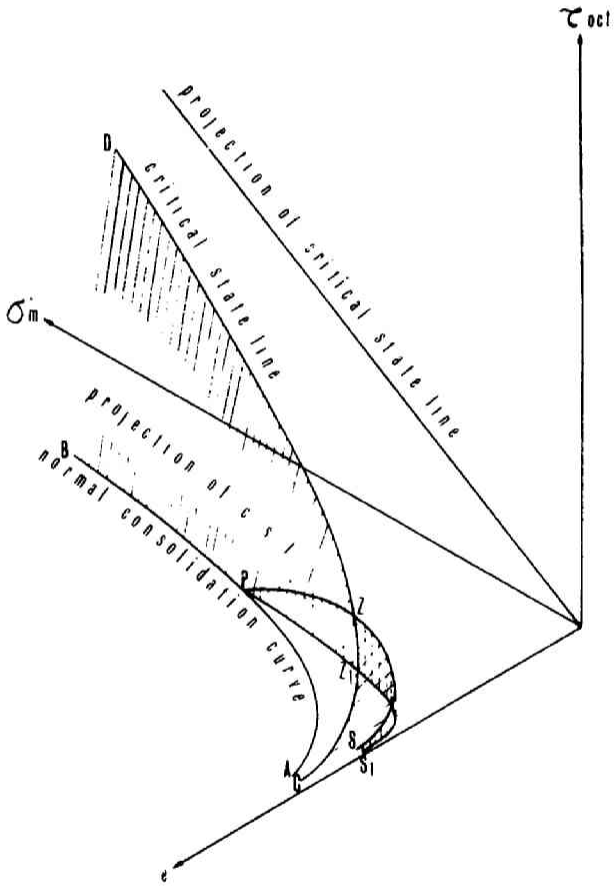


Fig.4.8. State surface and swelling wall of isotropically consolidated clay

$PZ_1S_1$ on the $\tau_{oct}=0$ plane is the swelling curve and the vertical wall on the swelling curve $S_1Z_1PZS$ is the "swelling wall". PZS is on the state surface, and the swelling curve $PZ_1S_1$ is under the state surface. The state surface should be limited by $e=e_{max}$ plane and $e=e_{min}$ plane.

When the clay specimen normally consolidated with the pressure of $\sigma'_{m0}$ is allowed to suck the water by reducing the confining pressure, its state point will move from the original point P in Fig.4.8 to the point on the swelling line $PZ_1S_1$ depending on the amount of reduced pressure. Such a clay is called to be in the overconsolidated state. Overconsolidation ratio (the ratio of the maximum pre-consolidation pressure $\sigma'_{m0}$ to the confining pressure $\sigma'_m$ after the reduction of consolidation pressure) gives the extent of overconsolidation of the specimen. Then the mechanical states of overconsolidated clay specimens (including the normally consolidated specimen as a special case of O.C.R.=1) whose maximum pre-consolidation pressure are $\sigma'_{m0}$ are represented by the state points on the swelling line $PZ_1S_1$ before the application of shear stress. Here these state points are called the initial state points.

Generally speaking, the stressed clay is in the elastic state under the stress state within the yield surface. But further increasing shear stress makes the clay yield and be in the elastic-plastic state accompanied by the work-hardening or work-softening effects, and finally makes the clay be in the perfectly plastic state, which is called the critical state by Roscoe *et al.*

In the perfectly plastic state, the shear strain in the clay specimen increases infinitely in spite of the unchanging stress state. Since the state point of the clay in elastic-plastic state should be on the state surface, the state point of the clay in perfectly plastic state (a special state of elastic-plastic state) must also be on the state surface. The state points representing the perfectly plastic state shape a curve on the state surface shown in Fig.4.8 as the critical state line. The curve PZS is called elastic limit curve

because it shows the boundary between the elastic state and elastic-plastic state.

Now, according to the definition by Roscoe, Schofield and Thurairajah (1963), we call the clay whose state point at its initial yielding is on the part PZ of the elastic limit curve in Fig.4.8 to be wetter than critical and the clay whose state point at its initial yielding is on the part ZS of the elastic limit curve in Fig.4.8 to be drier than critical. Fig.4.8 shows that the state points of elastic-plastic clays wetter than critical should be on the part BPZD of the state surface and those of elastic-plastic clays drier than critical should be on the part CZS of the state surface. From these considerations, it can be easily concluded that the elastic-plastic clays wetter and drier than critical are respectively the work-hardening and work-softening materials.

Fig.4.9 is the isometric view of state surface for clays pre-consolidated with the pressure of $\sigma'_{m0}$=1kg/cm$^2$. The state paths starting from the initial state points on the swelling line with the increasing shearing strain creep the swelling wall and then creep over the state surface, and they cannot enter the domain under the state surface but on the swelling wall. The critical state line does not allow the state paths to cross it. Then the state paths starting from the initial state points on $PZ_1$ with the increasing strain can be on the swelling wall $PZZ_1$ or on the state surface BPZXYW, and those starting from the initial state

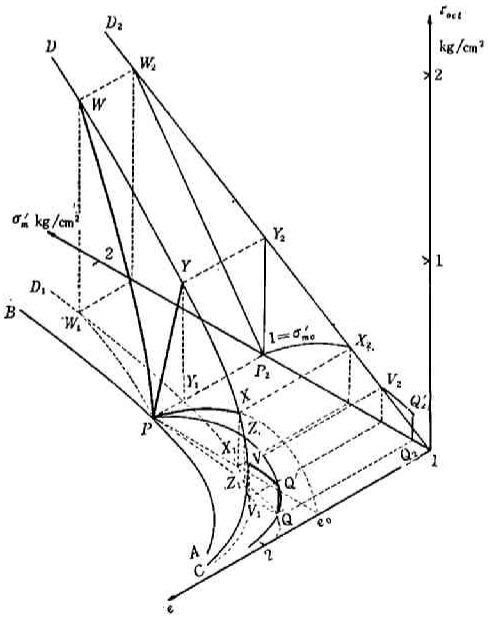


Fig.4.9. State surface and state paths

points on $Z_1Q$ can be on the swelling wall $Q'ZZ_1Q$ or on the state surface $Q'ZVC$. PW, PY, PX, $QQ'V$ are cited as instances of the state paths. When the restraint of increasing shearing strain is eliminated, for instance, loading and unloading cyclic shear, the state paths can enter the domain under the state surface as mentioned by Murayama and Kurihara (1968).

If $e$=constant, the following equation is derived from eq.(4.2.9):

$$\lim_{\sigma'_m \to 0} \tau_{oct} = \lim_{\sigma'_m \to 0} \frac{\sigma'_m}{(1+e_0)\mu}\left(e_0 - e - \ln\frac{\sigma'_m}{\sigma'_{m0}}\right) = 0 \qquad (4.2.10)$$

Eq.(4.2.10) means that $e$-axis is contained within the state surface. The fact that eq.(4.2.9) consists of consolidation term and dilatancy term suggests that consolidation and dilatancy may be essentially independent phenomena.

## 4.3 State Paths under Various Conditions

### 1. Undrained Shear

The state paths of clays whose initial state points are on the swelling curve including normally consolidated state point ($\tau_{oct}=0$, $\sigma'_m=\sigma'_{m0}$, $e=e_0$) creep the swelling wall and creep over the state surface.

When a saturated clay was sheared under undrained condition, void ratio $e$ is kept constant:

$$e=e_i \geqq e_0 \qquad (4.3.1)$$

where:

$$e_i=e_0-\kappa\ln\frac{\sigma'_{mi}}{\sigma'_{m0}} \qquad (4.3.2)$$

Then the state path starting from the initial point ($\tau_{oct}=0$, $\sigma'_m=\sigma'_{mi}\leqq\sigma'_{m0}$, $e=e_i\geqq e_0$) is given by the intersection of the state surface or the swelling wall with the $e=e_i$ plane. The intersection of the state surface with the $e=e_i$ plane is given by substituting eqs.(4.3.1),(4.3.2) into eq.(4.2.9):

$$\tau_{oct}=-\frac{\sigma'_m}{(1+e_0)\mu}\left(\lambda\ln\frac{\sigma'_m}{\sigma'_{m0}} - \kappa\ln\frac{\sigma'_{mi}}{\sigma'_{m0}}\right) \qquad (4.3.3)$$

If the initial state is the normally consolidated state, $\sigma'_{mi}=\sigma'_{m0}$, and then eq.(4.3.3) is reduced to:

$$\tau_{oct}=-\frac{\lambda}{(1+e_0)\mu}\sigma'_m \ln\frac{\sigma'_m}{\sigma'_{m0}} \tag{4.3.4}$$

This is the same equation derived by Roscoe, Schofield and Thurairajah (1963) for normally consolidated clays. Hata and Ohta (1969) discussed on the stress paths of normally consolidated clays under undrained shear represented by eq.(4.3.4).

Fig.4.10 shows the stress paths (projections of state paths onto the stress space) of normally consolidated clays for various value of $\lambda/((1+e_0)\mu)$, under $e=e_0$ condition. The state paths represented by eqs.(4.3.3). (4.3.4) are shown in Fig.11. All these state paths pass through the $e$-axis. The state paths of overconsolidated clays under undrained shear consist of two parts: one is $\sigma'_m=\sigma'_{mi}$ line on the swelling wall, PR′ or $Z_1Z$ or QQ′ in Fig.4.11, and the other is the curve from R′ or Q′ to the critical state point U or V (mentioned later) along the intersection of the state surface with $e=e_i$ plane. The state point R′ or Z or Q′ in Fig.4.11 is represented by:

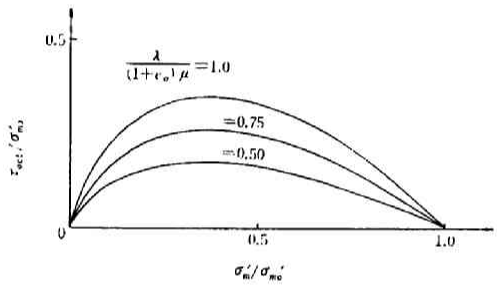


Fig.4.10. Undrained stress paths of normally consolidated clays

$$e=e_i, \qquad \sigma'_m=\sigma'_{mi}, \qquad \tau_{oct}=-\frac{\lambda-\kappa}{(1+e_0)\mu}\sigma'_{mi}\ln\frac{\sigma'_{mi}}{\sigma'_{m0}} \tag{4.3.5}$$

Fig.4.12 shows the stress paths of clays which have the same preconsolidation pressure $\sigma'_{m0}$. Fig.4.13 shows the stress paths of clays whose void ratios are the same of $e_i$.

2. Triaxial Drained Shear

When clays are sheared under drained condition, the stress state

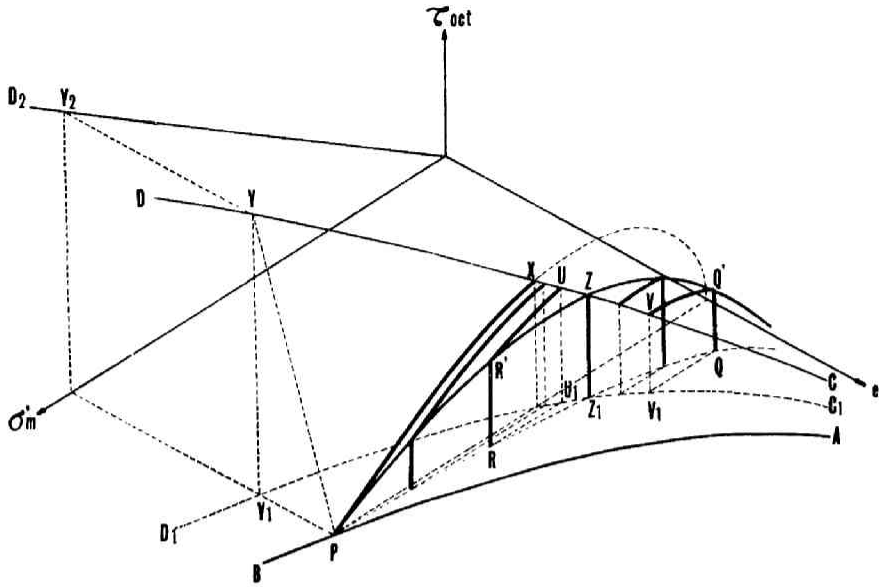


Fig.4.11. Undrained state paths

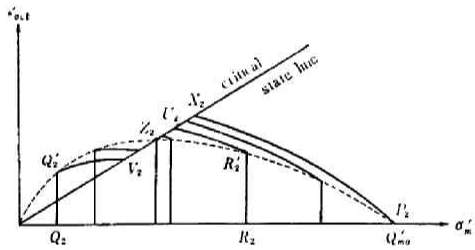


Fig.4.12. Undrained stress paths of the clays pre-consolidated with the same pressure of $\sigma'_m$

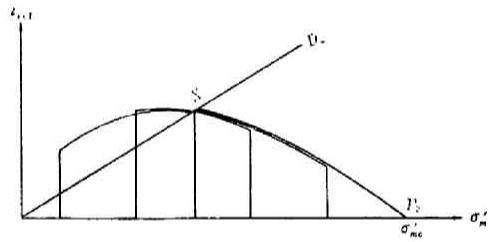

Fig.4.13. Undrained stress paths of the clays whose $e_i$ are identical

is defined directly as the applied stress state. In the conventional triaxial drianed tests, stress paths are represented by:

$$\tau_{oct}=\sqrt{2}(\sigma'_m-\sigma'_{mi}) \tag{4.3.6}$$

Then the state paths are given by substituting eq.(4.3.6) into eq. (4.2.9). For normally consolidated clays $\sigma'_{mi}=\sigma'_{m0}$, then the state

paths of conventional triaxial drained tests on normally consolidated clays are given by:

$$e=e_0-\lambda\ln\frac{\sigma'_m}{\sigma'_{m0}}-\sqrt{2}(1+e_0)\mu(1-\frac{\sigma'_{m0}}{\sigma'_m}) \qquad (4.3.7)$$

and eq.(4.3.6). Eq.(4.3.7) shows the projection of the state paths of normally consolidated clays under drained shear on $\tau_{oct}=0$ plane.

In Fig.4.14, the plane given by eq.(4.3.6) is $PWW_2P_2$, and the surface given by eq.(4.3.7) is $PWW_1$. Then the state paths of a normally consolidated clay under drained shear is given as the curve PW. The state paths of overconsolidated clays are shown as RHL and QKM. They consist of two parts; one is the intersection of the plane given by eq.(4.3.6) with the swelling wall, RH or QK and the other is the intersection of the plane given by eq.(4.3.6) with the state surface, HL or KM. The projection of HL or KM on $\tau_{oct}=0$ plane is given by:

$$e=e_0-\lambda\ln\frac{\sigma'_m}{\sigma'_{m0}}-\sqrt{2}(1+e_0)\mu(1-\frac{\sigma'_{mi}}{\sigma'_m}) \qquad (4.3.8)$$

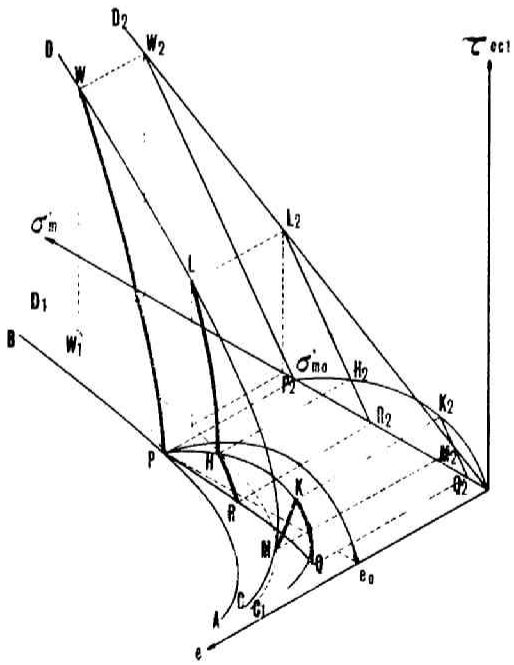


Fig.4.14. State paths in drained triaxial compression test

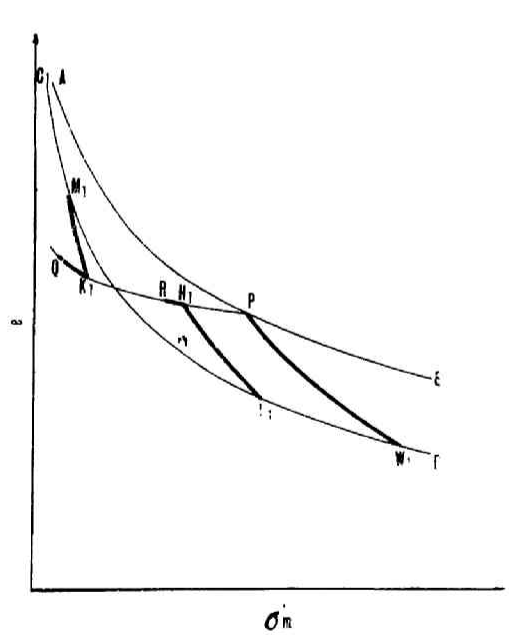


Fig.4.15. $e$-$\sigma'_m$ relations in drained triaxial compression test

the projections of these state paths on $\tau_{oct}=0$ plane are shown in Fig.4.15. Fig.4.15 reasons out the tendency of dilatancy of normally, slightly and heavily overconsolidated clays.

3. $\sigma'_m$-constant Shear

Substituting $\sigma'_m=\sigma'_{m0}$ into eq.(4.2.9), the term of consolidation is eliminated:

$$\tau_{oct}=-\frac{\sigma'_{m0}}{(1+e_0)\mu}(e-e_0) \tag{4.3.9}$$

Eq.(4.3.9) represents the projection of the state path of $\sigma'_m$- constant test on a normally consolidated clay on $\sigma'_m=0$ plane. Fig.4.16 shows this state path by PY as the intersection of the state surface with $\sigma'_m=\sigma'_{m0}$ plane. Substituting $\sigma'_m=\sigma'_{mi}\neq\sigma'_{m0}$ into eq.(4.2.9), $\sigma'_m=\sigma'_{mi}$-constant state paths are derived. $\sigma'_m$-constant state paths for overconsolidated clays are shown in Fig.4.16 as RR´S, $Z_1Z$, QQ´T.

The state paths on the state surface, R´S, Q´T are given by:

$$\tau_{oct}=-\frac{\sigma'_{mi}}{(1+e_0)\mu}\left(e-e_0+\lambda\ln\frac{\sigma'_{mi}}{\sigma'_{m0}}\right) \tag{4.3.10}$$

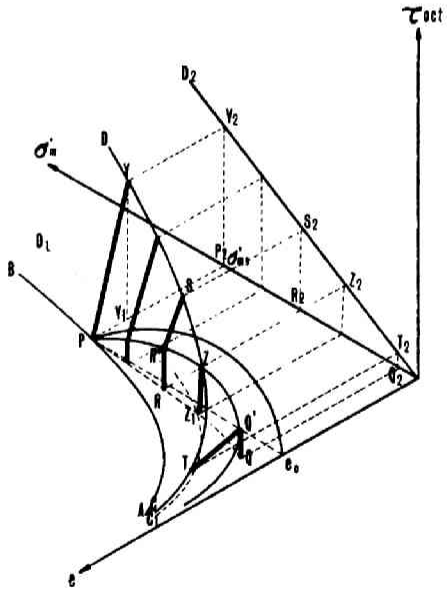

Fig.4.16. State paths in $\sigma'_m$-constant shear

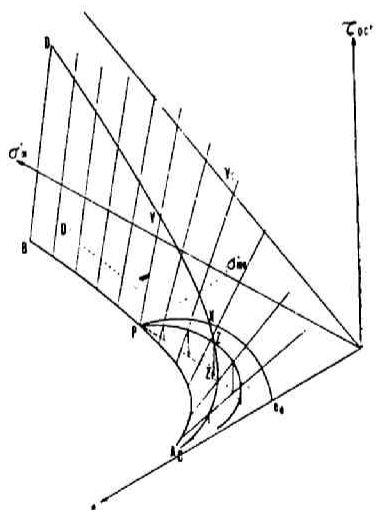

Fig.4.17 Construction of state surface

Eq.(4.3.10) shows that the intersections of the state paths with $\tau_{oct}=0$ plane are on the normal consolidation line which is given by:

$$e=e_0-\lambda \ln \frac{\sigma'_{mi}}{\sigma'_{m0}} \tag{4.3.11}$$

as shown in Fig.4.17. The obliquity of the state path is $-\sigma'_{mi}/((1+e_0)\mu)$. From these consideration, it is apparent that the state surface is the assemblage of inclined straight lines shown in Fig.4.17. At the stress state of $\sigma'_m=\sigma'_{mi}<\sigma'_{m0}$ state paths of overconsolidated clays climb up vetically along the swelling wall and then go straight ahead to the critical state line, along the inclined lines given by eq.(4.3.10).

When $\sigma'_{mi}=0$, the obliquity of the state path becomes zero and then it is apparent that $e$-axis is included in the state surface. Substituting $\sigma'_{mi}=0$ into eq.(4.3.11), $e$ becomes infinite and this does not seem to be supported by the experiments. But true $\sigma'_{mi}=0$ condition can hardly exist for clays then this problem should be discussed in future with more fundamental considerations. From the consideration of $e$-constant state paths and $\sigma'_m$-constant state paths, it is apparent that the mechanism of dilatancy of normally consolidated clays is essentially the same as that of overconsolidated clays. The difference of positive and negative dilatancy is derived from only the difference of the initial condition.

4. $\tau_{oct}/\sigma'_m$-constant Shear

Substituting $\tau_{oct}/\sigma'_m=k$ into eq.(4.2.9), straight lines parallel to the normal consolidation curve in $e$-$\ln\sigma'_m$ diagram are derived as follows:

$$e=-\lambda \ln \frac{\sigma'_m}{\sigma'_{m0}}+\{e_0+(1+e_0)\mu k\} \tag{4.3.12}$$

One of these lines shown in Fig.4.18 and Fig.4.19 shows the critical state line.

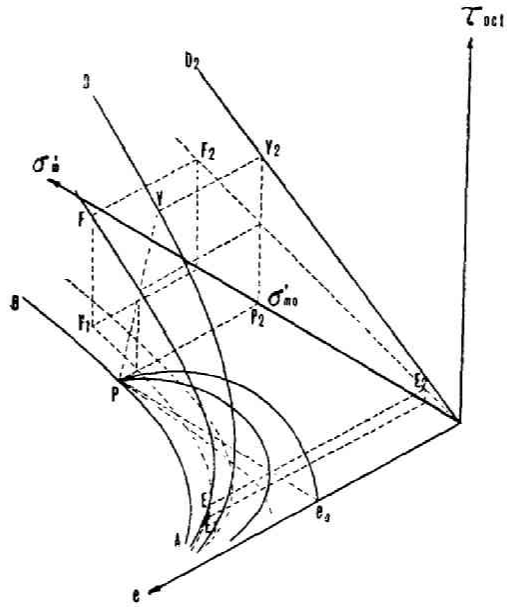


Fig.4.18. State paths in $\tau_{oct}/\sigma'_m$-constant shear

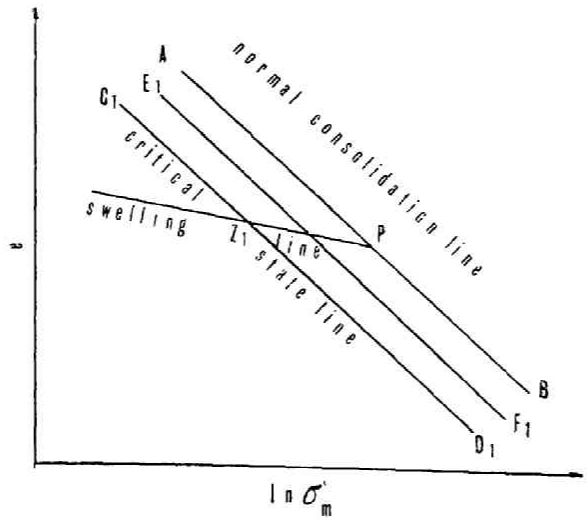


Fig.4.19. $e$-$\ln\sigma'_m$ relations in $\tau_{oct}/\sigma'_m$-constant shear

## 4.4 Stress-Strain Relations

### 1. Yield Surface

For a work-hardening material whose yield surfaces in the stress space are convex and time independent, Drucker (1951),(1959) reasoned out the concept of *normality* that the irreversible plastic component of incremental strain vector is normal to the current yield surface from his stability postulate. Palmer, Maier and Drucker (1967) extended Drucker's explanation to work-softening materials from the broader quasi-thermodynamic condition with some restriction on the extent of the falling of stress-strain curve.

Generally speaking, soils can be considered as work-hardening or work-softening materials, but the mechanical behavior of soils is not time independent. When an external agency is applied to a clay element, it deforms not only instantaneously but also time dependently. This time dependent deformation process has mainly two aspects: one is the pore water dissipating process and the other is time dependent deformability of the clay skelton constructed with clay particles. It is not unnatural to assume that the stress-strain curves for clays are defined uniquely while the clays are permitted to deform with sufficient duration. With such an assumption, the normality concept may be applicable to clays. In this thesis, the normality concept is applied to clays not only in the mechanical state of work-hardening but also of work-softening.

Many researchers have proposed various yield surfaces for soils. The yield surface of Mohr-Coulomb type associated with continuous dilation after yielding has played a dominant role in the stability analysis of soil structures. To the best of the author's knowledge, only a few researchers, Cox (1963), Poorooshasb, Holubec and Sherbourne (1967) and Davis (1968) have studied the stability analysis based on the non-associated flow rule. Drucker, Gibson and Henkel (1957) proposed the cone shaped yield surface with a spherical cap. Calladine (1963) proposed the yield surface as the intersection of the state surface with the swelling wall. Barden and Khayatt (1966)

proposed $\sigma_1'^K = A\sqrt{2}\sigma_3'$ as the plastic potential for sands. Poorooshasb, Holubec and Sherbourne (1966) proposed non-associated yield surface $\sigma_1'/\sigma_3'$=constant for sands accompanied with the plastic potential similarly shaped as the yield surface proposed by Calladine or by Barden and Khayatt. Some researchers considered soils as the materials ruled by the non-associated flow law. De Josselin de Jong (1964) and Palmer (1966) proposed an associated surface (g-surface) distinguished from the yield surface. Weidler and Paslay (1969) stated that the direction of the incremental plastic strain vector for a granular material may be related to the surface shffted from the yield surface.

These proposals mentioned above are based on the assumption that soils behave elastically under the stress state inside the current yield surface. This assumption is not supported by experimental data and therefore Roscoe and Burland (1968) and Chaplin (1969) proposed a double yield surface.

It is easy to draw inferences about yield locus from above discussion concerning state surface and swelling wall. As suggested by Calladine (1963), the border line between elastic state and elastic-plastic state is the intersection of the swelling wall and the state surface which is called *elastic limit curve*. The initial yield surface showing the stress condition for initial yielding is given as the projection of this elastic limit curve onto the stress space. Since the yield surface is a function of stress invariant for the initially isotropic soil skelton it is given by projecting the elastic limit curve onto $\tau_{oct}$-$\sigma_m'$ diagram. Therefore the initial yield surface is derived by eliminating void ratio $e$ from eq.(4.2.9) and eq.(4.2.10) as follows:

$$\frac{\tau_{oct}}{\sigma_m'} = -\frac{\lambda - \kappa}{(1+\ _0)\mu} \ln \frac{\sigma_m'}{\sigma_{m0}'} \tag{4.4.1}$$

The initial yield surface is the *yield locus* given by eq.(4.4.1) on $\tau_{oct}$-$\sigma_m'$ diagram.

Assuming the yield locus to expand or shrink proportionally with the increasing irreversible deformation, the current yield locus of

soil in elastic-plastic state is given by:

$$\frac{\tau_{oct}}{\sigma'_m} = -\frac{\lambda-\kappa}{(1+e_0)\mu}\ln\frac{\sigma'_m}{\sigma'_{my}} \tag{4.4.2}$$

where $\sigma'_m$ represents work-hardening or work-softening effect and corresponds to the value of $\sigma'_m$ for $\tau_{oct}/\sigma'_m=0$. The yield locus given by eq.(4.4.2) coincides with the one derived from energy balance by Roscoe, Schofield and Thurairajah (1963). For the stress ratio $\tau_{oct}/\sigma'_m=0$, state surface is reduced to normal consolidation curve and then the void ratio $e_y$ corresponding to $\sigma'_{my}$ is determined uniquely from the normal consolidation curve as follows:

$$e_y-e_0=-\lambda\ln\frac{\sigma'_{my}}{\sigma'_{m0}} \tag{4.4.3}$$

Inversely, $\sigma'_{my}$ of the current yield locus for the soil stressed by $\tau_{oct}$ and $\sigma'_m$ with void ratio $e$ is given as the effective mean principal stress of the intersecting point of the swelling curve passing the point $(e, \sigma'_m)$. Then:

$$e-e_0=-\kappa\ln\frac{\sigma'_m}{\sigma'_{my}} \tag{4.4.4}$$

and substituting eq.(4.4.3) into eq.(4.4.4). $\sigma'_{my}$ is given from the current applied mean stress $\sigma'_m$ and void ratio $e$ as follows:

$$e-e_0+\lambda\ln\frac{\sigma'_m}{\sigma'_{m0}}-(\lambda-\kappa)\ln\frac{\sigma'_m}{\sigma'_{my}}=0 \tag{4.4.5}$$

Fig.4.20 shows the yield conditions given by eqs.(4.4.1)-(4.4.5).

In the later section, it will be given that the stress condition of the critical state is represented by the stationary points of the yield loci in the $\tau_{oct}$-$\sigma'_m$ diagram as shown in Fig.4.20. For elastic-plastic clay wetter than critical, the current yield locus expands proportionally (work-hardening) and for elastic-plastic clay drier than critical, the current yield locus shrinks proportionally (work-softening) with the increasing plastic strain.

2. Incremental Stress-Plastic Strain Relations

Most of the incremental stress-plastic relations of work-

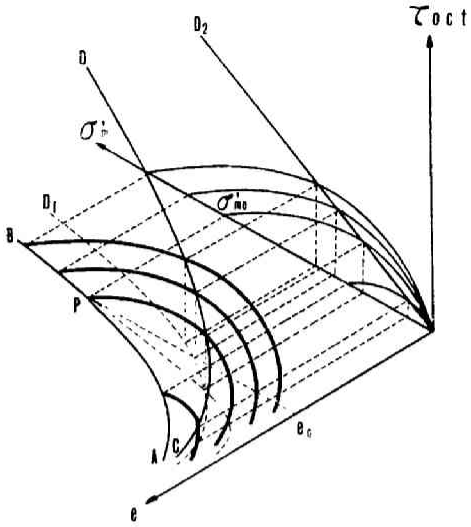


Fig.20. Yield condtions and yield loci

hardening or work-softening materials in the elastic-plastic state are able to be represented by:

$$d\varepsilon^p_{ij} = \Lambda \frac{\partial f}{\partial \sigma'_{ij}} \tag{4.4.6}$$

where $\varepsilon^p_{ij}$ is the plastic component of strain and $f$ is the plastic potential given as a function of stress. The yield locus is given by $f$=0.

Then, the plastic potential for soil can be derived from eq. (4.4.2) as:

$$f = \frac{\tau_{oct}}{\sigma'_m} + \frac{\lambda - \kappa}{(1+e_0)\mu} \ln \frac{\sigma'_m}{\sigma'_{my}} \tag{4.4.7}$$

$\Lambda$ in eq.(4.4.6) is a function of currently applied stress and stress increment. Eq.(4.4.6), an empirical law pointed out by von Mises, is called *associated flow law* and its reasonable interpretation is given by Drucker (1951), Palmer, Maier and Drucker (1967).

From eq.(4.4.6) plastic component of volume strain increment $dv^p$ is derived as:

$$dv^p = \delta_{ij} d\varepsilon^p_{ij} = \Lambda \delta_{ij} \frac{\partial f}{\partial \sigma'_{ij}} \tag{4.4.8}$$

The right hand side of eq.(4.4.8) is

$$\Lambda \delta_{ij} \frac{\partial f}{\partial \sigma'_{ij}} = \Lambda \delta_{ij} \left( \frac{\partial f}{\partial \tau_{oct}} \frac{\partial \tau_{oct}}{\partial \sigma'_{ij}} + \frac{\partial f}{\partial \sigma'_m} \frac{\partial \sigma'_m}{\partial \sigma'_{ij}} \right) \tag{4.4.9}$$

and substitution of eq.(4.4.7) into eq.(4.4.9) gives

$$\Lambda \delta_{ij} \frac{\partial f}{\partial \sigma'_{ij}} = \frac{\Lambda}{\sigma'_m} \left\{ \frac{\lambda - \kappa}{(1+e_0)\mu} - \frac{\tau_{oct}}{\sigma'_m} \right\} \tag{4.4.10}$$

Now, the plastic component of volume strain is defined by

$$dv^p = - \frac{de^p}{1 + e} \tag{4.4.11}$$

$$de^p = de - de^e \tag{4.4.12}$$

where $de^e$ and $de^p$ are elastic and plastic component of void ratio change respectively. Substituting eq.(4.2.7) and eq.(4.2.8) into eq.(4.4.12), $de^p$ is given as:

$$de^p = -(\lambda-\kappa)\frac{d\sigma'_m}{\sigma'_m} + (1+e_0)\mu\left(\frac{\tau_{oct}}{\sigma'_m}\frac{d\sigma'_m}{\sigma'_m} - \frac{d\tau_{oct}}{\sigma'_m}\right) \tag{4.4.13}$$

From eqs.(4.4.8),(4.4.10),(4.4.11) and (4.4.13), is derived as:

$$\Lambda = \mu\frac{1+e_0}{1+e}\left[d\sigma'_m + d\tau_{oct}\Big/\left\{\frac{\lambda-\kappa}{(1+e_0)\mu} - \frac{\tau_{oct}}{\sigma'_m}\right\}\right] \tag{4.4.14}$$

The void ratio $e$ in eq.(4.4.14) is given by eq.(4.2.10) as a function of stress. But in the case of small strain the volume strain is approximately defined by

$$dv = -\frac{de}{(1+e_i)} \tag{4.4.15}$$

where $e_i$ is the initial void ratio. Then $\Lambda$ is

$$\Lambda = \mu\frac{1+e_0}{1+e_i}\left[d\sigma'_m + d\tau_{oct}\Big/\left\{\frac{\lambda-\kappa}{(1+e_0)\mu} - \frac{\tau_{oct}}{\sigma'_m}\right\}\right] \tag{4.4.16}$$

Substituting eq.(4.4.7) into eq.(4.4.6), we get the incremental stress-plastic strain relations:

$$d\varepsilon^p_{ij} = \mu\frac{1+e_0}{1+e}\left[d\sigma'_m + d\tau_{oct}\Big/\left\{\frac{\lambda-\kappa}{(1+e_0)\mu} - \frac{\tau_{oct}}{\sigma'_m}\right\}\right]\frac{1}{3\sigma'_m}$$

$$\left[\left\{\frac{\lambda-\kappa}{(1+e_0)\mu} - \frac{\tau_{oct}}{\sigma'_m}\right\}\delta_{ij} + \frac{1}{\tau_{oct}}(\sigma'_{ij} - \sigma'_m\delta_{ij})\right] \tag{4.4.17}$$

where

$$e = e_0 - \lambda\ln\frac{\sigma'_m}{\sigma'_{m0}} - (1+e_0)\mu\frac{\tau_{oct}}{\sigma'_m} \qquad (bis\ 4.2.9)$$

in the case of large deformation, and

$$e = e_i$$

in the case of small deformation.

3. Stress-Elastic Strain Relations

It is assumed that a function $W$ of stress invariants gives the elastic component of strain $\varepsilon^e_{ij}$ as follows:

$$\varepsilon^e_{ij} = \frac{\partial W}{-\partial \sigma'_{ij}} \tag{4.4.18}$$

Assuming $W$ to be a function of $\sigma'_m$ only, it follows:

$$\varepsilon^e_{ij} = \frac{\partial W}{\partial \sigma'_m} \frac{\partial \sigma'_m}{\partial \sigma'_{ij}} = \frac{1}{3}\delta_{ij}\frac{dW}{d\sigma'_m} \tag{4.4.19}$$

Then $v^e = \delta_{ij}\varepsilon^e_{ij}$ is

$$v^e = \frac{dW}{d\sigma'_m} \tag{4.4.20}$$

The elastic component of volume strain $v^e$ is given by eq.(4.2.8) as:

$$dv^e = \frac{\kappa}{1+e} \frac{d\sigma'_m}{\sigma'_m} \tag{4.4.21}$$

For the infinitesimal strain, eq.(4.4.21) is approximately

$$dv^e = \frac{\kappa}{1+e_i} \frac{d\sigma'_m}{\sigma'_m} \tag{4.4.22}$$

Integrating eq.(4.4.22), $v^e$ is given as:

$$v^e = \frac{\kappa}{1+e_i} \ln \frac{\sigma'_m}{\sigma'_{mi}} \tag{4.4.23}$$

where $(e_i, \sigma'_{mi})$ is the initial state of soil and corresponds to a point on the swelling curve passing through $(e_0, \sigma'_{m0})$ on $e$-$\sigma'_m$ diagram. From eqs.(4.4.20) and (4.4.23), it follows:

$$\frac{dW}{d\sigma'_m} = \frac{\kappa}{e_i} \ln \frac{\sigma'_m}{\sigma'_{mi}} \tag{4.4.24}$$

And solving eq.(4.4.24), one gets:

$$W = \frac{\kappa}{1+e_i} \left[\sigma'_m\left(\ln \frac{\sigma'_m}{\sigma'_{mi}} - 1\right)\right] + \text{const.} \tag{4.4.25}$$

Substituting eq.(4.4.25) into eq.(4.4.19), the elastic strain is given as:

$$\varepsilon^e_{ij} = \frac{1}{3} \frac{\kappa}{1+e_i} \ln \frac{\sigma'_m}{\sigma'_{mi}} \delta_{ij} \tag{4.4.26}$$

And the incremental stress-elastic strain relation is given as:

$$d\varepsilon_{ij}^{e} = \frac{1}{3}\frac{\kappa}{1+e_i}\frac{d\sigma_m'}{\sigma_m'}\delta_{ij} \tag{4.4.27}$$

Eq.(4.4.26) shows that the assumption of $W$ to be a function of only $\sigma_m'$ leads to the conclusion of vanishing elastic (recoverable) shear strain. In the ordinary undrained shear test for clay, some recoverable axial strain is observed. Then, eq.(4.4.26) cannot give a reasonable explanation for such an experimental fact. This troublesome difficulty arising from the concept of elastic component defined immediately as the reversible component is also pointed out by Lee (1966), Barden, Khayatt and Wightman (1969) from another point of view. This difficulty might be overcome by assuming the double yield loci such as proposed by Roscoe and Burland (1968) and Chaplin (1969).

The theory mentioned above demands, the clays whose state points are on the swelling wall to behave recoverably or elastically. But this demand is not satisfied by the clays in a strict sense. The experiment carried on by Murayama and Kurihara (1968) shows the irreversible behaviors of clay whose state point is on the swelling wall. They sheared a clay with repeated loading under an undrained condition within a certain amount of axial strain. The stress path of this experiment does not behave recoverably. The normally consolidated clay under repeated load behaves gradually as an overconsolidated clay. In other words, repeated loading makes the clay change from the normally consolidated state to the overconsolidated state. Theoretical reasoning of these phenomena is not given in the present stage. But it might be possible to interpret these phenomena as follows. The stress-strain curve in a certain stage of the repeated loading test is shown in Fig.4.21. In Fig.4.21, elasticity means the equality between the energy released during unloading process BCDE and the work done by the applied stress in the loading process EFG when the distance BG is neglected. If the material yields plastically in the unloading and reloading process, the reloading stress-strain curve is to be on the right-hand side of

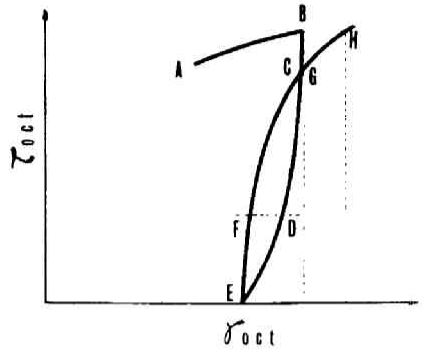


Fig.4.21. Loading cyclcle

the unloading stress-strain curve. Assuming that clays are not such materials, unreleased energy CDEFG might be spent for making the clay more heavily overconsolidated. Therefore, this unreleased energy might not be the plastically dissipated energy which is dissipated as the work for increasing the plastic strain. From these discussions it can be concluded that the shearing characteristics of the clays whose state points are on the swelling wall are not necessarily plastic, although they are not necessarily elastic in a strict sense. In this thesis, only the clays under shear with increasing shear strain are dealt with.

4. Critical State

Generally speaking, on the loading process, the elastic-plastic state path is to reach the final point on the critical state line which represents the perfectly plastic state, i.e., the state parameters $\tau_{oct}$, $\sigma_m'$ and $e$ do not change any more in spite of infinitely increasing shear strain at the perfectly plastic state. Fig.4.8 shows that the critical state line lying on the state surface intersects with the elastic limit curve at the point Z. An overconsolidated clay specimen whose initial state point is just under the point Z cannot experience the elastic-plastic state on the shearing process under undrained condition, because the state point arrives at the critical state line immediately when it reaches the

elastic limit curve after experiencing the purely elastic state.

The critical state is defined by Roscoe, Schofield and Wroth (1958) as:

$$\frac{de}{d\gamma_{oct}} = \frac{d\sigma'_m}{d\gamma_{oct}} = \frac{d\tau_{oct}}{d\gamma_{oct}} = 0 \tag{4.4.28}$$

which does not coincide, in general, with the so-called failure point defined by either $(\sigma'_1-\sigma'_3)_{max}$ or $(\sigma'_1/\sigma'_3)_{max}$. In eq.(4.4.27) $\tau_{oct}$ is defined as:

$$\tau_{oct} = \frac{1}{3}\sqrt{(\varepsilon_1-\varepsilon_2)^2+(\varepsilon_2-\varepsilon_3)^2+(\varepsilon_3-\varepsilon_1)^2}$$

Assuming the normality rule to be adaptable for clays, the critical state is represented as the stationary points of the yield loci in the $\tau_{oct}$-$\sigma'_m$ diagram.

From eq.(4.4.17), we can understand that the stress condition for the production of infinite shear strain increment is given by:

$$\left(\frac{\tau_{oct}}{\sigma'_m}\right)_{crit} = \frac{\lambda - \kappa}{(1+e_0)\mu} \tag{4.4.29}$$

Of course eq.(4.4.29) gives the stress condition for the critical state. Stress ratio $\tau_{oct}/\sigma'_m$ of the critical state is a constant value for the clays pre-consolidated with the pressure of $\sigma'_{m0}$. Little consideration shows that the stress condition given by eq. (4.4.29) represents the stationary point of current yield locus in the $\tau_{oct}$-$\sigma'_m$ diagram. Then the critical state point is given by a set of equations as:

$$\begin{aligned} \tau_{oct} &= \frac{\lambda - \kappa}{(1+e_0)\mu}\,\sigma'_{my}\exp.(-1) \\ \sigma'_m &= \sigma'_{my}\exp.(-1) \\ e &= e_0+\kappa+\lambda\ln\frac{\sigma'_{m0}}{\sigma'_{my}} \end{aligned} \tag{4.4.30}$$

Substituting eq.(4.4.29) into eq.(4.2.9) representing the state surface, parallel line to the normal consolidation curve on the $e$-$\ln\sigma'_m$ diagram is derived as follows:

$$e = e_0 - (\lambda-\kappa) - \lambda \ln \frac{\sigma'_m}{\sigma'_{m0}} \qquad (4.4.31)$$

This relation is supported by a lot of experimental data, for instance, by those of Bjerrum (1951), Henkel (1959) and Henkel and Sowa (1963).

The critical state line is closely neighboring the ordinary $(\sigma'_1-\sigma'_3)_{max}$ failure envelope on $\tau_{oct}-\sigma'_m$ diagram for clays wetter than critical state, but not for heavily overconsolidated clays drier than critical state. The intersection of $\tau_{oct}$ axis and the critical state line of the clays whose initial state points are on the same swelling curve is zero. If the critical state line is represented as follows:

$$\tau_{oct} = c' + \sigma'_m \tan\phi'$$

$c'$ is to be zero and $\tan\phi'$ is equal to eq.(4.4.29).

The $(\sigma'_1-\sigma'_3)_{max}$ failure envelope of clays wetter than critical coincides approximately with the critical state line, but the peak points of heavily overconsolidated clays do not necessarily coincide with the critical state points. From Figs.4.12, 4.13, it is apparent that the stress paths of overconsolidated clays under undrained shear can pass through the upside of $(\sigma'_1-\sigma'_3)_{max}$ failure envelope. This is supported experimentally by Murayama and Kurihara (1968). These results show that the stress state of clays can be outside the failure envelope substituted by the critical state line as shown in Fig.4.22.

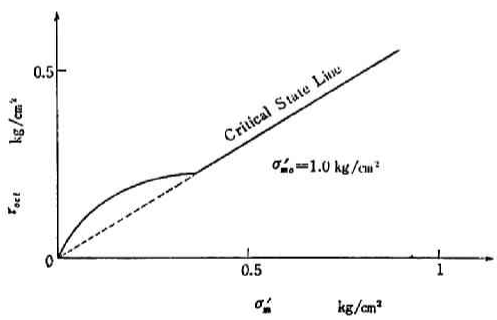


Fig.4.22. $(\sigma'_1 - \sigma'_3)_{max}$ envelope

The inherent physical meanings of Mohr-Coulomb failure criterion for clays are made vague by these results. Then supposing Mohr-Coulomb failure criterion to be true for clays, it may be merely fortuitous. The theory mentioned

here is based on the concept of octahedral stresses without clear reasons, but it can reason out many mechanical behaviors of clays systematically. These considerations do not support that Mohr-Coulomb criterion is more adaptable for clays than extended von Mises criterion.

5. Normality Rule in the Octahedral Stress Space

In the above discussions, we use the normality rule in the stress space. But as shown later, it is convenient to derive the stress-strain relations under various conditions to use the normality concept in the octahedral stress space. The proof given in the Appendix gives us the confidence that the following relations can be used:

$$\frac{1}{3}dv^p = \frac{\Lambda}{3}\frac{\partial f}{\partial \sigma'_m} \tag{4.4.32}$$

$$d\gamma^p_{oct} = \frac{\Lambda}{3}\frac{\partial f}{\partial \tau_{oct}} \tag{4.4.33}$$

if

$$f = f(\tau_{oct}, \sigma'_m) \tag{4.4.34}$$

and

$$d\varepsilon^p_i = \Lambda\frac{\partial f}{\partial \sigma'_i} \tag{4.4.35}$$

where $\varepsilon_i$ and $\sigma'_i$ are principal strain and principal stress respectively.

As shown in Fig.4.23, incremental stress-plastic strain relations for clays are to be deduced applying the normality concept in the octahedral stress space. Differentiating eq.(4.4.2), the tangent of the yield locus is given as:

$$\frac{d\tau_{oct}}{d\sigma'_m} = -\frac{\lambda - \kappa}{(1+e_0)\mu}\{\ln\frac{\sigma'_m}{\sigma'_{my}} + 1\} \tag{4.4.36}$$

and substituting eq.(4.4.2) into eq.(4.4.36), we get:

$$\frac{d\tau_{oct}}{d\sigma'_m} = \frac{\tau_{oct}}{\sigma'_m} - \frac{\lambda - \kappa}{(1+e_0)\mu} \tag{4.4.37}$$

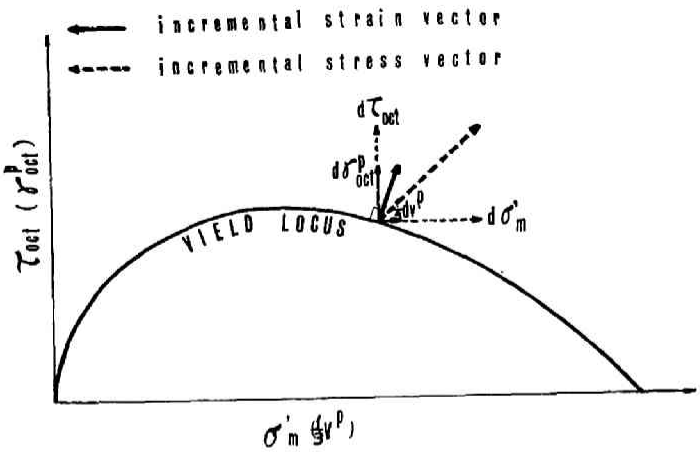


Fig.4.23. Associated flow rule

Normality demands that:

$$\frac{\frac{1}{3}dv^p}{d\gamma^p_{oct}} = -\frac{d\tau_{oct}}{d\sigma'_m} \tag{4.4.38}$$

on the yield locus. From eq.(4.4.17), the incremental plastic volumetric strain is given as:

$$dv^p = \frac{(1+e_0)\mu}{1+e}\left[\left\{\frac{\lambda-\kappa}{(1+e_0)\mu} - \frac{\tau_{oct}}{\sigma'_m}\right\}\frac{d\sigma'_m}{\sigma'_m} + \frac{d\tau_{oct}}{\sigma'_m}\right] \tag{4.4.39}$$

Therefore, substituting eq.(4.4.39) and eq.(4.4.37) into eq.(4.4.38), octahedral shear strain increment is given by:

$$d\gamma^p_{oct} = \frac{1}{3}\frac{(1+e_0)\mu}{1+e}\left\{\frac{d\sigma'_m}{\sigma'_m} + \frac{\dfrac{d\tau_{oct}}{\sigma'_m}}{\dfrac{\lambda-\kappa}{(1+e_0)\mu} - \dfrac{\tau_{oct}}{\sigma'_m}}\right\} \tag{4.4.40}$$

The incremental plastic shear strain given by eq.(4.4.40) is a function of $e$, $\sigma'_m$, $\tau_{oct}$ and the incremental stresses. Substituting the equation of the state surface into eq.(4.4.39) and (4.4.40), we get the incremental stress-plastic strain relation for clays as:

$$dv^p = \frac{1}{\frac{1}{\mu} - \frac{\tau_{oct}}{\sigma'_m} - \frac{\lambda}{(1+e_0)\mu} \ln \frac{\sigma'_m}{\sigma'_{m0}}} [\{\frac{\lambda - \kappa}{(1+e_0)\mu} - \frac{\tau_{oct}}{\sigma'_m}\}\frac{d\sigma'_m}{\sigma'_m} + \frac{d\tau_{oct}}{\sigma'_m}]$$

$$d\gamma^p_{oct} = \frac{1}{3} \frac{1}{\frac{1}{\mu} \quad \frac{\tau_{oct}}{\sigma'_m} - \frac{\lambda}{(1+e_0)\mu} \ln \frac{\sigma'_m}{\sigma'_{m0}}} \{\frac{d\sigma'_m}{\sigma'_m} + \frac{\frac{d\tau_{oct}}{\sigma'_m}}{\frac{\lambda - \kappa}{(1+e_0)\mu} - \frac{\tau_{oct}}{\sigma'_m}}\}$$

(4.4.41)

Eqs.(4.4.41) show the incremental linearity of stress-plastic strain relations for clays. Assuming that no plastic strains occur in the clays whose state points are on the swelling wall, the boundary condition for eqs.(4.4.41) are given as:

$$\gamma^p_{oct} = v^p = 0 \quad \text{at} \quad \frac{\tau_{oct}}{\sigma'_m} = - \frac{\lambda - \kappa}{(1+e_0)\mu} \ln \frac{\sigma'_m}{\sigma'_{m0}} \tag{4.4.42}$$

for the clays pre-consolidated with the pressure of $\sigma'_{m0}$. The solutions of eqs.(4.4.41) with the boundary condition given by eq.(4.4.42) give the surface in $\tau_{oct}$, $\sigma'_m$, $v^p$ space and $\tau_{oct}$, $\sigma'_m$, $\gamma^p_{oct}$ space. These two surfaces represent the general stress-strain relations.

## Appendix

The subject is to prove that:

$$\frac{1}{3}dv^p = \frac{\Lambda}{3} \frac{\partial f}{\partial \sigma'_m} \tag{A-1}$$

$$d\gamma^p_{oct} = \frac{\Lambda}{3} \frac{\partial f}{\partial \tau_{oct}} \tag{A-2}$$

when

$$f = f(\tau_{oct}, \sigma'_m) \tag{A-3}$$

$$d\varepsilon^p_i = \Lambda \frac{\partial f}{\partial \sigma'_i} \tag{A-4}$$

Defining the stress vector $\sigma$ and strain increment vector $d\varepsilon$ in the three dimensional coordinate whose base vectors are i, j, and k as

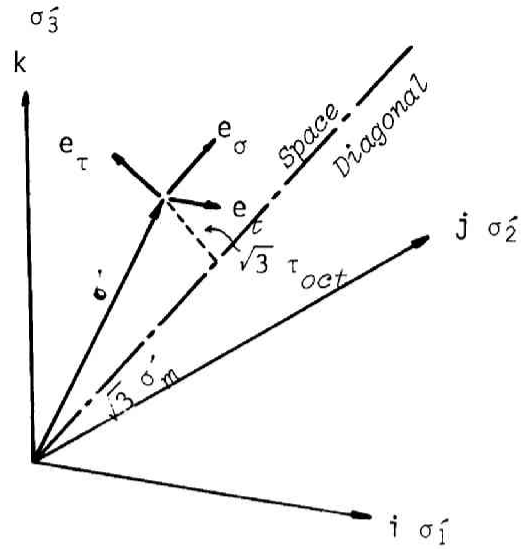


shown in the figure, we get:

$$\boldsymbol{\sigma}' = \sigma_1' \mathbf{i} + \sigma_2' \mathbf{j} + \sigma_3' \mathbf{k} \tag{A-5}$$

$$d\boldsymbol{\varepsilon}^p = d\varepsilon_1^p \mathbf{i} + d\varepsilon_2^p \mathbf{j} + d\varepsilon_3^p \mathbf{k} \tag{A-6}$$

Let us introduce another base vectors $e_\sigma$, $e_\tau$ and $e_t$. $e_\sigma$ is the vector directed to the same direction of the space diagonal. $e_\tau$ is defined as the unit vector lying on plane constructed by $e_\sigma$ and $\boldsymbol{\sigma}$ and normal to $e_\sigma$. $e_t$ is the unit vector normal to both $e_\sigma$ and $e_\tau$. Translations between these two sets of base vectors are as follows:

$$e_\sigma = \frac{1}{\sqrt{3}}(\mathbf{i} + \mathbf{j} + \mathbf{k})$$

$$e_\tau = \frac{1}{3\sqrt{3}\tau_{oct}} \{(2\sigma_1' - \sigma_2' - \sigma_3')\mathbf{i} + (2\sigma_2' - \sigma_3' - \sigma_1')\mathbf{j} + (2\sigma_3' - \sigma_1' - \sigma_2')\mathbf{k}\}$$

$$e_t = \frac{1}{3\tau_{oct}} \{(\sigma_3' - \sigma_1')\mathbf{i} + (\sigma_1' - \sigma_3')\mathbf{j} + (\sigma_2' - \sigma_1')\mathbf{k}\} \tag{A-7}$$

and

$$\mathbf{i} = \frac{\sqrt{3}}{3}\mathbf{e}_\sigma + \frac{1}{3\sqrt{3}\tau_{oct}}(2\sigma_1' - \sigma_2' - \sigma_3')\mathbf{e}_\tau + \frac{1}{3\tau_{oct}}(\sigma_3' - \sigma_2')\mathbf{e}_t$$

$$\mathbf{j} = \frac{\sqrt{3}}{3}\mathbf{e}_\sigma + \frac{1}{3\sqrt{3}\tau_{oct}}(2\sigma_2' - \sigma_3' - \sigma_1')\mathbf{e}_\tau + \frac{1}{3\tau_{oct}}(\sigma_1' - \sigma_3')\mathbf{e}_t$$

$$\mathbf{k} = \frac{\sqrt{3}}{3}\mathbf{e}_\sigma + \frac{1}{3\sqrt{3}\tau_{oct}}(2\sigma_3' - \sigma_1' - \sigma_2')\mathbf{e}_\tau + \frac{1}{3\tau_{oct}}(\sigma_2' - \sigma_1')\mathbf{e}_t \quad \text{(A-8)}$$

Substitution of eq.(A-8) into eq.(A-5) leads:

$$\boldsymbol{\sigma}' = \sqrt{3}\sigma_m'\mathbf{e}_\sigma + \sqrt{3}\tau_{oct}\mathbf{e}_\tau \quad \text{(A-9)}$$

Now partial derivation of $f$ is given by:

$$\frac{\partial f}{\partial \sigma_i'} = \frac{\partial f}{\partial \sigma_m'}\frac{\partial \sigma_m'}{\partial \sigma_i'} + \frac{\partial f}{\partial \tau_{oct}}\frac{\partial \tau_{oct}}{\partial \sigma_i'} \quad \text{(A-10)}$$

Substituting eqs.(A-4), (A-8) and (A-10) into eq.(A-6), we get:

$$d\boldsymbol{\varepsilon}^p = \sqrt{3}\,\frac{\Lambda}{3}\,\frac{\partial f}{\partial \sigma_m'}\mathbf{e}_\sigma + \sqrt{3}\,\frac{\Lambda}{3}\,\frac{\partial f}{\partial \tau_{oct}}\mathbf{e}_\tau \quad \text{(A-11)}$$

On the other hand, ombination of eqs.(A-6) and (A-8) gives:

$$\begin{aligned} d\boldsymbol{\varepsilon}^p = {} & \sqrt{3}\,\frac{1}{3}(d\varepsilon_1^p + d\varepsilon_2^p + d\varepsilon_3^p)\mathbf{e}_\sigma + \frac{1}{3\sqrt{3}\tau_{oct}}\{(2\sigma_1' - \sigma_2' - \sigma_3')d\varepsilon_1^p \\ & + (2\sigma_2' - \sigma_3' - \sigma_1')d\varepsilon_2^p + (2\sigma_3' - \sigma_1' - \sigma_2')d\varepsilon_3^p\}\mathbf{e}_\tau \\ & + \frac{1}{3\tau_{oct}}\{(\sigma_3' - \sigma_1')d\varepsilon_1^p + (\sigma_1' - \sigma_3')d\varepsilon_2^p + (\sigma_2' - \sigma_1')d\varepsilon_3^p\}\mathbf{e}_t \end{aligned} \quad \text{(A-12)}$$

Comparing eqs.(A-11) and (A-12), we get:

$$\frac{1}{3}dv^p = \frac{1}{3}(d\varepsilon_1^p + d\varepsilon_2^p + d\varepsilon_3^p) = \frac{\Lambda}{3}\,\frac{\partial f}{\partial \sigma_m'} \quad \text{(A-13)}$$

Then, from eqs.(A-6), (A-11) and (A-13), it is derived that:

$$\begin{aligned} d\boldsymbol{\varepsilon}^p &= d\varepsilon_1^p\mathbf{i} + d\varepsilon_2^p\mathbf{j} + d\varepsilon_3^p\mathbf{k} \\ &= \sqrt{3}\,\frac{1}{3}(d\varepsilon_1^p + d\varepsilon_2^p + d\varepsilon_3^p)\mathbf{e}_\sigma + \sqrt{3}\,\frac{\Lambda}{3}\,\frac{\partial f}{\partial \tau_{oct}}\,\mathbf{e}_\tau \end{aligned} \quad \text{(A-14)}$$

And by considering the absolute values of the plastic strain increment,vector we get:

$$d\gamma^{p}_{oct} = \frac{\Lambda}{3}\frac{\partial f}{\partial \tau_{oct}} \tag{A-15}$$

Eqs.(A-13) and (A-15) show that the plastic strain increment vector is normal to the $f$=0 locus in the octahedral space.

## 6. Stress-Strain Relations under Various Conditions

*Undrained Shear*

The initial state points of clays pre-consolidated with the pressure of $\sigma'_{m0}$ are given by:

$$\begin{aligned} \tau_{oct} &= 0 \\ \sigma'_m &= \sigma'_{mi} \leqq \sigma'_{m0} \\ e &= e_i \geqq e_0 \end{aligned} \tag{4.4.43}$$

The stress states of clays under undrained shear whose state points are on the state surface are given as:

$$\frac{\tau_{oct}}{\sigma'_m} = -\frac{\lambda}{(1+e_0)\mu}\ln\frac{\sigma'_m}{\sigma'_{m0}} + \frac{\kappa}{(1+e_0)\mu}\ln\frac{\sigma'_{mi}}{\sigma'_{m0}} \tag{bis 4.4.3}$$

Differentiating eq.(4.3.3), we get:

$$d\tau_{oct} = -\frac{1}{(1+e_0)\mu}\left(\lambda + \lambda\ln\frac{\sigma'_m}{\sigma'_{m0}} - \kappa\ln\frac{\sigma'_{mi}}{\sigma'_{m0}}\right)d\sigma'_m \tag{4.4.44}$$

Substituting eq.(4.3.3) and eq.(4.4.44) into eq.(4.4.41), we get:

$$dv^{p} = -\frac{\dfrac{\kappa}{(1+e_0)\mu}}{\dfrac{1}{\mu} - \dfrac{\kappa}{(1+e_0)\mu}\ln\dfrac{\sigma'_{mi}}{\sigma'_{m0}}}\frac{d\sigma'_m}{\sigma'_m}$$

$$d\gamma^{q}_{oct} = -\frac{1}{3}\frac{\kappa}{\dfrac{1}{\mu} - \dfrac{\kappa}{(1+e_0)\mu}\ln\dfrac{\sigma'_{mi}}{\sigma'_{m0}}}\left\{\frac{\dfrac{d\sigma'_m}{\sigma'_m}}{\lambda - \kappa - \kappa\ln\dfrac{\sigma'_{mi}}{\sigma'_{m0}} + \lambda\ln\dfrac{\sigma'_m}{\sigma'_{m0}}}\right\} \tag{4.4.45}$$

Solving eqs.(4.4.45) with the boundary condition:

$$v^p = 0, \ \gamma^p_{oct} = 0 \qquad \text{at} \qquad \sigma'_m = \sigma'_{mi} \tag{4.4.46}$$

we get:

$$v^p = -\frac{\kappa}{1+e_0 - \kappa \ln \frac{\sigma'_{mi}}{\sigma'_{m0}}} \ln \frac{\sigma'_m}{\sigma'_{mi}}$$

$$\gamma^p_{oct} = -\frac{1}{3} \frac{\frac{\kappa}{\lambda}}{\frac{1}{\mu} - \frac{\kappa}{(1+e_0)\mu} \ln \frac{\sigma'_{mi}}{\sigma'_{m0}}} \ln \frac{\lambda - \kappa - \kappa \ln \frac{\sigma'_{mi}}{\sigma'_{mo}} + \lambda \ln \frac{\sigma'_m}{\sigma'_{m0}}}{(\lambda - \kappa)\{\ln \frac{\sigma'_{mi}}{\sigma'_{m0}} + 1\}} \tag{4.4.47}$$

Eqs.(4.4.47) give the stress-plastic strain relations for clays under undrained shear. The graphical explanation of these deductions is given in Fig.4.24. Substituting eq.(4.3.3) into eq.(4.4.47), we get

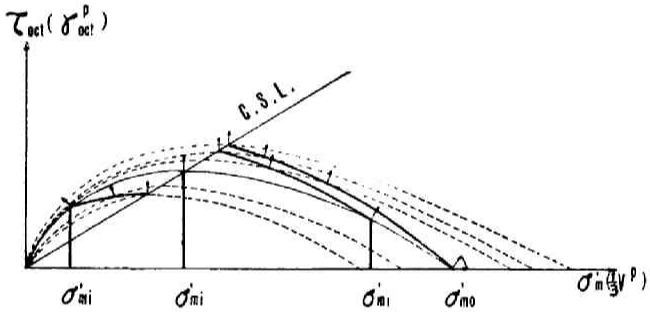


Fig.4.24. Stress paths and plastic strain increments (undrained shear)

the relation between $\tau_{oct}/\sigma'_m$ and $\gamma^p_{oct}$:

$$\gamma^p_{oct} = -\frac{1}{3} \frac{\frac{\kappa}{\lambda}}{\frac{1}{\mu} - \frac{\kappa}{(1+e_0)\mu} \ln \frac{\sigma'_{mi}}{\sigma'_{m0}}} \ln \frac{1 - \frac{(1+e_0)\mu}{\lambda - \kappa} \frac{\tau_{oct}}{\sigma'_m}}{1 + \ln \frac{\sigma'_{mi}}{\sigma'_{m0}}} \tag{4.4.48}$$

When the stress ratio $\tau_{oct}/\sigma'_m$ reaches the critical value $(\lambda-\kappa)/(1+e_0)\mu$, plastic shear strain becomes infinite. The critical value of the

stress ratio $\tau_{oct}/\sigma'_m$ corresponding to the value of $c_u/p$ is not constant for the clay elements consolidated with various pressures. The value of $\lambda$ tends to decrease slightly with an increase in consolidation pressure and the value of $\kappa$ conversely tends to increase with an increase in consolidation pressure. The value of $\mu$ tends to decrease very slightly with an increase in pressure judging from the data published by Shibata (1963). From this knowledge on $\lambda$, $\kappa$, $\mu$, $e_0$ it cannot be concluded whether the critical value of the stress ratio $\tau_{oct}/\sigma'_m$ increases or decreases with an increase in consolidation pressure. Therefore, the value of $c_u/p$ is not necessarily constant for a particlular clay and is the function of the consolidation pressure. It should be noted that this theory is based on the assumption of linearity of the $e$-$\ln\sigma'_m$ relation, i.e., the value of is constant which is valid for a limited range of the consolidation pressure. Eq.(4.4.48) suggests that for normally consolidated clays (and for overconsolidated clays which have the same overconsolidation ratios) the $\gamma^p_{oct}$-$\tau_{oct}/\sigma'_m$ relations coincide with each other while the values of $\kappa/\lambda$, $1/\mu$, $/(1+e_0)\mu$ and $(\lambda-\kappa)/(1+e_0)\mu$ are respectively the same.

Elastic volumetric strain is given by:

$$dv^e = \frac{\kappa}{1+e}\frac{d\sigma'_m}{\sigma'_m} = \frac{\kappa}{1+e_0-\kappa\ln\dfrac{\sigma'_m}{\sigma'_{m0}}}\frac{d\sigma'_m}{\sigma'_m} \tag{4.4.49}$$

and:

$$v^e = \frac{\kappa}{1+e_0-\kappa\ln\dfrac{\sigma'_m}{\sigma'_{mi}}}\ln\frac{\sigma'_m}{\sigma'_{mi}} \tag{4.4.50}$$

Then total volumetric strain under undrained condition is given from eq.(4.4.47) and eq.(4.4.49):

$$v = v^e + v^p = 0 \tag{4,4.51}$$

For normally consolidated clays, we have:

$$\sigma'_{mi} = \sigma'_{m0} \tag{4.4.52}$$

The stress-strain relation is deduced from eq.(4.4.47) as:

$$v^p = -\frac{\kappa}{1+e_0}\ln\frac{\sigma'_m}{\sigma'_{m0}}$$

$$\gamma^p_{oct} = -\frac{\kappa\mu}{3\lambda}\ln\frac{\lambda-\kappa+\lambda\ln\frac{\sigma'_m}{\sigma'_{m0}}}{\lambda-\kappa} \tag{4.4.53}$$

or from eq.(4.4.48) as:

$$v^p = \mu\frac{\kappa}{\lambda}\frac{\tau_{oct}}{\sigma'_m}$$

$$\gamma^p_{oct} = -\mu\frac{\kappa}{3\lambda}\ln\{1-\frac{(1+e_o)\mu}{\lambda-\kappa}\frac{\tau_{oct}}{\sigma'_m}\} \tag{4.4.54}$$

Eqs.(4.4.54) suggest that all equi-plastic strain curves for the clays normally consolidated with various pressures should be concentrated to the origin in the $\tau_{oct}$-$\sigma'_m$ diagram provided the shear strain rate is selected to be sufficiently slow.

*Drained Shear*

When the clays pre-consolidated with the pressure of $\sigma'_{m0}$ are compressed ($\sigma'_a$: increase, $\sigma'_r$: constant) under a fully drained condition in the conventional triaxial apparatus, the stress state is given by:

$$\tau_{oct} = \sqrt{2}(\sigma'_m - \sigma'_{mi}) \tag{4.4.55}$$

Theoretically it is assumed that plastic strains do not occur so far as the state paths are on the swelling wall. Therefore, the initial stress state ($\tau_{octp}$, $\sigma'_{mp}$) at which plastic strains begin to develop is determined as the intersecting point of the state surface, the swelling wall and the stress state plane defined by eq.(4.4.55). The point is shown as P or H or K in Fig.4.14. The intersection of the state surface with the swelling wall is given by:

$$\tau_{oct} = -\frac{\lambda-\kappa}{(1+e_0)\mu}\sigma'_m\ln\frac{\sigma'_m}{\sigma'_{m0}} \tag{4.4.56}$$

The initial stress state ($\tau_{oct}$ , $\sigma'_{mp}$) for plastic deformation is obtained by solving eq.(4.4.55) and eq.(4.4.56) simultaneously. Then the stress state for drained test is given by:

$$\tau_{oct} - \tau_{octp} = \sqrt{2}(\sigma'_m - \sigma'_{mp}) \tag{4.4.57}$$

Differentiating eq.(4.4.57), we get:

$$d\tau_{oct} = \sqrt{2}d\sigma'_m \tag{4.4.58}$$

Substituting eq.(4.4.57) and eq.(4.4.58) into eqs.(4.4.41) gives the incremental stress-plastic strain relation as:

$$dv^p = \frac{\dfrac{\lambda - \kappa}{(1+e_0)\mu} + \dfrac{\sqrt{2}\sigma'_{mp} - \tau_{octp}}{\sigma'_m}}{\dfrac{1}{\mu} - \sqrt{2} + \dfrac{\sqrt{2}\sigma'_{mp} - \tau_{octp}}{\sigma'_m} - \dfrac{\lambda}{(1+e_0)\mu}\ln\dfrac{\sigma'_m}{\sigma'_{m0}}}\,\frac{d\sigma'_m}{\sigma'_m}$$

$$d\gamma^p_{oct} = \frac{1}{3}\,\frac{1}{\dfrac{1}{\mu} - \sqrt{2} + \dfrac{\sqrt{2}\sigma'_{mp} - \tau_{octp}}{\sigma'_m} - \dfrac{\lambda}{(1+e_0)\mu}\ln\dfrac{\sigma'_m}{\sigma'_{m0}}}$$

$$\cdot\,\frac{\dfrac{\sqrt{2}\sigma'_{mp} - \tau_{octp}}{\sigma'_m} + \dfrac{\lambda - \kappa}{(1+e_0)\mu}}{\dfrac{\sqrt{2}\sigma'_{mp} - \tau_{octp}}{\sigma'_m} + \dfrac{\lambda - \kappa}{(1+e_0)\mu} - \sqrt{2}}\,\frac{d\sigma'_m}{\sigma'_m} \tag{4.4.59}$$

For normally consolidated clays, there exists:

$$\tau_{octp} = 0 \quad \text{and} \quad \sigma'_{mp} = \sigma'_{m0} \tag{4.4.60}$$

Solving eq.(4.4.59) with the initial condition of :

$$v^p = 0,\ \gamma^p_{oct} = 0 \text{ at } \sigma'_m = \sigma'_{mp} \tag{4.4.61}$$

we can obtain the stress-plastic strain relations for clays by the triaxial drained test. The graphical explanation of these deductions are given in Fig.4.25.

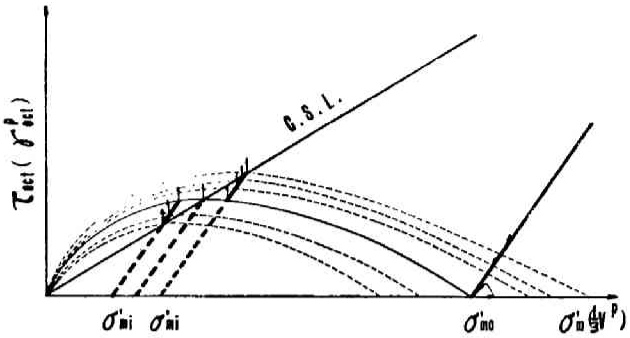


Fig.4.25. Stress paths and plastic strain increments (drained compression test)

$\sigma'_m$-*constant Shear*

For clays stressed keeping the effective bydrostatic pressure $\sigma'_m$ constant at the initial value of $\sigma'_{mi}$, the incremental stress-strain relations are given by substituting $\sigma'_m=\sigma'_{mi}$ and $d\sigma'_m=0$ into eq.(4.4.41):

$$dv^p = \frac{\dfrac{d\tau_{oct}}{\sigma'_{mi}}}{\dfrac{1}{\mu} - \dfrac{\tau_{oct}}{\sigma'_{mi}} - \dfrac{\lambda}{(1+e_0)\mu}\ln\dfrac{\sigma'_{mi}}{\sigma'_{m0}}}$$

$$d\gamma^p_{oct} = \frac{1}{3}\,\frac{\dfrac{d\tau_{oct}}{\sigma'_{mi}}}{\dfrac{1}{\mu} - \dfrac{\tau_{oct}}{\sigma'_{mi}} - \dfrac{\lambda}{(1+e_0)\mu}\ln\dfrac{\sigma'_{mi}}{\sigma'_m}\;\dfrac{\lambda-\kappa}{(1+e_0)\mu} - \dfrac{\tau_{oct}}{\sigma'_{mi}}} \qquad (4.4.62)$$

Solving eqs.(4.4.62) with the initial condition of:

$$v^p = 0, \quad \gamma^p_{oct} = 0 \quad \text{at} \quad \tau_{oct} = \tau_{octp} \qquad (4.4.63)$$

where $\tau_{octp}$ is given by eq.(4.3.5), we get stress-plastic strain relations for $\sigma'_m$-constant test as follows:

$$v^p = \ln\frac{\dfrac{1}{\mu} - \dfrac{\kappa}{(1+e_0)\mu}\ln\dfrac{\sigma'_{mi}}{\sigma'_{m0}}}{\dfrac{1}{\mu} - \dfrac{\tau_{oct}}{\sigma'_{mi}} - \dfrac{\lambda}{(1+e_0)\mu}\ln\dfrac{\sigma'_{mi}}{\sigma'_{m0}}} \qquad (4.4.64)$$

$$\gamma^p_{oct} = \frac{1}{3}\frac{1}{\frac{\lambda-\kappa}{(1+e_0)\mu} - \frac{1}{\mu} + \frac{\lambda}{(1+e_0)\mu}\ln\frac{\sigma'_{mi}}{\sigma'_{m0}}}$$

$$\cdot \ln\left\{\frac{\frac{1}{\mu} - \frac{\kappa}{(1+e_0)\mu}\ln\frac{\sigma'_{mi}}{\sigma'_{m0}}}{\frac{1}{\mu} - \frac{\tau_{oct}}{\sigma'_{mi}} - \frac{\lambda}{(1+e_0)\mu}\ln\frac{\sigma'_{mi}}{\sigma'_{m0}}}\;\frac{\frac{\lambda-\kappa}{(1+e_0)\mu} - \frac{\tau_{oct}}{\sigma'_{mi}}}{\left(1+\ln\frac{\sigma'_{mi}}{\sigma'_{m0}}\right)\frac{\lambda-\kappa}{(1+e_0)\mu}}\right\}$$

In this case the elastic volumetric strain $v^e=0$, and therefore $v^p$ means the total volumetric strain. For normally consolidated clays, i.e., $\sigma'_{mi}=\sigma'_{m0}$, eqs.(4.4.64) are rewritten as:

$$v = v^p = \ln\frac{1}{1-\mu\frac{\tau_{oct}}{\sigma'_{m0}}}$$

$$= \frac{1}{3}\frac{1}{\frac{\lambda-\kappa}{(1+e_0)\mu} - \frac{1}{\mu}}\ln\frac{1-\frac{(1+e_0)\mu}{\lambda-\kappa}\frac{\tau_{oct}}{\sigma'_{m0}}}{1-\mu\frac{\tau_{oct}}{\sigma'_{m0}}} \qquad (4.4.65)$$

It is apparent from eqs.(4.4.64) or eqs.(4.4.65) that when the stress ratio $\tau_{oct}/\sigma'_m$ reaches the critical value of $(\lambda-\kappa)/(1+e_0)\mu$, shear strain becomes infinite. The graphical explanation of these deduction is given in Fig.4.26.

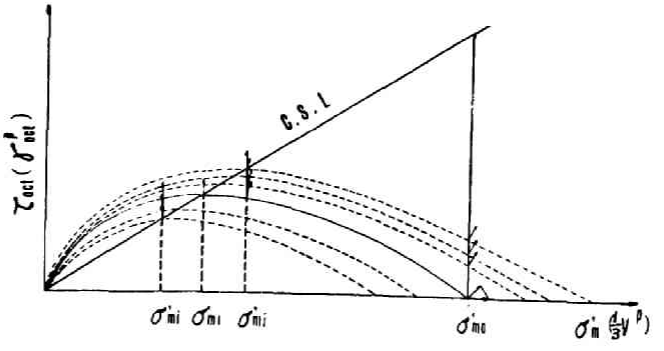


Fig.4.26. Stress paths and plastic strain increments ($\sigma'_m$-constant shear)

From eqs.(4.4.65), we get:

$$3\{\frac{\lambda - \kappa}{(1+e_0)\mu} - \frac{1}{\mu}\}\gamma^p_{oct} - v = \ln\{1 - \frac{(1+e_0)\mu}{\lambda - \kappa}\frac{\tau_{oct}}{\sigma'_{m0}}\} \qquad (4.4.66)$$

From eq.(4.4.54), we can see that the right-hand side of eq.(4.4.66) is enual to $-(3\lambda/\kappa\mu)(\gamma^p_{oct})$ undrained. Then we obtain the relation between the strains of normally consolidated clays stressed with the same stress ratio $\tau_{oct}/\sigma'_m$ under the condition of $\sigma'_m$-constant and under undrained shear as follows:

$$\frac{3\lambda}{\kappa\mu}(\gamma^p_{oct})_u = (v)_s - 3\{\frac{\lambda - \kappa}{(1+e_0)\mu} - \frac{1}{\mu}\}(\gamma^p_{oct})_s \qquad (4.4.67)$$

where the suffix $u$ and $s$ denote "undrained" and "$\sigma'_m$-constant" shear respectively. Assuming the elastic component of shear strain to be negligibly small compared with the plastic component, eq.(4.4.67) may be rewritten as:

$$\frac{3\lambda}{\kappa\mu}(\gamma_{oct})_u = (v)_s - 3\{\frac{\lambda - \kappa}{(1+e_0)\mu} - \frac{1}{\mu}\}(\gamma_{oct})_s \qquad (4.4.68)$$

Inversely, if the two constants are determined from the undrained and $\sigma'_m$-constant tests assuming that eq.(4.4.68) is valid, those two constants may be slightly different from $\lambda/\kappa\mu$ and $\{(\lambda-\kappa)/(1+e_0)\mu\}-\frac{1}{\mu}$ respectively because of the existence of the elastic component of shear strain.

*$\tau_{oct}/\sigma'_m$-constant Shear*

The incremental stress-plastic strain relations for clays sheared under $\tau_{oct}/\sigma'_m$-constant conditions, i.e., the anisotropic consolidation, are derived by substituting the following relations:

$$\tau_{oct}/\sigma'_m = k$$
$$\frac{d\tau_{oct}}{\sigma'_m} = k\frac{d\sigma'_m}{\sigma'_m} \qquad (4.4.69)$$

into eqs.(4.4.41) as follows:

$$dv^p = \frac{\dfrac{\lambda - \kappa}{(1+e_0)\mu}}{\dfrac{1}{\mu} - k - \dfrac{\lambda}{(1+e_0)\mu} \ln \dfrac{\sigma'_m}{\sigma'_{m0}}} \frac{d\sigma'_m}{\sigma'_m}$$

$$d\gamma^p_{oct} = \frac{1}{3} \frac{1}{\dfrac{1}{\mu} - k - \dfrac{\lambda}{(1+e_0)\mu} \ln \dfrac{\sigma'_m}{\sigma'_{m0}}} \cdot \frac{\dfrac{\lambda - \kappa}{(1+e_0)\mu}}{\dfrac{\lambda - \kappa}{(1+e_0)\mu} - k} \cdot \frac{d\sigma'_m}{\sigma'_m} \tag{4.4.70}$$

The intersection of the state surface with the swelling wall is given by:

$$\tau_{oct} = - \frac{\lambda - \kappa}{(1+e_0)\mu} \sigma'_m \ln \frac{\sigma'_m}{\sigma'_{m0}} \tag{bis 4.4.56}$$

Therefore, the intial stress state ($\tau_{octp}$, $\sigma'_{mp}$) for plastic deformation is given by solving eq.(4.4.69) and eq.(4.4.56) simultaneously. Then we get the following initial condition:

$$v^p = 0, \ \gamma^p_{oct} = 0 \quad \text{at} \quad \ln \frac{\sigma'_m}{\sigma'_{m0}} = - \frac{(1+e_0)\mu}{\lambda - \kappa} k \tag{4.4.71}$$

Solving eqs.(4.4.70) with the initial condition given by eq.(4.4.71), we get stress-plastic strain relation as:

$$v^p = - \frac{\lambda - \kappa}{\lambda} \ln \frac{\dfrac{1}{\mu} - k - \dfrac{\lambda}{(1+e_0)\mu} \ln \dfrac{\sigma'_m}{\sigma'_{m0}}}{\dfrac{1}{\mu} + \dfrac{\kappa}{\lambda - \kappa} k}$$

$$\gamma^p_{oct} = - \frac{\dfrac{\lambda - \kappa}{3\lambda}}{\dfrac{\lambda - \kappa}{(1+e_0)\mu} - k} \ln \frac{\dfrac{1}{\mu} - k - \dfrac{\lambda}{(1+e_0)\mu} \ln \dfrac{\sigma'_m}{\sigma'_m}}{\dfrac{1}{\mu} + \dfrac{\kappa}{\lambda - \kappa} k} \tag{4.4.72}$$

The graphical explanation of these deductions is given in Fig.4.27. Elastic volumetric strain is given from eq.(4.3.12) as:

$$dv^e = \frac{\kappa}{1 + e} \frac{d\sigma'_m}{\sigma'_m} = \frac{\kappa}{(1+e_0)(1 - \mu k) - \lambda \ln \dfrac{\sigma'_m}{\sigma'_{m0}}} \frac{d\sigma'_m}{\sigma'_m} \tag{4.4.73}$$

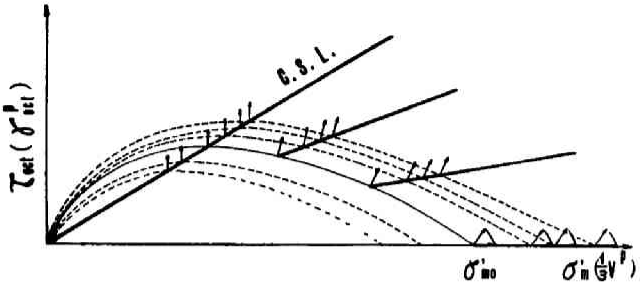


Fig.4.27. Stress paths and plastic strain increments ($\tau_{oct}/\sigma'_m$-constant shear)

Assuming that the initial state point of $\tau_{oct}/\sigma'_m$-constant test is on the state surface, namely:

$$v^e = 0 \quad \text{at} \qquad \ln \frac{\sigma'_m}{\sigma'_{m0}} = - \frac{(1+e_0)\mu}{\lambda - \kappa} k \tag{4.4.74}$$

we get:

$$v^e = - \frac{\kappa}{\lambda} \ln \frac{\frac{1}{\mu} - k - \frac{\lambda}{(1+e_0)\mu} \ln \frac{\sigma'_m}{\sigma'_{m0}}}{\frac{1}{\mu} + \frac{\kappa}{\lambda - \kappa} k} \tag{4.4.75}$$

Then, the total volumetric strain is derived from eqs.(4.4.72) and eq.(4.4.75) as:

$$v = - \ln \frac{\frac{1}{\mu} - k - \frac{\lambda}{(1+e_0)\mu} \ln \frac{\sigma'_m}{\sigma'_{m0}}}{\frac{1}{\mu} + \frac{\kappa}{\lambda - \kappa} k} \tag{4.4.76}$$

From eqs.(4.4.72) and eq.(4.4.76). we get:

$$\gamma^p_{oct} = \frac{\frac{\lambda - \kappa}{3\kappa}}{\frac{\lambda - \kappa}{(1+e_0)\mu} - k} v \tag{4.4.77}$$

It is noteworthy that eq.(4.4.77) is not defined for $k$=0, because the yield surface is cornered at the stress state $k$=0. The linearity of

the relation between the total shear strain and total volumetric strain for $\tau_{oct}/\sigma_m'$-constant test is supported by the experimental data by Roscoe and Poorooshasb (1963). Substituting eq.(4.4.76) into eq. (4.4.54), we get the relationship between the strains of normally consolidated clays tested by the same stress ratio $\tau_{oct}/\sigma_m'$ under the condition of undrained and $\tau_{oct}/\sigma_m'$-constant shear as follows:

$$\frac{3\lambda}{\kappa\mu}(\gamma_{oct})_u = -\ln\{\frac{(1+e_0)\mu}{3\lambda}(\frac{v}{\gamma^p_{oct}})_k\} \tag{4.4.78}$$

where the suffix $u$ and $k$ denote respectively "undrained" and "$k$-constant" shear. Assuming the elastic component of shear strain to be negligibly small compared with the plastic component, eq.(4.4.78) may be rewritten as:

$$\frac{3\lambda}{\kappa\mu}(\gamma_{oct})_u = -\ln\{\frac{(1+e_0)\mu}{3\lambda}(\frac{v}{\gamma_{oct}})_k\} \tag{4.4.79}$$

Inversely, if the two constants are determined from the undrained test and the $k$-constant test assuming that eq.(4.4.79) is valid, the so-obtained two constants may be slightly different from $\lambda/\kappa\mu$ and $(1+e_0)\mu/\lambda$, respectively, because of the existence of the elastic component of shear strain. Even in the case of the different value of $e_0$ for the undrained and $k$-constant test, eq.(4.4.79) is expected to be approximately valid provided the range of $\sigma_m'$ is not so wide that $(\lambda-\kappa)/(1+e_0)\mu$ and $\lambda/(1+e_0)\mu$ cannot be considered as the constants. In other words, it is valid while the stress $\sigma_m'$ is within the range where, for the clays normally consolidated under various pressures and stressed under the undrained condition so-called failure envelope, can be considered as a straight line and their stress paths can be considered similar. The author believes that eq.(4.4.79) may give the theoretical confirmation to the work of Roscoe and Poorooshasb (1963).

*$K_0$-consolidation*

The clays dealt with in this chapter are those which are isotropically pre-consolidated with the pressure of $\sigma_m'$ . When the clays whose state points are on the state surface are sheared in the conventioanl triaxial apparatus by keeping the stress ratio $k=\tau_{oct}/\sigma_m'$ at the certain value of $k_0$, it is experimentally confirmed that the lateral deformations of the specimen do not occur. Such a sort of shear process is generally called $K_0$-consolidation which is a special case of anisotropic consolidation. In $K_0$-consolidation, lateral strain $\varepsilon_2$ and $\varepsilon_3$ are to be zero and therefore we get:

$$\gamma_{oct}^p = \gamma_{oct} = \frac{\sqrt{2}}{3}\varepsilon_1$$
$$v = \varepsilon_1 \tag{4.4.80}$$

then:

$$\frac{\gamma_{oct}^p}{v} = \frac{\sqrt{2}}{3} \tag{4.4.81}$$

Substituting eq.(4.4.81) into eq.(4.4.77), we get:

$$\frac{\lambda - \kappa}{\lambda} = \sqrt{2}\{\frac{\lambda - \kappa}{(1+e_0)\mu} - k\} \tag{4.4.82}$$

and the true value of $k_0$ in $K_0$-consolidation is given by solving eq. (4.4.82) as follows:

$$k_0 = (\lambda - \kappa)\{\frac{1}{(1+e_0)\mu} - \frac{1}{\sqrt{2}\ \lambda}\} \tag{4.4.83}$$

Representing $\sigma_3'/\sigma_1'$ as $K$, we get:

$$k_0 = \frac{\sqrt{2}(1 - K_0)}{1 + 2K_0} \tag{4.4.84}$$

and then $K_0$-value is derived from eq.(4.4.83) and eq.(4.4.84) as:

$$K_0 = \frac{\dfrac{3\lambda - \kappa}{2\lambda} - \dfrac{\lambda - \kappa}{\sqrt{2}(1+e_0)\mu}}{\dfrac{\sqrt{2}(\lambda - \kappa)}{(1+e_0)\mu} + \dfrac{\kappa}{\lambda}} \tag{4.4.85}$$

## 4.5 Extension of the Theory to Sands and Silts

Clays, sands and silts are all the granular materials and then should behave mechanically ruled by the similar principles. The theory for clays mentioned above is based on the experimental laws about consolidation and dilatancy. If these assumptions are adaptable to sands and silts, the discussion for clays can be extended to all sorts of soils.

The linear relation between $e$ and $\ln\sigma_m'$ is valid for normally consolidated sands as shown in Fig.4.28 given by Vesić and Clough (1968). But it should be noted that sand is ordinarily in the overconsolidated state and becomes to be in the normally consolidated state by the application of hydrostatic effective pressure excessively large cimpared with clay. The attempt to point out the essential difference between the mechanical state of clay and sand in the normally consolidated state by means of the fact that the additional hydrostatic pressure to the normally consolidated sand causes crushing of sand grains might not prove successful. The additional hydrostatic effective pressure applied to normally consolidated clay crushes the aggregated clusters of flocculent structure into small clusters. In the author's opinion, the sand grains correspond to the aggregated clusters of clay, not to clay particles. Therefore, the author do not consider that there is any essential difference between the representation of their mechanical behaviors.

Normally consolidated state may be defined as the state that the maximum void ratio is maintained for the applied hydrostatic pressure. In this sense, normally consolidated state is quite sensitive to disturbance. The skelton of soil particles under normally consolidated state is prone to decrease the void ratio with

small disturbances.

Usually sands may be in overconsolidated state and this is supported by the undrained stress paths of sands as shown in Fig.4.29.

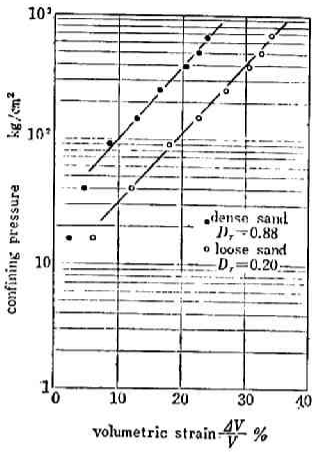


Fig.4.28. Consolidation of sands (after Vesić and Clough)

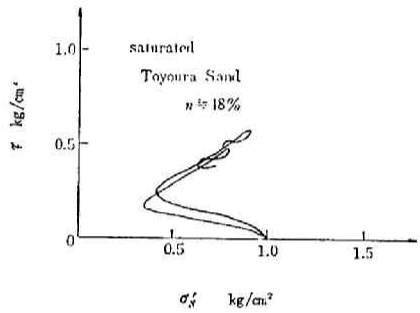


Fig.4.29. Undrained stress paths of loose sand

Silts may be in similar state judging from the data given by Schultze and Horn (1965). It is hard to put sands into normally consolidated state under the usual cell pressure, and therefore shear tests of normally consolidated sands are hardly carried on with a few exceptions. The stress paths of normally consolidated sands under undrained shear given by Bishop, Webb and Skinner (1965) are quite similar to those of normally consolidated clays. These facts suggest that the assumption on dilatancy. eq.(4.2.4) is adaptable to sands. Because of experimental difficulty, it can hardly be proved to be so directly by $\sigma'_m$-constant tests of normally consolidated sands. If the theory is adaptable to sands, the shearing properties of ordinary sands under $\sigma'_m$-constant condition should be similar to those of overconsolidated clays shown in Fig.4.16 as QQ'T. $\sigma'_m$-constant test carried by Yagi (1968) is quite similar to QQ'T in Fig.4.16. Such a datum was also given by Frydman and Zeitlen (1969).

From those facts, it can be concluded that the theory is adaptable to sands and silts. It is noteworthy that the theoretical state

paths of soils in overconsolidated state are quite similar to those given by Rowe (1962).

Ordinary sand compressed in the conventional triaxial apparatus under drained condition decreases its volume in the beginning of the shear process and then, with the increase of shear stress, tends to dilate. This tendency can be easily reasoned by the curve $QK_1M_1$ in Fig.4.15. Based on these considerations, it can be suggested that the so-called negative and positive dilatancy for sand and heavily overconsolidated clay do not have important physical meanings, and are not the inherent nature of sand and overconsolidated clay, because the negative dilatancy of them does not take place in the extension drained test by the conventional triaxial apparatus as shown by Tatsuoka (1971).

Schofield and Wroth (1968) extended their theory to sand which they call "*Granta Gravel*" in order to distinguish their idealized sand from the real sand. Barden, Khayatt and Wightman (1969) showed that the deformation of sand, which should be completely reversible in the range of considerable stress according to the author's theory, consisted of recoverable and irreversible components. And they suggested the latter component of deformation of sand was due to the grain to grain slip behavior. Rowe (1969) has also pointed out the slip component of deformation of sand during unloading.

In the author's opinion, this irreversible deformation is arising from the considerablly unstable packing of sand grains at the initial state, and this instability of packing can be eliminated by the application of small amplitude cyclic loading, for instance, vibration. Murayama (1964) gave the experimental data which seem to support this idea. This troublesome difficulty in the extension of the theory to granular materials does exist even in the mechanical behavior of overconsolidated clay, and prevents expanding the theory to the case of cyclic loading.

## 4.6 Stress-Strain-Temperature Relations

The discussion mentioned above is restricted by the condition: (a) sufficiently slow strain rate and (b) constant temperature. Here we examine the influence of temperature on the stress-strain relations of the clay based on some of the experimental facts. The influence of temperature on the consolidation characteristics was studied by Matsuo and Kamon (1970). Their conclusion is shown in Fig.4.30 briefly. From Fig.4.30, we can realize that the temperature effect on the consolidation process causes the parallel shifts of the normal consolidation line and swelling line in the order of temperature. Then the coefficients $\lambda$ and $\kappa$ are independent of temperature. It should be noted that the experiments were carried without varying temperature during the tests. Therefore our discussion should be limited to the constant temperature condition. Parallel shifts of the normal consolidation line and swelling line can be described by making $e_0$ a function of temperature $T$:

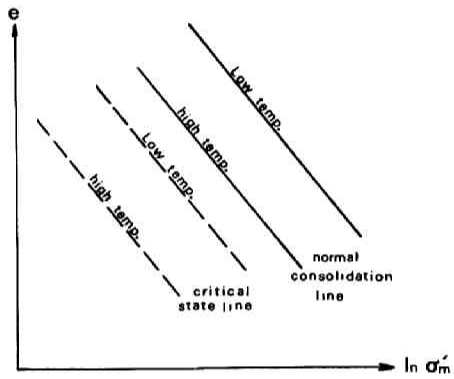


Fig.4.30. Influence of temperature (after Matsuo and Kamon)

$$e_0 = e_0(T) \tag{4.6.1}$$

In order to confirm the temperature independence of the consolidation coefficients $\lambda$ and $\kappa$, let us examine the relationship between the normal consolidation line and the critical state line on $e$-$\sigma'_m$diagram. The critical state is nothing but the perfectly plastic state of clay and therefore is the special state of elastic-plastic state of clay then it should be on the state surface representing the stress-void ratio relation of clay in elastic-plastic state.

It has already shown that the critical state line on the

$e$-$\ln\sigma_m'$ diagram is nothing but the shifted normal consolidation line by amount of $\lambda-\kappa$ to the direction parallel to $e$-axis. If the coefficients $\lambda$ and $\kappa$ are independent of temperature $T$, the distance between the normal consolidation line and the critical state line on $e$-$\ln\sigma_m'$ diagram must be also independent of temperature. The experimental data given by Matsuo and Kamon (Fig.4.30) show that this reasoning is satisfactorily correct.

The influence of the temperature on the dilatancy characteristics has not yet been detected directly. But we have some experimental works for constant volume shear tests of the clay.

The stress path for the constant volume shear test of the normally consolidated clay in elastic-plastic state is given by eq. (4.3.4). The constant volume shear test data under the condition of various constant temperatures are given by Matsuo and Kamon (1970) as shown in Fig.4.31 briefly. It is apparent that the coefficient $\lambda/(1+e_0)\mu$ for high temperature is larger than that for low temperature. But for the consolidation characteristics, we have already realized, $e_0$ is a monotonously decreasing function of temperature $T$ and $\lambda$ is independent of temperature. Therefore the coefficient $\mu$ should be highly monotonously increasing function of temperature as follows:

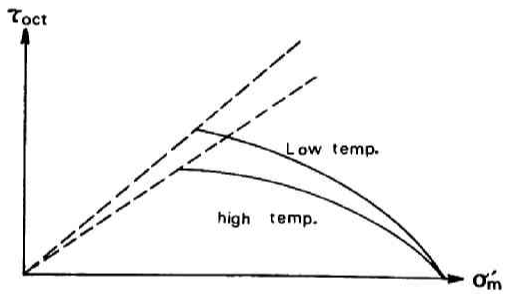


Fig.4.31. Influence of temperature (after Matsuo and Kamon)

$$\mu = \mu(T) \tag{4.6.2}$$

Eq.(4.6.2) can be confirmed by Matsuo and Kamon's experiments data that the stress ratio $\tau_{oct}/\sigma_m'$ of the critical state line for clay sheared under the constant volume condition is decreasing in accordance with temperature. Therefore from eq.(4.4.29), we can

derive eq.(4.6.2). Eq.(4.6.2) shows that the dilatancy effect is eminent for the case under high temperature. Introducing eqs.(4.6.1) and (4.6.2) into the stress-strain relations represented by eqs. (4.4.17) and (4.4.27), we get the incremental stress-strain-temperature relations which are applicable for the case of constant temperature as follows:

$$d\varepsilon^{p}_{ij} = \frac{\mu(T)}{3\sigma'_m}\frac{1+e_0(T)}{1+e_i(T)}\left[\left\{\frac{\lambda-\kappa}{[1+e_0(T)]\mu(T)} - \frac{\tau_{oct}}{\sigma'_m}\right\}\delta_{ij}\right. \tag{4.6.3}$$

$$\left. + \frac{1}{\tau_{oct}}(\sigma'_{ij} - \sigma'_m\delta_{ij})\right]\left[d\sigma'_m + \frac{d\tau_{oct}}{\frac{\lambda-\kappa}{[1+e_0(T)]\mu(T)} - \frac{\tau_{oct}}{\sigma'_m}}\right]$$

$$d\varepsilon^{e}_{ij} = \frac{1}{3}\frac{\kappa}{1+e_i(T)}\frac{d\sigma'_m}{\sigma'_m}\delta_{ij} \tag{4.6.4}$$

where $e_i$ is also the monotonously decreasing function of temperature like $e_0$. The incremental stress-strain-temperature relations given by eqs.(4.6.3) and (4.6.4) are adaptable only to analyze the deformation of the clay stressed under the conditions of constant temperature and sufficiently slow loading rate. The deformation of clay stressed with the changing temperature cannot be represented by these equations, because the normality rule in such a case may not be valid for elastic-plastic materials. In order to estimate the influence of changing temperature or rate dependent viscous behavior of clay, new flow rule theory based on the thermodynamical assumptions is necessary. In other words, such a problem cannot be analyzed until the thermoplasticity theory is constructed. In this thesis the failure condition of frictional material was derived from the concept of normality in plasticity. The stress condition of the critical state given by eq.(4.4.29) seems to be the failure condition of the frictional material, but none of the coefficients in the right-hand side of eq.(4.4.29) do not relate to the frictional behavior. Generally the granular material like clay is considered to behave as a frictional material. It seems to the author that macroscopic

frictional behavior of granular material might be merely apparent behavior. In other words, soils in elastic-plastic state might resist to the applied load mainly by the deformation of the frame work constructed with the soil particles accompanied with the rotation of soil particles, not mainly by interparticle frictional slide. The soil may resist to the load by the interparticle frictional slide, but such a resistence is that of the soil in elastic state. It is inconsistent to consider the interparticle frictional slide, which is irreversible process, in so-called elastic state. Indeed soil deforms plastically even in unloading process. This irreversible process of the soil in so-called elastic state makes soil mechanics very complex. At the present stage, we cannot avoid to neglect, in this theory, this irreversible process in the so-called elastic state.

## 4.7 Conclusions

In this investigation, mechanical states of isotropically pre-consolidated clay are shown to be governed by a logically self-consistent theory based on the concepts of state surface and swelling wall derived from the characteristics of consolidation and dilatancy of clays in elastic and elastic-plastic state. For example, the mechanical behaviors of clay stressed under various conditions are derived.

Combining the concepts of the state surface and swelling wall and the concept of normality, fundamental equations of incremental stress-strain relations of isotropically consolidated clays in elastic and elastic-plastic state are presented.

Based on the incremental stress-strain relations, the concept of critical state is clarified. And integration of the incremental stress-strain relations leads to the various stress-strain relations with the various restricting conditions. These stress-strain relations are to be used as the fundamental equations in the analyses of practical problems which the soil engineers often encounter in their routine works concerning the design and construction of soil structures.

In the last part of this chapter, the theory is shown to be applicable not only to clay but also to sand and silt. The influence of temperature on these stress-strain relations is also discussed and the constitutive equations are derived.

# CHAPTER 5

# CONSTITUTIVE RELATIONS FOR ANISOTROPICALLY CONSOLIDATED SOILS

## 5.1 Introduction

In this chapter constitutive relations for anisotropically consolidated soils are derived by means of the theoretical expansion of the results presented in Chapter 4. We have the isotropically consolidated clay only in the laboratory. All the natural clay deposits are consolidated under the anisotropic stress condition. Therefore we have to get a systematic understanding of the mechanical behavior especially of the constitutive relations of anisotropically consolidated soils. In this chapter, the anisotropically consolidated clays are of interest. But as discussed in Chapter 4, the theory is considered to be adaptable for sands and silts.

The eminent nature of anisotropically consolidated clay is that it behaves mechanically in quite different styles depending on the loading conditions in spite of the same conditions of stress invariants and void ratio. This difference can be easily examined by comparing the compression and extension test results of anisotropically consolidated clay stressed in the conventional triaxial apparatus.

## 5.2 State Surface and Swelling Wall

### 1. State Surface and Swelling Wall

Let us consider the anisotropically consolidated clay which is consolidated by keeping the stress ratio $\tau_{oct}/\sigma_m'$ at the constant value of $k$ on the process of normal consolidation. The characteristics of consolidation of anisotropically consolidated clays are similar to those of isotropically consolidated clays, as shown by Walker and Reymond (1969). They show that the $e$-$\ln\sigma_m'$ lines for the various stress ratio $\tau_{oct}/\sigma_m'$ are parallel and coincide each other by shifting them. Then, assuming that the anisotropically consolidated clay is an elastic-plastic material, the infinitesimal void ratio changes due to the consolidation, i.e., $\tau_{oct}/\sigma_m'$-constant deformation

process, of the clay in state of elastic-plastic and elastic states are respectively given as follows:

$$de = -\lambda d(\ln\sigma_m') \quad : \text{ elastic-plastic state} \qquad (5.2.1)$$

$$de = -\kappa d(\ln\sigma_m') \quad : \text{ elastic state} \qquad (5.2.2)$$

where $\lambda$ and $\kappa$ are the obliques of normal consolidation line and swelling line on $e$-$\ln\sigma_m'$ plot. In Chapter 4, the dilatancy is characterized by:

$$de = -(1 + e_0)\mu d(\frac{\tau_{oct}}{\sigma_m'}) \quad : \text{ elastic-plastic state} \qquad (5.2.3)$$

$$de = 0 \quad : \text{ elastic state} \qquad (5.2.4)$$

But for the anisotropically consolidated clay, eq.(5.2.3) is conside considered to be altered in the form as:

$$de = \mp(1 + e_0)\mu d(\frac{\tau_{oct}}{\sigma_m'}) \quad : \text{ elastic-plastic state} \qquad (5.2.5)$$

where the upper and lower signs are corresponding to the cases in which the applied stress ratio $\tau_{oct}/\sigma_m'$ is greater or smaller than the initial value $k$ of the stress ratio respectively. These two loading states are defined here as the active state and passive state respectively. The compression test and extension test in conventional triaxial apparatus are corresponding to the active and passive state respectively. The alternation of eq.(5.2.3) into eq.(5.2.5) will be rationalized later in this chapter.

A specimen of anisotropically consolidated clay stressed by the application of increasing stress ratio $\tau_{oct}/\sigma_m'$ is to reach the critical state. On the other hand, when the specimen is stressed by decreasing stress ratio $\tau_{oct}/\sigma_m'$ from the initial value of $k$, we say that it is in the passive state. On this passive shear process of clay specimen, the value of applied stress ratio $\tau_{oct}/\sigma_m'$ becomes smaller than $k$ and then reaches zero. And after reaching the state of $\tau_{oct}/\sigma_m'=0$, the direction of the maximum principal stress rotates 90° in the case of extension test in conventional triaxial apparatus. Then with the progress of extension test, the stress ratio $\tau_{oct}/\sigma_m'$

begins to increase (because $\tau_{oct}$ is defined as non-negative) and finally reaches the critical state value. But here, for the convenience of mathematical expressions, we define the negative value of $\tau_{oct}$ in the case of passive loading after the stress ratio $\tau_{oct}/\sigma'_m$ reaches the value of zero.

From eqs.(5.2.1)-(5.2.5). we get the differential equations of state surface and swelling wall for anisotropically consolidated clay as follws:

$$de = -\lambda\frac{d\sigma'_m}{\sigma'_m} \mp (1+e_0)\mu\left(\frac{d\tau_{oct}}{\sigma'_m} \quad \frac{\tau_{oct}}{\sigma'_m} - \frac{d\sigma'_m}{\sigma'_m}\right)$$

: elastic-plastic state (5.2.6)

$$de = -\kappa\frac{d\sigma'_m}{\sigma'_m}$$

: elastic state (5.2.7)

These infinitesimal void ratio changes are the functions of stress invariants even for the anisotropically consolidated clay. It is reasonable to consider that the deformation of the initially isotropic material is represented by a function of the stress invariants. But it is apparent that the anisotropically consolidated clay cannot be assumed to be intially isotropic material because the clay particles of anisotropically consolidated clay with no lateral displacement tend to be aligned parallel. Therefore there is no reason to rationalize the deformation of anisotropically consolidated clay to be represented by the stress invariants. Nevertheless, we assume the validity of eqs.(5.2.6) and (5.2.7) here, hoping that the microscopic anisotropy of clay skelton does not affect seriously on the macroscopic mechanical behavior of anisotropically consolidated clay.

The boundary condition for eqs.(5.2.6) and (5.2.7) is given by the initial state of normally anisotropically consolidated clay as follows:

$$\tau_{oct}/\sigma'_m = \tau_{oct0}/\sigma'_{m0} = k$$

$$\sigma'_m = \sigma'_{m0}$$

$$e = e_0$$

Then, we get the general stress-void ratio relations for the anisotropically pre-consolidated clay as follows:

$$e - e_0 + \lambda \ln \frac{\sigma'_m}{\sigma'_{m0}} \pm (1 + e_0)\mu\left(\frac{\tau_{oct}}{\sigma'_m} - k\right) = 0$$

: elastic-plastic state (5.2.8)

$$e - e_0 + \kappa \ln \frac{\sigma'_m}{\sigma'_{m0}} = 0$$

: elastic state (5.2.9)

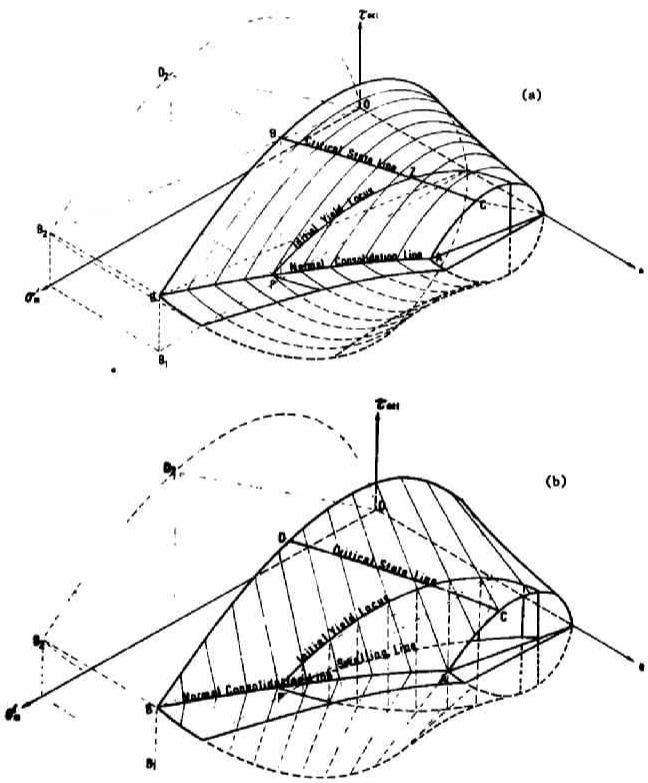


Fig.5.1(a),(b).

Isometric view of State surface of anisotropically consolidated clay

Eqs.(5.2.8) and (5.2.9) give the state surface and swelling wall whose physical meanings are discussed in Chapter 4. The isometric view of state surface is shown in Figs.5.1(a),(b) and that of wetter side of swelling wall is shown in Fig.5.2.

As presented in Chapter 4, the mechanical state of elastic limit is represented by the intersection of state surface and swelling wall as shown in Figs.5.1(a),(b) and 5.2. Eliminating the void ratio from eqs.(5.2.8) and (5.2.9), we get the stress condition for the initial yielding as follows:

$$\pm\left(\frac{\tau_{oct}}{\sigma'_m} - k\right) + \frac{\lambda - \kappa}{(1+e_0)\mu} \ln \frac{\sigma'_m}{\sigma'_{m0}} = 0 \qquad (5.2.10)$$

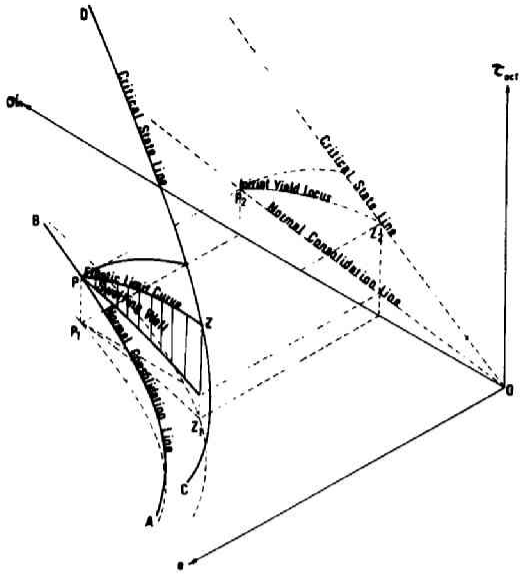


Fig.5.2. Swelling wall of anisotropically consolidated clay (wetter side)

2. State Paths under Various Conditions

*Undrained Shear*

The initial state of normally consolidated clay anisotropically compressed with the pressure of $\sigma'_{m0}$ keeping the stress ratio $\tau_{oct}/\sigma'_m$ constant is as follows:

$$e = e_0$$

$$\sigma'_m = \sigma'_{m0}$$

$$\frac{\tau_{oct}}{\sigma'_m} = \frac{\tau_{oct0}}{\sigma'_{m0}} = k$$

The initial state of overconsolidated clay rebounded from the normally consolidated state with the constant stress ratio $\tau_{oct}/\sigma'_m = k$ is given by:

$$e = e_i \geqq e_0$$

$$\sigma'_m = \sigma'_{mi} \leqq \sigma'_{m0}$$

$$\frac{\tau_{oct}}{\sigma'_m} = \frac{\tau_{octi}}{\sigma'_{mi}} = k$$

Then the state points of normally and over consolidated clay should

be on the swelling wall as shown in Fig.5.3. In the case of anisotropically consolidated clay, the state points of over-consolidated clay are not necessarily on the swelling curve lying on the $\tau_{oct}/\sigma'_m=k$ plane. For instance, on the swelling process of $K_0$-consolidated clay with no lateral displacement, the stress ratio $\tau_{oct}/\sigma'_m$ decreasingly changes as shown by Henkel and Sowa (1963). The initial state point on the swelling wall passing through the point ($\tau_{oct0}$, $\sigma'_{m0}$, $e_0$) is represented by ($\tau_{octi}$, $\sigma'_{mi}$, $e_i$) where

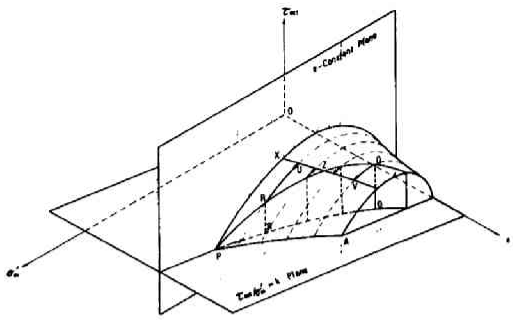

Fig.5.3. State paths in undrained shear

$$\frac{\tau_{octi}}{\sigma'_{mi}} = k_i \tag{5.2.11}$$

and

$$e_i = e_0 - \kappa \ln \frac{\sigma'_{mi}}{\sigma'_{m0}} \geqq e_0 \tag{5.2.12}$$

For normally consolidated clay, it follows:

$$e_i = e_0$$

$$\sigma'_{mi} = \sigma'_{m0}$$

$$\tau_{octi} = \tau_{oct0}$$

It is apparent that the state path of anisotropically consolidated clay stressed under undrained condition, i.e., with the constant void ratio $e_i$ is given by the intersection between $e=e_i$ plane and the swelling wall or the state surface. The equation representing the swelling wall is given by eq.(5.2.9), and from eqs. (5.2.9) and (5.2.12) the intersection of the swelling wall and $e=e_i$ plane is given as:

$$e = e_i$$
$$\sigma'_m = \sigma'_{mi} \tag{5.2.13}$$

Eqs.(5.2.13) show a line normal to the $e$-$\sigma'_m$ plane. As mentioned above, the state point of a volume element of clay in the purely elastic state is on the swelling wall and after it reaches the elastic limit curve which is given as the intersection of swelling wall and state surface the clay element begins to yield with work-hardening or work-softening effect. Then the line given by eqs. (5.2.13) must lead to the intersection of state surface and $e=e_i$ plane across the elastic limit curve. The initial yield locus given as the projection of the elastic limit curve onto the stress space given by eq.(5.2.10).

The height $\tau_{octp}$ of the line represented by eq.(5.2.13) is given from eqs.(5.2.10) and (5.2.13) as follows:

$$\tau_{octp} = \sigma'_{mi}\{k \mp \frac{\lambda - \kappa}{(1+e_0)\mu} \ln \frac{\sigma'_{mi}}{\sigma'_{m0}}\} \tag{5.2.14}$$

and depends on the value of $\sigma'_m$ . In Fig.5.3, the normal anisotropic consolidation curve is AP and the point P on the normal consolidation curve is ($e=e_0$, $\sigma'_m=\sigma'_{m0}$, $\tau_{oct}=\tau_{oct0}$). XZV lying on the state surface is the curve showing the perfectly plastic state and named the critical void ratio line by Roscoe, Schofield and Wroth (1958), and renamed the critical state line by Roscoe, Schofield and Thurairajah (1963). The projection of this critical state line onto $\tau_{oct}$-$\sigma'_m$ plane is the straight line passing the origin. Further consideration about the critical state line is given later.

For normally consolidated clay, eq.(5.2.14) becomes

$$\tau_{octp} = k\sigma'_{m0} = \tau_{oct0}$$

with $\sigma'_{mi}=\sigma'_{m0}$, then it can be concluded that there is no purely elastic state for normally consolidated clay stressed under the undrained condition. Now, the state path of the element of yielding

clay is represented by the intersection between the state surface and $e=e_i$ plane under undrained condition. Such a state path can be derived from eq.(5.2.8) by substituting $e=e_i$ as follows:

$$e_i - e_0 + \lambda \ln \frac{\sigma'_m}{\sigma'_{m0}} \pm (1 + e_0) \left( \frac{\tau_{oct}}{\sigma'_m} - k \right) = 0 \qquad (5.2.15)$$

Eq.(5.2.15) shows that the state path of clay stressed under undrained condition is dependent on the initial value of void ratio $e_0$. In Fig. 5.3, the state paths lying on the state surface for active loading are represented by PX, RU and VQ. For normally consolidated clay, $e_i=e_0$ and therefore eq.(5.2.15) becomes

$$\frac{\tau_{oct}}{\sigma'_m} = \mp \frac{\lambda}{(1+e_0)\mu} \ln \frac{\sigma'_m}{\sigma'_{m0}} + k \qquad (5.2.16)$$

giving the state path PX for the active loading state.

On the loading process, the elastic-plastic state path mentioned above is to reach the final point on the critical state line which represents the perfectly plastic state, i.e., the state parameter $\tau_{oct}$, $\sigma'_m$ and $e$ do not change any more at the perfectly plastic state. Fig.5.3 shows that the critical state line lying on the state surface for the active loading state intersects with the elastic limit curve at the point Z. An overconsolidated clay specimen whose initial state point is just under Z cannot experience the elastic-plastic state on the active shearing process under undrained condition, because the state point arrives at the critical state line immediately when it reaches the elastic limit curve after experiencing the purely elastic state. The stress path is defined as the projection of the state path onto the stress space, for instance, the $\tau_{oct}$-$\sigma'_m$ plane, as shown in Fig.5.4. The projections of the state paths on $e$-$\sigma'_m$ diagram are also shown in Fig.5.5.

In the above discussion, the domain enclosed by state surface, $\tau_{oct}=0$ plane, $\sigma'_m=0$ plane and $e=0$ plane is considered to show the purely elastic state. Then, the plastic deformation should not be found even in the repeated loading and unloading process so far as

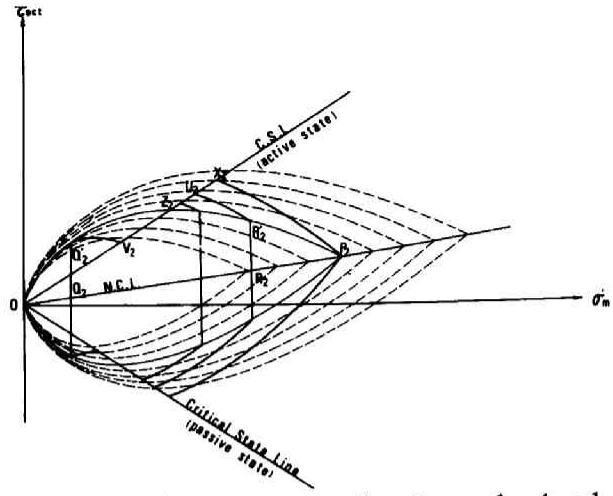


Fig.5.4. Stress paths in undrained shear

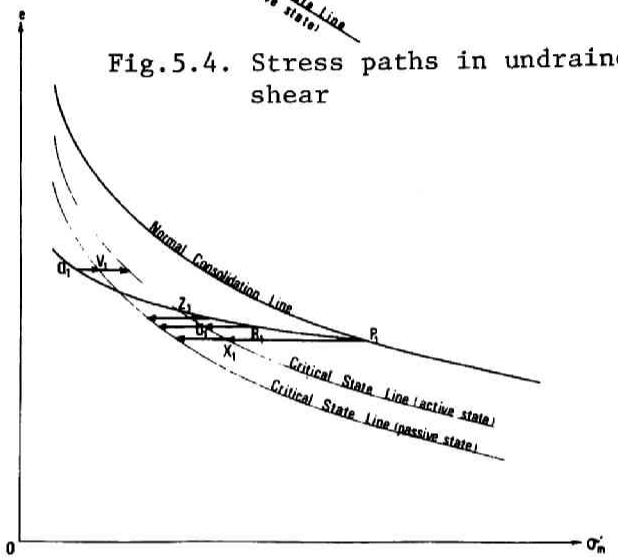


Fig.5.5. $e$-$\sigma_m'$ relations in undrained shear

the state point is in the elastic domain, i.e., on such a process the loading and unloading state path should coincide each other. However, on the contrary. experimental data given by Murayama and Kurihara (1969), Sangrey, Henkel and Esrig (1969) show that the induced pore pressure in the normally consolidated clay increases monotonously on the undrained shear process. This means that the state paths for loading and unloading process do not coincide each other and furthermore the state path shifts to the negative direction of $\sigma_m'$ axis in accordance with the repetition. To eliminate such a difficulty, only the loading processes with monotonously increasing shear strain are to be treated in this thesis.

The undrained state paths obtained in the above discussion are corresponding to the case of increasing shear stress from the initial state (active state). Let us consider the case of decreasing octahedral shear stress from the initial state of $\tau_{oct}=\tau_{octi}$ (passive state). Judging from the data on normally consolidated clay given by Skempton and Sowa (1963), the state path for this case seems to be represented by eq.(5.2.16) with the lower sign. This is the reason why the characteristics of dilatancy given by eq.(5.2.5) are assumed.

*Triaxial Drained Shear*

Generally speaking, the mean effective stress $\sigma_m'$ and octahedral shear stress $\tau_{oct}$ are able to be applied to clay specimen independently from each other under drained condition. The state path of a clay element in elastic-plastic state can be obtained by subsituting the applied stresses $\sigma_m'$ and $\tau_{oct}$ into eq.(5.2.8). Here, let us consider a few cases corresponding to some special stress paths. The stress path for the conventional triaxial drained test carried on by changing the axial stress with constant radial stress is given as follows:

$$\tau_{oct} = \sqrt{2}(\sigma_m' - \sigma_{mi}') + k\sigma_{mi}' \tag{5.2.17}$$

And for the loading system of changing radial stress with constant axial stress, the stress path is represented as:

$$\tau_{oct} = -\frac{1}{\sqrt{2}}(\sigma_m' - \sigma_{mi}') + k\sigma_{mi}' \tag{5.2.18}$$

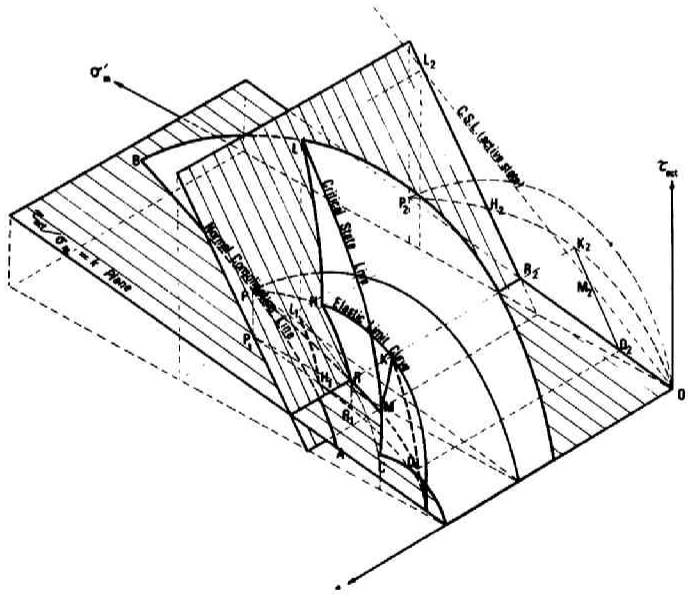


Fig.5.6. State paths in drained shear
($\sigma_a$; increase, $\sigma_r$; constant)

Eqs.(5.2.17) and (5.2.18) are both representing the planes in the state space. Then the state paths corresponding to such cases should be on these planes. From the above consideration, it can be concluded that: (a) the stress path in elastic state is given as the intersection of the plane defined by eq.(5.2.17) or (5.2.18) with the swelling wall given by eq.(5.2.9) and (b) the stress path in elastic-plastic state is given as the intersection of the plane defined by eq.(5.2.17) or (5.2.18) with the state surface given by eq.(5.2.8). These state paths, in the case of changing axial stress with constant radial stress, are shown in Fig.5.6 for the active loading systems with the condition $(\tau_{oct}/\sigma_m') \geqq k$. In Figs.5.7 (a) and (b), the stress paths of conventional drained tests of the clay wetter and drier than critical are shown respectively for the active loading state. Fig.5.8 shows the projections of these state paths for active loading, in the case of changing axial stress with constant radial stress, onto the $e$-$\sigma_m'$ plane. It is the well accepted experimental result that the volume of the heavily overconsolidated clay specimen or sand specimen decreases in the beginning of conventional drained compression test and then increases afterwards. Fig.5.8 suggests that such a

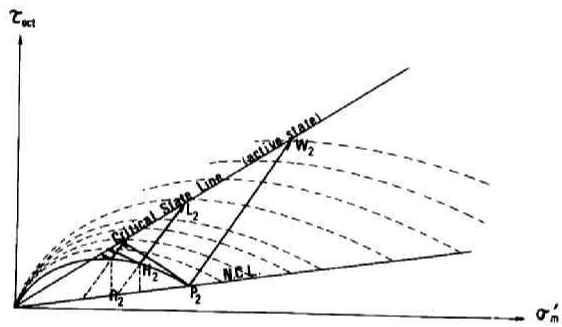


Fig.5.7(a). Stress paths of conventional drained tests (wetter than critical)

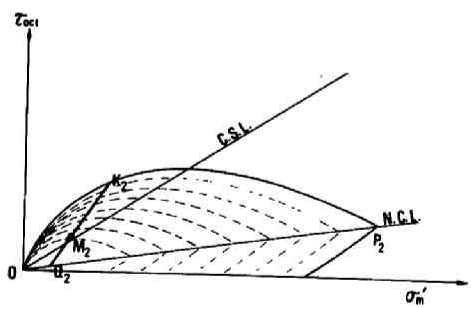


Fig.5.7(b). Stress paths of conventional drained tests (drier than critical)

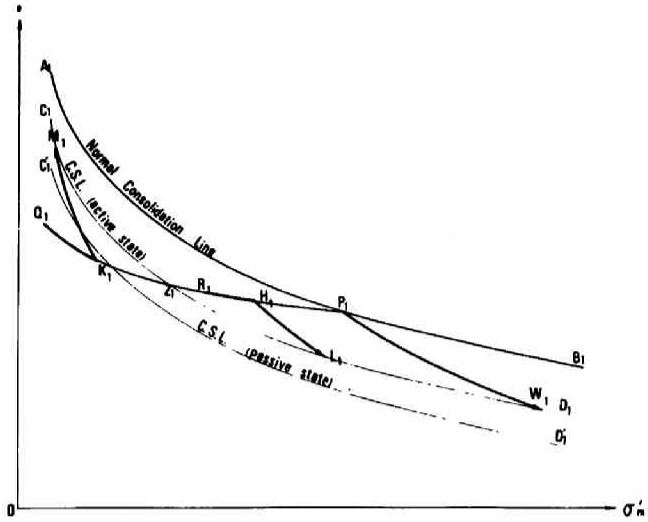


Fig.5.8. $e$-$\sigma'_m$ relations in drained shear ($\sigma_q$: increase $\sigma_r$: constant)

tendency is merely arising from the initial state and the stress path and is not the general mechanical behavior of such a soil stressed under the drained condition. In the text-books of soil mechanics, the volume increase and volume derease of soil induced by the shear stress are called positive and negative dilatancy respectively. But in the author's opinion, such a definition of dilatancy is not physically important. So-called positive and negative dilatancy do not represent the essential mechanical behavior of soil. They can be controlled by the combination of the initial state and the stress condition of loading system.

*$\sigma'_m$-constant Shear*

Now let us consider the case of drained shear under constant effective mean stress $\sigma'_m$ in which the stress path is confined on the plane defined as follows:

$$\sigma'_m = \sigma'_{mi} \quad (5.2.19)$$

where $\sigma'_{mi}$ is the initial effective mean stress. In elastic state, the state path is given by the intersection of the swelling wall and the plane given by eq.(5.2.19). And the state path in elastic-plastic state is given as the intersection between the

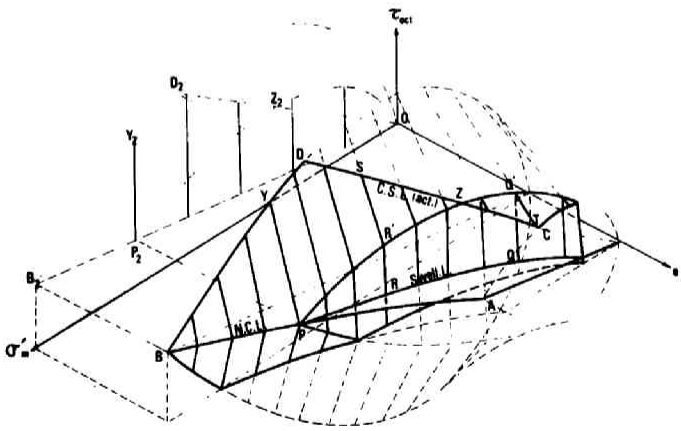


Fig.5.9. State paths in $\sigma'_m$-constant shear

state surface and $\sigma'_m=\sigma'_{mi}$ plane. The isometric view of these state paths for the active loading condition of $(\tau_{oct}/\sigma'_m)\geqq k$ is shown in Fig.5.9. Substituting $\sigma'_m=\sigma'_{mi}$ into eq.(5.2.8) for the stress condition $(\tau_{oct}/\sigma'_m)\geqq k$ leads to

$$e - e_0 + \lambda \ln \frac{\sigma'_{mi}}{\sigma'_{m0}} \pm (1 + e_0)\mu\left(\frac{\tau_{oct}}{\sigma'_{mi}} - k\right) = 0 \qquad (5.2.20)$$

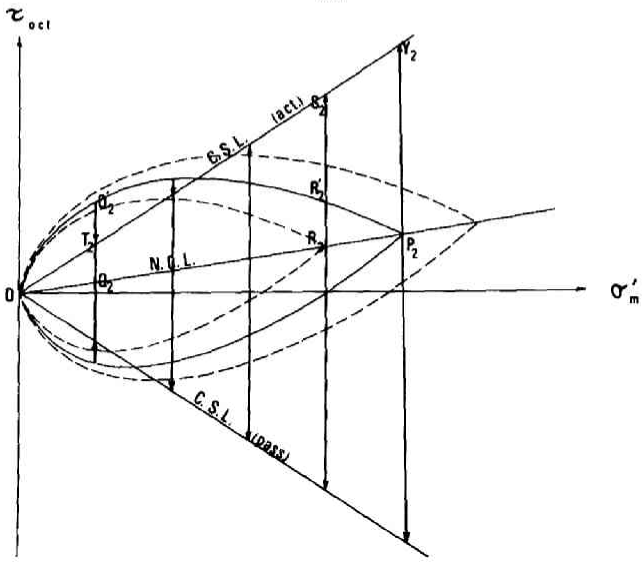


Fig.5.10. Stress paths in $\sigma'_m$-constant shear

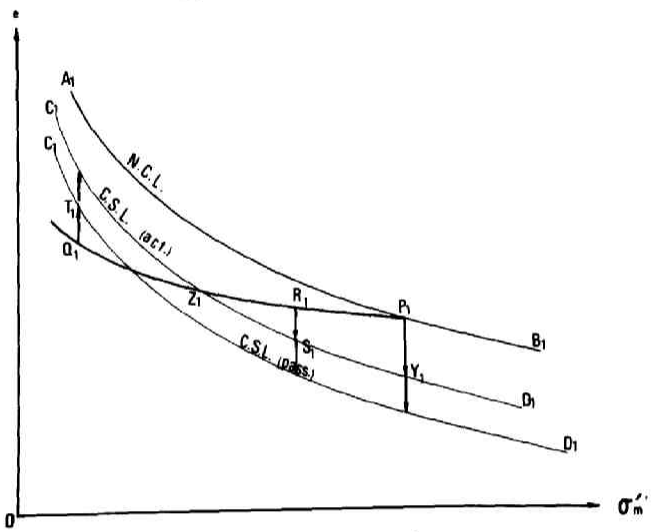


Fig.5.11. $e$-$\sigma'_m$ relations in $\sigma'_m$-constant shear

and it can be concluded that the void ratio $e$ and octahedral shear stress $\tau_{oct}$ are linearly related under constant effective mean stress $\sigma'_m$. Then we can see that the intersection of the state surface with the $\sigma'_m=\sigma'_{mi}$ plane is always a straight line regardless of $\sigma'_{mi}$. The intersecting point of $(\tau_{oct}/\sigma'_m)=k$ plane with this straight line is given from eq.(5.2.20) by eliminating the third term as follows:

$$e - e_0 + \lambda \ln \frac{\sigma'_{mi}}{\sigma'_{m0}} = 0 \qquad (5.2.21)$$

Eq.(5.2.21) shows that the intersecting point is to be on the normal consolidation curve. In other words, the straight lines given by eq.(5.2.20)

intersect with the normal consolidation curve passing through the point $(e_0, \sigma'_{m0})$ on $(\tau_{oct}/\sigma'_m)=k$ plane. Because the obliquities of these straight lines are represented by $\sigma'_{mi}/(1+e_0)\mu$, the obliquity of the line corresponding to $\sigma'_{mi}=0$ is to be zero. From the above consideration, it can be concluded that the state surface is constructed with inifnite number of straight lines whose obliquities increase in order of the value of $\sigma'_m$. Figs.5.10 and 5.11 shows the projections of $\sigma'_m$-constant state paths onto $\tau_{oct}$-$\sigma'_m$ plane and $e$-$\sigma'_m$ plane respectively.

## 5.3 Stress-Strain Relations

### 1. Critical State

The critical state is defined as the perfectly plastic state of soil. Roscoe, Schofield and Wroth (1958) defined the critical state by

$$\frac{de}{d\gamma_{oct}} = \frac{d\sigma'_m}{d\gamma_{oct}} = \frac{d\tau_{oct}}{d\gamma_{oct}} = 0$$

where $\gamma_{oct}$ is the octahedral shear strain. Assuming anisotropically consolidated clay to yield according to the associated flow rule, the the critical state can be defined as the stationary points of the yield loci on the $\tau_{oct}$-$\sigma'_m$ diagram. The initial yield locus is already given by eq.(5.2.10). After the initial yielding, the yield locus expands or shrinks according to the work-hardening or work-softening effect. Then the current yield loci are given by

$$\pm\left(\frac{\tau_{oct}}{\sigma'_m} - k\right) + \frac{\lambda - \kappa}{(1+e_0)\mu} \ln \frac{\sigma'_m}{\sigma'_{my}} = 0 \qquad (5.3.1)$$

where $\sigma'_{my}$ is the parameter representing the hardening effect.

Now the critical state, the stationary points of the yield loci, is given by differentiating eq.(5.2.1) as follows:

$$\left(\frac{\tau_{oct}}{\sigma'_m}\right)_{crit} = \frac{\lambda - \kappa}{(1+e_0)\mu} \quad \text{for} \quad \frac{\tau_{oct}}{\sigma'_m} \geqq k \text{ (active state)} \qquad (5.3.2)$$

$$\left(\frac{\tau_{oct}}{\sigma'_m}\right)_{crit} = -\frac{\lambda - \kappa}{(1+e_0)\mu} \text{ for } \frac{\tau_{oct}}{\sigma'_m} < k \text{ (passive state)} \qquad (5.3.3)$$

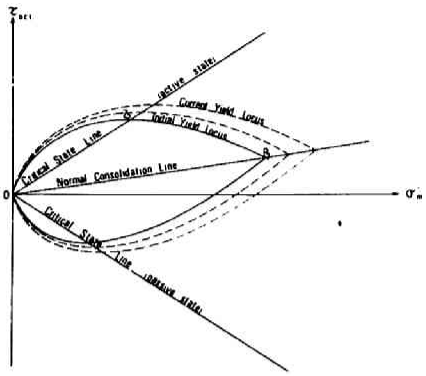


Fig.5.12(a). Critical state line and yield loci (wetter than critical)

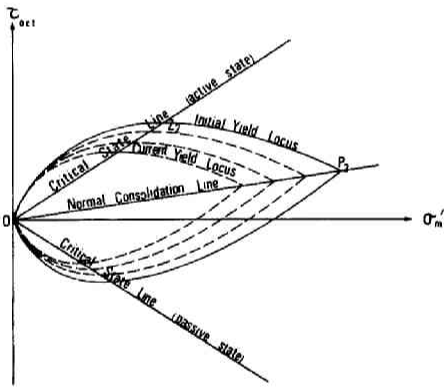


Fig.5.12(b). Critical state line and yield loci (drier than critical)

Figs.5.12(a),(b) show the critical state line and yield loci on $\tau_{oct}$-$\sigma'_m$ plane for the clays wetter and drier than critical respectively. It should be noted that the value of the stress ratio $\tau_{oct}/\sigma'_m$ at the critical state is independent of its initial value $(\tau_{oct}/\sigma'_m)_{initial}=k$. This leads to the conclusion that the critical states of clays anisotropically consolidated with various stress ratio $\tau_{octi}/\sigma'_{mi}$ are uniquely determined by

$$\frac{\tau_{oct}}{\sigma'_m} = \frac{\lambda - \kappa}{(1+e_0)\mu},$$ if the coefficients $\lambda$, $\kappa$, $\mu$ do not vary according to the value of $\tau_{octi}/\sigma'_{mi}$. In order to clarify the shape of the critical state line in the state space, eqs.(5.3.2) and (5.3.3) are to be substituted into eq.(5.2.8) representing the state surface as follows:

$$e - e_0 + \lambda \ln \frac{\sigma'_m}{\sigma'_{m0}} + \lambda - \kappa \mp k(1 + e_0)\mu = 0 \qquad (5.3.4)$$

Eq.(5.3.4) gives the projections of critical state lines onto the $e$-$\sigma'_m$ plane. The critical state line on the $e$-$\sigma'_m$ plane coincides to the shifted normal consolidation curve by the amount of $\lambda-\kappa \mp k(1+e_0)\mu$ parallel to the $e$-axis downward.

2. Stress-Strain Relations under Various Conditions

*Incremental Stress-Strain Relations*

From the current yield loci for anisotropically consolidated clay given by eq.(5.3.1), we get the plastic potential as follows:

$$f = \pm\left(\frac{\tau_{oct}}{\sigma'_m} - k\right) + \frac{\lambda - \kappa}{(1+e_0)\mu} \ln \frac{\sigma'_m}{\sigma'_{my}} \tag{5.3.5}$$

The intersection of the current yield surface with the Rendulic plane is shown in Fig.5.13.

By means of similar reducing process used in Chapter 4, the incremental stress-plastic strain relation is derived as:

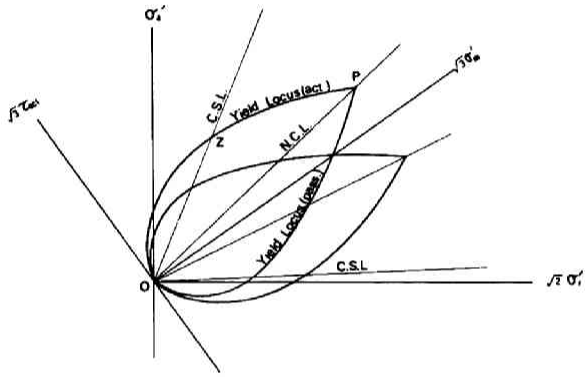


Fig.5.13. Yield locus in the Rendulic plane

$$d\varepsilon^p_{ij} = \frac{1+e_0}{1+e}\left[d\sigma'_m + d\tau_{oct}\Big/\left\{\frac{\lambda-\kappa}{(1+e_0)\mu} \mp \frac{\tau_{oct}}{\sigma'_m}\right\}\right] \frac{1}{3\sigma'_m}$$
$$\left[\left\{\frac{\lambda-\kappa}{(1+e_0)\mu} \mp \frac{\tau_{oct}}{\sigma'_m}\right\}\delta_{ij} \pm \frac{1}{\tau_{oct}}(\sigma'_{ij} - \sigma'_m\delta_{ij})\right] \tag{5.3.6}$$

where

$$e = e_0 - \lambda \ln \frac{\sigma'_m}{\sigma'_{m0}} \mp (1+e_0)\mu\left(\frac{\tau_{oct}}{\sigma'_m} - k\right) \qquad (bis\ 5.2.8)$$

in the case of large deformation, and

$$e = e_i$$

in the case of small deformation. The incremental stress-elastic strain relation is also derived, in the same way explained in Chapter 4, as:

$$d\varepsilon^{e}_{ij} = \frac{1}{3}\frac{\kappa}{1+e_i}\frac{d\sigma'_m}{\sigma'_m}\delta_{ij} \tag{5.3.7}$$

Applying the normality rule to the current yield surface in the octahedral stress space, as shown in Fig.5.14, we get the following relations:

$$dv^{p} = \frac{(1+e_0)\mu}{1+e}\left[\left\{\frac{\lambda-\kappa}{(1+e_0)\mu} \mp \frac{\tau_{oct}}{\sigma'_m}\right\}\frac{d\sigma'_m}{\sigma'_m} \pm \frac{d\tau_{oct}}{\sigma'_m}\right] \tag{5.3.8}$$

$$d\gamma^{p}_{oct} = \frac{1}{3}\frac{(1+e_0)\mu}{1+e}\left[\pm\frac{d\sigma'_m}{\sigma'_m} + \frac{\dfrac{d\tau_{oct}}{\sigma'_m}}{\dfrac{\lambda-\kappa}{(1+e_0)\mu} \mp \dfrac{\tau_{oct}}{\sigma'_m}}\right] \tag{5.3.9}$$

where $e$ is given by eq.(5.2.8). The elastic strain increments are given by:

$$dv^{e} = \frac{\kappa}{1+e}\frac{d\sigma'_m}{\sigma'_m} \tag{5.3.10}$$

$$d\gamma^{e}_{oct} = 0 \tag{5.3.11}$$

Then from eqs.(5.3.8)-(5.3.11), general relations between stress and strain increment for the clay in elastic-plastic state as follows:

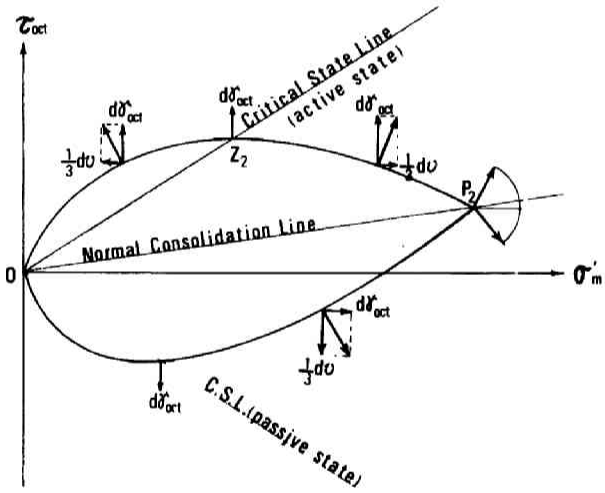


Fig.5.14. Associated flow rule

$$dv = \frac{\left\{\dfrac{\lambda}{(1+e_0)\mu} \mp \dfrac{\tau_{oct}}{\sigma'_m}\right\}\dfrac{d\sigma'_m}{\sigma'_m} \pm \dfrac{d\tau_{oct}}{\sigma'_m}}{\dfrac{1}{\mu} - \dfrac{\lambda}{(1+e_0)\mu}\ln\dfrac{\sigma'_m}{\sigma'_{m0}} \mp \left(\dfrac{\tau_{oct}}{\sigma'_m} - k\right)} \tag{5.3.12}$$

$$d\gamma_{oct} = \frac{\frac{1}{3}[\pm \frac{d\sigma'_m}{\sigma'_m} + \frac{1}{\frac{\lambda - \kappa}{(1+e_0)\mu} \mp \frac{\tau_{oct}}{\sigma'_m}} \frac{d\tau_{oct}}{\sigma'_m}]}{\frac{1}{\mu} - \frac{\lambda}{(1+e_0)\mu} \ln \frac{\sigma'_m}{\sigma'_{m0}} \mp (\frac{\tau_{oct}}{\sigma'_m} - k)} \tag{5.3.13}$$

*Undrained Shear*

The stress state of the clay in elastic-plastic state under undrained condition is derived from eqs.(5.2.12) and (5.2.15) as:

$$\frac{\tau_{oct}}{\sigma'_m} = k \mp \frac{1}{(1+e_0)\mu}\{\lambda \ln \frac{\sigma'_m}{\sigma'_{m0}} - \kappa \ln \frac{\sigma'_{mi}}{\sigma'_{m0}}\} \tag{5.3.14}$$

Then, differentiating eq.(5.3.14), we know that the stress increments are restricted by the following equation:

$$d\tau_{oct} = kd\sigma'_m - \frac{1}{(1+e_0)\mu} \{\lambda + \lambda \ln \frac{\sigma'_m}{\sigma'_{m0}} - \kappa \ln \frac{\sigma'_{mi}}{\sigma'_{m0}}\}d\sigma'_m \tag{5.3.15}$$

Substitution of eq.(5.3.14) into eq.(5.3.15) leads:

$$d\tau_{oct} = \{\frac{\tau_{oct}}{\sigma'_m} \mp \frac{\lambda}{(1+e_0)\mu}\}d\sigma'_m \tag{5.3.16}$$

With eq.(5.3.16), eqs.(5.3.15) and (5.3.16) are rewritten as:

$$dv = 0 \tag{5.3.17}$$

$$d\gamma_{oct} = \mp \frac{\frac{\kappa}{3}}{\frac{1}{\mu} - \frac{\kappa}{(1+e_0)\mu} \ln \frac{\sigma'_{mp}}{\sigma'_{m0}}} \{\frac{\frac{d\sigma'_m}{\sigma'_m}}{\lambda - \kappa \mp (1+e_0)\mu k + \lambda \ln \frac{\sigma'_m}{\sigma'_{m0}} - \kappa \ln \frac{\sigma'_{mi}}{\sigma'_{m0}}}\} \tag{5.3.18}$$

Solving eqs.(5.3.17) and (5.3.18) with the boundary condition:

$$v = 0, \qquad \gamma_{oct} = 0$$

$$\text{at} \quad \sigma'_m = \sigma'_{mi}, \qquad \tau_{oct} = k\sigma'_{mi} \mp \frac{\lambda - \kappa}{(1+e_0)\mu} \ln \frac{\sigma'_{mi}}{\sigma'_{m0}}$$

we get:

$$v = 0 \tag{5.3.19}$$

$$\gamma_{oct} = \mp \frac{\dfrac{\kappa}{3\lambda}}{\dfrac{1}{\mu} - \dfrac{\kappa}{(1+e_0)\mu} \ln \dfrac{\sigma'_{mi}}{\sigma'_{m0}}} \ln \frac{\dfrac{\lambda - \kappa}{(1+e_0)\mu} \mp \dfrac{\tau_{oct}}{\sigma'_m}}{\dfrac{\lambda - \kappa}{(1+e_0)\mu}\left\{\ln \dfrac{\sigma'_{mi}}{\sigma'_{m0}} + 1\right\} \mp k} \tag{5.3.20}$$

as the stress-strain relations for anisotropically pre-consolidated clay stressed under undrained condition. Figs.5.15 (a) and (b) show the stress paths and plastic strain increments of clay wetter and drier than critical respectively. The obtained stress-strain relations are given in Fig.5.16.

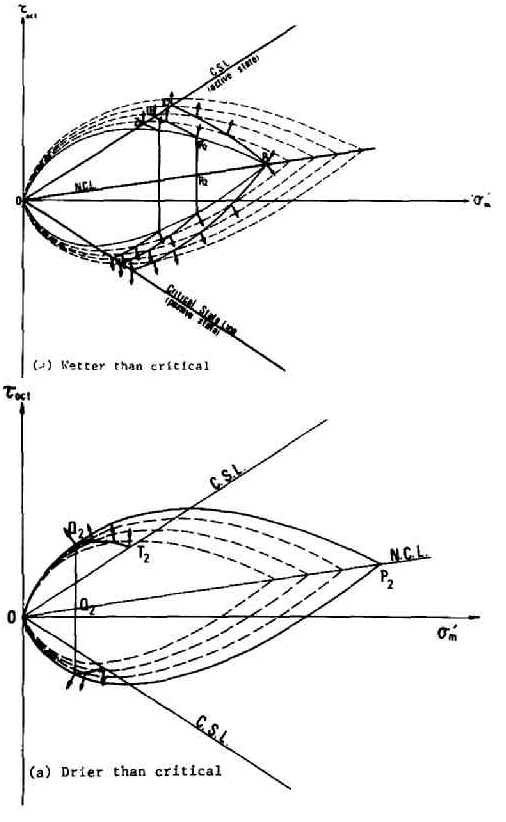


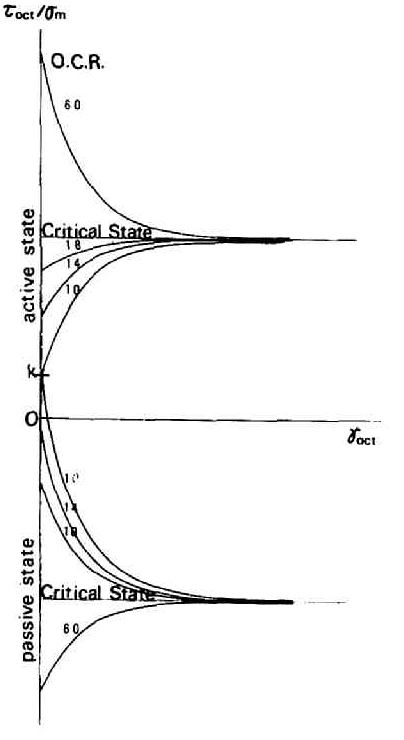


Fig.5.16. Stress-strain relations (undrained shear)

Fig.5.15. Stress paths and plastic strain increments

(a) undrained shear, wetter than critical
(b) undrained shear, drier than critical

*Triaxial Drained Shear*

Let us consider the stress-strain relations of anisotropically pre-consolidated clay stressed with constant cell pressure in the conventional triaxial apparatus under undrained condition. The stress path for such a test is given by:

$$\tau_{oct} = \sqrt{2}(\sigma'_m - \sigma'_{mi}) + \tau_{octi} \tag{5.3.21}$$

where $(\tau_{octi}, \sigma'_{mi})$ is the initial stress state of the clay before shear. Then, the stress state $(\tau_{octp}, \sigma'_{mp})$ for the initial yielding is given by solving the following equations simultaneously:

$$\tau_{octp} = k\sigma'_{mp} \mp \frac{\lambda - \kappa}{(1+e_0)\mu} \sigma'_{mp} \ln \frac{\sigma'_{mp}}{\sigma'_{m0}} \tag{5.3.22}$$

$$\tau_{octp} = \sqrt{2}(\sigma'_{mp} - \sigma'_{mi}) + \tau_{octi} \tag{5.3.23}$$

The incremental stress-strain relations of clay in elastic-plastic state are given by substituting the differential form of eq.(5.3.21):

$$d\tau_{oct} = \sqrt{2}d\sigma'_m$$

into eqs.(5.3.12) and (5.3.13) as follows:

$$dv = \frac{\left\{\frac{\lambda}{(1+e_0)\mu} \mp \frac{\sqrt{2}\sigma'_{mp} - \tau_{octp}}{\sigma'_m}\right\}\frac{d\sigma'_m}{\sigma'_m}}{\frac{1}{\mu} - \frac{\lambda}{(1+e_0)\mu} \ln \frac{\sigma'_m}{\sigma'_{m0}} \pm (k - \sqrt{2}) \pm \frac{\sqrt{2}\sigma'_{mp} - \tau_{octp}}{\sigma'_m}} \tag{5.3.25}$$

$$d\gamma_{oct} = \frac{\frac{1}{3}\left[\pm 1 + \frac{\sqrt{2}}{\frac{\lambda - \kappa}{(1+e_0)\mu} \mp \left(\sqrt{2} - \frac{\sqrt{2}\sigma'_{mp} - \tau_{octp}}{\sigma'_m}\right)}\right]\frac{d\sigma'_m}{\sigma'_m}}{\frac{1}{\mu} - \frac{\lambda}{(1+e_0)\mu} \ln \frac{\sigma'_m}{\sigma'_{m0}} + (k - \sqrt{2}) \pm \frac{\sqrt{2}\sigma'_{mp} - \tau_{octp}}{\sigma'_m}} \tag{5.3.26}$$

Eqs.(5.3.25) and (5.3.26) cannot be solved analytically. Figs.5.17 (a) and (b) show the stress paths and plastic strain increments in this case. The obtained stress-strain relations by the numerical method are shown in Fig.5.18 for the active loading state. It is interesting to compare the stress-strain relations of clay stressed

under undrained and drained condition in the conventional triaxial apparatus. The stress paths and stress-shear strain relations in each case are shown in Figs.5.19 (a) and (b).

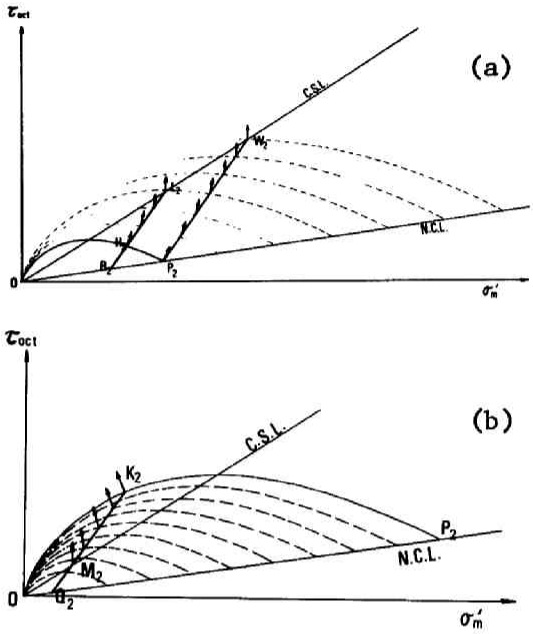


Fig.5.17. Stress paths and plastic strain increments
($\sigma_a$: increase, $\sigma_r$: constant)
(a) wetter than critical (b) drier than critical

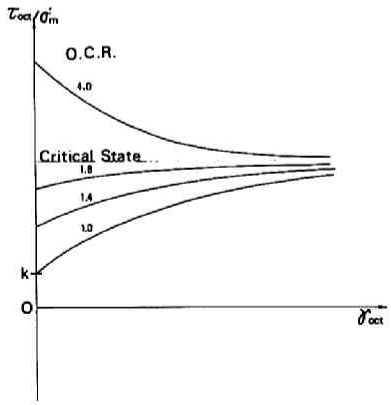


Fig.5.18. Stress-strain relations ($\sigma_a$: increase, $\sigma_r$: constant)

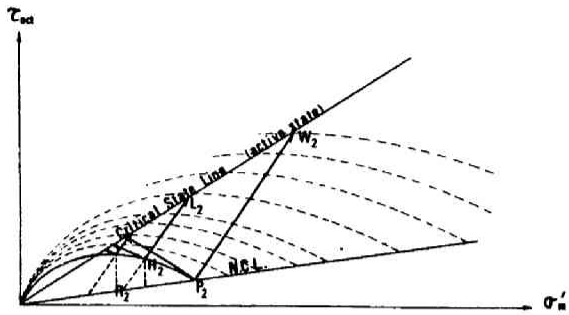


Fig.5.19 (a). Stress paths in undrained and drained shear

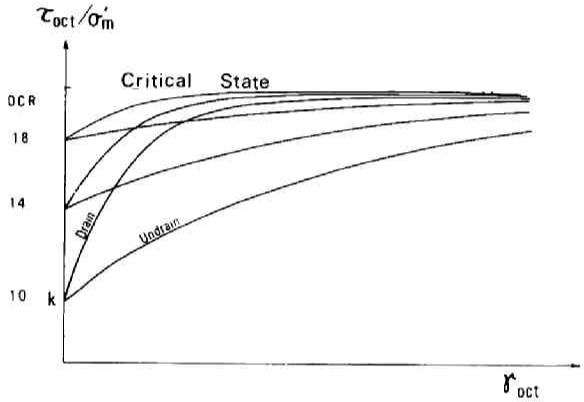


Fig.5.19 (b). Stress-strain relations in undrained and drained shear

*$\sigma'_m$-constant Shear*

In this case, the stress condition is given by:

$$\sigma'_m = \sigma'_{mi} \tag{5.3.27}$$

$$d\sigma'_m = 0 \tag{5.3.28}$$

Substituting eqs.(5.3.27) and (5.3.28) into eqs.(5.3.12) and (5.3.13), we get:

$$dv = \frac{\pm \dfrac{d\tau_{oct}}{\sigma'_m}}{\dfrac{1}{\mu} - \dfrac{\lambda}{(1+e_0)\mu} \ln \dfrac{\sigma'_{mi}}{\sigma'_{m0}} \mp \left(\dfrac{\tau_{oct}}{\sigma'_{mi}} - k\right)} \tag{5.3.29}$$

$$d\gamma_{oct} = \frac{\frac{1}{3}\frac{1}{\frac{\lambda-\kappa}{(1+e_0)\mu} \mp \frac{\tau_{oct}}{\sigma'_{mi}}}\frac{d\tau_{oct}}{\sigma'_{mi}}}{\frac{1}{\mu} - \frac{\lambda}{(1+e_0)\mu}\ln\frac{\sigma'_{mi}}{\sigma'_{m0}} \mp \left(\frac{\tau_{oct}}{\sigma'_{mi}} - k\right)} \tag{5.3.30}$$

The clay begins to yield when the applied $\tau_{oct}$ reaches the value of $\tau_{octp}$ given by subsitution of $\sigma'_{mp}=\sigma'_{mi}$ into eq.(5.3.22) as:

$$\tau_{octp} = k\sigma'_{mi} \mp \frac{\lambda-\kappa}{(1+e_0)\mu}\sigma'_{mi}\ln\frac{\sigma'_{mi}}{\sigma'_{m0}} \tag{5.3.31}$$

Then, solving eqs.(5.3.29) and (5.3.30) with such a boundary condition, we get the stress-strain relations of anisotropically pre-consolidated clay under $\sigma'_m$-constant shear as follows:

$$v = \ln\frac{\frac{1}{\mu} - \frac{\kappa}{(1+e_0)\mu}\ln\frac{\sigma'_{mi}}{\sigma'_{m0}}}{\frac{1}{\mu} - \frac{\lambda}{(1+e_0)\mu}\ln\frac{\sigma'_{mi}}{\sigma'_{m0}} \mp \left(\frac{\tau_{oct}}{\sigma'_{mi}} - k\right)} \tag{5.3.32}$$

$$\gamma_{oct} = \pm\frac{1}{3}\frac{1}{\frac{\lambda-\kappa}{(1+e_0)\mu} \mp k - \frac{1}{\mu} + \frac{\lambda}{(1+e_0)\mu}\ln\frac{\sigma'_{mi}}{\sigma'_{m0}}}$$

$$\ln\left[\frac{\frac{\lambda-\kappa}{(1+e_0)\mu} \mp \frac{\tau_{oct}}{\sigma'_m}}{\frac{\lambda-\kappa}{(1+e_0)\mu}\left\{\ln\frac{\sigma'_{mi}}{\sigma'_{m0}}+1\right\} \mp k}\right.\frac{\frac{1}{\mu} - \frac{\kappa}{(1+e_0)\mu}\ln\frac{\sigma'_{mi}}{\sigma'_{m0}}}{\frac{1}{\mu} - \frac{\lambda}{(1+e_0)\mu}\ln\frac{\sigma'_{mi}}{\sigma'_{m0}} \mp \left(\frac{\tau_{oct}}{\sigma'_m} - k\right)} \tag{5.3.33}$$

The stress paths and plastic strain increments in this case are shown in Figs.5.20. Stress-shear strain relations in this case are also given in Fig.5.21.

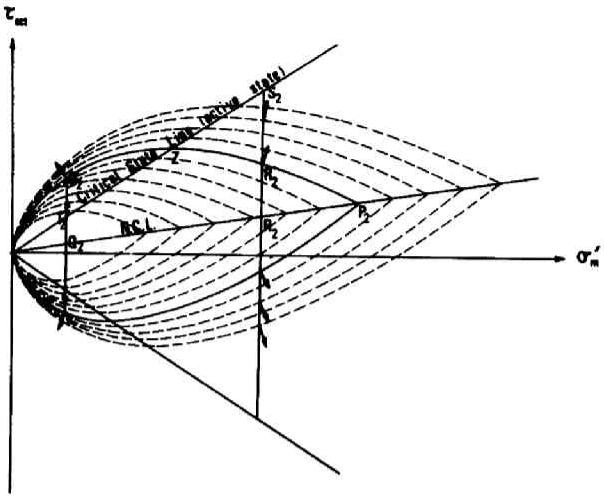


Fig.5.20. Stress paths and plastic strain increments ($\sigma_m'$-constant shear)

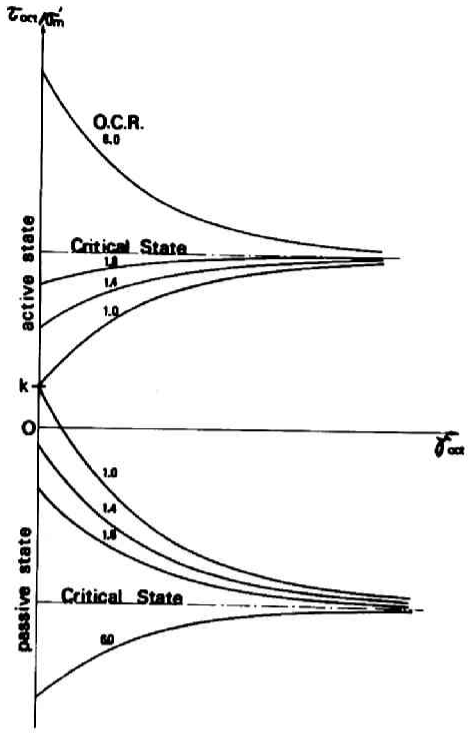


Fig.5.21. Stress-strain relations in $\sigma_m'$-constant shear

## 5.4 Stress Condition for Plane Strain Deformation

The practical design of engineering soil structure using the general stress-strain relations mentioned above will need considerable laboriousness and a computer with large capacity. But most of the engineering problems are able to be treated as plane strain two dimensional problems. Then it is useful to find the plane-strain stress-strain relations by means of the stress condition for plane strain.

Plane strain condition is derived from intermediate pricipal strain increment $d\varepsilon_2=0$. But, here, plane strain condition is assumed to be $d\varepsilon_2^p=0$ approximately. Then, the stress condition for plane strain is given as:

$$\frac{\partial f}{\partial \sigma_2} = 0 \tag{5.4.1}$$

From eqs.(5.3.5) and (5.4.1) the stress condition for plane strain deformation is given by

$$\frac{\sigma_2'}{\sigma_m'} = 1 \mp \frac{\tau_{oct}}{\sigma_m'}\{\frac{\lambda - \kappa}{(1+e_0)\mu} \mp \frac{\tau_{oct}}{\sigma_m'}\} \tag{5.4.2}$$

Approximate plane strain deformation can be maintained when the stress state is controlled to satisfy eq.(5.4.2) throughout the shearing process. If the stress state is controlled to satisfy eq. (5.4.2) for some part of shearing process, the change of the intermediate principal strain $d\varepsilon_2^p$ will not take place for this while.

The shearing process of anisotropically consolidated soil is performed by increasing or decreasing the stress ratio $\tau_{oct}/\sigma_m'$ until it reaches a certain critical value. This final state called critical state is such that shear strain increases and volume strain remains unchanged in spite of constant value of stress ratio $\tau_{oct}/\sigma_m'$. The critical value of stress ratio $\tau_{oct}/\sigma_m'$ is given by:

$$(\frac{\tau_{oct}}{\sigma_m'})_{crit} = \pm \frac{\lambda - \kappa}{(1+e_0)\mu} \tag{5.4.3}$$

Then the stress ratio $\tau_{oct}/\sigma_m'$ changes from the initial value of to the critical value $\pm(\lambda-\kappa)/(1+e_0)\mu$ through the shearing process.

Eq.(5.4.2) shows that the intermediate principal stress $\sigma_2'$ is equal to the mean principal stress $\sigma_m'$ at the zero stress ratio ($\tau_{oct}/\sigma_m'=0$) and at the critical state [$\tau_{oct}/\sigma_m'=\pm(\lambda-\kappa)/(1+e_0)\mu$].

This conclusion is rather convenient for the practical designs, for instance, the stability problem under plane strain condition can be analyzed by using the theory of characteristics line field with the stress condition given by:

$$\sigma_2' = \frac{\sigma_1' + \sigma_3'}{2} \tag{5.4.4}$$

Eq.(5.4.2) gives a quadric parabolas of $\tau_{oct}/\sigma_m'$. In the active case the value of $\tau_{oct}/\sigma_m'$ changes from to $(\lambda-\kappa)/(1+e_0)\mu$, then the range of $\sigma_2'/\sigma_m'$ is given by:

$$1 - \frac{1}{4}\{\frac{\lambda - \kappa}{(1+e_0)\mu}\}^2 \leqq \frac{\sigma_2'}{\sigma_m'} \leqq 1 \qquad (5.4.5)$$

Since the value of $(\lambda-\kappa)/(1+e_0)\mu$ is about 0.6-0.7 for the common clay, the minimum value given by eq.(5.4.5) is about 0.9. Therefore in the case that the error of 10% is permitted, the stress condition for plane strain deformation is approximately given by eq.(5.4.5). On the other hand, in the case of passive loading state, the range of $\sigma_2'/\sigma_m'$ is given by:

$$1 - \frac{1}{4}\{\frac{\lambda - \kappa}{(1+e_0)\mu}\}^2 \leqq \frac{\sigma_2'}{\sigma_m'} \leqq 1 + k\{\frac{\lambda - \kappa}{(1+e_0)\mu} + k\} \qquad (5.4.6)$$

For $K_0$-consolidated natural clay deposit, the value of $K_0$ is about 0.5 and this corresponds to $k$=0.35. Then, the range of $\sigma_2'/\sigma_m'$ for the passive loading state is given as:

$$0.9 \leqq \frac{\sigma_2'}{\sigma_m'} \leqq 1.3$$

with the value of $(\lambda-\kappa)/(1+e_0)\mu$ =0.65.

Then we can realize that in the passive case, the error arising from the approximation of eq.(5.4.4) is considerable. But since eq.(5.4.2) is rather complex to use in the practical design works, we conclude that the approximate stress state for plane strain deformation is given by eq.(5.4.4) from the view point of practical engineering.

Experimental works carried on by Henkel and Wade (1966), Karube and Harada (1967) show the rather small value of $\sigma_2'/\sigma_m'$ compared with unit. But this small value of $\sigma_2'/\sigma_m'$ in experiments may arises from the end friction of clay specimens to some extent.

## 5.5 Comparison with the Cambridge Energy Theory

The relationship between Cambridge theories (original energy theory and modified energy theory) and the present theory is mentioned in Chapters 2 and 4 briefly. Here we make further discussions. To say briefly, the original energy theory constructed by Roscoe, Schofield and Thurairajah (1963) and by Schofield and Wroth (1968) can be considered as a special case of the present theory. Of course, the author appreciates their originality, since their works were published before the publication of the present theory.

In the original energy theory, the stress condition for the critical state is given by:

$$\left(\frac{q}{p}\right)_{critical} = M \tag{5.5.1}$$

where

$$q = \sigma_1' - \sigma_3'$$

$$p = \frac{1}{3}(\sigma_1' + 2\sigma_2') = \sigma_m'$$

$M$ : constant

According to the present theory, the stress condition of the critical state for the active state is given as follows:

$$\left(\frac{\tau_{oct}}{\sigma_m'}\right)_{critical} = \frac{\lambda - \kappa}{(1+e_0)\mu} \tag{5.5.2}$$

Substituting $\sigma_2'=\sigma_3'$ and $\sigma_{m0}'=1$ and $e_0=e_a$ into the present theory for the active state brings the derivatives of the original energy theory. In other words, the original energy theory is a special case of the present theory. In the original energy theory, the critical state line in the stress space is uniquely defined by eq.(5.5.1). But in the present theory, the inclination of the critical state line in the stress space depends on the maximum pre-consolidation pressure $\sigma_{m0}'$, because $e_0$, $\mu$ and $\kappa$ depend on the value of $\sigma_{m0}'$. Therefore the shape of the state surface in the present theory is dependent on the maximum pre-consolidation pressure $\sigma_{m0}'$. This is the reason why we

do not call the state surface the state boundary surface. It is not the boundary in the present theory. The critical state of the present theory can be represented as follows in Roscoe style:

$$\left(\frac{q}{p}\right)_{critical} = \frac{3}{\sqrt{2}} \frac{\lambda - \kappa}{(1+e_a)\mu} \tag{5.5.3}$$

Now it is noteworthy to comment about the basic assumption of the original energy theory that is the estimation of energy dissipation during the deformation process of clay, i.e.:

$$dW = Mpd\varepsilon^p \tag{5.5.4}$$

where $dW$ is the dissipated energy and

$$d\varepsilon = \frac{2}{3}(d\varepsilon_1 - d\varepsilon_3)$$

Eq.(5.5.4) shows that the dissipated energy during shear process of clay does not depend on the volumetric strain. And this assumption cannot easily be accepted by our intuitive feelings as pointed out by Rowe, Barden and Lee (1964), Burland (1965) and by Palmer (1967). The modified energy theory was developed by the research group at Cambridge starting from the assumption of dissipative energy estimated by the following equation initially proposed by Burland (1965):

$$dW = p\sqrt{(dv^p)^2 + (Md\varepsilon^p)^2} \tag{5.5.5}$$

Eq.(5.5.5) shows that the dissipative energy depends both on the plastic volumetric strain and on the plastic shear strain, and so seems to be more adequate than that of original energy theory.

In the present theory, the fundamental incremental stress-plastic strain relation can be given by:

$$\frac{dv^p}{d\gamma^p_{oct}} = \pm 3\left(\frac{\lambda - \kappa}{(1+e_0)\mu} \mp \frac{\tau_{oct}}{\sigma'_m}\right) \tag{5.5.6}$$

Rewriting the eq.(5.5.6) for the active loading state into Roscoe style, we get:

$$\frac{dv^p}{d\varepsilon^p} = M - \frac{q}{p} \tag{5.5.7}$$

The dissipated energy is defined as:

$$dW = pdv^p + qd\varepsilon^p$$

and the substituting eq.(5.5.7) into eq.(5.5.8), we get the estimation of energy dissipation as follows:

$$dW = p(M - \frac{q}{p})d\varepsilon^p + qd\varepsilon^p = Mpd\varepsilon^p \tag{5.5.9}$$

Eq.(5.5.9) shows that the dissipated energy estimation, eq.(5.5.4), in the original energy theory coincides with that derived from the present theory.

Although Roscoe, Schofield and Thurairajah (1963) did not mention that their estimation of dissipated energy contained the effect of the plastic volumetric strain, it is clear that their estimation included the effect of the plastic volumetric strain on the process of deformation.

## 5.6 Conclusions

In this chapter, the theoretical extension of Chapter 4 to be applicable to anisotropically consolidated soils. It is emphasized that the mechanical behavior of anisotropically consolidated soil seems apparently quite different in the active and passive state. The discussions presented in this chapter are of use to analyse the practical problems in the field of soil mechanics and foundation engineering. For convenience of such an application of the theory, stress condition for plane strain deformation is derived. In the last part of this chapter, it is shown that the original energy theory at Cambridge, which has been well confirmed experimentally, is included in the present theory as the special case.

# CHAPTER 6

# EXPERIMENTAL EXAMINATIONS

## 6.1 Introduction

In this chapter, some experimental investigations are presented in order to give the theory mentioned in Chapters 4 and 5. The objects of the presented experimental works carried on by the author are the isotropically pre-consolidated clays.

The experiments are carried on with quite small strain rate or loading rate in order to eliminate the rate dependent behavior of clays. In the ordinary undrained shear tests on clays, the strain rate is selected sufficientlt slow to realize the complete equalization of pore pressure throughout the clay specimen. But in the author's opinion, such a criterion for the determination of strain rate is only the necessary condition. This thought is supported by the data given by Akai, Yamamoto and Ozawa (1962) and Richardson and Whitman (1963).

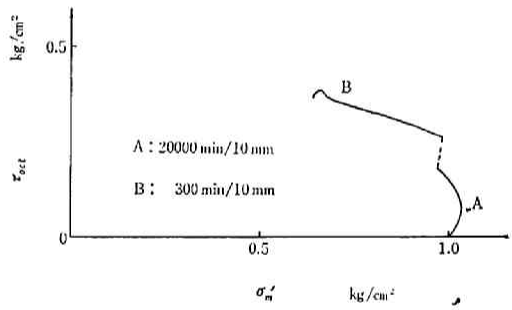


Fig.6.1. Time dependent behavior of of a clay under undrained shear

Fig. 6.1 is the stress path of a strain controlled triaxial test on a clay (P.L. = 31.2%, L.L. = 51.5%, P.I = 20.3%). The strain rates of the beginning part and the following part of the test were 20000 min/10 mm and 300 min/10 mm respectively (35 mm diameter and 80 mm height specimen). About 10 minutes were spent for the exchange of gears to change the shearing speed. This datum shows that the strain rate affects not only the development of pore water pressure but also the mobilization of shearing resistance.

## 6.2 Sample Preparation and Test Procedures

### 1. The Clay Used in the Investigations

The clay used in the investigations is Osaka alluvial clay containing shells deposited in the sea water. The index properties of the clay, percentage of clay particles ($\leq 2\mu$), activity and specific gravity are shown in Table 6.1. The water was added to the clay and then this clay paste was made to pass the 0.074 mm screen to elliminate the shells and was left still in a bucket for about two months.

| L.L. | P.L. | P.I. | $\leq 2\mu$ | Activity | Specific gravity |
|---|---|---|---|---|---|
| 69.2% | 32.5% | 36.7% | 25% | 1.47 | 2.64 |

Table 6.1. Physical properties of clay specimen

Then the clay paste was consolidated with its own weight. This half consolidated clay paste was mixed again and consolidated in a cilinder (30 cm diameter, 15 cm height) with about 0.3 kg/cm$^2$ for four weeks. The consolidated clay was coated with parchment paper and wax and then was preserved in the machine oil for several months. The water content of the clay in this state was about 88%. This high water content of the clay seemed to be derived from the high water content of the clay paste before consolidation.

### 2. Test Procedure

*Triaxial Test*

The clay specimens (35 mm diameter, 80 mm height) covered with drainage filter and thin rubber membranes were mounted directly on the pedestal in the triaxial cell. Porous stone was not used because of the possibility of residual air bubbles. Cell pressure and pore pressure were measured by the height difference of mercury columns. Consolidation time was about 5 days and swelling time was about 15 days. Back pressure was applied for the undrained tests. Strain rate was selected quite slow. Loading rate of the stress controlled drained tests were about a few weeks for one loading step. Area correction

was put in with natural strain.

*Shear Box Test*

Constant volume tests were carried. In constant volume test, the volume of the specimen (60 mm diameter and about 10 mm thickness) is maintained constant during the test by increasing or decreasing the normal pressure keeping free drainage condition. Area correction was not put in because of the reasons given by Matsuo and Karube (1966). Loading rate of the test was selected quite slow.

## 6.3 Consolidation Test

In order to obtain the values of the coefficients $\lambda$ and $\kappa$, a consolidation test is carried on in the oedometer. The sample is in 60 mm diameter and 18 mm thickness. Loading rate is 24 hours for each step. This loading rate is not sufficient to get the final settlement of the clay specimen. But the values of $\lambda$ and perhaps $\kappa$ are not so sensitive to the loading rate as shown by Crawford (1964). Test data are shown in Fig. 6.2.

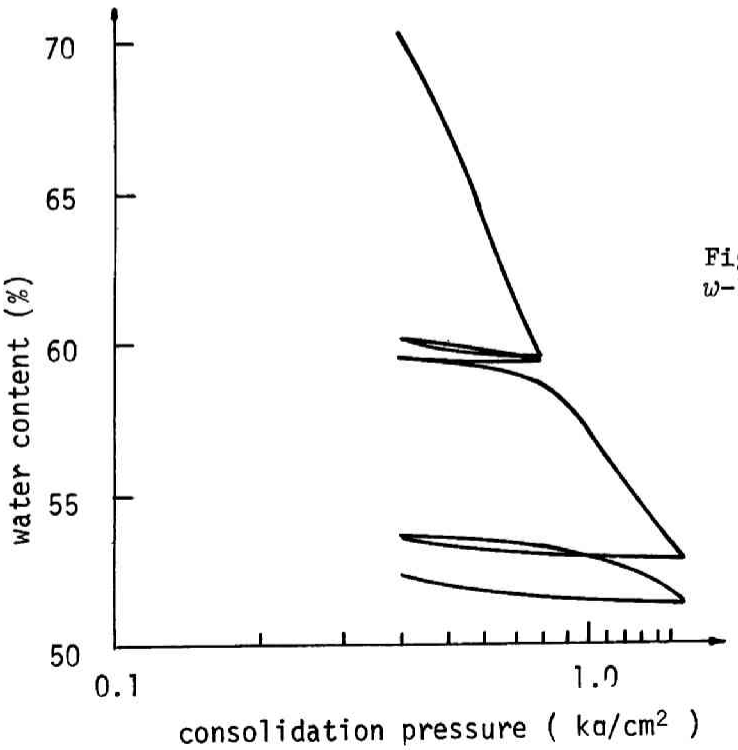


Fig.6.2.
$w$-log p plot

The reliable values of $\lambda$ and $\kappa$ corresponding to the consolidation pressure of 1 kg/cm$^2$ are 0.25 and 0.03 respectively. The value of coefficient $\mu$ is given in the following section.

## 6.4 Undrained Stress Paths

### 1. Normally Consolidated Clay

A normally isotropically consolidated clay specimen (initial $w$ = 88.34%) was consolidated with the cell pressure of about 0.998 kg/cm$^2$ (the cell pressure was changed from 0.967 kg/cm$^2$ to 1.029 kg/cm$^2$ by the friction of the constant pressure apparatus) for 5 days. The void ratio $e_0$ of the specimen after consolidation was 1.594. The stress path of the clay under strain controlled shear with the strain rate of 4.40 x 10$^{-4}$ mm/min (22719.98 min/10 mm) is given in Fig. 6.3.

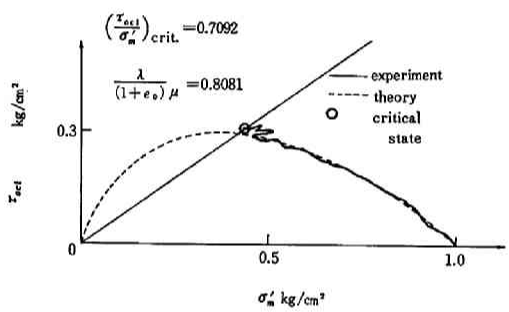


Fig.6.3. Stress path of the normally consolidated clay under undrained shear

The strict determination of the critical state point on the stress path is quite difficult. In this case the author would like to select the 0 point as the critical state point.

The theoretical stress path of a normally consolidated clay under undrained shear for $\frac{\lambda}{(1 + e_0)\mu}$ = 0.8081 is suitable with the experimental stress path. At the experimental critical state point, $\tau_{oct}$ = 0.3058 kg/cm$^2$ and $\sigma_m'$ = 0.4312 kg/cm$^2$, then the stress ratio $(\tau_{oct}/\sigma_m')_{crit.}$ = 0.7092. The theoretical stress ratio at the critical state is given by:

$$\left(\frac{\tau_{oct}}{\sigma_m'}\right)_{crit.} = \frac{\lambda - \kappa}{(1 + e_0)\mu}$$

Substituting the values of $e_0$ = 1.59, $\lambda$ = 0.25, $\kappa$ = 0.03 and $\left(\frac{\tau_{oct}}{\sigma_m'}\right)_{crit.}$ = 0.71 into the above equation, we get $\mu$ = 0.12.

All following calculations for the theoretical analysis will be carried with $\lambda = 0.25$, $\kappa = 0.03$ and $\mu = 0.12$.

2. Overconsolidated Clay

An overconsolidated clay (initial water content was 88.44%) was consolidated with the cell pressure of 1.010 ± 0.001 kg/cm$^2$ for 5 days and rebound to the pressure of 0.296 ± 0.031 kg/cm$^2$ for 16 days. This specimen was sheared under strain controlled undrained condition. The strain rate was selected as $3.049 \times 10^{-4}$ mm/min (32800 min/10 mm).

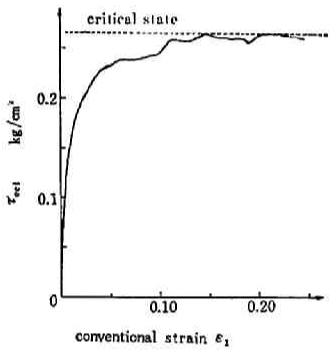


Fig.6.4. Stress-strain relation of the overconsolidated clay

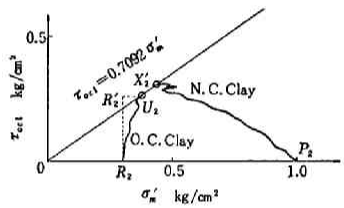


Fig.6.5. Stress paths of the clays under undrained shear

Judging from the stress strain relation shown in Fig. 6.4, the author would like to select the 0 point in Fig. 6.5 as the critical state point. The stress path of this overconsolidated clay is shown in Fig.6.5 and the stress ratio ($\tau_{oct}/\tau'_m$) of the 0 point of the overconsolidated clay is 0.7049.

The critical state line in Fig. 6.5 derived from ($\tau_{oct}/\sigma'_{m\cdot crit.}$) = 0.7092 is suitable with the experimental critical state point of the overconsolidated clay. The theoretical stress path is $R_2R'_2U_2$ for the overconsolidated clay in Fig. 6.5.

3. Shear Box Test

Stress paths of normally consolidated clays under shear in shear box are shown in Fig. 6.6. Strain rates are given in Table 2.

Assuming that the stress state ($\tau$, $\sigma'_N$) is synonymous with that on the $\phi'$ maximum mobilized plane as shown in Fig. 6.7, the theoretical stress paths are calculated as shown in Fig. 6.8. The stress state in the shear box seems to be approximately plane strain. Karube and Harada (1967) showed that the value of $N = (\sigma'_2 - \sigma'_3)/(\sigma'_1 - \sigma'_3)$ varied from 0.2 to 0.4. Then the theoretical stress paths of normally consolidated clays under plane strain shear may be substituted approximately by the theoretical curves for $N$ = 0.35. The value of $\lambda/\mu$ of the theoretical stress paths in Fig. 6.6 is derived from $\lambda$ = 0.25 and $\mu$ = 0.12. The theoretical curves agree with the experimental stress paths. And this agreement suggests the appropriateness of the assumption about the stress state in the shear box.

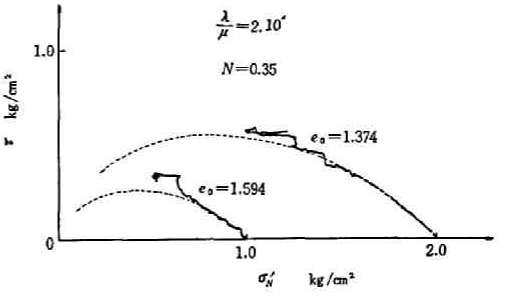


Fig.6.6. Stress paths of normally consolidated clays under shear in shear box

| Consolidation Pressure 2 kg/cm² | |
|---|---|
| Displacement ($\times 10^{-2}$ mm) | Strain rate mm/min |
| 0~70 | 0.01 |
| 70~140 | 0.02 |
| 140~300 | 0.04 |
| 300~500 | 0.05 |
| 500~600 | 0.10 |
| Consolidation Pressure 1 kg/cm² | |
| Displacement ($\times 10^{-2}$ mm) | Strain rate mm/min |
| 0~20 | 0.005 |
| 20~50 | 0.01 |
| 50~100 | 0.02 |
| 100~200 | 0.04 |
| 200~600 | 0.05 |

Table 6.2. Strain rate of the shear box test

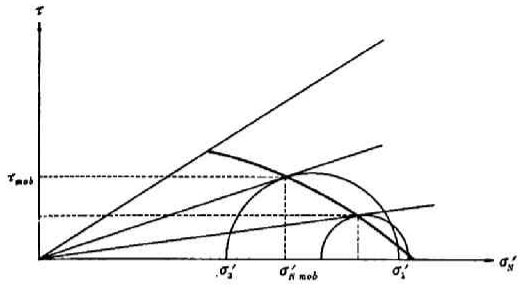

Fig.6.7. Stress state on the $\phi'$ maximum mobilized plane

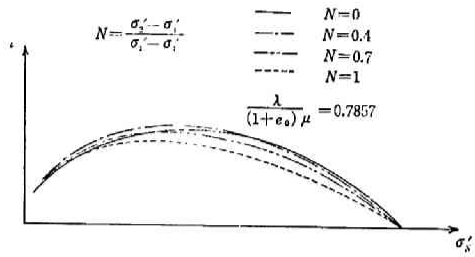


Fig.6.8. Theoretical stress paths of clays in shear box

## 6.5 Analysis on Drained Tests

### 1. Normally Consolidated Clay

A normally consolidated clay specimen (initial water content was 86.18%) was consolidated with the cell pressure of 0.967 ± 0.050 kg/cm$^2$ for 2 days and then sheared under stress controlled drained condition. The void ratio after consolidation was 1.606. The axial stress was increased with 5 steps remaining the radial stress constant. The expelled water is shown in Fig. 6.9.

Fig. 6.10 shows the experimental data comparing with the theoretical curve derived from the data of $\lambda$ = 0.25, $\kappa$ = 0.03 and $\mu$ = 0.12 and it suggests the possibility of the incomplete drainage in spite of the very long duration for each step of loading. The clay specimen could not arrive at the critical state point, because the deformation of the specimen was too

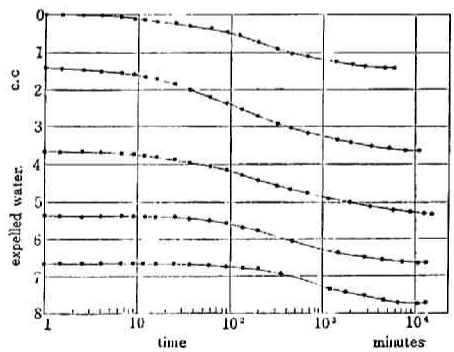


Fig.6.9. Expelled water~time relation of consolidated clay

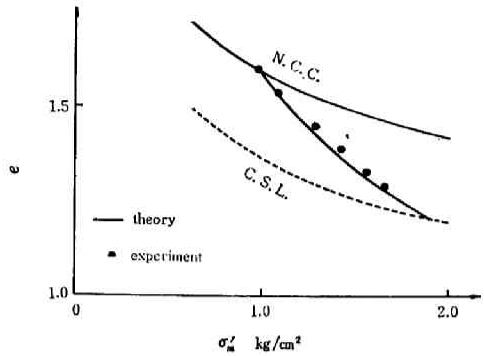


Fig.6.10. $e$-$\sigma'_m$ relation of the normally consolidated clay under drained shear

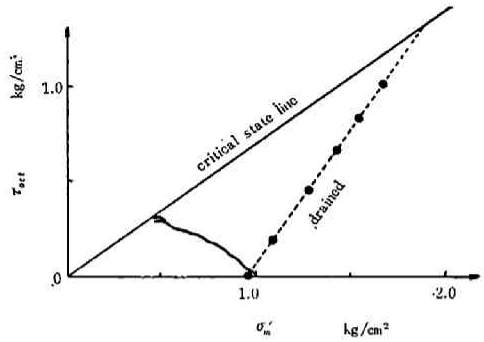


Fig.6.11. Stress paths of the normally consolidated clays

large to continue the test with the next step of loading. The stress paths of the undrained and drained tests on the normally consolidated clay and the theoretical critical state line are shown in Fig. 6.11. Fig. 6.12 shows the projection of the state paths of the undrained and drained test to the $\tau_{oct}$ = 0 plane, and the two points combined with the dotted line is the pair of the same stress ratio $\tau_{oct}/\sigma'_m$. The theory requires that these dotted lines are parallel to the normal consolidation curve.

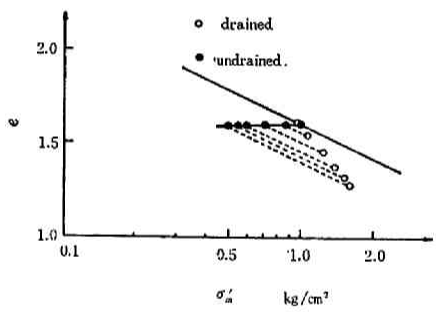


Fig.6.12. $\tau_{oct}/\sigma'_m$ : constant lines for the normally consolidated clays

Judging from the experimental data shown in Fig. 6.12 (including the possibility of incomplete drainage in drained test), the theory is generally acceptable.

2. Overconsolidated Clay

An overconsolidated clay specimen (initial water content was 87.46%) was consolidated with the pressure of 1.892 ± 0.051 kg/cm$^2$ for 16 days ($e_0$ = 1.3738) and rebounded to the pressure of 0.9189 ± 0.0364 kg/cm$^2$ for 9 days. This specimen was sheared under stress controlled drained condition with 3 steps of loading. The effective mean stress $\sigma_m'$ was kept nearly constant because the $\sigma_m'$ - constant test in strict sense cannot be carried on by the difficulties in the exact expection of the shear strain and of the radial stress. The shear strain increased suddenly about 5 minutes after the last step of loading and it was apparent that the last load was over the critical load.

Fig. 6.13 shows the state path of this test. The last step of loading was carried rather under the undrained condition than under $\sigma_m'$ - constant condition, because the pore pressure could not dissipate. The point 0, 1, 2, 3 are the experimental data and the point $S_0$ and $S_2$ are the critical points for $\sigma_m'$ = 0.9189 - constant and $\sigma_m'$ = 1.0232 - constant test respectively. The section of the swelling wall and the state surface are shown in Fig. 6.13 as $RR'$ and $R'S_0$ respectively for $\sigma_m'$ = 0.92 . Fig. 6.13 shows that the swelling wall is standing vertically on the swelling curve.

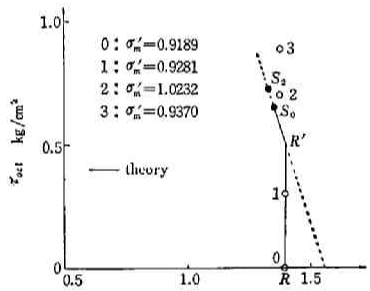


Fig.6.13. $\sigma_m'$ - constant test on the overconsolidated clay

These experimental data can be reasoned out approximately by the theory mentioned above.

## 6.6 Stress-Shear Strain Relations

As shown in the previous sections, excellent agreements exist between experimental data and the theoretical results. Here we examine the stress-shear strain relations. In Fig. 6.14, presented are the stress-shear strain relations for undrained and drained tests of normally consolidated clays. The theoretical curves can represent the tendencies of experimental curves. But the accuracy is not so satisfactory. In the author's opinion, this discrepancy is mainly arising from the nonuniformity of shear strain in the specimen caused by the end friction

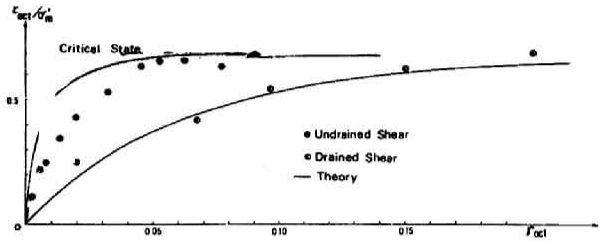


Fig.6.14. Stress-shear strain relations in the cases of undrained and drained shear

## 6.7 Experimental Results by Other Researchers

As mentioned in chapter 5, the Cambridge original theory is the special case of the present theory. The derivatives of the Cambridge original theory are completely coincident with those of the present theory in the case of conventional triaxial tests on isotropically consolidated soils. In Fig. 6.15 (a), (b), Roscoe, Schofield and Thurairajah (1963) gave some experimental confirmations of their hypothesis about the energy balance which is theoretically justified from the viewpoint of the present theory in chapter 5. They also showed that the stress ratio-constant lines on the $e$-log $p$ ($\sigma_m'$) diagram constructed a set of paralled lines as shown in Fig. 6.16 (a), (b). Such relations were also given by Walker and Reymond (1969).

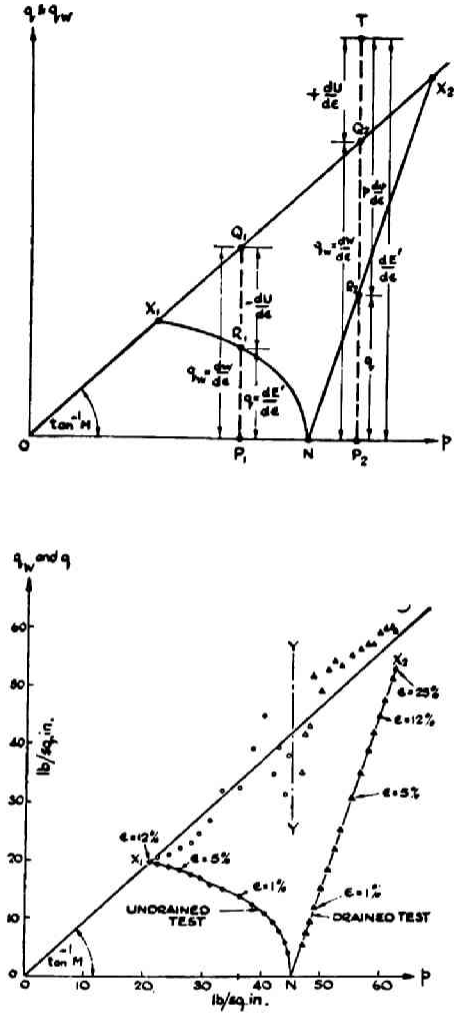


Fig.6.15.

Energy balance
(After Roscoe et al.)

(a) Theory
(b) Experiments

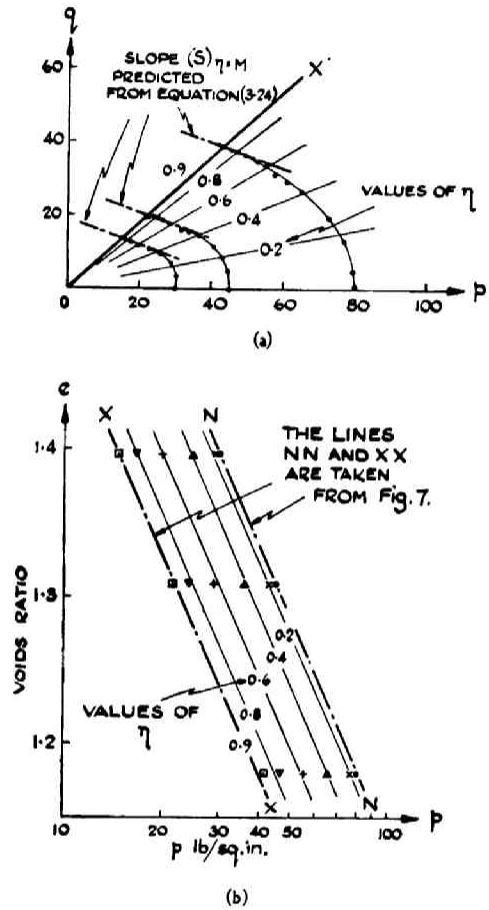


Fig.6.16.

Stress ratio-constant lines
(After Roscoe et al.)

(a) In the stress space
(b) On the $e$ - $p$ diagram

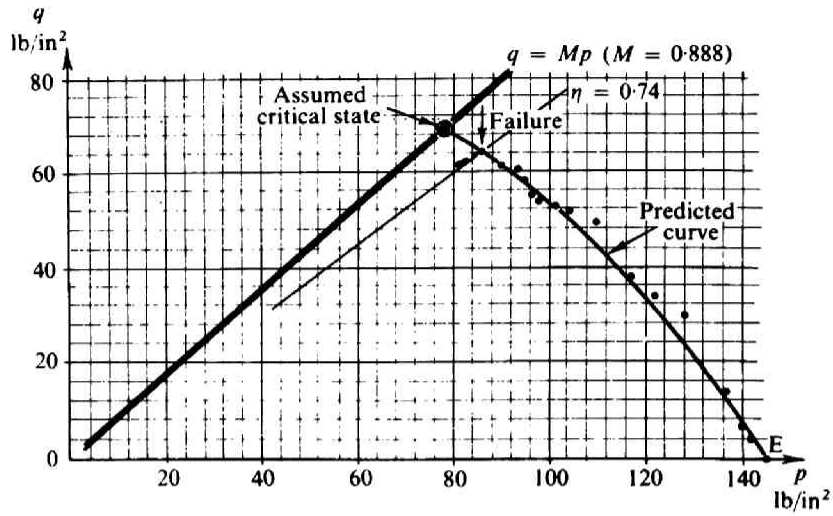


Fig.6.17. Stress path in undrained shear
(After Schofield and Wroth)

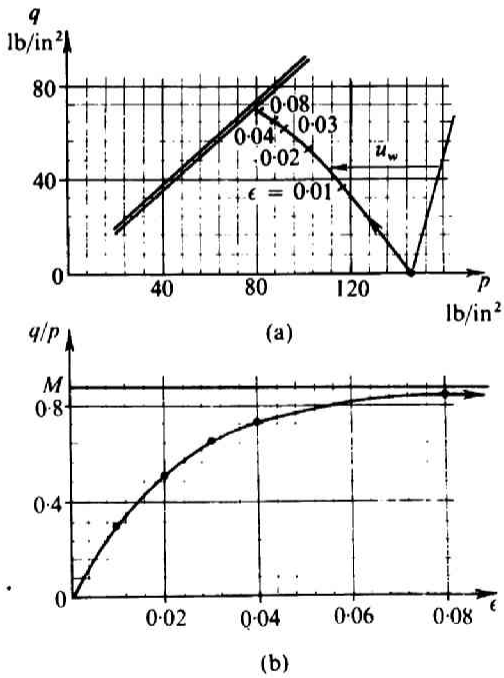


Using the experimental data of Bishop, Webb and Lewin (1965), Schofield and Wroth (1968) showed that the Cambridge original energy theory could excellently predict the stress path and stress-strain relation of undrained shear test on normally consolidated clay. Their results are shown in Fig. 6.17 and Figs. 6.18. (a), (b).

Fig.6.18. Undrained shear test (After Schofield and Wroth)

(a) Stress path
(b) Stress-shear strain relation

## 6.8 Conclusions

In this chapter, some experimental confirmations of the present theory are given. The conclusions are as follows:

(a) In order to obtain the unique stress-deformation relations, strain rate or loading rate is to be thoroughly slow. Equalization of pore water pressure throughout the specimen stressed under undrained condition is only the necessary condition, not the sufficient condition. In the case of drained test, complete expulsion of the pore water is to be expected.

(b) Theoretical state surface for the isotropically consolidated clay shows the excellent agreement with the experimental results.

(c) Theoretical swelling wall for the isotropically consolidated clay does describe the mechanical behavior of clay in elastic state to the satisfactory extent.

(d) The tendencies of stress-shear strain relations are predicted by the theory to some extent. But experimental and theoretical curves for the undrained test do not coincide completely. This is considered to be caused by the remarkable non-uniformity of shear strain in the specimen arising from the end friction.

# CHAPTER 7

# THREE DIMENSIONAL CONSOLIDATION ANALYSIS

## 7.1 Introduction

Consolidation analysis has been one of the most popular topics in the field of soil mechanics. The term "consolidation" used in this chapter is defined as the dissipating process of excess pore water pressure set up by the application of load. Therefore it is quite different phenomenon mentioned in the previous chapters. The term "consolidation" in this chapter is of the current usage.

The one dimensional consolidation theory initially constructed by Terzaghi in 1924 (introduced by Aboshi, 1969) is based on the assumption that the clay is able to be substituted by spring which deforms reversely in one particular direction. Biot (1941) constructed a three dimensional consolidation theory based on elasticity. Akai (1953) gave two dimensional consolidation theory based on elasticity, too. There have been too many research works about one dimensional, and two or three dimensional consolidation theory to introduce here. But most of them are based on the linear recoverable stress-strain assumptions for clay. Davis and Reymond (1965) constructed a non-linear theory of one dimensional consolidation based on the $e$-$\ln\sigma'_m$ linear relation. But as presented in the previous chapters, the stress-void ratio relations for clay under the general stress state are not represented by $e$-$\ln\sigma'_m$ linearity. In this chapter, a three dimensional analysis of consolidation is presented based on the general stress-strain relations for clay. In addition to that, some considerations on the anisotropic consolidation are made. It should be noted that the experimental confirmation of the present analysis by the conventional consolidation test in triaxial cell is hardly carried on, because the stress-strain relations, presented in the previous chapters and used in this chapter as the basic relations, are to be applied in the case of sufficient slow loading and strain rates.

It is apparent that the duration for the complete expulsion of the pore water is rather short compared with the duration for the rearrangement of the clay particles accompanied by deformation in the case of consolidation test on a considerablly small specimen. In the author's opinion, the secondary consolidation is arising from the time lag between the compulsion of the pore water and rearrangement of the clay particles.

## 7.2 Three Dimensional Consolidation Process

### 1. Stress-strain Relations

The incremental stress-strain relation for anisotropically pre-consolidated clay in elastic state is given by:

$$d\varepsilon_{ij} = \frac{1}{3}\frac{\kappa}{1+e_i}\frac{d\sigma'_m}{\sigma'_m}\delta_{ij} \tag{7.2.1}$$

when the stress state is within the range given by initial yield condition, i.e.:

$$\pm\left(\frac{\tau_{oct}}{\sigma'_m} - k\right) \leq -\frac{\lambda-\kappa}{(1+e_0)\mu}\ln\frac{\sigma'_m}{\sigma'_{m0}} \tag{7.2.2}$$

where the upper and lower sign are respectively corresponding to the active ($\tau_{oct}/\sigma'_m > k$) and passive ($\tau_{oct}/\sigma'_m < k$) state. From eq.(7.2.1), we get the incremental stress-void ratio relation in this case derived as:

$$dv = \frac{\kappa}{1+e_i}\frac{d\sigma'_m}{\sigma'_m} \tag{7.2.3}$$

When the stress state of the anisotropically pre-consolidated clay is beyond the initial yield condition, i.e.:

$$\pm\left(\frac{\tau_{oct}}{\sigma'_m} - k\right) > -\frac{\lambda-\kappa}{(1+e_0)\mu}\ln\frac{\sigma'_m}{\sigma'_{m0}} \tag{7.2.4}$$

the incremental stress-strain relation is given by:

$$d\varepsilon_{ij} = \frac{\mu}{3\sigma'_m}\frac{1+e_0}{1+e_i}[\{\frac{\lambda-\kappa}{(1+e_0)\mu} \mp \frac{\tau_{oct}}{\sigma'_m}\}\delta_{ij} \pm \frac{1}{\tau_{oct}}(\sigma'_{ij} - \sigma'_m\delta_{ij})]$$

$$[d\sigma'_m \pm \frac{d\tau_{oct}}{\frac{\lambda-\kappa}{(1+e_0)\mu} \mp \frac{\tau_{oct}}{\sigma'_m}}] + \frac{\kappa}{3\sigma'_m}\frac{d\sigma'_m}{1+e_i} \qquad (7.2.5)$$

The first and second terms of the right hand side of eq.(7.2.5) are representing the plastic and elastic component of incremental strain. Applying $\delta_{ij}$ to eq.(7.2.5), we get:

$$dv = \frac{(1+e_0)\mu}{1+e_i}[\frac{d\sigma'_m}{\sigma'_m}\{\frac{\lambda}{(1+e_0)\mu} \mp \frac{\tau_{oct}}{\sigma'_m}\} \pm \frac{d\tau_{oct}}{\sigma'_m}] \qquad (7.2.6)$$

2. Dissipation Process of Pore Water Pressure

Here we discuss the dissipation process of pore water pressure in the same manner that was used by many of the previous researchers.

*Continuity of the Water*

Assuming that the clay is completely saturated and neglecting the compressibilities of clay particle and pore water, the rate of the change of volumetric strain must equal to the volume of expelled water per unit time. Then we get:

$$\frac{\partial v}{\partial t} = \frac{\partial V_x}{\partial x} + \frac{\partial V_y}{\partial y} + \frac{\partial V_z}{\partial z} \qquad (7.2.7)$$

where $V_x$, $V_y$, $V_z$ are the x-, y-, z- component of the water velocity as shown in Fig.7.1.

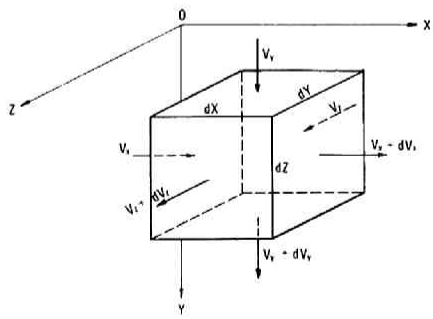


Fig.7.1. Continuity of the water

*Darcy's Law*

Assuming the validity of Darcy's law, we get:

$$V_x = -\frac{k_x}{\rho_w}\frac{\partial u}{\partial x}$$

$$V_y = -\frac{k_y}{\rho_w}\frac{u}{y} \tag{7.2.8}$$

$$V_z = -\frac{k_z}{\rho_w}\frac{u}{z}$$

where $k_x$, $k_y$, $k_z$ are the coefficients of permeability in x, y, z direction, $\rho_w$ and $u$ are respectively the density of pore water and pore pressure. It is noted that the values of $k_x$, $k_y$, $k_z$ depend on both the position (x, y, z) of the element and time t.

*Fundamental Equation for Clay in Elastic-Plastic State*

Substituting eqs.(7.2.7) and (7.2.8) into eq.(7.2.6), we get the fundamental equation for the pore pressure dissipation due to the consolidation of anisotropically pre-consolidated clay in elastic-plastic state as follows:

$$-\frac{\partial}{\partial x}\left(\frac{k_x}{\rho_w}\frac{\partial u}{\partial x}\right) - \frac{\partial}{\partial y}\left(\frac{k_y}{\rho_w}\frac{\partial u}{\partial y}\right) - \frac{\partial}{\partial z}\left(\frac{k_z}{\rho_w}\frac{\partial u}{\partial z}\right)$$

$$= \frac{(1+e_0)\mu}{1+e_i}\left[\left\{\frac{\lambda}{(1+e_0)\mu} \mp \frac{\tau_{oct}}{\sigma_m - u}\right\}\frac{1}{\sigma_m - u}\left(\frac{\partial \sigma_m}{\partial t} - \frac{\partial u}{\partial t}\right) \pm \frac{1}{\sigma_m - u}\frac{\partial \tau_{oct}}{\partial t}\right] \tag{7.2.9}$$

Eq.(7.2.9) gives a constraint on the pore pressure $u$ and applied total stresses $\tau_{oct}$ and $\sigma_m$. Generally speaking, deformation of clay accompanied by the expulsion pore water induces the change of total stresses applied to the clay element. Therefore $\tau_{oct}$ and $\sigma_m$ are not independent of time t. But here we pay our attention to the case of constant total stresses, i.e.:

$$\frac{\partial \tau_{oct}}{\partial t} = 0 \tag{7.2.10}$$

$$\frac{\partial \sigma_m}{\partial t} = \frac{\partial \sigma_m}{\partial t} + \frac{\partial u}{\partial t} = 0 \tag{7.2.11}$$

Then eq.(7.2.9) is reduced as:

$$- \frac{\partial}{\partial x}\left(\frac{k_x}{\rho_w}\frac{\partial u}{\partial x}\right) - \frac{\partial}{\partial y}\left(\frac{k_y}{\rho_w}\frac{\partial u}{\partial y}\right) - \frac{\partial}{\partial z}\left(\frac{k_z}{\rho_w}\frac{\partial u}{\partial z}\right)$$

$$= \frac{1}{1+e_i}\frac{1}{\sigma_m - u}\left[-\lambda \pm (1+e_0)\mu\frac{\tau_{oct}}{\sigma_m - u}\right]\frac{\partial u}{\partial t} \qquad (7.2.12)$$

Eq.(7.2.12) is the differential equation about pore pressure $u$, because $\tau_{oct}$ and $\sigma_m$ are assumed to be constant.

*Fundamental Equation for Clay in Elastic State*

With the similar procedure mentioned above, we get the fundamental equation for clay in elastic state as follows:

$$- \frac{\partial}{\partial x}\left(\frac{k_x}{\rho_w}\frac{\partial u}{\partial x}\right) - \frac{\partial}{\partial y}\left(\frac{k_y}{\rho_w}\frac{\partial u}{\partial y}\right) - \frac{\partial}{\partial z}\left(\frac{k_z}{\rho_w}\frac{\partial u}{\partial z}\right)$$

$$= - \frac{\kappa}{1+e_i}\frac{1}{\sigma_m - u}\frac{\partial u}{\partial t} \qquad (7.2.13)$$

Eq.(7.2.13) corresponds to eq.(7.2.12) in the case of elastic-plastic state.

*Discussion*

Dissipating process of the pore water pressure set up in the natural clay deposit loaded by the construction of buildings and embankments or by the another sort of external agency can be clarified by solving eq.(7.2.12) or eq.(7.2.13) with initial state of total stress distribution and initial pore pressure distribution and with the boundary condition of pore pressure. Unfortunately, eqs.(7.2.12) and (7.2.13) are in too complicated forms to be solved analytically. Then we have to carry the numerical calculation in order to obtain the practical informations.

In advance of the numerical computation, we must define the values of $e_i$ and $e_0$ and soil constants $\lambda$, $\kappa$ and $\mu$. The total stresses $\tau_{oct}$ and $\sigma_m$ are also to be defined to each point in the clay deposit throughout. The initial pore water distribution can be known as follows from the total stress distribution. Immediately after the loading, the clay deforms under undrained condition. Then the stress

state of a clay element located at any arbitrary point in the clay deposit must be on the undrained stress path obtained in Chapter 5.

As mentioned in Chapters 4 and 5, the stress state of clay element sheared under undrained condition is defined by the intersection of the $e=e_i$ plane ($e_i=e_0$ for the normally consolidated clay) with the swelling wall in the case of elastic state, and with the state surface in the case of elastic-plastic state.

Summing up these discussions

(a) elastic state

When the applied octahedral shear stress $\tau_{oct}$ is smaller than $\tau_{octp}$ which is given by:

$$\tau_{octp} = \sigma'_{mi}\{k \mp \frac{\lambda - \kappa}{(1+e_0)\mu} \ln \frac{\sigma'_{mi}}{\sigma'_{m0}}\} \qquad (7.2.14)$$

(bis5.2.14)

($\tau_{octp} = \sigma'_{m0}$ for normally consolidated clay)

The effective mean principal stress remains unchanged, i.e.:

$$\sigma'_m = \sigma'_{mi} \qquad (7.2.15)$$

and therefore the pore water pressure set up in the clay element is given by:

$$u = \sigma_m - \sigma'_{mi} \qquad (7.2.16)$$

where $\sigma_m$ is the applied total mean principal stress.

(b) elastic-plastic state

When the applied octahedral shear stress $\tau_{oct}$ is larger than $\tau_{octp}$ given by eq.(7.2.14), the effective mean principal stress $\sigma'_m$ must be related with $\tau_{oct}$ in the way given by:

$$e_i - e_0 + \lambda \ln \frac{\sigma'_m}{\sigma'_{m0}} \pm (1+e_0)\mu(\frac{\tau_{oct}}{\sigma'_m} - k) = 0 \qquad (7.2.17)$$

(bis5.2.15)

and the pore water pressure set up in the clay element is also given by numerical method.

With the initial values of the coefficients of permeability which are also defined to each point in the clay layer, and with the knowledge of initial pore water pressure distribution, we can begin

to solve eq.(7.2.12) or eq.(7.2.13) numerically. On the progress of pore pressure dissipation accompanied with the expulsion of pore water from the clay layer, the values of coefficients of permeability may change in the way that should be clarified before the computation. In this way, the dissipation process of pore water pressure set up in the clay deposit by the loading can be known.

It should be noted that eqs.(7.2.12) and (7.2.13) are based on the assumption of constant total stress. But constant total stress condition can be hardly realized in general practical problems, but only in the artificially controlled experimental works. Generally speaking, the progress of deformation of clay deposit due to the pore pressure dissipation causes the change in total stress distribution throughout the clay. But in some of the practical engineering problems, this change in total stress distribution may not be serious because of the small deformation of clay layer. Therefore we can conclude that the three dimensional analysis presented in this section is of practical use with sufficient accuracy compared with that of the current Terzaghi's one dimensional consolidation theory or with those of three dimensional consolidation theories in Terzaghi-Rendulic type.

Now let us consider the transition of effective stress state during the pore water pressure dissipation. The stress states of the clay in elastic-plastic state just after the loading, are to be represented by the points on the current yield locus shown in Fig.7.2. It is easily understood that the points on the current yield locus begin to move to the right hand direction parallel to the $\sigma_m'$-axis with the dissipation of pore water pressure under the condition of constant total stresses.

It is apparent from Fig.7.2 that the clay initially in elastic-plastic state can never become to be in elastic state. Such a clay wetter than critical must continue to yield with work-hardening effect during the dissipation process of pore water pressure. When the total stress ratio $\tau_{oct}/\sigma_m$ is smaller than $k$, it is possible that

the clay which is wetter than critical and initially in the active loading state becomes to be in the passive loading state on the process of pore water pressure dissipation. And now the clay wetter than critical yields with work-hardening effect and it will never reach the critical state.

On the other hand, the stress state of the clay initially in the elastic-plastic state which is represented by the point on the drier side of the current yield locus is rather unstable. When the pore water pressure decrease, the clay must experience further yielding with the work-hardening effect and then becomes to be in the critical state, if the applied total stress ratio $|\tau_{oct}/\sigma_m|$ is smaller than the critical value.

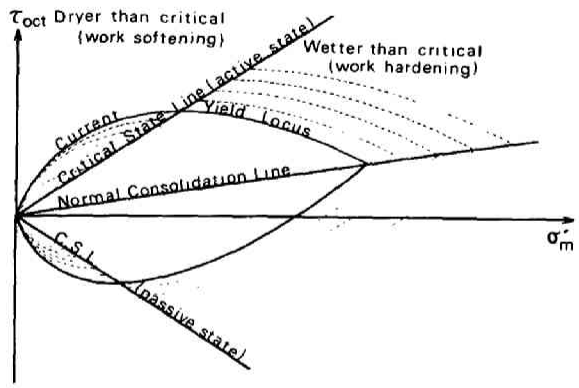


Fig.7.2. Yielding of clay

The stress state of the clay in the elastic state just after the loading is to be represented by a point within the domain enclosed by the current yield locus. In this case, the current yeild locus is nothing other than the initial yield locus. Accompanied with the dissipation of pore water pressure, i.e., with the increase of effective mean principal stress $\sigma'_m$, the stress point of clay in elastic state moves to the right hand direction of Fig.7.2. It is easily found that the stress point will finally reach the initial yield locus and then enters the elastic-plastic domain. After arriving at the initial yield locus, the situation is quite the same as for the stress point of clay in elastic-plastic state. It is noted that the clay initially in elastic state cannot become to be in the elastic-plastic state drier than critical under the constant total stresses. Seeing Fig.5.8, we can easily realize that the characteristics of

void ratio change of clay in elastic and elastic-plastic state are considerablly different from each other. Therefore many complicated difficulties will be encountered in the analysis of pore water pressure dissipation of pre-consolidated clay, especially of clay drier than critical.

3. Deformation of Clay due to the Dissipation of Pore Water Pressure

In the current analysis of consolidation process, the settlement is calculated from the void ratio change of clay element induced by the expulsion of pore water. But it is the physical reality that the reduction of pore water pressure causes not only the void ratio change but also the further distortional deformation of clay in elastic-plastic state.

From eqs.(7.2.1) and (7.2.5), we get the time derivatives of strain as follows:

$$\frac{\partial \varepsilon_{ij}}{\partial t} = \frac{1}{3}\frac{\kappa}{1+e_i}\frac{1}{\sigma'_m}\frac{\partial \sigma'_m}{\partial t}\delta_{ij} \quad : \text{ elastic state} \qquad (7.2.18)$$

$$\frac{\partial \varepsilon_{ij}}{\partial t} = \frac{\mu}{3\sigma'_m}\frac{1+e_0}{1+e_i}\left[\left\{\frac{\lambda}{(1+e_0)\mu} \mp \frac{\tau_{oct}}{\sigma'_m}\right\}\delta_{ij} \pm \frac{1}{\tau_{oct}}(\sigma'_{ij} - \sigma'_m\delta_{ij})\right]\frac{\partial \sigma'_m}{\partial t} \quad : \text{ elastic-plastic state} \qquad (7.2.19)$$

The terms in right hand side of eqs.(7.2.18) and (7.2.19) are already obtained by the way mentioned in the previous section. Then, we can easily get the rate of deformation per unit time. But it is noteworthy that the obtained change in strain distribution throughout the clay deposit, i.e., the change in configuration of clay deposit cannot satisfy the boundary condition of displacement completely.

## 7.3 Anisotropic Consolidation

In this section the stress path on the consolidation process of isotropically consolidated clay specimen with some special constraints of deformation in conventional triaxial apparatus is to be presented. Such an analysis presented here is of little use in the practical

engineering problems, but of academic interest.

Now we consider the consolidation process of isotropically consolidated clay specimen with no lateral deformation. This is similar process to so-called $K_0$-consolidation on which Akai and Adachi (1965) gave some contributions. Under the condition of $\sigma_2=\sigma_3$, the octahedral stresses are reduced as:

$$\sigma'_m = \frac{1}{3}(\sigma'_1 + 2\sigma'_3) \tag{7.3.1}$$

$$\tau_{oct} = \frac{\sqrt{2}}{3}(\sigma'_1 - \sigma'_3) \tag{7.3.2}$$

and the plastic potential given in Chapter 4 is reduced as:

$$f = \frac{\tau_{oct}}{\sigma'_m} + \frac{\lambda - \kappa}{(1+e_0)\mu} \ln \frac{\sigma'_m}{\sigma'_{my}} \qquad (bis\ 4.4.7)$$

$$= \frac{\sqrt{2}(\sigma'_1 - \sigma'_3)}{\sigma'_1 + 2\sigma'_3} + \frac{\lambda - \kappa}{(1+e_0)\mu} \ln \frac{\frac{1}{3}(\sigma'_1 + 2\sigma'_3)}{\sigma'_{my}} \tag{7.3.3}$$

It is already shown in Chapter 4 that the plastic strain increment is given by:

$$d\varepsilon^p_{ij} = \Lambda \frac{\partial f}{\partial \sigma'_{ij}} \qquad \begin{matrix}(7.3.4)\\ (bis\ 4.4.6)\end{matrix}$$

where

$$\Lambda = \mu \frac{1 + e_0}{1 + e} [d\sigma'_m + d\tau_{oct} / \{\frac{\lambda - \kappa}{(1+e_0)\mu} - \frac{\tau_{oct}}{\sigma'_m}\}] \qquad (bis\ 4.4.14)$$

which is reduced as:

$$\Lambda = \mu \frac{1 + e_0}{1 + e} [\frac{1}{3} d\sigma'_1 + \frac{2}{3} d\sigma'_3 + \frac{\frac{\sqrt{2}}{3} d\sigma'_1 - \frac{\sqrt{2}}{3} d\sigma'_3}{\frac{\lambda - \kappa}{(1+e_0)\mu} - \frac{\sqrt{2}(\sigma'_1 - \sigma'_3)}{\sigma'_1 + 2\sigma'_3}}] \tag{7.3.5}$$

Elastic strain increment is given by:

$$d\varepsilon^e_{ij} = \frac{1}{3} \frac{\kappa}{1 + e} \frac{d\sigma'_m}{\sigma'_m} \delta_{ij} \tag{7.3.6}$$

Combining these equations, we get the differential equation for

$$d\varepsilon^p_3 + d\varepsilon^e_3 = 0 \tag{7.3.7}$$

as follows:

$$\{-3\sqrt{2}\,\frac{\sigma_1'}{\sigma_1' + 2\sigma_3'} + 2\,\frac{\lambda - \kappa}{(1 + e_0)\mu}\}(1 + e_0)\mu[d\sigma_1' + 2d\sigma_3' + \frac{\sqrt{2}d\sigma_1' - \sqrt{2}d\sigma_3'}{\frac{\lambda - \kappa}{(1 + e_0)\mu} - \frac{\sqrt{2}(\sigma_1' - \sigma_3')}{\sigma_1' + 2\sigma_3'}}]$$

$$= \kappa(d\sigma_1' + 2d\sigma_3') \qquad (7.3.8)$$

Introducing,

$$A \equiv \{-\frac{3\sqrt{2}}{1 + 2K} + 2\,\frac{\lambda - \kappa}{(1 + e_0)\mu}\}\ (1 + e_0)\mu \qquad (7.3.9)$$

$$B \equiv \frac{\lambda - \kappa}{(1 + e_0)\mu} - \sqrt{2}\,\frac{1 - K}{1 + 2K} \qquad (7.3.10)$$

where

$$K = \frac{\sigma_3'}{\sigma_1'} \qquad (7.3.11)$$

we get the differential equation which the effective stresses and their increments should satisfy as follows:

$$\frac{d\sigma_3'}{d\sigma_1'} = \frac{A(B + \sqrt{2}) - \kappa B}{2\kappa B - A(2B - \sqrt{2})} \qquad (7.3.12)$$

Now let us consider the change in effective stress on the consolidation process of isotropically consolidated clay carried on with no axial displacement, i.e.:

$$d\varepsilon_1 = d\varepsilon_1^p + d\varepsilon_1^e = 0 \qquad (7.3.13)$$

In this case, we get the identical form of eq.(7.3.12) with the slight alternation of A as:

$$A \equiv \{\frac{3\sqrt{2}\ K}{1 + 2K} + \frac{\lambda - \kappa}{(1 + e_0)\mu}\}(1 + e_0)\mu \qquad (7.3.14)$$

## 7.4 Conclusions

In this chapter, three dimensional consolidation analysis based on the non-linear stress-strain relations for anisotropically consolidated clay presented in Chapter 5 is presented. This analysis is characterized as follows compared with the previously proposed three dimensional consolidation theories:

(a) The stress-strain relations used in the analysis are much realistic. They describe the effect of dilatancy and are consistent with the description of general mechanical behavior of anisotropically pre-consolidated clay.

(b) The situation of the deformation due to the progress of pore pressure dissipation is able to be described in detail connecting with the change in the mechanical state of clay from the elastic state to the elastic-plastic state and to the perfectly plastic state (critical state).

(c) The difference between mechanical behaviors of anisotropically pre-consolidated clay stressed in active state and passive state is described.

In the last part of this chapter, some discussions on the stress paths of isotropically consolidated clay specimen consolidated in the conventional triaxial cell with some restraints on its deformation are made.

# CHAPTER 8

# IMMEDIATE SETTLEMENT OF EMBANKMENTS ANALYSED BY FINITE ELEMENT METHOD

## 8.1 Introduction

In this chapter, the immediate deformation of anisotropically normally consolidated clay layer loaded by the construction of an embankment is analysed by the finite element method using the stress-strain relation presented in Chapter 5.

Immediate settlement of clay layer stressed by the uniform strip load has been analysed by the theory of elasticity. But the elastic constants suitable for the analysis are hardly determined from the soil tests. Then recently many researchers, Höeg, Christian and Whitman (1968), Girijavallabhan and Reese (1968), Dunlop, Duncan and Seed (1968), Christian (1968), Christian and Boehmer (1970), Duncan and Chang (1970) and Chang and Duncan (1970), have begun to analyse the deformation problems by the numerical analyses using the non-linear stress-strain relations for soils.

The stress-strain relations used in their analyses are to be obtained from the soil testing. But it should be noted that the stress-strain relations of clays are quite different depending on the maximum pre-consolidation pressures, initial states, drainage conditions and loading states as mentioned in Chapters 4 and 5. Even if we discuss only the case of anisotropically normally consolidated clays, stressed under undrained condition, their stress-strain relations depend on their consolidation pressure and loading states. In addition to those, we must take the plane strain condition into account. Therefore we can say that to determine the reliable stress-strain relations of clays directly from the undrained tests on clays is hardly possible practically.

In this chapter, the stress-strain relations of anisotropically normally consolidated clay presented in Chapter 5 are used. Broms and Casbarian (1965) showed that pore water pressure induced by the

undrained shear depends on the rotation of principal stress axes. It is noted that this effect is neglected in this thesis.

## 8.2 Procedures of Analysis

The immediate settlement of anisotropically normally consolidated clay layer stressed by the construction of an embankment is to be analysed. The embankment is replaced by the uniform strip load whose width is 8 m. The thickness of the clay layer is assumed to be 20 m. The maximum pre-consolidation pressure $\sigma'_{m0}$ is assumed to be distributed proportionally to the depth of clay layer. The values of $\sigma'_{m0}$ of the clay elements located at the surface and bottom of the clay layer are respectively 0.9483 t/m$^2$ and 13.5923 t/m$^2$.

Here, the clay layer is devided into the quadrilateral elements. A quadrilateral element can be devided into two triangles in two distinct ways as shown in Fig.8.1. The stiffness of the quadrilateral element is obtained by averaging the stiffness of elements 1, 2, 3 and 4.

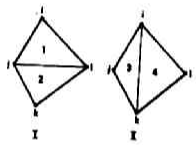

Fig.8.1. Division of quadrilateral element

The initial stress state of the clay element located at the depth y is given by:

$$\sigma_y^i = \rho y \tag{8.2.1}$$

$$\sigma_x^i = K_0 \rho y \tag{8.2.2}$$

$$\tau_{xy}^i = 0 \tag{8.2.3}$$

where $\rho$ and $K_0$ are respectively the weight of the clay element per unit volume and coefficient of earth pressure at rest. Here the value of $K_0$ is assumed to be 0.5 and then corresponding value $k_0$ is 0.3536. From eqs.(8.2.1)-(8.2.3), we get:

$$\sigma_m^i = \frac{1 + 2K_0}{3} \rho y \tag{8.2.4}$$

$$\tau_{oct}^i = \frac{\sqrt{2}}{3}(1 - K_0)\rho y \tag{8.2.5}$$

In this analysis, the stress increments due to the application of the load are calculated by finite element method regardless of the effect of the own weight of the clay. Then the stress state in the clay layer is obtained from the summation of the initial stress state and stress increment. The effective mean principal stress $\sigma_m'$ in each clay element is determined by numerically solving the undrained stress path:

$$\frac{\tau_{oct}}{\sigma_m'} = \mp \frac{\lambda}{(1+e_0)\mu} \ln \frac{\sigma_m'}{\sigma_{m0}'} + k_0 \qquad (bis\ 5.2.16)$$

The stress-strain relations of the clay elements are linearized by the incremental-variable elasticity procedure indtroduced by Zienkiewicz and Cheung (1967). The stress-strain relations of the clay elements are obtained by substituting the stress condition for plane strain deformation:

$$\sigma_2' = \sigma_m' \quad \text{and} \quad e_i = e_0 \quad , \quad k = k_0 \qquad (8.2.6)$$

into the general undrained stress-strain relation:

$$\gamma_{oct} = \mp \frac{\dfrac{\kappa}{3\lambda}}{\dfrac{1}{\mu} - \dfrac{\kappa}{(1+e_0)\mu} \ln \dfrac{\sigma_m'}{\sigma_{m0}'}} \ln \frac{\dfrac{\lambda - \kappa}{(1+e_0)\mu} \mp \dfrac{\tau_{oct}}{\sigma_m'}}{\dfrac{\lambda - \kappa}{(1+e_0)\mu}\{\ln \dfrac{\sigma_m'}{\sigma_{m0}'} + 1\} \mp k} \qquad (bis\ 5.3.20)$$

where the upper and the lower signs correspond to the active and the passive states respectively. On the computation process, one must judge whether the clay elements are in the active state or not, and apply the stress-strain relations corresponding to each case. The poison's ratio $\nu$ is assumed to be 0.49.

## 8.3 Remarks on the Calculation Results

The values of the coefficients used in the calculation are as follows:

$\rho = 1.6322$ t/m , $\lambda = 0.3112$, $\kappa = 0.1089$,

$\mu = 0.1150$, $k_0 = 0.3536$ ($K_0 = 0.5$)

and the value of $e_0$ corresponding to $\sigma'_{m0}$ = 10 t/m$^2$is 1.594.

Calculation is carried on for the following three cases:

Case 1: load intensity q = 0.15 t/m$^2$

Case 2: load intensity q = 0.225 t/m$^2$

Case 3: load intensity q = 0.30 t/m$^2$

with the boundary conditions:

(a) No lateral displacement on the line just under the center of the uniform strip load and on the line 32 m apart from the center line.

(b) No vertical displacement at the bottom of clay layer.

The stress increments due to the application of uniform strip load are shown in Figs.8.2(a)-(c), 8.3(a)-(c) and 8.4(a)-(c). In these figures we find some elements in which the stress increments are negative. The physical meaning of this tendency is clarified by seeing Figs.8.5(a)-(c).

In Figs.8.5(a)-(c), the elements with the mark P are in passive loading state, i.e., the stress ratios $\tau_{oct}/\sigma'_m$ in these elements decrease from their initial value $k_0$. Figs.8.5(a)-(c) show that the passive region is developing with the increase of load intensity. It is noted that the passive region approximately includes the so-called passive region derived from the theory of characteristics field. The value of $\tau_{oct}/\sigma'_m$ at the critical state for the clay layer is about 0.7. Then no element is in the critical state. But in Case 3, the clay elements just under the strip load are almost reaching to be in the critical state.

In Figs.8.6(a)-(c). the distributions of pore water pressures set up by the loads are shown.

The strain fields are given in Figs.8.7(a)-(c), Figs.8.8(a)-(c) and Figs.8.9(a)-(c). In all cases, the strains in the clay elements just under the strip load are meaninglessly large. This arises from their comparatively large stress ratios. From Fig.5.16, we can easily understand the rapidly increasing tendenc[illegible]r strain in a clay element stressed by the considerablly hi[illegible] ratio.

(a)

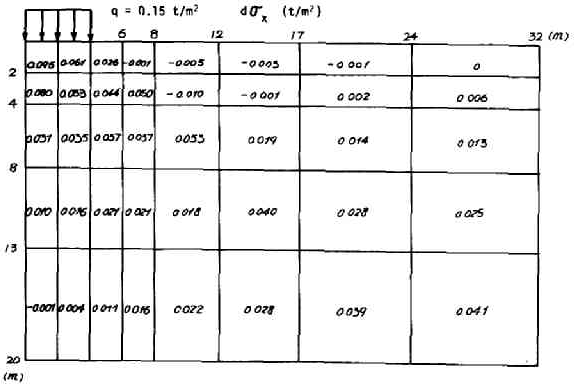


(b)

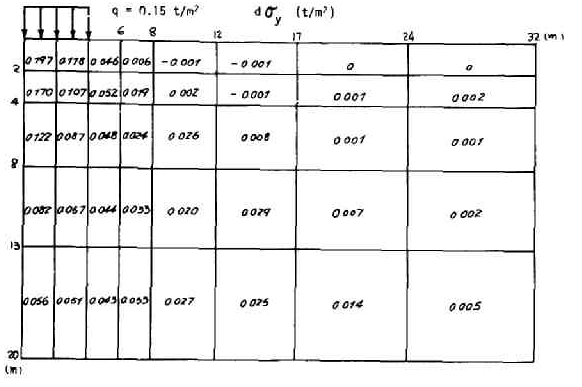


(c)

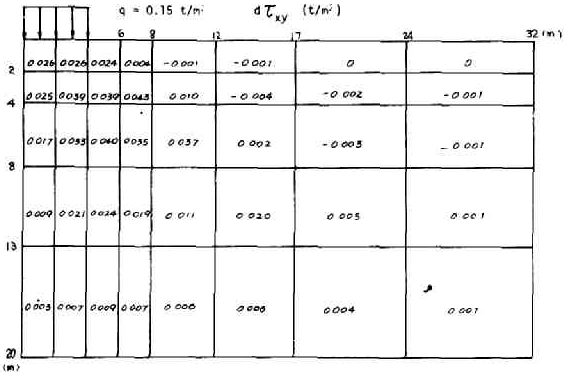


Fig.8.2. Stress increments (Case 1)
(a) increments of $\sigma_x$
(b) increments of $\sigma_y$
(c) increments of $\tau_{xy}$

(a)

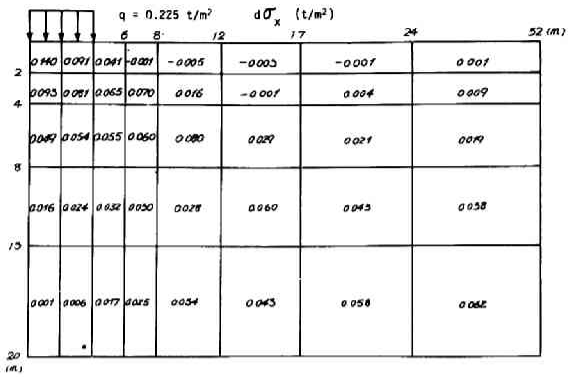


(b)

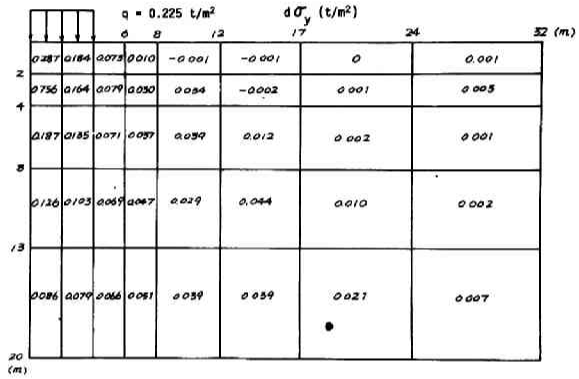


(c)

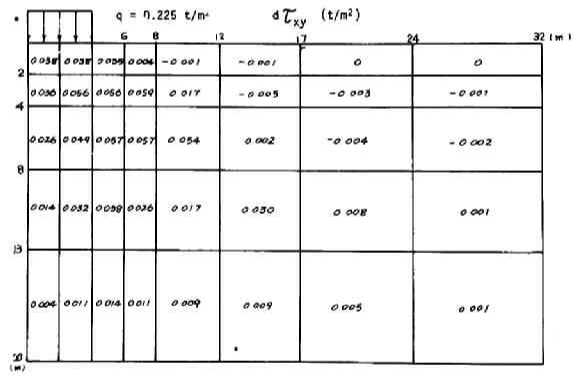


Fig.8.3. Stress increments (Case 2)
(a) increments of $\sigma_x$
(b) increments of $\sigma_y$
(c) increments of $\tau_{xy}$

(a)

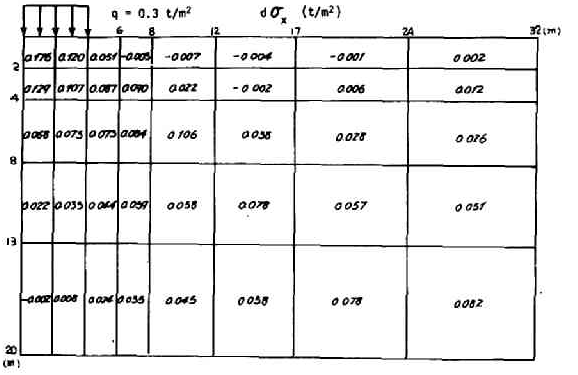


(b)

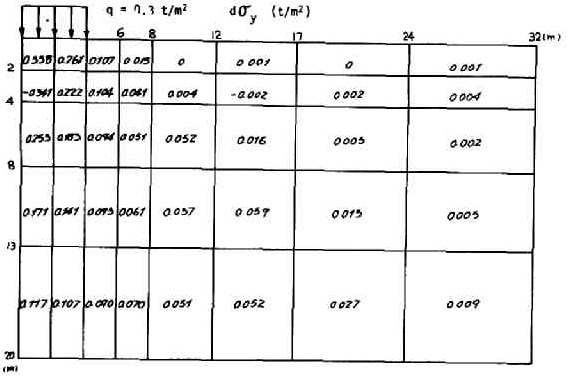


(c)

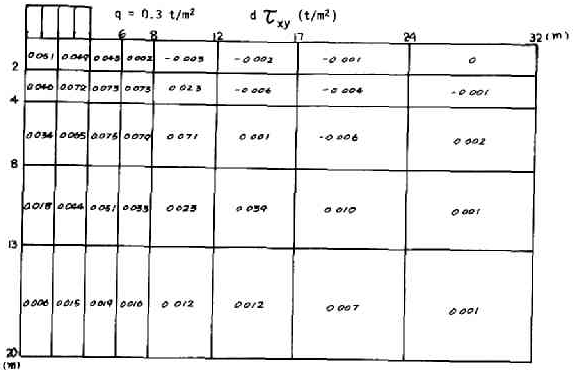


Fig.8.4. Stress increments (Case 3)
(a) increments of $\sigma_x$
(b) increments of $\sigma_y$
(c) increments of $\tau_{xy}$

(a)

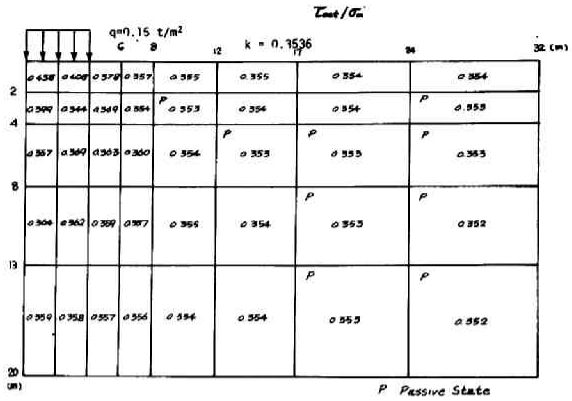


(b)

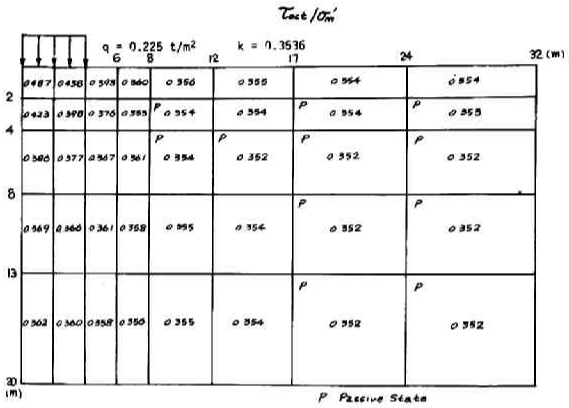


(c)

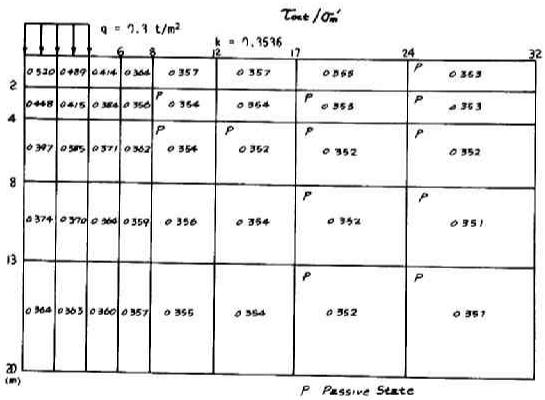


Fig.8.5. Stress ratios
(a) Case 1
(b) Case 2
(c) Case 3

(a)

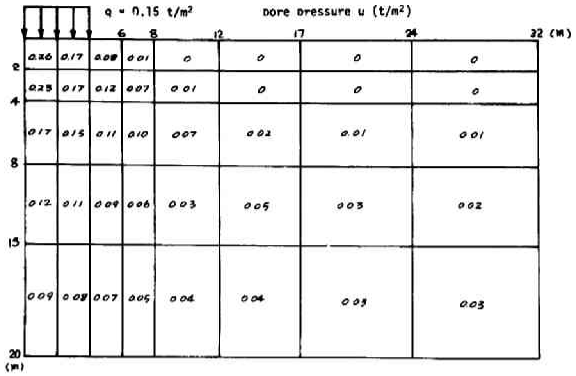


(b)

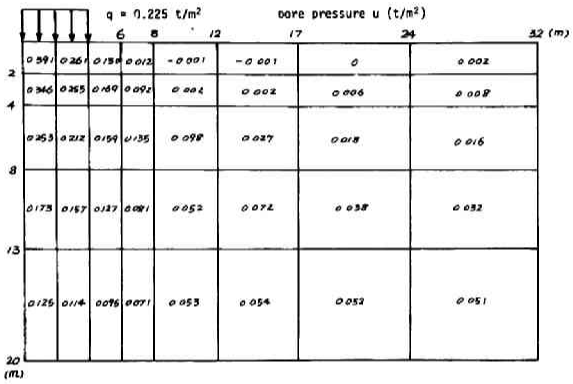


(c)

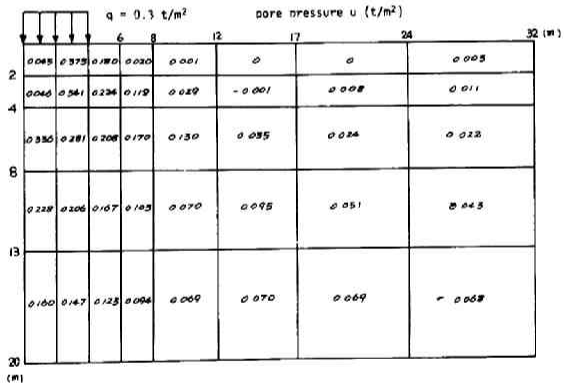


Fig.8.6. Induced pore water pressure
(a) Case 1
(b) Case 2
(c) Case 3

(a)

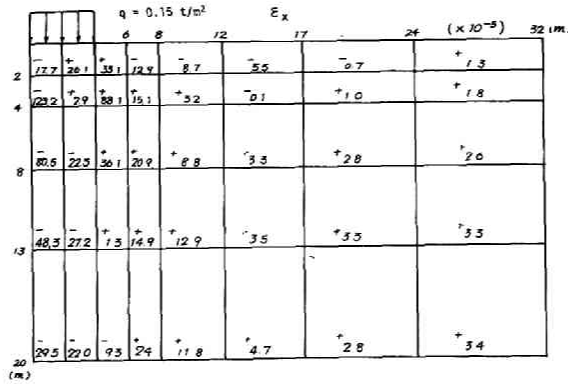


(b)

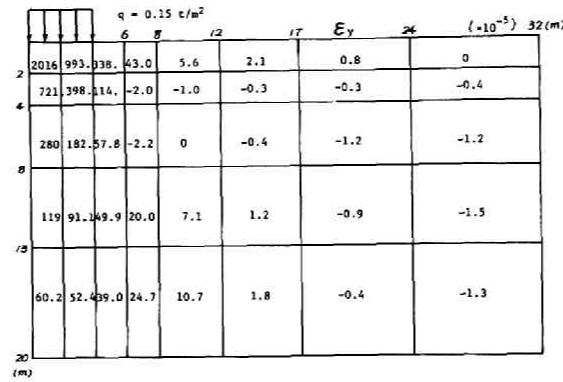


(c)

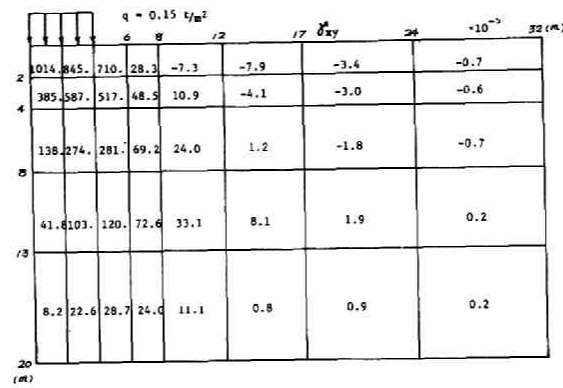


Fig.8.7. Strain increments (Case 1)
(a) increments of $\varepsilon_x$
(b) increments of $\varepsilon_y$
(c) increments of $\gamma_{xy}$

(a)

q = 0.225 t/m² $\varepsilon_x$ ($\times 10^{-5}$)

| (m) | 6 | 8 | 12 | 17 | 24 | 32 (m) |
|---|---|---|---|---|---|---|
| 2 | 34.7 -78 | 41.0 -25.2 | -13.4 | -8.3 | -0.9 | 2.0 |
| 4 | -185.9 0.5 | 187.2 21.0 | 5.3 | -0.2 | -1.7 | 2.8 |
| 8 | -194.5 -32.8 | 52.1 24.9 | 13.4 | 5.0 | 4.3 | 4.0 |
| 15 | -66.4 -32.7 | 1.09 17.1 | 17.9 | 5.1 | 5.0 | 5.0 |
| 20 (m) | -39.3 -29.3 | -17.6 2.5 | 15.2 | 5.4 | 4.2 | 5.1 |

(b)

q = 0.225 t/m² $\varepsilon_y$ ($\times 10^{-5}$)

| (m) | 6 | 8 | 12 | 17 | 24 | 32 (m) |
|---|---|---|---|---|---|---|
| 2 | 478.8 1145.7 | 607.5 75.1 | 9.1 | 3.2 | 1.1 | 0 |
| 4 | 1148.2 | 652.4 190.2 | -1.7 | -1.6 | -0.3 | -0.4 | -0.6 |
| 8 | 446.8 | 271.5 89.1 | -1.9 | 0 | -0.4 | -1.8 | -1.9 |
| 15 | 156.2 | 127.6 70.6 | 30.0 | 12.2 | 2.0 | -1.4 | -2.2 |
| 20 (m) | 71.6 | 69.3 | 51.7 | 33.2 | 14.6 | 2.4 | -0.7 | -2.0 |

(c)

q = 0.225 t/m² $\gamma_{xy}$ $\times 10^{-5}$

| (m) | 6 | 8 | 12 | 17 | 24 | 32 (m) |
|---|---|---|---|---|---|---|
| 2 | 2451. 1506. | 1111. 25.7 | -15.4 | -12.8 | -5.0 | -1.0 |
| 4 | 619. 889. | 783. 65.9 | 18.8 | -5.5 | -4.1 | -1.0 |
| 8 | 202. 388. | 400. 84.5 | 35.4 | 1.2 | -2.7 | -1.0 |
| 15 | 58.0 141. | 164. 94.8 | 50.5 | 11.9 | 3.0 | 0.4 |
| 20 (m) | 11.0 30.0 | 37.9 31.2 | 16.4 | 1.6 | 1.3 | 0.3 |

Fig.8.8. Strain increments (Case 2)
(a) increments of $\varepsilon_x$
(b) increments of $\varepsilon_y$
(c) increments of $\gamma_{xy}$

(a)

q = 0.3 t/m²  $\varepsilon_x$  (x 10⁻⁵)

| | 6 | 8 | 12 | 17 | 24 | 32 (m) |
|---|---|---|---|---|---|---|
| 2 | 6912 -4800 -510 | -686 | -26.7 | -14.3 | -14 | 27 |
| 4 | -2351 -152 1885 | 218 | 73 | -11 | 23 | 38 |
| 8 | -1415 -454 612 | 280 | 17.9 | 66 | 57 | 54 |
| 15 | -852 -486 08 | 19.4 | 25.2 | 67 | 68 | 67 |
| 20 (m) | -485 -359 -16.0 | 26 | 18.8 | 62 | 56 | 68 |

(b)

q = 0.3 t/m²  $\varepsilon_y$  X10⁻⁵

| | 6 | 8 | 12 | 17 | 24 | 32 (m) |
|---|---|---|---|---|---|---|
| 2 | — 4872 1099 | 1321 | 16.8 | 54 | 17 | -01 |
| 4 | 1824 981 286 | -12 | -24 | -05 | -05 | -08 |
| 8 | 5574 3703 1235 | -14 | -01 | -06 | -26 | -24 |
| 15 | 2165 1660 922 | 408 | 17.5 | 26 | -19 | -30 |
| 20 (m) | 998 868 648 | 400 | 18.5 | 29 | -10 | -27 |

(c)

q = 0.3 t/m²  $\gamma_{xy}$  ×10⁻⁵

| | 6 | 8 | 12 | 17 | 24 | 32 (m) |
|---|---|---|---|---|---|---|
| 2 | — 3004 1526 | 31.9 | -49.4 | -24.2 | -7.9 | -1.2 |
| 4 | 887. 1229. 1080. | 82.8 | 25.0 | -8.4 | -5.3 | -1.3 |
| 8 | 270. 510. 526. | 100. | 46.8 | 0.8 | -3.8 | -1.4 |
| 15 | 75.2 180. 210. | 118. | 68.4 | 15.7 | 4.0 | 0.5 |
| 20 (m) | 14.0 37.8 47.4 | 38.8 | 21.9 | 2.5 | 1.7 | 0.3 |

Fig.8.9. Strain increments (Case 3)
(a) increments of $\varepsilon_x$
(b) increments of $\varepsilon_y$
(c) increments of $\gamma_{xy}$

(a)

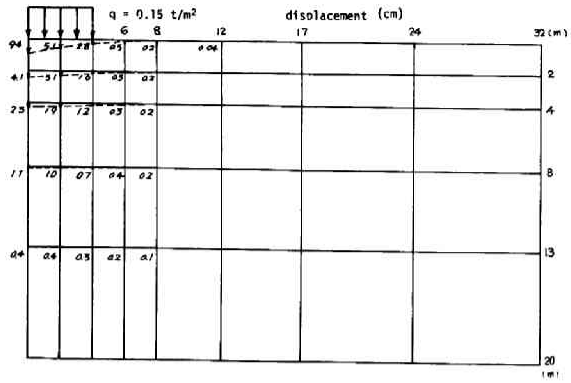


(b)

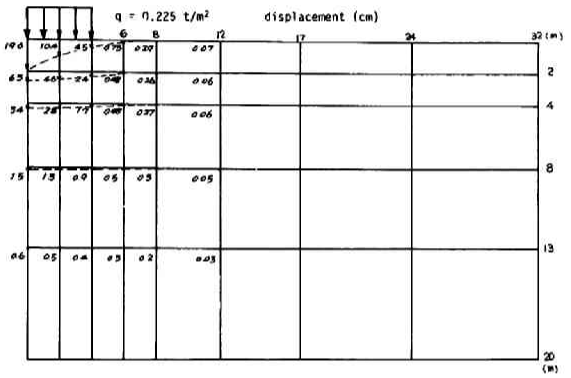


(c)

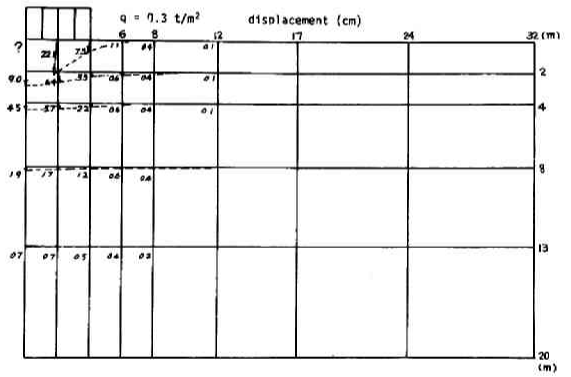


Fig.8.10. Immediate settlement
(a) Case 1
(b) Case 2
(c) Case 3

Unfortunately such a characteristic of the shear strain brings the difficulty into the computation and gives remarkablly limited usage of the present analysis in the practical engineering problems.

The immediate settlement for each case is shown in Figs.8.10(a)-(c) respectively. In spite of the undrained condition, the calculated deformations show the volume decrease of clay layer. This is considered to arise from the character of shear strain mentioned above.

## 8.4 Conclusions

In this chapter analysed is the immediate settlement of embankments constructed on the anisotropically normally consolidated clay layer. When considerablly rapid construction of embankments is performed, the pore water pressures set up in the clay layer are not allowed to dissipate. Stress and strain field induced by the application of load are to be analysed with a set of equilibrium equations accompanied by the stress-strain relations. This sort of analysis is the logically consistent procedure applicable to any continuum. In the case of saturated clay stressed under undrained condition, pore water pressure is to be taken into account.

In the investigations presented in this chapter, these theoretical requirements are completely satisfied. And stress and strain field in the clay layer are obtained numerically. As mentioned above, the analysing method presented here is logically self-consistent, but the computation results are not so satisfactory because of their rough accuracy. In addition to the question of the accuracy, some difficulties arising from the rapidly increasing tendency of shear strain in the clay element stressed by high stress ratio $\tau_{oct}/\sigma'_m$. Shear strain in such a clay element is hardly determined in the computation process.

This investigations given in this chapter were not achieved to the present stage without the cooperation of Mr.S.Yoshitani.

# CHAPTER 9

# CONSOLIDATION SETTLEMENT OF EMBANKMENTS

## 9.1 Introduction

As mentioned in the previous chapter, the logically consistent analysis of stress and strain field in the ground loaded by the construction of an embankment is too laborious and its accuracy is not so satisfactory. Then, in this chapter, the immediated and consolidation settlement of embankments are deducted based on the stress-strain relations and three dimensional consolidation theory presented in Chapter 5 and 7 respectively. And with the informations obtained from the computation, discussed is the accuracy of current estimation methods of immediate settlement, consolidation settlement and final settlement of embankments.

## 9.2 Procedures of Analysis

1. Stress Distributions

The embankment constructed on the anisotropically consolidated clay layer is replaced by the uniform load.

*Initial Stress Distribution*

The initial stress distribution in the clay layer before the application of the load is determined from the own weight of clay as follows:

$$\sigma_y^i = \rho y \tag{9.2.1}$$

$$\sigma_x^i = \sigma_z = K_0\sigma_y = K_0\rho y \tag{9.2.2}$$

$$\tau_{xy}^i = 0 \tag{9.2.3}$$

where y is the depth and x, z are the lateral distances of the clay element and $\rho$ is the specific dencity of the clay element.

*Additional Stress Distribution due to the Loading*

The additional stress distribution due to the loading is assumed to be determined from the theory of elasticity. Fortunately, stress

distribution given by the theory of elasticity is independent of the elastic constants in this case. The stress distribution derived from the finite element method is rather symilar to that given by the theory of elasticity as shown in Chapter 8. Then, the stress distribution in this case is considered not to be so sensitive to the stress-strain relations. Then we assume that the additional stress distribution is given by:

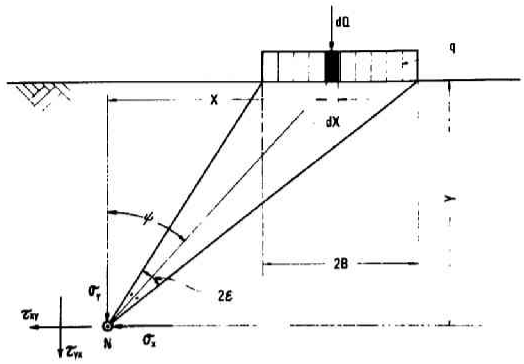


Fig.9.1. Stress field induced by strip loading (after Akai)

$$\sigma_y^l = \frac{q}{\pi}(2\varepsilon + \sin 2\varepsilon \cos 2\phi) \tag{9.2.4}$$

$$\sigma_x^l = \frac{q}{\pi}(2\varepsilon - \sin 2\varepsilon \cos 2\phi) \tag{9.2.5}$$

$$\tau_{xy}^l = \frac{q}{\pi}\sin 2\varepsilon \sin 2\phi \tag{9.2.6}$$

where q, ε and ϕ are shown in Fig.9.1.

*Total Stress Distribution*

The total stress distribution is assumed to be given by the sum of the initial stress and additional stress as follows:

$$\sigma_y = \rho y + \frac{q}{\pi}(2\varepsilon + \sin 2\varepsilon \cos 2\phi) \tag{9.2.7}$$

$$\sigma_x = K_0 \rho y + \frac{q}{\pi}(2\varepsilon - \sin 2\varepsilon \cos 2\phi) \tag{9.2.8}$$

$$\tau_{xy} = \frac{q}{\pi}\sin 2\varepsilon \sin 2\phi \tag{9.2.9}$$

As mentioned in Chapter 5, the intermediate principal stress is approximately equal to the mean principal stress in the case of plane strain deformation. Then, we get the distributions stress invariants of total stress after loading as follows:

$$\sigma_m \mp \frac{1 + 2K_0}{3} \rho h + \frac{q}{\pi} 2\varepsilon \tag{9.2.10}$$

$$\tau_{oct} = \frac{1}{6}(\sigma_x - \sigma_y)^2 + \frac{2}{3}\tau_{xy}^2 \tag{9.2.11}$$

*Effective Stress Distribution (just after loading)*

Just after the loading, the clay layer is considered to deform under the undrained condition. The stress path of the anisotropically normally consolidated clay is given by:

$$\tau_{oct} = k_0\sigma_m' \mp \frac{\lambda}{(1+e_0)\mu} \sigma_m' \ln \frac{\sigma_m'}{\sigma_{m0}'} \tag{9.2.12}$$

where the upper and lower signs show the active and passive loading states. The octahedral shear stresses in terms of effective stress and total stress are coincident. Then from eqs.(9.2.11) and (9.2.12), we can obtain the effective mean principal stress $\sigma_m'$. In such a way, the effective stress distribution is determined throughout the clay layer. At the same time, the pore water pressure distribution is calculated as the difference between $\sigma_m$ and $\sigma_m'$.

2. Immediate Settlement

*Stress-Strain Relation*

Stress-strain relation of normally consolidated clay is given as:

$$d\varepsilon_{ij} = \frac{\mu}{3\sigma_m'}[\{\frac{\lambda - \kappa}{(1+e_0)\mu} \mp \frac{\tau_{oct}}{\sigma_m'}\}\delta_{ij} \pm \frac{1}{\tau_{oct}} (\sigma_m' - \sigma_m'\delta_{ij})]$$

$$[d\sigma_m' \pm \frac{d\tau_{oct}}{\frac{\lambda - \kappa}{(1+e_0)\mu} - \frac{\tau_{oct}}{\sigma_m'}}] + \frac{\kappa}{3\sigma_m'} \frac{d\sigma_m'}{1+e_0} \delta_{ij} \tag{9.2.13}$$

We must integrate the strain increments along the loading history in order to obtain the strain field in the clay layer stressed by the uniform load q. In this chapter, we devide the load into 100 load increments, and calculate the strain field by the repetitious

integration of the strain increments induced by the imaginary load increments q/100.

*Immediate Settlement*

From the strain distribution obtained in the way mentioned above, the immediate deformation (undrained deformation) of the clay layer is to be deduced. Strain is defined as:

$$\varepsilon_x = \frac{\partial S_x}{\partial x} \tag{9.2.14}$$

$$\varepsilon_y = \frac{\partial S_y}{\partial y} \tag{9.2.15}$$

$$\gamma_{xy} = \frac{1}{2}\left(\frac{\partial S_y}{\partial x} + \frac{\partial S_x}{\partial y}\right) \tag{9.2.16}$$

where $S_x$ and $S_y$ are the displacements in x and y direction respectively In this chapter, we obtain the difference between the displacement of any neighboured points as follows:

$$\Delta S = \varepsilon_x \Delta x \tag{9.2.17}$$

$$\Delta S = \varepsilon_y \Delta y \tag{9.2.18}$$

where $\Delta x$ and $\Delta y$ are the distances of any neighboured points in the clay layer.

3. Consolidation Settlement

*Dissipation of Set up Pore Water Pressure*

In Chapter 7, we have already constructed the three dimensional consolidation theory based on the stress-strain relations presented in Chapters 4 and 5. Reducing the fundamental equation of three dimensional consolidation into the two dimensional consolidation, with the assumption that the values of coefficients of permeablity $k_x$, $k_y$, $k_z$ are identical to $k$ and do not change during the consolidation process, we get:

$$-\frac{k}{\rho_w}\left(\frac{\partial^2 u}{\partial x^2} + \frac{\partial^2 u}{\partial y^2}\right) = \frac{1}{\sigma_m' - u}\left\{\pm\mu\frac{\tau_{oct}}{\sigma_m' - u} - \frac{\lambda}{(1+e_0)}\right\}\frac{\partial u}{\partial t} \tag{9.2.19}$$

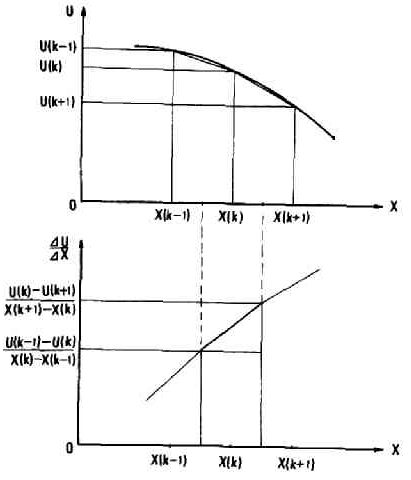


Fig.9.2. Distribution of pore water pressure

As shown in Fig.9.2, we know the pore water pressures at the neighboured points $k-1$, $k$ and $k+1$.

The pore pressure gradient is approximately represented as:

$$\frac{\partial u}{\partial x} = \frac{\Delta u}{\Delta x} \tag{9.2.20}$$

Then we get:

$$\frac{\partial^2 u}{\partial x^2} = \frac{\dfrac{u(k-1) - u(k)}{x(k) - x(k-1)} - \dfrac{u(k) - u(k+1)}{x(k+1) - x(k)}}{\frac{1}{2}\{x(k+1) - x(k-1)\}} \tag{9.2.21}$$

If all the distances between neighboured points are coincident to , eq.(9.2.21) is reduced to:

$$\frac{\partial^2 u}{\partial x^2} = \frac{u(k-1) - 2u(k) + u(k+1)}{(\Delta x)^2} \tag{9.2.22}$$

In the same way as mentioned above, we obtain the left hand side of eq.(9.2.19), and then the pore water pressure change $\Delta u$ in the duration of $\Delta t$.

*Consolidation Settlement*

Using the infinitesimal pore pressure decrease $\Delta u$, we get the effective stress increment after $\Delta t$ as follows:

$$\Delta\sigma'_{ij} = -\Delta u \delta_{ij} \tag{9.2.23}$$

Then the effective stress after $\Delta t$ is $\sigma'_{ij} + \Delta\sigma'_{ij}$. From eq.(9.2.13), we can calculate the strain increment $\Delta\varepsilon_{ij}$. By adding the strain increments to the previous strains, we know the strain field at the time $t+\Delta t$, and the deformation of the clay layer.

## 9.3 Immediate Settlement

Clay layer is assumed to be normally consolidated. The strengths of the clay elements located at the surface of clay layer are zero. Therefore the clay. to the depth of 1 m from the surface, is assumed to be replaced by sands. But on the calculation, the strength and deformation of the sand layer is neglected, i.e., the sand layer is assumed to deform following the settlement of clay layer without mobilizing its shear resistence. Grand water table is assumed to be at 1 m below the ground surface.

Sand layer is also assumed to exist under the clay layer. The clay elements located at the bottom boundary between the clay and sand layer is assumed to displace only laterally. The vertical displacements $S_y$ of the clay elements are calculated by integrating $\varepsilon_y$ from the bottom of the clay layer. The points located just under the center of uniform load are not allowed to move laterally. The lateral displacements $S_x$ of the clay elements are calculated by integrating $\varepsilon_x$ from the line just under the center of the load.

The values of the coefficients used in the calculation are as follows:

$$\rho = 1.6322\ \mathrm{t/m^3}, \qquad \lambda = 0.3112, \qquad \kappa = 0.1089,$$

$$\mu = 0.1150, \qquad k_0 = 0.3536\ (K_0 = 0.5)$$

$$k_x = k_y = 1.0\mathrm{x}10^{-6}\ \mathrm{cm/sec}$$

and the value of $e_0$ corresponding to $\sigma'_{m0} = 10\ \mathrm{t/m^2}$ is 1.594. These constants are identical with those used in Chapter 8.

Calculation is carried on for the following four cases:

Case 1: Load intensity $q = 0.5\ \mathrm{t/m^2}$

Thickness of clay layer: 20 m

Case 2: Load intensity q = 0.3 t/m
Thickness of clay layer: 20 m

Case 3: Load intensity q = 0.15 t/m
Thickness of clay layer: 20 m

Case 4: Load intensity q = 0.3 t/m
Thickness of clay layer: 10 m

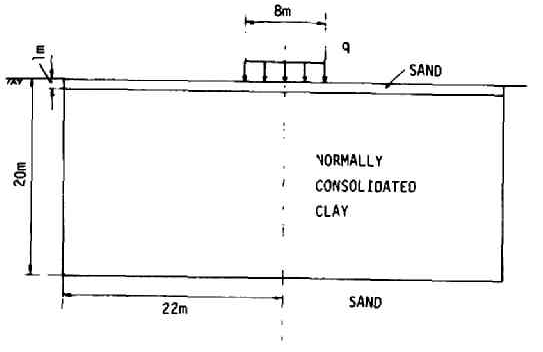


Fig.9.3. Key sketches of the problem

(a) Cases 1,2,3

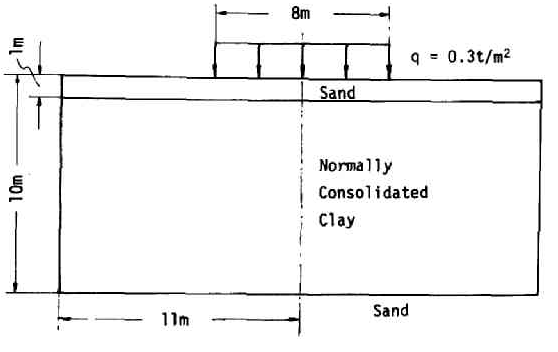


(b) Case 4

The brief descriptions of the problems are shown in Fig.9.3(a) (Case 1,2,3) and Fig.9.3(b) (Case 4).

The stress distributions in the Case 1 and Case 4 are shown in Figs.9.4(a)-(c) and in Figs.9.5(a)-(c). These stress fields are rather similar to those given in Chapter 8.

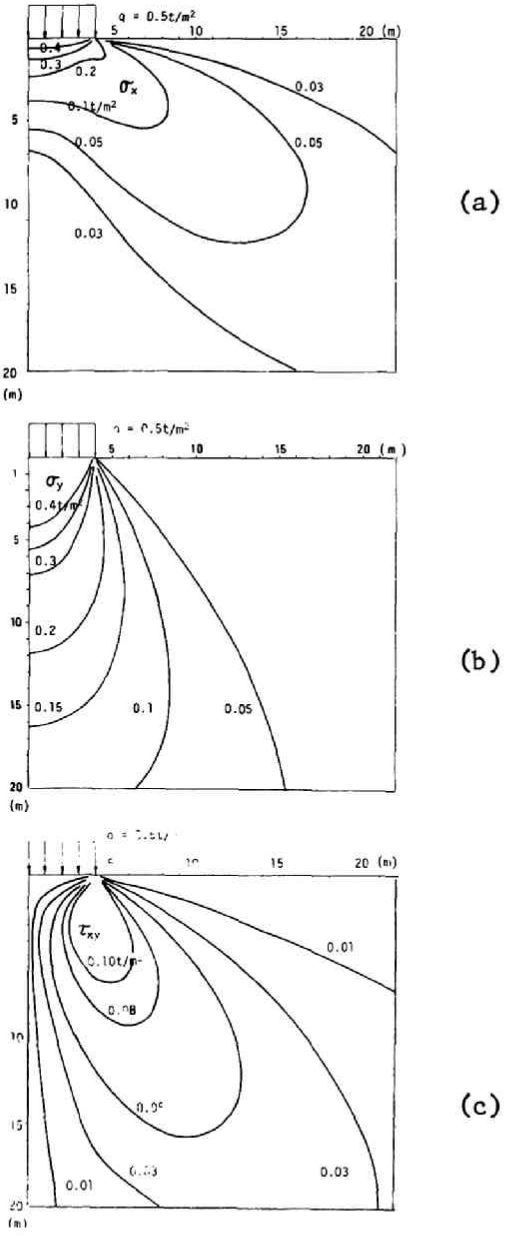


(a)

(b)

(c)

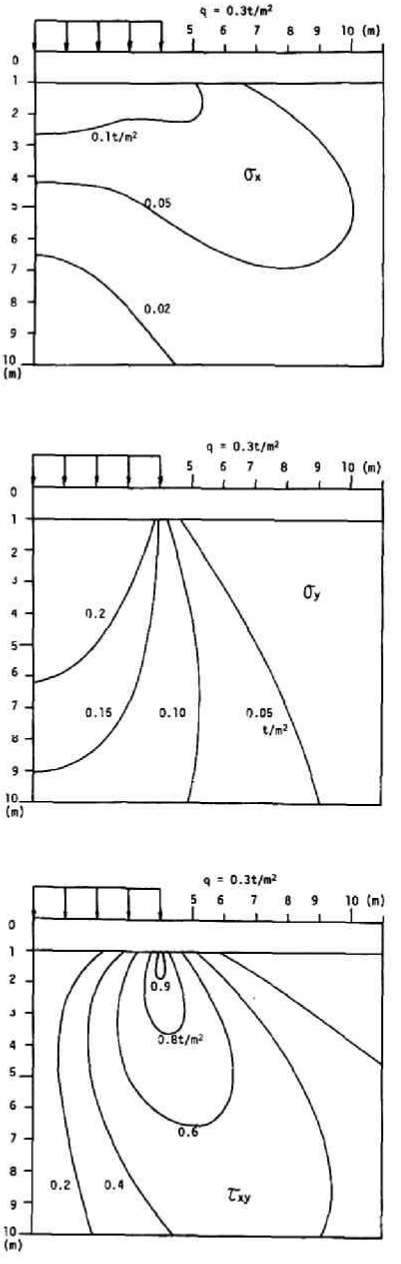


(a)

(b)

(c)

Fig.9.4. Stress field (Case 1)
(a) $\sigma_x$
(b) $\sigma_y$
(c) $\tau_{xy}$

Fig.9.5. Stress field (Case 2)
(a) $\sigma_x$
(b) $\sigma_y$
(c) $\tau_{xy}$

The pore water pressure distributions set up by the loading are given in Figs.9.6(a)-(d). It is noteworthy that the induced pore water pressures in the clay elements located near the load are larger than the applied load intensities. This phenomenon is caused by the effect of dilatancy and eminent in the clay with large μ. This arises from the present theory which takes account of the effect of dilatancy and remarkablly distinguishes the present theory from the current consolidation theory.

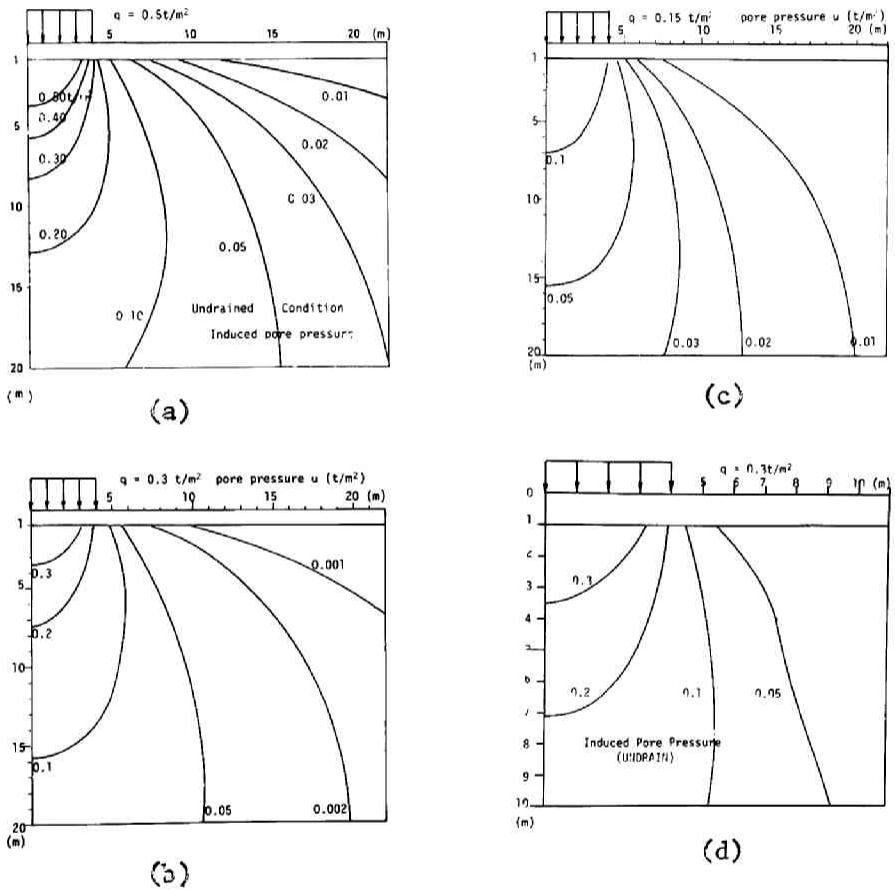


Fig.9.6. Induced pore water pressure

(a) Case 1 (b) Case 2 (c) Case 3 (d) Case 4

The strain fields just after the loading in the Cases 1-4 are shown in Figs.9.7(a)(b)(c), Figs.9.8 (a)(b), Figs.9.9(a)(b) and Figs.9.10 (a)(b) respectively.

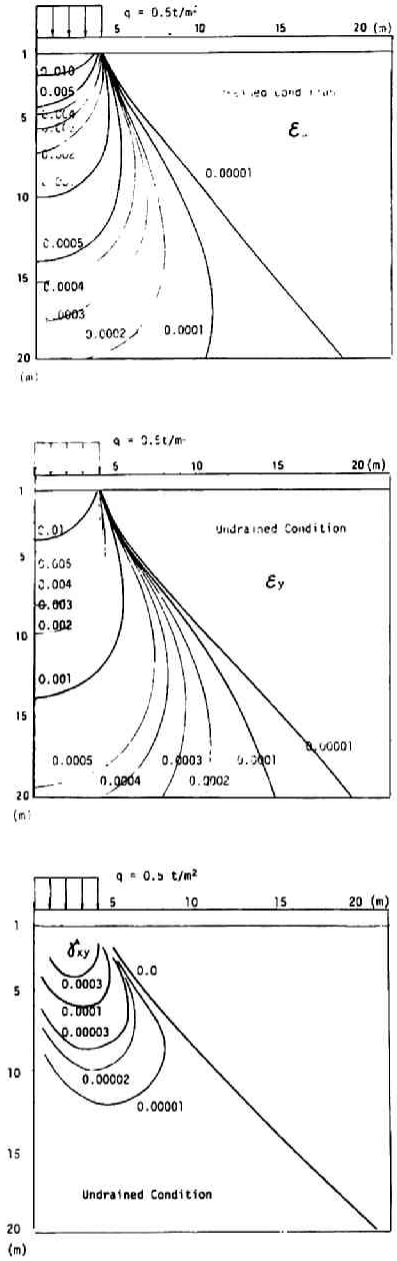


Fig.9.7. Strain field
(undrained, Case 1)
(a) $\varepsilon_x$
(b) $\varepsilon_y$
(c) $\gamma_{xy}$

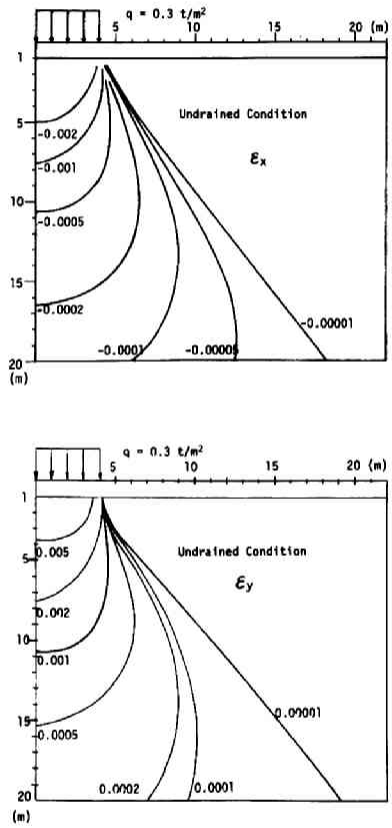


Fig.9.8. Strain field
(undrained, Case 2)
(a) $\varepsilon_x$
(b) $\varepsilon_y$

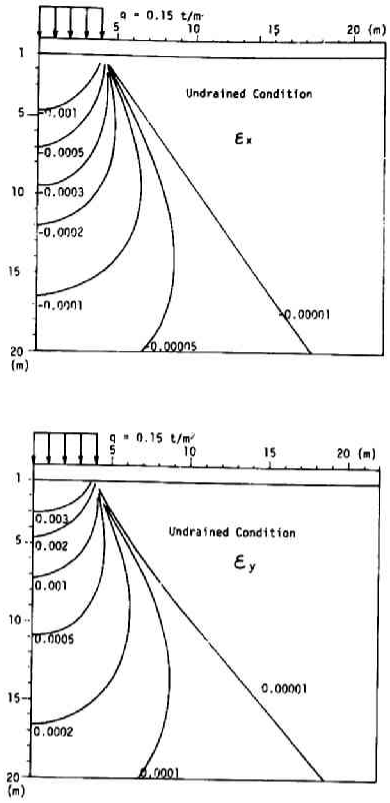


Fig.9.9. Strain field
(undrained, Case 3)
(a) $\varepsilon_x$
(b) $\varepsilon_y$

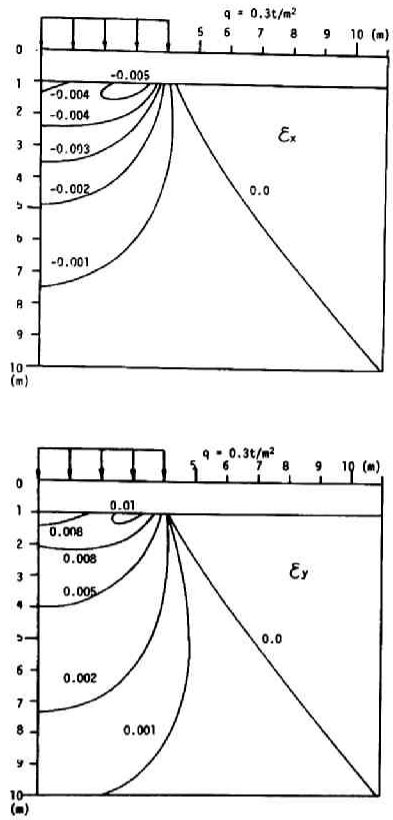


Fig.9.10. Strain field
(undrained, Case 4)
(a) $\varepsilon_x$
(b) $\varepsilon_y$

The immediate settlement (undrained deformation) of each case is given in Figs.9.11(a)-(d) respectively. In the case of real embankments, the swelling of the clay surface beside the embankment is often observed just after the construction. But the calculation results presented above do not show such a swelling. This is caused by the incomplete set of boundary conditions and by the stress distribution derived from the theory of elasticity. This sort of calculation was also presented by Burland (1969) based on the Cambridge modified energy theory.

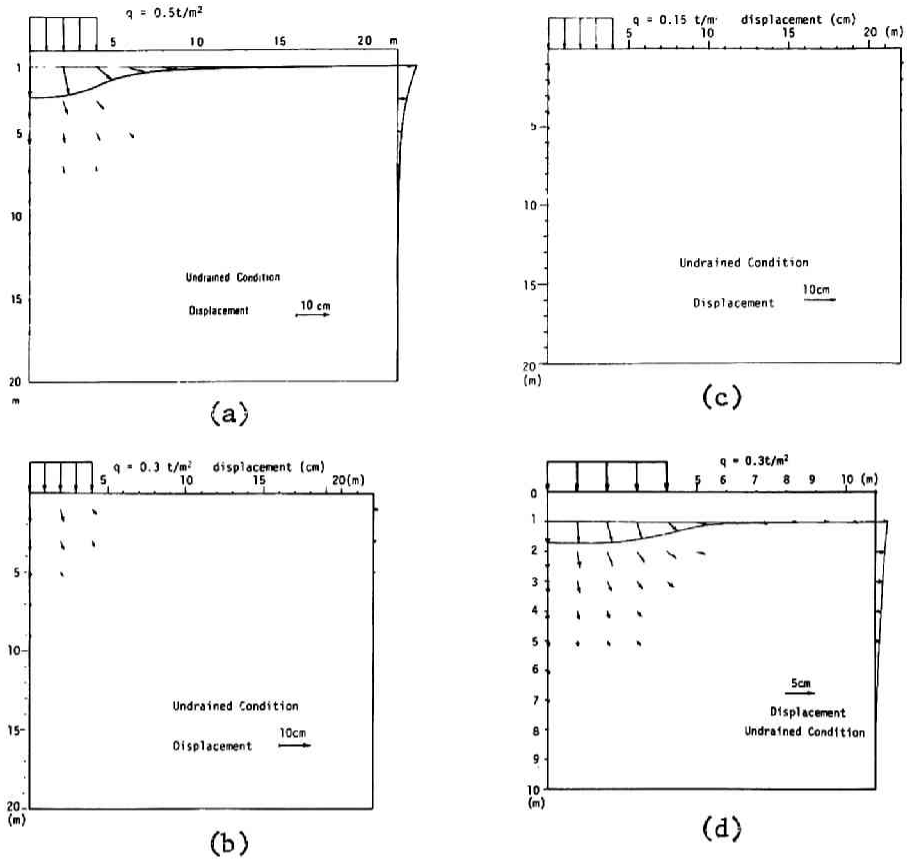


Fig.9.11. Immediate settlement
(a) Case 1 (b) Case 2 (c) Case 3 (d) Case 4

The development of the critical state zone with the increase of load intensity is shown in Fig.9.12. Fig.9.12 shows that the critical state zone is developed in the region just under the load. This is a great contrast with the assumption that the region just under the load remains sound in the current stability analyses.

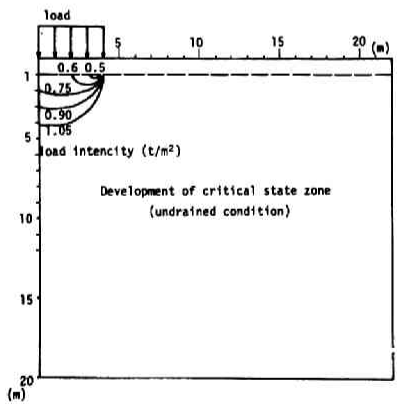


Fig.9.12. Development of critical state zone (undrained condition)

## 9.4 Consolidation Settlement

With the boundary condition that the pore water pressure is always vanished at the boundary between sand and clay layer, the consolidation settlement (additional deformation due to the dissipation of pore water) is calculated for the Case 1 and Case 4. The infinitesimal time $\Delta t$ in the calculation is:

$\Delta t$ = 1 day for 1-10 days,

$\Delta t$ = 10 days for 10-100 days,

$\Delta t$ = 100 days for 100-1000 days,

in the Case 1. But t determined in this way does not seem to be so adequate because the stage of consolidation in every clay element is different from each other depending on its location in the clay layer. In Case 4, $\Delta t$ = 10 days throughout the dissipation process of pore water pressure.

Fig.9.13 shows the dissipating processes of pore water pressures in the clay elements located just under the tip of the load (4m apart from the center of the load).

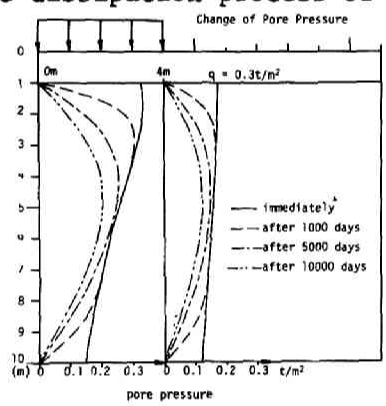


Fig.9.13. Description of pore water pressure (Case 4)

The situations of pore water pressure dissipation at the typical points and the surface settlements are shown in Figs.9.14(a)-(d) and Figs.9.15(a)(b) for Case 1 and Case 4 respectively. They show that the immediate settlement of embankments is considerablly larger than the consolidation settlement.

Fig.9.16 shows the deformation of clay layer after 100 days in Case 1. Fig.9.17 shows also the deformation after 10000 days in C Case 4. We can easily realize that the clay elements flowed laterally at the moment of loading come back to their original positions accompanied with the vertical settlement with the progress of pore water expulsion. But it is notes that on this process the clay

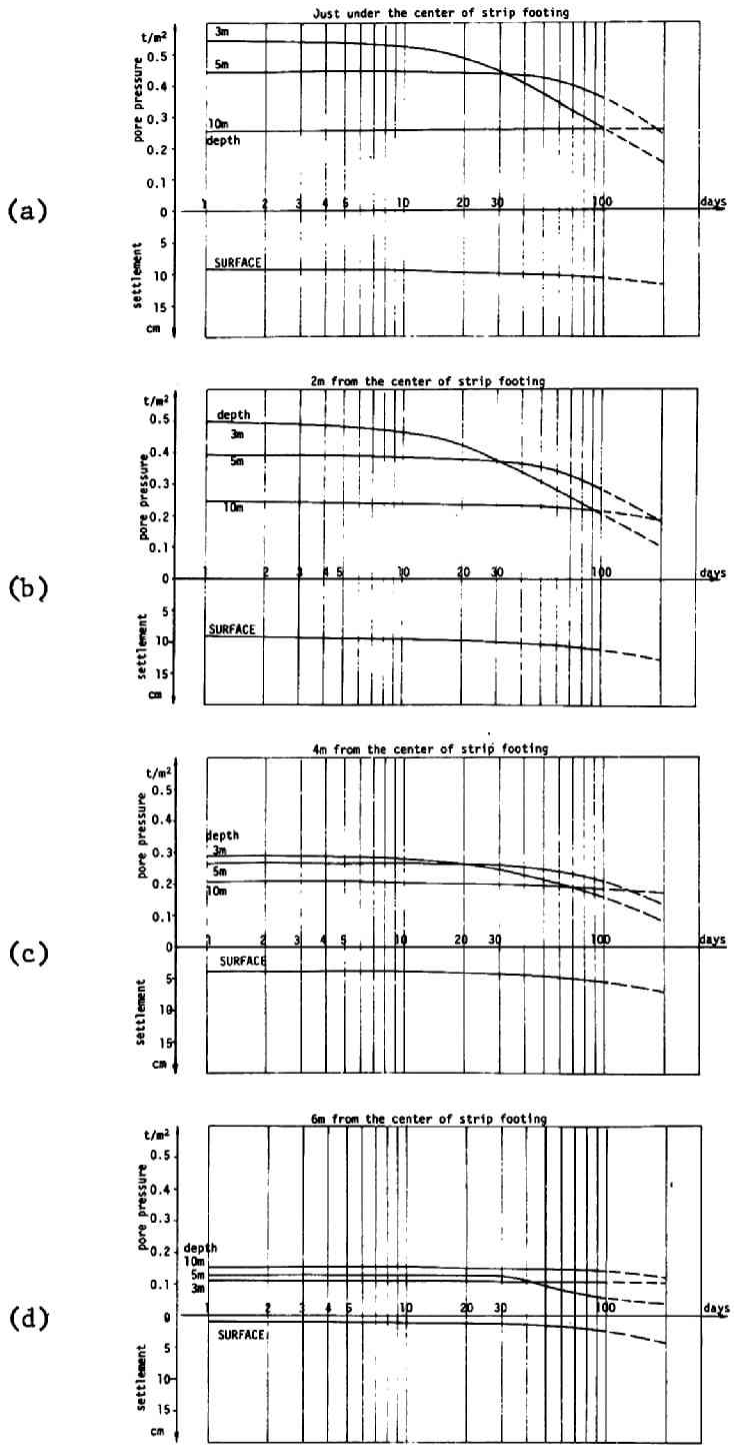


Fig.9.14. Pore pressure dissipation and surface settlement (Case 1)

(a)

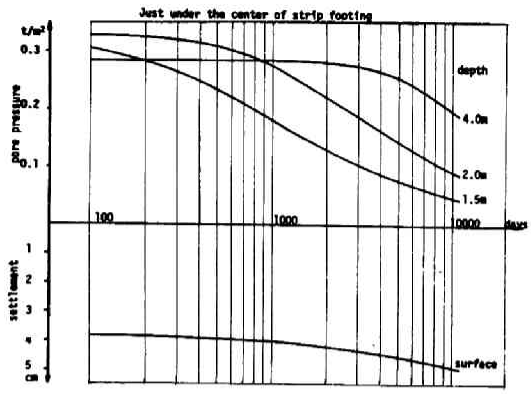


(b)

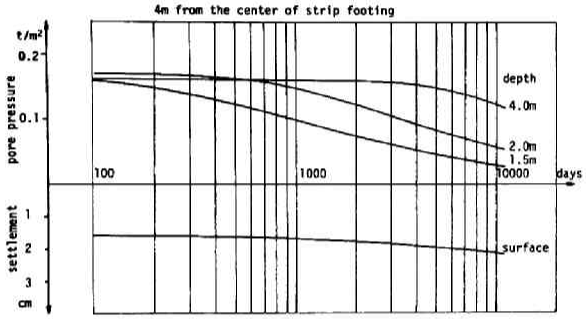


Fig.9.15. Pore pressure dissipation and surface settlement (Case 4)
(a) just under the center of strip load
(b) 4m from the center of strip load

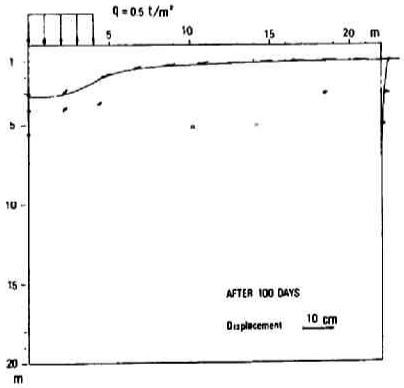


Fig.9.16. Deformation after 100 days (Case 1)

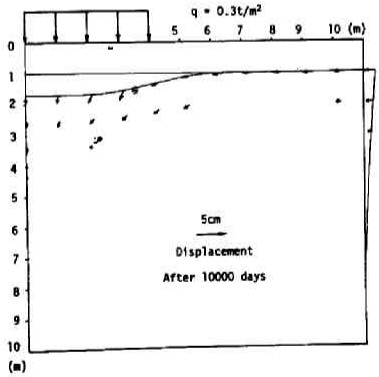


Fig.9.17. Deformation after 10000 days (Case 4)

elements deform distortionally further. Then, the clay elements in the uniformly loaded clay layer deform one-demensionally consequent on the undrained shear and following dissipation of pore water pressure.

The calculations presented here are still in the primitive stage and contain a lot of questions concerning the computation procedure. In order to make the analyses useful in the practical design and construction of embankments, further improvements are expected.

## 9.5 Final Settlement due to Consolidation

To analyse the progress of consolidation settlement, electronic computers are necessary. In the practical engineering activity, we often have to know the approximate consolidation settlement of embankment. In such a case, the simplified analysing method is to be used.

As clarified in the previous section, the displacements of the points in the clay layer stressed by uniform strip load can approximately be assumed to be one dimensional. This suggests that the settlement of embankments can be calculated from only the void ratio changes of clay elements. Here the calculation by such a simplified method is presented. The void ratio change is obtained from the concepts of state surface and swelling wall presented in Chapter 5. The brief description of the example is given in Fig.9.18. And calculated settlement is shown in Fig.9.19. This method is so simple that we can perform the calculation in a few hours without computers.

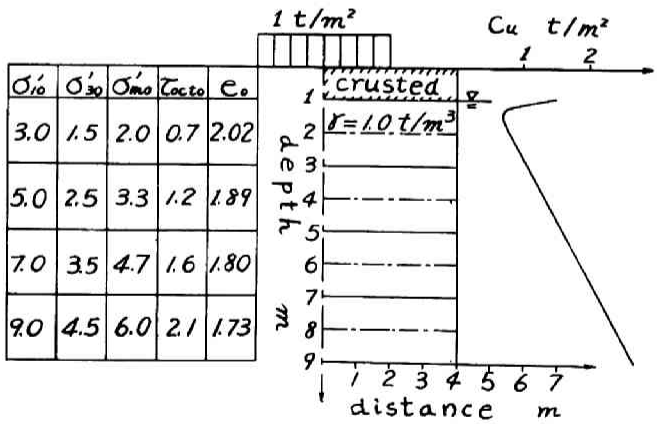


Fig.9.18. Key sketch of the problem

In the clay elements located just under the center of the strip

load, no volume change due to dilatancy can occur. Then, the void ratio changes of such clay elements can be predicted from the $e$-ln$p$ curve. This consideration gives the rationalization of the current method of final settlement estimation.

This simplified method p presented above is based on the similar phylosophy proposed by Lamb (1967). His "*stress path method*" requires the engineers to perform a lot of experimental works, because systematic description of mechanical behavior of soils is not established.

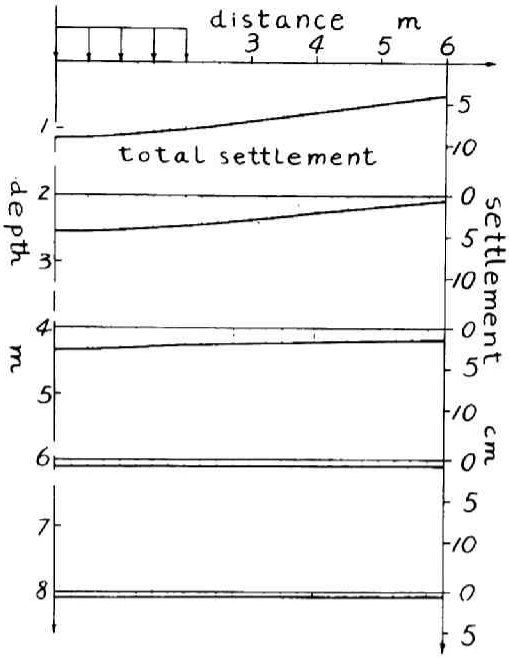


Fig.9.19. Final settlement

The deformation analyses presented in this chapter are considered to be much reliable compared with those proposed by Skempton and Bjerrum (1957) and improved by Davis and Poulos (1968).

## 9.6 Conclusions

In this chapter, presented are the mechanical states of the anisotropically normally consolidated clay layer stressed by the uniform strip load (embankment) just after the loading, and on the process of pore water expulsion and at the final stable state. And in the discussions the accuracy and limitation of the current methods of settlement estimation are evaluated.

In the analysis of the immediate settlement of embankments, we can see the progress of the shear deformation of clay layer with the increase of applied load. The situations are easily accepted by our intuitive feelings. The distributions of the induced pore water pressure obtained by the analysis tell us that the pore water pres-

sures set up just under the strip load are a little larger than the load intensity. This tendency caused by the dilatancy effect shows us some aspects of the characters of the present theory. The development of the critical state zone (so-called plastically flowing zone) with the increase of load intensity is clarified. The calculation results are in the remarkable contrast with those derived from the theory of elasticity or from the theory of characteristics field.

In the analysis of the consolidation settlement of embankments, we can also see the progress of shear deformation of the clay layer which suggests the appropriateness of the current estimation method of the final consolidation settlement of the embankments.

Based on the informations given by these analyses, a simplified estimation method of final settlement of the ground surface is proposed. This simplified method gives the same estimation of settlement so far as the center of the uniform strip load is concerned.

# CHAPTER 10

# CRITICAL STATE OF EMBANKMENTS

## 10.1 Introduction

In this chapter, the critical state of embankment is discussed. This sort of engineering problem has been called the "*stability problem*". It can be said that the soil mechanics has been developed with the stability problem as the central topic. The main subjects in the stability problem are considered to be the following two:

(a) The strength of soil

(b) The analytical method to solve the stability problem based on the failure condition of soil.

Here we try to construct a field theory of stress characteristics line based on the description of the mechanical behavior of soil presented in Chapters 4 and 5. And with the informations obtained in the process of construction of the theory, some practical considerations on the current failure conditions of soils and stability analyses that are based on the concepts of effective stress and total stress. In those considerations, the necessity of the proper understanding of the change in mechanical state of soils in the practical design and constructing works is emphasized.

## 10.2 Failure Conditions

### 1. Failure Conditions in Terms of Effective Stress

The stress state of normally consolidated natural clay layer is generally anisotropic. In the case of $K_0$-state, the stress ratio $\tau_{oct}/\sigma'_m$ in the normally and over-consolidated clay is kept constant at $K_0$ on the normal consolidation process and decreases on the swelling process as shown in Fig. 10.1. Here we consider the natural clay layer in normally or over-consolidated state. The stress ratio $\tau_{oct}/\sigma'_m$ of the clay in normally consolidated state is represented by $K_0$. Maximum pre-consolidation pressure is $\sigma'_{m0}$ and the void ratio corresponding to the maximum pre-consolidation pressure $\sigma'_{m0}$ is $e_0$.

In order to discuss in general the failure condition of clay, let us deal with the over-consolidated clays in which the normally consolidated clay is included as a special case. Then the initial state of the clay is represented by a set of ($\tau_{octi}$, $\sigma'_{mi}$, $e_i$).

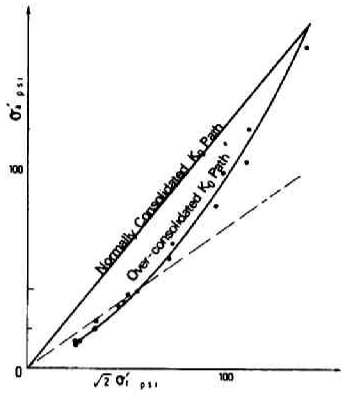


Fig.10.1.
Consolidation and swelling process without lateral deformation

As mentioned in Chapter 5, the stress condition for critical state is given by:

$$\frac{\tau_{oct}}{\sigma'_m} = \pm \frac{\lambda - \kappa}{(1+e_0)\mu}$$

where the upper and lower signs are corresponding to the active and passive loading state respectively. But it is noted that the negative value of $\tau_{oct}$ is defined in Chapter 5 for the sake of convenience. Then here we can rewrite this relation as follows in mathematically correct form:

$$\frac{\tau_{oct}}{\sigma'_m} = \frac{\lambda - \kappa}{(1+e_0)\mu} \equiv M \qquad (10.2.1)$$

In eq. (10.2.1). the values of $\kappa$, $\mu$ and $e_0$ are dependent on the maximum pre-consolidation pressure $\sigma'_{m0}$. Therefore the value of $M$ cannot be determined uniquely for the sonsidered clay layer, because the maximum pre-consolidation pressure depends on the depth of the clay element. But many experimental data show that the value of $M$ itself can be assumed to be a constant for the clay layer regardless of $\sigma'_{m0}$ with quite excellent accuracy. Fortunately, eq. (10.2.1) represents not only the critical state of normally consolidated clay

but also that of over-consolidated clay.

The most strict definition of the failure condition of clay we have had is proposed by Hvorslev in 1937 and given further physical meanings by Hvorslev (1960). Hvorslev's failure condition arises from the recognition that the mechanical behavior of clay depends on the water content of clay. Eq. (10.2.1) is also derived from the concept that the mechanical behavior of clay is closely related to the void ratio. But experimental data and considerations on the Hvorslev's paramenters given by Gibson (1953), Bjerrum (1954) and Noorany and Seed (1965) show that the difference between the Hvorslev's parameters and eq. (10.2.1) is seriously large. This difference is considered to be caused by the definition of the failure used in these research works.

As mentioned before, the failure state defined by the maximum stress deviator does not coincide with the critical state. The influence of this difference on the practical stability analysis will be discussed later in this chapter.

Eq. (10.2.1) suggests that the stress state of the critical state of soil is of von Mises type. On the other hand the experimental works carried on by Kirkpatrick (1957), Wu, Loh and Malvern (1963) and Shibata and Karube (1965) show that the failure condition of soil is approximately of Mohr-Coulomb type. Judging from the experimental data presented in Chapter 6, especially from those given by Henkel and Wade (1966), the mechanical behavior of clay on the shearing process is considered to be governed by the octahedral stresses. It is natural to consider that the failure state and the critical state are nothing else but the special states included in the shearing precess of clay. This dilemma must be vanished in future based on the much reliable experimental data. In the author's opinion, the extension test of soil in the conventional triaxial apparatus and the triaxial test by means of the devices of independent application of three principal stresses had many difficulties in the reliable measurement.

Many stability problems can be simplified to the plane strain problems. The stress condition for the plane strain deformation is discussed in Chapter 5. And we get the approximate stress condition for plane strain deformation as follows:

$$\sigma_2' = \frac{\sigma_1' + \sigma_3'}{2} = \frac{\sigma_x' + \sigma_y'}{2} \tag{10.2.2}$$

Substituting eq. (10.2.2) into eq. (10.2.1), we get the stress condition for the critical state under plane strain deformation as:

$$\begin{aligned} \sigma_x' &= \sigma_m'(1 + \sqrt{\tfrac{2}{3}}\, M \cos 2\theta\ ) \\ \sigma_y' &= \sigma_m'(1 - \sqrt{\tfrac{2}{3}}\, M \cos 2\theta\ ) \\ \sigma_{xy}' &= \sigma_m' \sqrt{\tfrac{2}{3}}\, M \sin 2\theta \end{aligned} \tag{10.2.3}$$

where $\theta$ is the direction of maximum principal stress as shown in Fig. 10.2. It should be noted that eqs. (10.2.3) are in the identical forms with those of Mohr-Coulomb failure condition in terms of effective stress without $c'$-parameter if the coefficient $\sqrt{\frac{2}{3}}\, M$ in eqs. (10.2.3) is substituted by $\sin\phi'$. This relation is rather convenient to develop our discussion further.

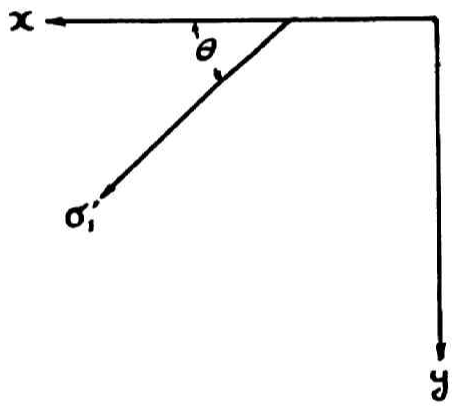


Fig. 10.2.
Direction of maximum principal stress

2. Failure Conditions in Terms of Total Stress

Skempton (1955) proposed the coefficients of pore water pressure A and B in order to represent the pore water pressure set up in clay specimens stressed in the conventional triaxial apparatus under undrained condition. Skempton's pore pressure coefficients are

theoretically extended by Skempton (1960) and Henkel and Wade (1960).

Here we try to derive the pore water pressure set up in the anisotropically pre-consolidated clay in the critical state. In this case we must use again the expression of the conventional definition of negative octahedral shear stress. Then the critical state is:

$$\frac{\tau_{oct}}{\sigma'_m} = \pm \frac{\lambda - \kappa}{(1 + e_0)\mu} \equiv \pm M \tag{10.2.4}$$

The current yield locus is given by:

$$\frac{\tau_{oct}}{\sigma'_m} - k_0 = \mp M \ln \frac{\sigma'_m}{\sigma'_{my}} \tag{10.2.5}$$

From eqs. (10.2.4) and (10.2.5) we get:

$$\ln \frac{\sigma'_m}{\sigma'_{my}} = - (1 \mp \frac{k_0}{M}) \tag{10.2.6}$$

The initial void ratio $e_i$ is given by:

$$e_i - e_0 = - \kappa \ln \frac{\sigma'_{mi}}{\sigma'_{m0}} \tag{10.2.7}$$

As shown in Fig. 10.3, the relationship between $e_i$ and $\sigma'_{my}$ is given by:

$$e_i = e_y - \kappa \ln \frac{\sigma'_m}{\sigma'_{my}} \tag{10.2.8}$$

Since the point ($\sigma'_{my}$, $e_y$) is on the normal consolidation line we get:

$$e_y = e_0 - \lambda \ln \frac{\sigma'_{my}}{\sigma'_{m0}} \tag{10.2.9}$$

From eqs. (10.2.8) and (10.2.9). it leads:

$$e_i = e_0 - \lambda \ln \frac{\sigma'_{my}}{\sigma'_{m0}} - \kappa \ln \frac{\sigma'_m}{\sigma'_{my}} \tag{10.2.10}$$

With eq. (10.2.7), eq. (10.2.10) is rewritten as:

$$\kappa \ln \frac{\sigma'_{mi}}{\sigma'_{m0}} = \lambda \ln \frac{\sigma'_{my}}{\sigma'_{m0}} + \kappa \ln \frac{\sigma'_m}{\sigma'_{my}} \tag{10.2.11}$$

Then, we get:

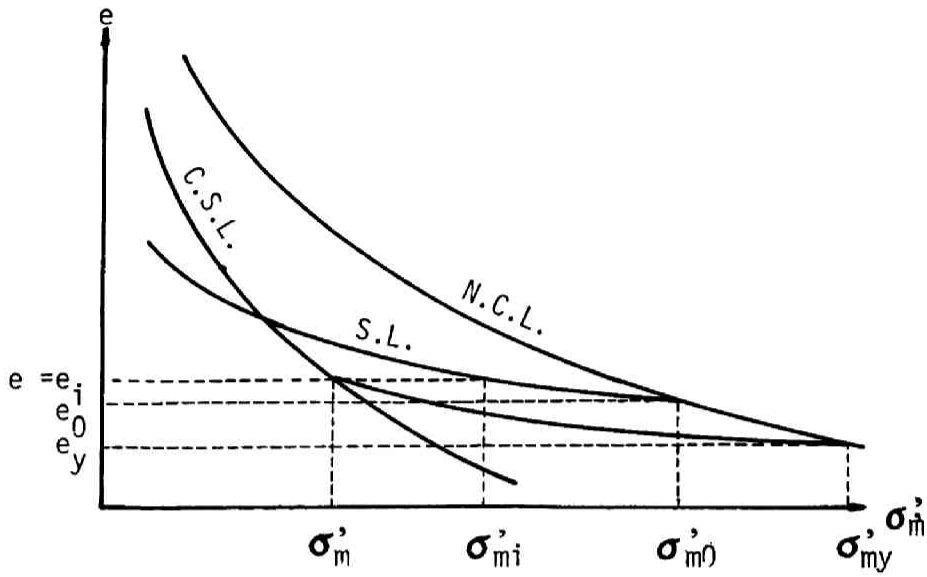


Fig. 10.3.
Effective mean principal stress at the critical state

$$\ln\sigma'_{my} = \ln\sigma'_{m0} + \frac{\kappa}{\lambda - \kappa} \ln \frac{\sigma'_{mi}}{\sigma'_m} \tag{10.2.12}$$

Substitution of Eq. (10.2.12) into eq. (10.2.6) gives:

$$\ln\sigma'_m = \frac{\lambda - \kappa}{\lambda} \{\ln\sigma'_{m0} - (1 \mp \frac{k_0}{M})\} + \frac{\kappa}{\lambda} \ln\sigma'_{mi} \tag{10.2.13}$$

then:

$$\sigma'_m = \sigma'_{m0} \exp. [ - (1 - \frac{\kappa}{\lambda})(1 \mp \frac{k_0}{M}) + \frac{\kappa}{\lambda} \ln \frac{\sigma'_{mi}}{\sigma'_{m0}}] \tag{10.2.14}$$

Defining:

$$C \equiv \exp. [ - (1 - \frac{\kappa}{\lambda})(1 \mp \frac{k_0}{M}) + \frac{\kappa}{\lambda} \ln \frac{\sigma'_{mi}}{\sigma'_{m0}}] \tag{10.2.15}$$

we get the effective mean principal stress $\sigma'_m$ at the critical state as follows:

$$\sigma'_m = C\ \sigma'_{m0} \tag{10.2.16}$$

It is noted that the value of C is different in the cases of active and passive loading state. But these value of C is uniquely determined when the $\sigma'_{m0}$ and $\sigma'_{mi}$ of the clay element are known.

For the normally consolidated clay deposit, the coefficient C is reduced as:

$$C = \exp.\ [\ -\ (1 - \frac{\kappa}{\lambda})(1 \mp \frac{k_0}{M})\ ] \qquad (10.2.17)$$

and is considered to be approximately constant throughout the clay layer. For the over-consolidated clay deposit, the value of C is not necessarily constant throughout the clay layer, because the initial effective mean principal stress $\sigma'_{mi}$ is the function of the depth of clay element and therefore the over-consolidation ratio $\frac{\sigma_{m0}}{\sigma'_{mi}}$ is not constant throughout the clay layer in general. But even for the over-consolidated clay layer, C can be assumed to be constant with adequate accuracy in the practical sense.

As mentioned above, the C value is not generally constant throughout the clay layer, but is uniquely determined for any clay element. From (10.2.16). the induced pore pressure at the critical state is given by:

$$\begin{aligned} \Delta u &= \sigma_m - \sigma'_m \\ &= \sigma_m - C\ \sigma'_{m0} \end{aligned} \qquad (10.2.18)$$

where $\sigma_m$ is the total mean principal stress applied to clay element in critical state. Since the initially applied mean principal stress is $\sigma'_{mi}$, the increase of total mean principal stress $\Delta\sigma_m$ is given by:

$$\Delta\sigma_m = \sigma_m - \sigma'_{mi} \qquad (10.2.19)$$

Then from eqs. (10.2.18) and (10.2.19), we get:

$$\Delta u = \Delta\sigma_m + \sigma'_{mi} - C\sigma'_{m0} \qquad (10.2.20)$$

Eq. (10.2.20) shows that the set up pore pressure in the clay element in critical state is given by the summation of $\Delta\sigma_m$ and a constant which is differently defined in the cases of active and passive loading state. Eq. (10.2.20) is remarkably in different form compared with Skempton's pore-pressure coefficients. In the author's opinion, it is more adequate and simpler to represent the effective mean stress at the critical state in the form given by (10.2.16) than

to represent the set up pore pressure at the critical state in terms of applied total stresses.

Now using eq. (10.2.16), let us rewrite eqs. (10.2.3) as follows:

$$\sigma_x = \sigma_m + \sqrt{\frac{2}{3}}\, M\, C\, \sigma'_{m0} \cos 2\theta$$
$$\sigma_y = \sigma_m - \sqrt{\frac{2}{3}}\, M\, C\, \sigma'_{m0} \cos 2\theta \qquad (10.2.21)$$
$$\tau_{xy} = \sqrt{\frac{2}{3}}\, M\, C\, \sigma'_{m0} \sin 2\theta$$

These are the stress conditions for the critical state in terms of total stresses. It is noteworthy that eqs. (10.2.21) are in different style of Mohr-Coulomb failure condition in terms of total stresses.

## 10.3 Characteristics Field

The equilibrum equations of a volume element located in the clay layer is given as follows:

$$\frac{\partial \sigma_x}{\partial x} + \frac{\partial \tau_{xy}}{\partial y} = 0$$
$$\frac{\partial \tau_{xy}}{\partial x} + \frac{\partial \sigma_y}{\partial y} = \gamma \qquad (10.2.22)$$

where $\gamma$ is the weight of the unit volume element. Eq. (10.2.22) is in terms of total stresses. In the place of total stress, one may construct the theory based on the equilibrium equations in terms of effective stresses and determine the field of effective stress characteristics, in such an analysis, the obtained bearing capacity of clay layer in the state of the end of construction is also in terms of effective stresses. This bearing capacity may be called effective bearing capacity. But in the practical engineering problems, such an effective bearing capacity is of no or little use. It is considered to be only of academic interest.

The total stress conditions for the critical state of clay stressed with no time allowance for the expulsion of pore water is

given by eqs. (10.2.21). Assuming that the every point in clay layer is in the critical state simultaneously, substitution of eqs. (10.2.21) into eqs. (10.2.22) is required:

$$\frac{\partial \sigma_m}{\partial x} - X \frac{\partial \theta}{\partial x} + Y \frac{\partial \theta}{\partial y} = - \gamma \sqrt{\frac{2}{3}} M \text{ C } \sin 2\theta$$

$$\frac{\partial \sigma_m}{\partial y} + X \frac{\partial \theta}{\partial x} + X \frac{\partial \theta}{\partial y} = \gamma \{1 + \sqrt{\frac{2}{3}} M \text{ C } \cos 2\theta\} \qquad (10.2.23)$$

where,

$$X \equiv 2 \sqrt{\frac{2}{3}} M \text{ C } (a + \gamma y) \sin 2\theta$$

$$Y \equiv 2 \sqrt{\frac{2}{3}} M \text{ C } (a + \gamma y) \cos 2\theta$$

On the process to derive eqs. (10.2.23), it is assumed that:

$$\sigma'_{m0} = a + \gamma y \qquad (10.2.24)$$

where a is a constant corresponding to the own weight of clay removed, for instance, by the erosion.

The inclinations of the stress characteristics are obtained by solving the characteristic equation of eqs. (10.2.23) as follows:

$$\frac{dy}{dx} = \tan (\theta \pm \frac{\pi}{4}) \qquad (10.2.25)$$

The upper and lower sign in eq. (10.2.25) are corresponding to the first and second family of stress characteristics. A little consideration shows that eq. (10.2.26) can be obtained with much broader assumption that the maximum pre-consolidation pressure $\sigma'_{m0}$ of the clay element is given by a smoothly continuous function of the position of the element, i.e.:

$$\sigma'_{m0} = \sigma'_{m0} (x, y) \qquad (10.2.26)$$

Eqs. (10.2.23) can be solved numerically with eq. (10.2.25). But it may be convenient in calculation to transform them as:

$$\sin(\theta + \frac{\pi}{4}) \frac{d\sigma_m}{ds_1} - \{X\sin(\theta + \frac{\pi}{4}) + Y\cos(\theta + \frac{\pi}{4})\} \frac{d\theta}{ds_1}$$

$$
\begin{aligned}
&- \sin(\theta - \frac{\pi}{4}) \frac{d\sigma_m}{ds_2} + \{X\sin(\theta - \frac{\pi}{4}) + Y\cos(\theta - \frac{\pi}{4})\} \frac{d\theta}{ds_2} \\
&= - \gamma \frac{2}{3} M \text{ C } \sin 2\theta \qquad\qquad (10.2.27) \\
&- \cos(\theta + \frac{\pi}{4}) \frac{d\sigma_m}{ds_1} - \{X\cos(\theta + \frac{\pi}{4}) - Y\sin(\theta + \frac{\pi}{4})\} \frac{d\theta}{ds_1} \\
&+ \cos(\theta - \frac{\pi}{4}) \frac{d\sigma_m}{ds_2} + \{X\cos(\theta - \frac{\pi}{4}) - Y\sin(\theta - \frac{\pi}{4}) \frac{d\theta}{ds_2} \\
&= \gamma(1 + \sqrt{\frac{2}{3}} M \text{ C } \cos 2\theta)
\end{aligned}
$$

where $ds_1$ and $ds_2$ are respectively the line element of first and second family of stress characteristics.

Solving eqs. (10.2.25) and (10.2.27) numerically with the adequate boundary condition of stress, we can define the stress field completely. But it should be noted that the coefficient C and therefore $X$ and $Y$ in eqs. (10.2.27) are of different values in the cases of active and passive loading state. This difference causes the quite troublesome difficulty in the stability analyses; not only in the present theory but also in the theories proposed by a lot of researchers and engineers.

The difference in the undrained strength of anisotropically consolidated clay in the state of active and passive loading and its influence on the safety factor for the sliding of soil structures are considered to be of vital importance in the practical sense. And stability analyses logically consistent with this sort of strength character of anisotropically consolidated clay are expected to be proposed.

Brinch Hansen and Gibson (1948) gave an excellent theoretical interpretation to the anisotropy of undrained strength of anisotropically consolidated clay and discussed the remarks to be considered in the practical designing. Taylor (1948) showed that the undrained strengths of anisotropically consolidated clay in the state of active and passive loading are uniquely defined in terms of effective stresses. Lowe and Karafiath (1960) also discussed the pore-pressure coefficient at failure of anisotropically consolidated

clay. But their theory cannot be supported by the present theory. Bailey (1964) showed that the c/p-value for the passive state is about half of that for the active state. Duncan and Seed (1966 (a), (b)) showed the experimental data on this subject and stated that its influence on the safety factor of sliding of slope was not so serious.

Now let us consider the velocity characteristics. It is apparent that the theories of stress characteristics field are generally based on the assumption that the considered material can be idealized as the rigid-plastic material. Therefore the deformation of the material is not induced while the material remains in the rigid state. After the beginning of plastic flow in the material, the accompanied deformation is considered to be ruled by the associated or non-associated flow law. Most of the analyses of the stability problems in the field of soil mechanics and foundation engineering are in modified or simplified forms of the theory of characteristics field with the tacit assumption that soils deform plascically in accordance with the associated flow law.

Drucker and Prager (1952), Drucker (1954), Cox, Eason and Hopkins (1961) discussed the soil plasticity considering the yield condition for soils to be Mohr-Coulomb criterion with the assumption of associated flow rule. Cox (1963) and Davis (1968) gave the strict treatment of stress and velocity characteristics field based on the non-associated flow rule and Mohr-Coulomb criterion. Applying the associated flow rule (normality rule) to the Mohr-Coulomb criterion, the deduced plastic strain increment vector should be directed to the normal direction of Mohr-Coulomb envelope, i.e. soils do not change its volume before the stress state reaches the failure envelope, and after yielding. They are to continue to dilate.

As mentioned before, the stress condition for critical state under plane strain deformation is equivalent to Mohr-Coulomb criterion in terms of effective stresses. But at the critical state, soils deform distortionally without changing their volume. This suggests that the non-associated flow rule should be assumed when one con-

structs the effective stress and velocity field in the soil medium. To say briefly the stress condition for the critical state and the Mohr-Coulomb criterion are not adequate to be used as the yield surface to which the normality concept is applied. Nevertheless we use this sort of stress condition in the analysis of stability problems for the sake of convenience. To avoid the irrelevant consequences arising from the above mentioned logical inconsistency, we must firstly recognize that the stress characteristics and velocity characteristics, one of which is the slip line as shown by Roscoe (1970) experimentally, are essentially indifferent. They coincide with each other only when the associated flow rule can be assumed, i.e., the continuous dilation of soil in plastic state.

## 10.4 Critical State of Embankments

### 1. Short-Term Stability

The analysis of stress characteristics field presented in the previous section is a sort of $\phi = 0$ analysis in terms of total stress. In this case the stress characteristics is directed to $\pm 45^{\circ}$ from the maximum principal stress direction as shown in eq. (10.2.25) and is coincident with the velocity characteristics. In the routine stability analysis of the embankments at the end of construction, the slip surface is assumed to be circular. This assumption will lead to the slight under-estimation of the bearing capacity of the clay layer, because the length of the assumed circular slip line is slightly shorter than the stress characteristics given by the present theory.

But in the current $\phi = 0$ analysis, the undrained strength of anisotropically consolidated clay is determined from the unconfined compression test on the undisturbed clay specimen. Therefore the undrained strength used in the current $\phi = 0$ analysis is rather conservative compared with the active state strength in the ground even if the sampling is completely carried on as shown by Ladd and Lambe (1963) , Skempton and Sowa (1964) and Ladd and Bailey (1964). Ladd and Bailey (1964) also pointed out that the passive state strength in the ground is much smaller than the compression strength

of completely sampled clay. In the case of the stability problems of embankments, the area of passively loaded failure zone is considerable. Then, the $\phi = 0$ analysis using the strength obtained from unconfined compression test on unditurbed clay specimen leads to the considerable over-estimation of bearing capacity. But on the practical sampling and testing processes, the clay specimen is considerably weakened by the disturbance.

As mentioned by Ladd and Bailey, it is likely that these effects are cancelled by each other. But it is noteworthy that current $\phi = 0$ analysis on the stability problem in which the passively loaded zone is dominant will lead to the remarkable over-estimation of critical bearing capacity. For instance, in the design works of sheet piles correct estimation of the strength of clay in the passive state is vital. The theoretical basis of $\phi = 0$ analysis for the stability of soil structures at the end of construction was discussed by Skempton (1948). The limitation of its use was shown by Bishop and Bjerrum (1960). But its usefulness in the short-term stability problems was emphasized by Nakase (1967). In the author's opinion, $\phi = 0$ analysis is of use in the short-term stability problems with sufficient understanding of the difference between active and passive state strength of anisotropically consolidated clay.

2. Long-Term Stability

In the practical sense, the long-term stability analysis of embankments on the clay layer which is in the normally consolidated or lightly over consolidated state is not so necessary except in the special problems, because the strength of such a clay layer increases due to the dissipation of excess pore water pressure. But when engineers encounter the necessity to know the bearing capacity of such a clay layer stressed under fully drained condition, they have only to analyse based on the theory of stress characteristics field. In this case $\sqrt{\frac{2}{3}}\,M$ corresponds to $\sin\phi$ and is assumed to be zero and the strength difference for the active and passive loading state vanishes. But it is noted that the slip line differs remarkably from

the stress characteristics, because normally consolidated or lightly over-consolidated clay considerably shrinks itself on the shearing process to the critical state contrary to the requirement of the associated flow rule that the clay is to continuously dilate after yielding.

The use of effective stress analysis in the form derived by Bishop (1954) for the long-term problems has been recommended by Bishop and Bjerrum (1960), KjÆrnsli and Simons (1962) and their coworkers. It is vital to have proper knowledges about the change in effective stresses and accompanied change in the mechanical state of clay in the case of analysing the long-term stability problems of embankments or cuts. But the use of effective stress analysis with the circular slip line has to be reconsidered from the view point of stress and velocity characteristics. Mikasa (1963) and Nakase, Kobayashi and Katsuno (1969) recommended the useage of the total stress analysis even in the long-term stability problems because of its simplicity.

The stability of embankments constructed on heavily over-consolidated clay or sand under the condition of full drainage of pore water can be analysed with the theory of characteristics field by substituting $\sqrt{\frac{2}{3}}\,M$ for $\sin\phi$ and C for zero. But the critical state of such soils corresponds to the residual strength introduced by Skempton (1964). In the ordinary stability problems of embankments, this analysis gives considerable under-estimation of bearing capacity of the ground. But on the contrary, the use of peak strength in the analysis leads to remarkable over-estimation of the bearing capacity, because the theory is based on the assumption that the yielding soils have constant shear strength regardless of increasing shear strain. Matsuo and Karube (1966) suggested an idea about the conventional reduction of peak strength. It is noted that such soils considerably dilate during the shear process, and therefore the associated flow rule can be assumed.

## 10.5 Conclusions

In this chapter, constructed is the theory of characteristics field of stress and velocity in the anisotropically pre-consolidated clay layer forced into the critical state under undrained condition by the construction of an embankment. In the analysis, the difference in strengths of the clays in the active and passive loading states is taken into account. This difference remarkablly influences the value of critical bearing capacity of clay layer. Nevertheless, to the best of the author's knowledge, none but the present theory do not take the difference in the strengths of clay elements in the active and passive loading states into account.

The present analysis is based on the realization that the characteristics field of stress and velocity do not, in general, coincide with each other. But most of the previous analyses of stability problems are indifferent to this basic theory of charateristics field.

In this chapter, some considerations are made on the accuracies and limitations of the current analyses used in the stability problems of embankments with the evaluation of the influences of the above mentioned two effects on the calculated critical bearing capacity.

# CHAPTER 11

# CONCLUSIONS

Through these investigations on the analysis of deformations of soils based on the theory of plasticity and on its application to settlement of embankments, the following features are considered to be clarified:

1. The current definition of effective stress is not appropriate as the definition of the allotted stress to the soil skelton in the special case of boundary condition of the stress in the clay.
2. The micro-mechanism of the consolidation and dilatancy of clay is considered to be described by the buckling of the frame works of clay skelton and by the breakdown of the links connecting the aggregated clusters of clay particles.
3. The flow rule of rate dependent elastic-plastic material is described by the existence of two sorts of free energy.
4. With some restrictions, the normality rule for the flow rule of plastic materials is rationalized.
5. The stress-void ratio relations for both the isotropically and anisotropically pre-consolidated clay in the elastic-plastic state are described by the concept of state surface which is derived from the characteristics of consolidation and dilatancy.
6. The stress-void ratio relations for both the isotropically and anisotropically pre-consolidated clay in the elastic state are described by the concept of swelling wall which is derived from the characteristics of consolidation and dilatancy.
7. Stress-strain relations for both the isotropically and anisotropically pre-consolidated clay in the elastic-plastic state are derived from the normality rule with the yield loci obtained by the combination of the concepts of state surface and swelling wall.
8. Stress-strain relations for both the isotropically and anisotropically pre-consolidated clay in the elastic state are derived from the concept of swelling wall.

9. The concepts of state surface and swelling wall are applicable for sandy and silty soils.

10. The effect of temperature on the mechanical state of the soil can be represented by the shift of the state surface and swelling wall in the state surface under the condition of constant temperature.

11. The intermediate principal stress in the clay deforming under the plane strain condition approximately coincides with the mean principal stress.

12. The derivatives of Cambridge original energy theory is derived from the present theory as a special case.

13. The constitutive relations for soils derived from the concepts of state surface and swelling wall predict the experimental results with a satisfactory accuracy.

14. Three dimensional consolidation analysis is established based on the constitutive relations of soils given by the present theory.

15. The effective stress paths of the clays on the process of consolidation with some special boundary conditions are analysed.

16. Stress and strain field in the anisotropically normally consolidated clay layer stressed by the construction of embankments are numerically computed with the assumption of undrained condition. And immediate settlement of the embankment is obtained.

17. Based on the stress field given by the theory of elasticity, the immediate deformation of the anisotropically normally consolidated clay layer stressed by the construction of the embankment is computed. And the development of deformation of the clay layer with the progress of the expulsion process of pore water is clarified.

18. A simplified estimation method of consolidation settlement of embankments is proposed.

19. An analysis of the critical state of embankments at the end of construction is established using the theory of characteristics field.

## REFERENCES


Aboshi,H.(1969): Consolidation, *Soil Mechanics* (edited by Mogami,T.), Gihodo, Tokyo, (in Japanese).

Adachi,T. and Ohta,H.(to appear): Thermodynamical Base of the Flow Rule of Plastic Materials.

Akai,K.(1953): Study on the Two Dimensional Consolidation of Embankment, *Trans. J.S.C.E.*, 51 - 59, (in Japanese).

Akai,K.(1966): *Soil Mechanics*, Asakura-Shoten, Tokyo, (in Japanese).

Akai,K. and Adachi,T.(1965): Study on the One-dimensional Consolidation and the Shear Strength Characteristics of Fully Saturate Clay, in Terms of Effective Stress, *Proc.6th I.C.S.M.F.E.*, Canada, Vol.2 146 -150.

Akai,K., Yamamoto,J. and Ozawa,R.(1962): On the Behavior of Pore Pressure during the Shear of Saturated Clay, *Trans.J.S.C.E.*, No.85, 1 - 6.

Barden,L. and Khayatt,A.J.(1966): Incremental Strain Rate Ratios and Strength of Sand in the Triaxial Test, *Géotechnique*, Vol.16, 338 - 357.

Barden,L., Khayatt,A.J. and Wightman,A.(1969): Elastic and Strip Components of the Deformation of Sand, *Canadian Geotechnical Journal*, Vol.6, 227 - 240.

Biot,M.A.(1941): General Theory of Three-dimensional Consolidation, *Journ.Appl.Phys.*, Vol.12, 155 - 164.

Biot,M.A.(1955): Theory of Elasticity and Consolidation for a Porous Anisotropic Solid, *Journ.Appl.Phys.*, Vol.26, No.2, 182 - 185.

Bishop,A.W.(1954): The Use of the Slip Circle in the Stability Analysis of Slopes, *Géotechnique*, Vol.5, 7 - 17.

Bishop,A.W.(1955): The Principle of Effective Stress, *Norwegian Geotechnical Institute*, No.32(1960), 1 - 5.

Bishop,A.W. and Bjerrum,L.(1960): The Relevance of the Triaxial Test to the Solution of Stability Problems, *A.S.C.E. Research Conference on Shear Stregth of Cohesive Soils*, 437 - 501.

Bishop,A.W., Webb,D.L. and Skinner,A.E.(1965): Triaxial Tests on Soil at Elevated Cell Pressure, *Proc.6th Int.Conf.Soil Mech.Found.Eng.*, Vol.1, 170 - 174.

Bjerrum,L.(1951): Fundamental Considerations on the Shear Strength of Soil, *Géotechnique*, Vol.2, 209 - 218.

Bjerrum,L.(1954): Theoretical and Experimental Investigations on the Shear Strength of Soils, *Norwegian Geotechnical Institute*, Publication No.5.

Broms,B.B. and Casbarian,A.O.(1965): Effects of Rotation of the Principal Stress Axes and of the Intermediate Principal Stress on the Shear Strength, *Proc.6th Int.Conf.Soil Mech.Found.Eng.*, Vol.1, 179 - 183.

Burland,J.B.(1965): The Yielding and Dilation of Clay, Correspondence, *Géotechnique*, Vol.15, 211 - 214.

Burland,J.B.(1969): Deformation of Soft Clay beneath Loaded Areas, *Proc.7th Int.Conf.Soil Mech.Found.Eng.*, Vol.1, 55 - 63.

Calladine,C.R.(1963): Correspondence, *Géotechnique*, Vol.13, No.3, 250.

Chang,C.Y. and Duncan,J.M.(1970): Analysis of Soil Movement around a Deep Excavation, *Proc.A.S.C.E.*, SM 5, Sept., 1655 - 1681.

Chaplin,T.K.(1970): Inner and Outer Plastic Yield Surfaces in Clays, *Proc.7th Int.Conf.Soil Mech.Found.Eng.*, Vol.1, 73 - 80.

Christian,J.T.(1968): Undrained Stress Distribution by Numerical Methods, *Proc.A.S.C.E.*, SM 6, Nov., 1333 - 1345.

Christian,J.T. and Boehmer,J.W.(1970): Plane Strain Consolidation by Finite Elements, *Proc.A.S.C.E.*, SM 4, July, 1435 - 1457.

Coleman,B.D. and Gurtin,M.E.(1967): Thermodynamics with Internal State Valiables, *Journ.Chem.Phys.*, Vol.47, 597 - 613.

Coleman,B.D. and Mizel,V.J.(1964): Existence of Caloric Equations of State in Thermodynamics, *Journ.Chem.Phys.*, Vol.40, 1116 - 1125.

Coleman,B.D. and Noll,W.(1963): The Thermodynamics of Elastic Materials with Heat Conduction and Viscosity, *Arch.Rational Mech. Anal.*, Vol.13, 167 - 178.

Cox,A.D.(1963): The Use of Non-associated Flow Rules in Soil

Plasticity, *Royal Armament Research and Development Establishment Report*, (B)2/63.

Cox,A.D., Eason,G. and Hopkins,H.G.(1961): Axially Symmetric Plastic Deformations in Soils, *Philosophical Transactions of the Royal Society of London*, Vol.254, A-1036, 1 - 45.

Crawford,C.B.(1964): Interpretation of the Consolidation Test, *Proc.A.S.C.E.*, SM 5, 87 - 90.

Davis,E.H.(1968): Theories of Plasticity and the Failure of Soil Masses, *Soil Mechanics-selected topics* (edited by Lee,I.K.). Butterworths, London, 341 - 380.

Davis,E.H. and Poulos,H.G.(1968): The Use of Elastic Theory for Settlement Prediction under Three-dimensional Condition, *Géotechnique*, Vol.18, 67 - 91.

Davis,E.H. and Raymond,G.P.(1965): A Non-linear Theory of Consolidation, *Géotechnique*, Vol.15, 161.

De Josselin de Jong,G.(1964): Lower Bound Collapse Theorem and Lack of Normality of Strain-rate to Yield Surface for Soils, *Proc.I.U.T.A.M.Symposium on Rheology and Soil Mech.*, Grenoble, 69 - 75.

Drucker,D.C.(1951): A More Fundamental Approach to Stress-strain Relations, *Proc.1st U.S.National Congr.Appl.Mech.*,A.S.M.E. 487 - 491.

Drucker,D.C.(1954): Coulomb Friction, Plasticity and Limit Load, *Journ.Appl.Mech.*, Vol.21, 71 - 74.

Drucker,D.C.(1958): Plasticity, Structural Mechanics, *Proc. of the 1st Symposium on Naval Structural Mechanics*, 407 - 455.

Drucker,D.C.(1959): A Definition of Stable Inelastic Material, *Journ. Appl.Mech.,Trans.A.S.M.E.*, Vol.26, 101 - 106.

Drucker,D.C.(1962): Stress-strain-time Relations and Irreversible Thermodynamics, *Int.Symposium on Second-Order Effects in Elasticity, Plasticity and Fluid Dynamics*, International Union of Theoretical and Applied Mechanics, 331 - 351.

Drucker,D.C. and Gibson,R.E. and Henkel,D.J.(1957): Soil Mechanics and Work-hardening Theories of Plasticity, *Trans.A.S.C.E.*,338 - 346.

Drucker,D.C. and Prager,W.(1952): Soil Mechanics and Plastic Analysis on Limit Design, *Quarterly of Applied Mathematics*, Vol.10, No.2, 157 - 165.

Duncan,J.M. and Chang,C.T.(1970): Nonlinear Analysis of Stress and Strain in Soils, *Proc.A.S.C.E.*, SM 5, Sept., 1629 - 1653.

Duncan,J.M. and Seed,H.B.(1966)[a]: Anitotropy and Stress Reorientation in Clay, *Proc.A.S.C.E.*, SM 5, 21 - 80.

Duncan,J.M. and Seed,H.B.(1966)[b]: Strength Voriation along Failure Surfaces in Clay, *Proc.A.S.C.E.*, SM 6, 81 - 104.

Dunlop,P. Duncan,J.M. and Seed,H.B.(1968): Finite Element Analysis of Slope in Soil, *Report No.TE-68-3 to U.S. Army Engineers*, Waterways Experiment Station, Univ. of California, Berkley.

Frydman,S. and Zeitlen,J.G.(1969): Some Pseudo-elastic Properties of Granular Media, *Proc.7th Int.Conf.Soil Mech.Found.Eng.*, Vol.1, 135 - 141.

Gibson, R.E.(1953): Experimental Determination of the True Cohesion and True Angle of Internal Friction in Clays, *Proc.3rd Int.Conf. Soil Mech.Found.Eng.*, Vol.1, 126 - 130.

Girijavallabhan,C.V. and Reese,L.C.(1968): Finite-element Method for Problems in Soil Mechanics, *Proc.A.S.C.E.*, SM 2, 473 - 496.

Green,A.E. and Naghdi,P.M.(1965): A General Theory of an Elastic-Plastic Continuum, *Arch.Rational Mech.Anal.*, Vol.18, 253 - 281.

Green,A.E. and Naghdi,P.M.(1967): A Class of Viscoelastic-Plastic Media, *Acta Mechanica*, Vol.4, 289 - 295.

Hansen,J.Brinch.(1963): Discussion, *Proc.A.S.C.E.*, July, 241.

Hansen,J.Brinch and Gibson,R.E.(1948): Undrained Shear Strengths of Anisotropically Consloidated Clays, *Géotechnique*, Vol.1, 189 - 204.

Hata,S.and Ohta,H.(1968): A Consideration on the Pore Pressure in Clays under Undrained Shear, *Trans.J.S.C.E.*, No.155, 18 - 24.

Hata,S. and Ohta,H.(1968): On the Effective Stress Paths of Normally Consolidated Clays under Undrained Shear, *Proc.J.S.C.E.*, No.162, 21 - 29.

Hata,S., Ohta,H. and Yoshitani,S.(1969)[a]: On the State Surface of Soils,

*Proc.J.S.C.E.*, No.172, 71 - 92.

Hata,S., Ohta,H. and Yoshitani,S.(1969)[b]: A Theoretical Approach to Stress-strain relations of Clays, *Land Subsidence*, Publication No.89, IASH-UNESCO, Vol.2, 563 - 572.

Henkel,D.J.(1956): The Effect of Overconsolidation on the Behavior of Clays during Shear, *Géotechnique*, Vol.6.

Henkel,D.J.(1959): The Relationships between the Strength, Pore-water Pressure and Volume-change Characteristics of Saturated Clay, *Géotechnique*, Vol.9, 119 - 135.

Henkel,D.J.(1960): The Relationships between the Effective Stresses and Water Content in Saturate Clays, *Géotechnique*, Vol.10, 41 - 54.

Henkel,D.J. and Sowa,V.A.(1963): The Influence of Stress History on Stress Paths in Undrained Triaxial Tests on Clay, *Laboratory Shear Testing of Soils*, A.S.T.M. Special Publication, No.361, 280 - 294.

Henkel,D.J. and Wade,N.H.(1966): Plane Strain Tests on a Saturated Remoulded Clay, *Proc.A.S.C.E.*, SM6, 67 - 79.

Höeg,K., Christian,J.T. and Whitman,R.V.(1968): Settlement of Strip Load on Elastic-Plastic Soil, *Proc.A.S.C.E.*, SM 2, 431 - 445.

Hvorslev,M.J.(1960): Physical Components of the Shear Strength of Saturated Clays, *Research Conference on Shear Strength of Cohesive Soils*, 169 - 273.

Karube,D. and Harada,S.(1967): Plane Strain Tests on Remoulded Clay, *Trans.J.S.C.E.*, No.147.

Karube,D. and Kurihara,N.(1966): Dilatancy and Shear Strength of Saturated Remoulded Clay, *Trans.J.S.C.E.*, No.135.

Kirkpatrik,W.H.(1957): The Condition of Failure for Sands, *Proc.4th Int.Conf.Soil Mech.Found.Eng.*, Vol.1, 172 - 178.

KjAErnsli,B. and Simons,N.(1962): Stability Investigations of the North Bank of the Drammer River, *Géotechnique*, Vol.12, 147 - 167.

Kondner,R.L.(1963): Hyperbolic Stress-strain Response; Cohesive Soils, *Proc.A.S.C.E.*, SM 1, 115 - 143.

Kondner,R.L. and Zelasko,J.S.(1963): Void Ratio Effects on the Hyperbolic Stress-strain Response of a Sand, *Laboratory Shear*

*Testing of Soils*, A.S.T.M.Special Technical Publication, No.361, 250 - 257.

Kratochvil,J. and Dillon,O.W.Jr.(1969): Thermodynamics of Elastic-Plastic Materials as a Theory with Internal State Variables, *Journ.Appl.Phys.*, Vol.40, No.8, 3207 - 3218.

Lambe,T.W.(1967): Stress Path Method, *Proc.A.S.C.E.*, SM 6, 309 - 331.

Ladd,C.C. and Bailey,W.A.(1964): Correspondence to A.W.Skempton and V.A.Sowa, *Geotechnique*, Vol.14, 353 - 358.

Ladd,C.C. and Lambe,T.W.(1963): The Strength of "Undisturbed" Clay Determined from Undrained Tests, *Laboratory Shear Testing of Soils*, A.S.T.M.Special Technical Publication, No.361, 342 - 371.

Leigh,D.C.(1969): On the Restriction of Processes by the Clausius-Duhem Inequality, *Zeit.Ang.Math.Phys.*, Vol.20, 167 - 175.

Lewin,P.I. and Burland,J.B.(1970): Stress-probe Experiments on Saturated Normally Consolidated Clay, *Geotechnique*, Vol.20, No.1, 38 - 56.

Lowe,J.III and Karafiath,L.(1960): Effect of Anisotropic Consolidation on the Undrained Shear Strength of Compacted Clays, *Research Conference on Shear Strength of Cohesive Soils*, 837 - 858.

Matsuo,S. and Kamon,M.(1970): *Proc. Anual Meeting of J.S.C.E.(25th)*, 187.

Matsuo,M. and Karube,D.(1966): A Few Consideration on the Application of the Shear Test Results for Design, *11th Symposium on Soil Engineering*, Tokyo.

Mikasa,M.(1963): The Interpretation of the Strength of Clay; the Criticism on $c'$, $\phi'$ Analysis, *Soil Mechanics and Foundation Engineering*, Vol.11, No.3, 31 - 43 (in Japanese).

Murayama,S.(1964): A Theoretical Consideration on a Behavior of Sand, *Proc.I.U.T.A.M. Symposium on Rheology and Soil Mech.*, 146 - 159, Grenoble.

Murayama,S.(1968): Mechanical Behavior of Soils under Shearing Stress (In the Case of Cohesionless Soil), *Bulletin of the Disaster Prevention Research Institute*, Vol.18, 97 - 109, Kyoto

University.

Murayama,S. and Kurihara,N.(1968): On the Effect of Stress History on the Strength of Clays, *23rd Annual Meeting of J.S.C.E.*

Murayama,S. and Kurihara,N.(1969): Mechanical Properties of Clay under the Repetitious Loads, *Disaster Prevention Research Institute Annuals*, No.12B, Kyoto University.

Murayama,S. and Matsuoka,H.(1971): The Mechanism of Shearing and its Similarity for Sands and Clays, *Disaster Prevention Research Institute Annuals*, No.14B, 551 - 563.

Nakase,A.(1967): The $\phi_u$=0 Analysis of Stability and Unconfined Compression Strength, *Soil and Foundation*, Vol.7, No.2, 33 - 50.

Nakase,A., Kobayashi,M. and Katsuno,M.(1969): Change in Undrained Shear Strength of Saturated Clays through Consolidation and Rebound, *Report of the Port and Harbour Research Institute*, Vol.8, No.4, 103 - 143 (in Japanese).

Noorany,I. and Seed,H.B.(1965): A New Experimental Method for the Determination of Hvorslev Strength Parameters for Sensitive Clays, *Proc.6th Int.Conf.Soil Mech.Found.Eng.*, Vol.1, 318 - 322.

Ohta,H. and Hata,S.(1971)[a]: Plane-strain Stress-strain Relations for Soils, *Proc.4th Asian Regional Conf. on Soil Mech. and Found.Eng.*, Vol.1, 57 - 62.

Ohta,H. and Hata,S.(1971)[b]: A Theoretical Study of the Stress-strain Relations for Clays, *Soils and Foundations*, Vol.11, No.3, 45 - 70.

Ohta,H. and Hata,S.(to appear)[a]: Stress-strain-temperature Relations for Granular Material as Clay.

Ohta,H. and Hata,S.(to appear)[b]: On the State Surface of Anisotropically Consolidated Clays.

Palmer,A.C.(1965): *On Stress Strain Relations for Soils*, Division of Engineering, Brown University, National Science Foundation Research Grant, GP 1115.

Palmer,A.C.(1966): A Limit Theorem for Materials with Non-associated Flow Laws, *Journal de Méchanique*, Vol.5, No.2, 217 - 222.

Palmer,A.C.(1967): Stress-strain Relations for Clays; an Energy

Theory, *Géotechnique*, Vol.17, 348 - 358.

Palmer,A.C., Maier,G. and Drucker,D.C.(1967): Normality Relations and Convexity of Yield Surfaces for Unstable Materials or Structural Elements, *Journ.Appl.Mech.,Trans.A.S.M.E.*, 464 - 470.

Poorooshasb,H.B., Holubec,I. and Sherbourne,A.N.(1966): Yielding and Flow of Sand in Triaxial Compression; Part 1, *Canadian Geotechnical Journal*, Vol.3, No.4, 179 - 190.

Poorooshasb,H.B., Holubec,I. and Sherbourne,A.N.(1967): Yielding and Flow of Sand in Triaxial Compression; Part 2 and 3, *Canadian Geotechnical Journal*, Vol.4, No.4, 377 - 397.

Pusch,R.(1970): Microstructural Changes in Soft Quick Clay at Failure, *Canadian Geotechnical Journal*, Vol.7, No.1, 1 - 7.

Rendulic,L.(1936): Relation between Void Ratio and Effective Principal Stresses for a Remoulded, Silty Clay, Discussion, *Proc.1st Int. Conf.Soil Mech.Found.Eng.*, Vol.3, 48 -51.

Richardson,A.M. and Whitman,R.V.(1963): Effect of Strain-rate upon Undrained Shear Resistence of a Saturated Remoulded Fat Clay, *Géotechnique*, Vol.13, 310 - 324.

Roscoe,K.H.(1970): The Influence of Strains in Soil Mechanics, *Géotechnique*, Vol.20, No.2, 129 - 170.

Roscoe,K.H. and Burland,J.B.(1968): On the Generalized Stress-strain Behaviour of 'Wet' Clay. *Engineering Plasticity*, Cambridge Univ. Press, 535 - 609.

Roscoe,K.H. and Poorooshasb,H.B.(1963): A Theoretical and Experimental Study of Strains in Triaxial Compression Tests on Normally Consolidated Clays, *Géotechnique*, Vol.13, 12 - 38.

Roscoe,K.H., Schofield,A.N. and Thurairajah,A.(1963): Yielding of Clays in States Wetter than Critical, *Géotechnique*, Vol.13, 211 - 240.

Roscoe,K.H., Schofield,A.N. and Wroth,C.P.(1958): On the Yielding of Soils, *Géotechnique*, Vol.8, 22 - 53.R

Rowe,P.W.(1962): The Stress-dilatancy Relation for Static Equilibrium of an Assembly of Particles in Contact, *Proc. of the Royal Society*

*of London*, Series A, Vol.269, 500 - 527.

Rowe,P.W.(1969): The Relation between the Shear Strength of Sands in Triaxial Compression, Plane Strain and Direct Shear, *Géotechnique*, Vol.19, 75 - 86.

Rowe,P.W., Barden,L. and Lee,I.K.(1964): Energy Components during the Triaxial Cell and Direct Shear Tests, *Géotechnique*, Vol.14, 247 - 261.

Sangrey,D.A., Henkel,D.J. and Esrig,M.I.(1969): The Effective Stress Response of a Saturate Clay Soil to Repeated Loading, *Canadian Geotechnical Journal*, Vol.6, 240 - 252.

Schofield,A.N. and Wroth,C.P.(1968): *Critical State Soil Mechanics*, McGraw-Hill, London.

Schultze,E. and Horn,A.(1965): The Shear Strength of Silt, *Proc.6th Int.Conf.Soil Mech.Found.Eng*, Vol.1, 350 - 354.

Shibata,T.(1963): On the Volume Change of Normally Consolidated Clays, *Disaster Prevention Research Institute Annuals*, No.6, Kyoto Univ.

Shibata,T. and Karube,D.(1965): Influence of the Variation of the Intermediate Principal Stress on the Mechanical Properties of Normally Consolidated Clays, *Proc.6th Int.Conf.Soil Mech.Found.Eng.*, Vol.1, 359 - 363, Canada.

Skempton,A.W.(1948): The $\phi$=0 Analysis of Stability and its Theoretical Basis, *Proc.2nd Int.Conf.Soil Mech.Found.Eng*, Vol.1, 72 - 78.

Skempton,A.W.(1954): The Pore-pressure Coefficients A and B, *Géotechnique*, Vol.4, 143 - 147.

Skempton,A.W.(1960): Effective Stress in Soils, Concrete and Rocks, *Pore Pressure and Suction in Soils (1961)*, 4 - 16.

Skempton,A.W.(1964): Long-term Stability of Clay Slopes, *Géotechnique*, Vol.14, 77 - 102.

Skempton,A.W. and Bjerrum,L.(1957): A Contribution to the Settlement Analysis of Foundations on Clay, *Géotechnique*, Vol.7, 168 - 178.

Skempton,A.W. and Sowa,V.A.(1963): The Behavior of Saturated Clays during Sampling and Testing, *Géotechnique*, Vol.13, No.4, 269 - 290.

Tatsuoka,F.(1971): Stress-strain Relations of Sands under Triaxial

Compression, *Proc.26th Annual Meeting of J.S.C.E. III*, 63 - 66.

Taylor,D.W.(1948): *Fundamentals of Soil Mechanics*, J.Wiley, N.Y., 383.

Truesdell,C. and Toupin,R.A.(1960): The Classical Field Theories, *The Encyclopedia of Physics*,Vol.III/1 (edited by Flugge,S.), Berlin-Göttingen-Heidelberg, Springer.

Valanis,K.C.(1970): On the Thermodynamic Foundation of Classical Plasticity, *Acta Mechanica*, Vol.9, 278 - 291.

Vesić,A.S. and Clough,G.W.(1968): Behavior of Granular Materials under High Stresses, *Proc.A.S.C.E.*, SM 3.

Walker,L.K. and Raymond,G.P.(1969): Anisotropic Consolidation of Leda Clay, *Canadian Geotechnical Journal*, Vol.6, 271 - 286.

Weidler,J.B. and Paslay,P.R.(1969): Analytical Description of Behavior of Granular Media, *Proc.A.S.C.E.*, EM 2, 379 - 395.

Whitman,R.V.(1960): Some Considerations and Data regarding the Shear Strength of Clay, *Research Conf. on Shear Strength of Cohesive Soils*, 581 - 614.

Wroth,C.P.(1965): The Prediction of Shear Strains in Triaxial Tests on Normally Consolidated Clays, *Proc.6th Int.Conf.Soil Mech.Found. Eng.*, Vol.1, 417 - 420, Canada.

Wroth,C.P. and Bassett,R.H.(1965): A Stress-strain Relationship for the Shearing Behavior of a Sand, *Géotechnique*, Vol.15, No.1, 32 - 56.

Wu,T.H., Loh,A.K. and Malvern,L.E.(1963): Study of Failure Envelope of Soils, *Proc.A.S.C.E.*, Vol.89, SM 1, 145 - 181.

Yagi,N.(1968): On the Shear Resistence of Sands, *23rd Annual Meeting of J.S.C.E.*

Zienkiewicz,O.C. and Cheung,Y.K.(1967): *The Finite Element Method in Structural and Continuum Mechanics*, McGraw-Hill, London.